Final Report

Application of Microbial Induced Calcite Precipitation to Stabilize Florida High-Organic Matter Soils for Roadway Construction

FDOT Project No. BDV34-977-06

Submitted To:

Project Manager, David Horhota, Ph.D., P.E.
Florida Department of Transportation

Submitted By:

Principal Investigator, Raphael Crowley, Ph.D., P.E.
Co-Principal Investigator, Andrew Zimmerman, Ph.D.
Nick Hudyma, Ph.D., P.E., and Scott Wasman, Ph.D., E.I., Collaborators
Matthew Davies, Mohammed Yahaya, and Jennie Ford, Graduate Students

University of North Florida
Taylor Engineering Research Institute
School of Engineering
Building 4, Room 1501
Jacksonville, FL 32224

March 2019

DISCLAIMER

The opinions, findings, and conclusions expressed in this publication are those of the author(s) and not necessarily those of the State of Florida Department of Transportation or the U.S. Department of Transportation.

APPROXIMATE CONVERSIONS TO SI UNITS

SYMBOL	WHEN YOU KNOW	MULTIPLY BY	TO FIND	SYMBOL
LENGTH				
in	inches	25.4	millimeters	mm
ft	feet	0.305	meters	m
yd	yards	0.914	meters	m
mi	miles	1.61	kilometers	km
SYMBOL	**WHEN YOU KNOW**	**MULTIPLY BY**	**TO FIND**	**SYMBOL**
AREA				
in^2	square inches	645.2	square millimeters	mm^2
ft^2	square feet	0.093	square meters	m^2
yd^2	square yard	0.836	square meters	m^2
ac	acres	0.405	hectares	ha
mi^2	square miles	2.59	square kilometers	km^2
SYMBOL	**WHEN YOU KNOW**	**MULTIPLY BY**	**TO FIND**	**SYMBOL**
VOLUME				
fl oz	fluid ounces	29.57	milliliters	mL
gal	gallons	3.785	liters	L
ft^3	cubic feet	0.028	cubic meters	m^3
yd^3	cubic yards	0.765	cubic meters	m^3
NOTE: volumes greater than 1000 L shall be shown in m^3				
SYMBOL	**WHEN YOU KNOW**	**MULTIPLY BY**	**TO FIND**	**SYMBOL**
MASS				
oz	ounces	28.35	grams	g
lb	pounds	0.454	kilograms	kg
T	short tons (2000 lb)	0.907	megagrams (or "metric ton")	Mg (or "t")
SYMBOL	**WHEN YOU KNOW**	**MULTIPLY BY**	**TO FIND**	**SYMBOL**
TEMPERATURE (exact degrees)				
°F	Fahrenheit	5 (F-32)/9 or (F-32)/1.8	Celsius	°C
SYMBOL	**WHEN YOU KNOW**	**MULTIPLY BY**	**TO FIND**	**SYMBOL**
ILLUMINATION				
fc	foot-candles	10.76	lux	lx
fl	foot-Lamberts	3.426	candela/m^2	cd/m^2
SYMBOL	**WHEN YOU KNOW**	**MULTIPLY BY**	**TO FIND**	**SYMBOL**
FORCE and PRESSURE or STRESS				
lbf	pound force	4.45	newtons	N
lbf/in^2	pound force per square inch	6.89	kilopascals	kPa

APPROXIMATE CONVERSIONS TO ENGLISH UNITS

SYMBOL	WHEN YOU KNOW	MULTIPLY BY	TO FIND	SYMBOL
LENGTH				
mm	millimeters	0.039	inches	in
m	meters	3.28	feet	ft
m	meters	1.09	yards	yd
km	kilometers	0.621	miles	mi
SYMBOL	**WHEN YOU KNOW**	**MULTIPLY BY**	**TO FIND**	**SYMBOL**
AREA				
mm^2	square millimeters	0.0016	square inches	in^2
m^2	square meters	10.764	square feet	ft^2
m^2	square meters	1.195	square yards	yd^2
ha	hectares	2.47	acres	ac
km^2	square kilometers	0.386	square miles	mi^2
SYMBOL	**WHEN YOU KNOW**	**MULTIPLY BY**	**TO FIND**	**SYMBOL**
VOLUME				
mL	milliliters	0.034	fluid ounces	fl oz
L	liters	0.264	gallons	gal
m^3	cubic meters	35.314	cubic feet	ft^3
m^3	cubic meters	1.307	cubic yards	yd^3
SYMBOL	**WHEN YOU KNOW**	**MULTIPLY BY**	**TO FIND**	**SYMBOL**
MASS				
g	grams	0.035	ounces	oz
kg	kilograms	2.202	pounds	lb
Mg (or "t")	megagrams (or "metric ton")	1.103	short tons (2000 lb)	T
SYMBOL	**WHEN YOU KNOW**	**MULTIPLY BY**	**TO FIND**	**SYMBOL**
TEMPERATURE (exact degrees)				
^oC	Celsius	1.8C+32	Fahrenheit	^oF
SYMBOL	**WHEN YOU KNOW**	**MULTIPLY BY**	**TO FIND**	**SYMBOL**
ILLUMINATION				
lx	lux	0.0929	foot-candles	fc
cd/m^2	$candela/m^2$	0.2919	foot-Lamberts	fl
SYMBOL	**WHEN YOU KNOW**	**MULTIPLY BY**	**TO FIND**	**SYMBOL**
FORCE and PRESSURE or STRESS				
N	newtons	0.225	pound force	lbf
kPa	kilopascals	0.145	pound force per square inch	lbf/in^2

*SI is the symbol for the International System of Units. Appropriate rounding should be made to comply with Section 4 of ASTM E380.(Revised March 2003)

TECHNICAL REPORT DOCUMENTATION

1. Report No. BDV34 977-06	2. Government Accession No.	3. Recipient's Catalog No.
4. Title and Subtitle Application of Microbial Induced Calcite Precipitation to Stabilize Florida High-Organic Matter Soils for Roadway Construction		5. Report Date December 2018 6. Performing Organization Code
7. Author(s) Raphael Crowley, Andrew R. Zimmerman, Nick Hudyma, and Scott Wasman		8. Performing Organization Report No.
9. Performing Organization Name and Address School of Engineering University of North Florida Building 4, Room 3201 Jacksonville, FL 32224		10. Work Unit No. 11. Contract or Grant No. BDV34-977-06
12. Sponsoring Agency Name and Address Florida Department of Transportation 605 Suwannee Street, MS 30 Tallahassee, FL 32399		13. Type of Report and Period Covered Final Report, 01/2016 – 03/2019 14. Sponsoring Agency Code
15. Supplementary Notes		

16. Abstract

Microbially induced calcite precipitation (MICP) was used to treat Ottawa 50-70 sand and organic soil (from Polk County, FL, with 50% organic content) in the lab via injection at the bottom of specimens. Results showed that the technique was effective in sands, although calcification was variable and not uniform over the height of each specimen, which resulted in variability in the laboratory strength tests. In an effort to create specimens with uniform calcification, a pre-mixing treatment methodology was developed. Results from pre-mixing showed that more-uniform specimens were created. Both injection and pre-mixing MICP techniques were used to treat the organic soil. Results showed that very little calcite was created using either treatment technique. However, the pre-mixing technique was slightly more effective for specimens with lower organic content (10%). Exopolysaccharide (EPS) formation and the role it plays in MICP was investigated. EPS was observed in samples of MICP-treated Ottawa sand and appears to be a necessary component in the process for successful calcification. The inability to calcify in the organic soil may be due to the lack of EPS, which suggests its formation is inhibited by organic matter. A preliminary study was conducted to assess the feasibility of using bio-stimulation (stimulating native soil microbes) to induce calcite formation in Florida soils. While results showed that the treatment was ineffective, this was expected based upon results from bio-augmented treatments. In an attempt to induce calcification in the organic soil, sodium dodecyl sulfate (SDS) was added to the MICP recipe. While preliminary results were very promising, further investigation showed that specimens treated with SDS-MICP were dissolvable. In addition, results showed an unintended formation of a calcium dodecyl sulfate (CDS) complex that when stoichiometrically balanced, yielded specimens that were very strong and insoluble. This new, unstudied, non-traditional soil treatment technique has been dubbed surfactant-induced soil stabilization (SISS). The SISS method was further investigated as a viable means for treating Florida soils, although a thorough investigation of this soil treatment technique was outside the scope of this project. Preliminary results of SISS-treated specimens are very promising and warrant further investigation.

17. Keywords. Microbial Induced Calcite Precipitation Organic Soil		18. Distribution Statement No restrictions	
19. Security Classif. (of this report) Unclassified	20. Security Classif. (of this page) Unclassified	21. Pages 216	22. Price

EXECUTIVE SUMMARY

Microbially induced calcite precipitation (MICP) was used to treat Ottawa 50-70 sand and organic soil (from Polk County, FL, with 50% organic content) in the lab via injection at the bottom of specimens. Results showed that the technique was effective in sands, although calcification was variable and not uniform over the height of each specimen, which resulted in variability in the laboratory strength tests. In an effort to create specimens with uniform calcification, a pre-mixing treatment methodology was developed. Results from pre-mixing showed that more-uniform specimens were created. Both injection and pre-mixing MICP techniques were used to treat the organic soil. Results showed that very little calcite was created using either treatment technique. However, the pre-mixing technique was slightly more effective for specimens with lower organic content (10%). Exopolysaccharide (EPS) formation and the role it plays in MICP was investigated. EPS was observed in samples of MICP-treated Ottawa sand and appears to be a necessary component in the process for successful calcification. The inability to calcify in the organic soil may be due to the lack of EPS, which suggests its formation is inhibited by organic matter. A preliminary study was conducted to assess the feasibility of using bio-stimulation (stimulating native soil microbes) to induce calcite formation in Florida soils. While results showed that the treatment was ineffective, this was expected based upon results from bio-augmented treatments. In an attempt to induce calcification in the organic soil, sodium dodecyl sulfate (SDS) was added to the MICP recipe. While preliminary results were very promising, further investigation showed that specimens treated with SDS-MICP were dissolvable. In addition, results showed an unintended formation of a calcium dodecyl sulfate (CDS) complex that when stoichiometrically balanced, yielded specimens that were very strong and insoluble. This new, unstudied, non-traditional soil treatment technique has been dubbed surfactant-induced soil stabilization (SISS). The SISS method was further investigated as a viable means for treating Florida soils, although a thorough investigation of this soil treatment technique was outside the scope of this project. Preliminary results of SISS-treated specimens are very promising and warrant further investigation.

TABLE OF CONTENTS

page

LIST OF TABLES

LIST OF FIGURES

Figure page

CHAPTER 1
INTRODUCTION, BACKGROUND, AND LITERATURE REVIEW

1.1 Organic Soils and Peat in Florida

The presence of organic-rich soil and peat beneath Florida roadways has resulted in significant maintenance and associated costs due to settlements that result from the material's secondary compression (creep) and consolidation. Soper and Osbon (1922) noted that peat deposits in Florida are in a large abundance (more than 1,000,000,000 tons), third behind Minnesota and Wisconsin. Figure 1 illustrates 14 Florida soil regions as presented by Soper and Osbon (1922). The seven regions with significant extensive organic-rich soil deposits in Figure 1 are 6-Middle Flatwood, 7-Gulf Hammock, 8-Lake, 9-East Flatwood, 10-East Coast, 11-South Flatwood, and 12-Miami Limestone.

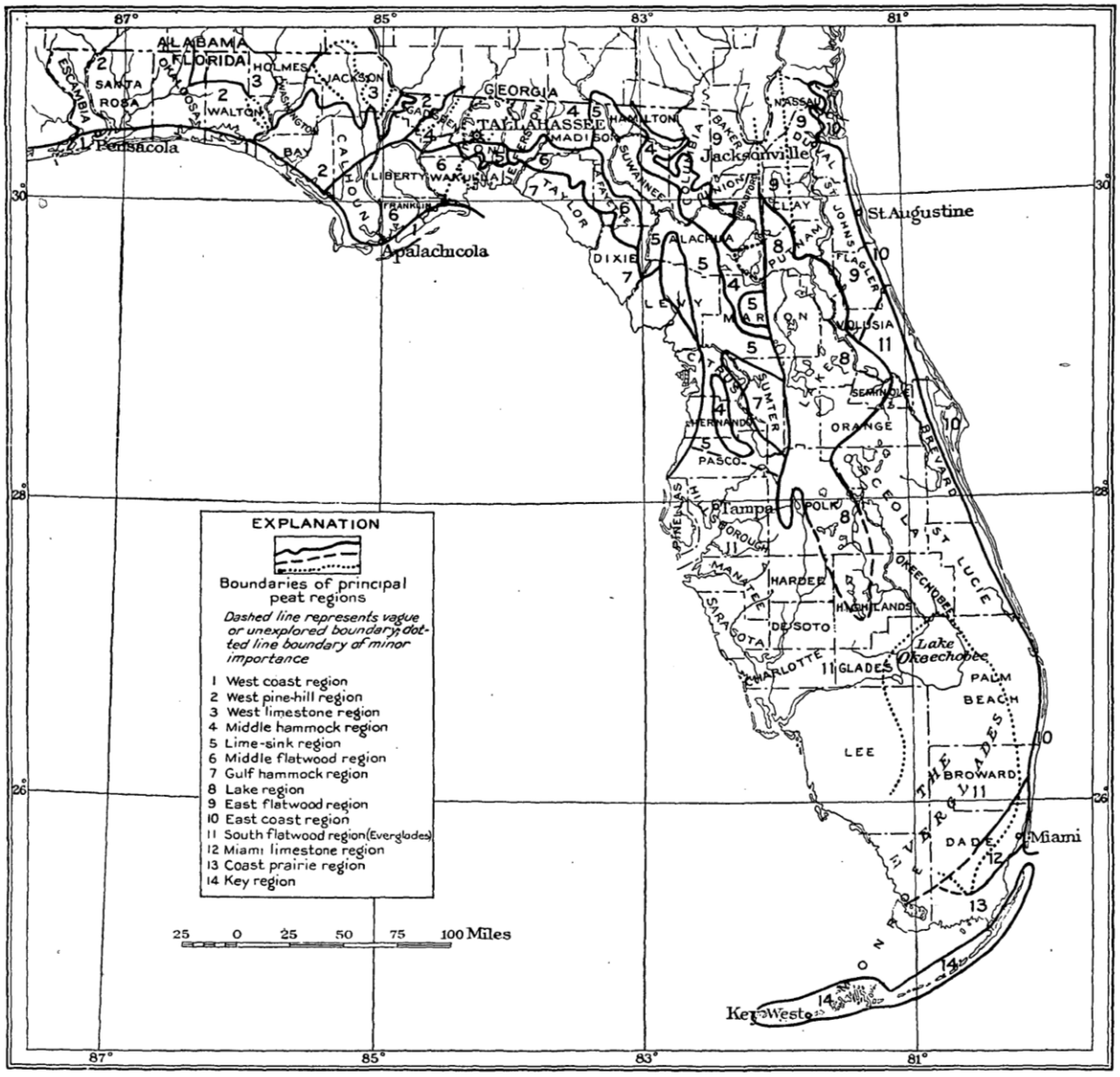

Figure 1-1. Peat Deposit Regions in Florida (Soper and Osbon 1922)

The Middle Flatwood region covers the southeastern part of the panhandle from southern Calhoun County (Apalachicola) to northern Dixie County. The Gulf Hammock region runs along the gulf coast from Wakula County to Pasco County. The Lake region runs north-south down the center of the state from Clay County to central Highlands County. The East Flatwood region covers the northeast of the state from the state line near Jacksonville south to northern Volusia County. The East Coast region is a narrow band along the east coast from the state line to South Beach Miami. The South Flatwood region is predominately the Everglades of Florida and runs north to central Florida on the east and west of the Lake Region. The Miami Limestone region is a small area in the southeastern part of Miami-Dade County and primarily originates from swaps and estuaries.

Organic-rich soil and peat are unique in terms of engineering and biological characteristics when compared to mineral soils. A few unique characteristics are their ability to absorb large amounts of moisture (natural moisture contents up to 1500 %), high compressibilities (large volume changes), high hydraulic conductivities, very low shear strengths (S_u = 0.73-2.9 psi or 5-20 kPa [Huat et al., 2014]), and rate of decomposition in different environmental conditions.

Usually, organic-rich soils and peats are the result of plant remains. They can easily be identified by evidence of decomposition, particular textures, colors, and odors. Peat and organic-rich soil are typically dark black or brown in color and have an organic odor. Peat is predominately composed of plant matter and is lightweight compared to organic-rich soil (Jarret 1995). Organic-rich soils have a noticeable mineral component and less plant matter, although it is sometimes identified as peat due to its high organic content and humus content. The term "muck" is commonly used to describe peat, although muck is fully decomposed peat (Huat, et al., 2014).

The Unified Soil Classification System (USCS) provides a classification for organic-rich soils that is separate from fine-grained soil and coarse-grained soil. The symbol "Pt" is used to describe highly organic soils which are composed of primarily organic matter, dark in color, and having an organic odor. For classification based on measured properties, the Florida Department of Transportation's (FDOT) Soils and Foundation Handbook (FDOT, 2018) recommends guidelines based on the percentage of organic content (OC), determined according to ASTM D2974. These are:

- Organic Material with organic content> 5% and < 20%,
- Highly Organic Material with organic content> 20% but < 75% (Highly Organic Material is also referred to as Muck)
- Peat with organic content> 75%.

A more thorough classification can be made according to ASTM standard D4427 (ASTM, 2013) which classifies peat according to fiber content (ASTM D1997), ash content (ASTM D2974), acidity (ASTM D2976), absorbency (ASTM D2980), and botanical composition. The basis for the classification of peat according to ASTM D4427 are:

Fiber Content:

- Fibric – less than 67 % fibers.
- Hemic – between 33 % and 67 % fibers.

- Sapric – more than 33 % fibers.

Ash Content:
- Low Ash – less than 5 % ash.
- Medium Ash – between 5 % and 15 % ash.
- High Ash – more than 15 % ash.

Acidity:
- Highly Acidic – pH less than 4.5.
- Moderately Acidic – pH between 4.5 and 5.5.
- Slightly Acidic – pH greater than 5.5 and less than 7.
- Basic – pH equal to or greater than 7.

Absorbency:
- Extremely Absorbent – water-holder capacity greater than 1500 %.
- Highly Absorbent – water-holding capacity between 800 % and 1500 %.
- Moderately Absorbent – water-holding capacity greater than 300 % and less than 800 %.
- Slightly Absorbent – water-holding capacity less than or equal to 300%.

Botanical Composition:
- Name the predominant type of plant in the peat sample.
- Refrain from using a botanical designation for samples with less than 33 % fibers.

1.2 Stabilization of Organic-Rich Soils

As a result of the creep/compressibility issues associated with organic rich soils discussed above, much research over the last several years has consisted of finding methods to stabilize these soils. Due to the significant presence of organic rich soil in Florida cited above, FDOT has a significant interest in finding solutions to issues faced with roadways on this soil. There are a number of options when dealing with organic soil. The following is a discussion of common stabilization techniques for organic-rich soils that have been previously used.

1.2.1 Cut and Replace

Cut-and-replace is commonly used as a stabilization technique for organic-rich soils when practical. The issues with this technique are (1) cost; and (2) feasibility. For deeper deposits, replacement is often not practical because its expense is cost-prohibitive (Mullins and Gunaratne, 2015). Gue et al. (2002) found that excavation and replacement is viable to a maximum depth of 15 feet (4.5 m). Additionally, removal of organic rich soil will lead to organic decomposition; decomposition will lead to carbon atmospheric carbon release; and the carbon may contribute to global warming.

1.2.2 Modification of Applied Loads

The modification of applied loads can be accomplished in a number of ways. This technique is addressed during the design phase and implemented during construction. The techniques associated with this methodology include increasing the bearing area of foundation elements and the use of light weight fills.

1.2.2.1 Increasing Bearing Area

Increasing the bearing area of foundation elements or embankments will decrease the stresses applied to the organic materials which will, in turn, decrease the settlement and decrease the chance of bearing capacity failure. Increasing the bearing area is directly related to costs; increasing the bearing area means a larger foundation or increased widths of embankments. There are both material costs and potentially right-of-way acquisition costs associated with this technique.

1.2.2.2 Lightweight Fills

Lightweight fills can be used to reduce the applied stresses from geotechnical assets. Some of the most common lightweight fills are lightweight expanded clay and ESP (expanded polystyrene) geofoam. Expanded clay is a vitrified shale produced in a rotary fired kiln. Each aggregate has a highly porous interior with a vitrified outer shell. The aggregates come in a variety of sizes. Typically, the unit weights of these materials range between 2 and 65 pounds per cubic foot (pcf).

EPS was successfully used in Hollywood, Florida for the construction of an elevated roadway. The project utilized approximately 1,150 cubic meters of Type II EPS geofoam to raise grades up to 1.7 meters (Meyer et al., 2004).

1.2.3 Construction Techniques

Mitigation of the effects of organic soils on engineered structures can be often be realized by adopting different construction techniques. Normally multiple construction techniques are adopted to address the issues raised by organic materials. These techniques include soft soil expulsion, surcharging, and staged construction.

1.2.3.1 Soft Soil Expulsion

Soft soil expulsion, also known by displacement fills or mud wave technique, utilizes the weight of soil to displace the organic material. Strategically placing the soil will cause the problematic soils to be expelled from the construction zone leaving the fill material in its place (Zayen et. al, 2003).

1.2.3.2 Surcharge with or without Wick Drains

In 2004, McVay and Nguyen investigated the distress of an embankment over organic-rich soils. The investigation consisted of field monitoring of a site with an existing roadway and a proposed roadway. Soil surcharging was used to stabilize the soils. While results were mostly positive, the surcharging technique appeared to be appropriate only for new roadways.

As discussed in Mullins and Gunaratne (2015) wick drains may be an effective means to reduce the consolidation time of organic-rich soils by shortening their drainage paths. These drains are installed prior to surcharging throughout the treatment area. While they are usually prefabricated drains but they may also be stone or sand columns. Their efficiency is dependent on spacing, drain diameter, and material disturbance / interface smear formed during installation.

Several drains are readily available from wick drain manufacturers, and for stabilization programs involving soil mixing, installation of these drains may be very useful. However, as Mullins and Gunaratne (2015) point out, these are only an effective treatment method when primary consolidation dominates relative to secondary consolidation. This behavior should only be expected in organic clays.

1.2.3.3 Staged Construction

One option that is often utilized for construction over weak soils is staged construction. In this technique, only a portion of the asset is constructed and the weak soils are allowed to deform and consolidate prior to the next portion being placed. Staged construction is often used when constructing embankments of soft soils.

1.2.4 Ground Modification

As discussed in Mullins and Gunaratne (2015), ground modification consists of a broad range of techniques including stone columns, sand columns, dynamic replacement, dynamic compaction, and soil mixing. Many of these techniques are in detail in Mullins and Gunaratne (2015). A brief summary is presented below:

1.2.4.1 Stone Columns

Stone columns, or inclusions installed by packing sand or stone into a borehole, are often used to stabilize some soils – particularly sinkhole prone areas. However, as discussed by Mullins and Gunaratne (2015), soil columns would not appear to be a suitable method for stabilizing high-OM soils because of the progressive loss of confinement stress necessary for radial support of the columns.

1.2.4.2 Dynamic Compaction

Dynamic compaction (DC) is a method of densifying soil via successive drops of a heavy weight (up to 40 tons) from a significant height (up to 100 feet). While this may be an effective treatment technique, construction difficulties can occur if the water table is not maintained at least six to seven feet below the ground surface (Lukas, 1986; Mullins and Gunaratne, 2015).

1.2.4.3 Dynamic Replacement

Dynamic replacement and mixing (DRM) is a technique whereby consolidation can be accelerated by dynamic replacement (DR) and DRM of deposits with sand columns. In short, the technique consists of using DR to create a sand column and then dropping a heavy mass onto the sand column

to burst the column and shoot jets of sand into the surrounding soil (Mullins and Gunaratne, 2015). This technique is considered an in situ mechanical soil mixing method that does not use a binder.

According to the Mullins and Gunaratne (2015), soils treated with this technique may show excellent improvement in terms of compressibility and strength because DRM can transform in situ peaty clay deposits into an upper sand raft with pockets of peaty sand underlain by a relatively uniform layer of sand and peat. Examples of improvement using this technique include Lo et al, (1990), Lee and Lo (1985), and Terashi and Tanaka (1981).

1.2.4.4 Soil Mixing

Mullins and Gunaratne (2015) discuss soil mixing in-depth. To summarize, numerous proprietary methods for soil mixing exist where a binder such as lime, slag, or cement is mixed with in situ material to improve its engineering characteristics. In particular, soil-cement has been used for decades. The soil-cement is prepared via an above-ground process and added to the soil via jet grouting, wet mixing, or dry mixing.

The Mullins and Gunaratne (2015) study involved several bench tests and large-scale laboratory tests, and full-scale mixing tests. Results showed consistent improvement, and design guidelines were developed for soil mixing implementation. While these are positive benefits, the issue with soil mixing in general is its sustainability in that addition of large quantities of cement, lime, or slag may cause environmental issues. Specifically, the presence of some substances in concrete, particularly some of its additives, may cause health concerns due to toxicity and radioactivity. Additionally, many studies indicate that Portland cement/concrete production is a significant contributor of global CO_2 (up to 5 %) through chemical processes and manufacturing energy. In addition, large quantities of cement/grout are required using this method. At higher organic contents, it is thought that much of this material acts as void fill and not as a cementing agent. Using such large quantities of material may be very expensive.

1.3 Microbially Induced Calcite Precipitation (MICP)

An alternative approach for soil improvement that has gained traction in recent years is microbially induced calcite precipitation (MICP). This technique has been primarily developed and tested for sands, although other soils have also been studied on a limited basis. Sumner (1926) was the first to crystallize the enzyme urease from the jack bean, which is the catalyst for the MICP reaction most commonly used today (Mobley et al., 1995). The common use of MICP for soil strengthening or ground improvement today is preceded by a number of applications including:

1. Microbial enhanced oil recovery (MEOR) (Kantzas et al., 1992)

2. Restoration of calcareous stone materials (Tiano, 1995; Castanier et al., 2000; Stocks-Fisher et al., 1999; Rodriguez-Navarro et al., 2003)

3. Wastewater treatment (Hammes et al., 2003)

4. Bioremediation (Ferris et al., 2003; Fujita et al., 2000; Warren et al., 2001; Achal et al., 2011b)

5. Concrete crack repair (Ramachandran et al., 2001; Wong, 2015)

6. As a sealant and structural measure (Gollapudi et al., 1995)

7. As a bioclogging mechanism for brick (Sarda et al., 2009; Soon, 2013)

Beyond MICP, other biomediated subsurface geochemical processes include: gas generation (microbial excretion of biogases reducing the saturation of soil with implications of reducing soil susceptibility to liquefaction), biofilm formation (microorganisms adhering to surface and excreting extracellular polymer substances creating a biofilm which has the potential to trap and stabilize sediments) , and biopolymer generation (can reduce hydraulic conductivity and increase shear strength) (DeJong et al., 2013).

The advantage to using MICP as a geotechnical improvement technique as opposed to the more traditional methods discussed in Section 1.2 is that MICP's sustainability as an organic process (DeJong et al., 2009). Applications where MICP may be used in lieu of traditional geotechnical improvement methods may eventually include liquefaction prevention, damage mitigation, building settlement reduction, and dam/levee piping prevention (DeJong et al., 2009). Additionally, much research has been conducted on reducing hydraulic conductivity via geomicrobial bioclogging. More recently, it has been suggested that MICP may be used to stabilize slopes (Salifu et al., 2016) or mitigate wind erosion (Maleki et al., 2016). Because of this project's scope, the focus of this literature review is potential geotechnical improvement applications. This topic will be discussed in-depth in Section 1.3.4. However, before discussing ground improvement specifically, the chemistry and microbes associated with the MICP process are discussed in-depth below.

1.3.1 MICP Chemistry

MICP involves utilizing naturally-occurring ureolytic bacteria to induce chemical reactions that strengthen soil. Usually, the soil is supplemented with ureolytic bacteria such as *Sporosarcina pasteurii*. Then, urea and calcium chloride are added to the soil/bacteria. The urea is metabolized by the bacterial urease enzymes to induce the classical MICP reactions:

$$CO(NH_2)_2 + 2H_2O \rightarrow 2NH_3 + H_2CO_3 \text{ (Urea Lysis)} \quad (1\text{-}1)$$

Ammonia from reaction 1-1 combines with water to form ammonium ions and hydroxide ions:

$$NH_3 + H_2O \leftrightarrow NH_4^+ + OH^- \quad (1\text{-}2)$$

Ammonium is a weak acid and hydroxide is a strong base. As such, the pH of the system increases to an optimal value of approximately 9.5. Under these basic conditions, two moles of hydroxide ions react with the carbonic acid formed in the urea lysing step to generate a carbonate ion (Equation 1-3 and Equation 1-4), which then combines with dissolved calcium (from the calcium chloride) to form calcium carbonate (Equation 1-5). Calcium ions can also directly combine with bicarbonate ion to form calcium carbonate, carbon dioxide, and water (Equation 1-6).

$$H_2CO_3 + 2OH^- \leftrightarrow HCO_3^- + H_2O + OH^- \text{ (Carbonic acid to bicarbonate)} \quad (1\text{-}3)$$

$$HCO_3^- + H_2O + OH^- \leftrightarrow CO_3^{2-} + 2H_2O \text{ (Bicarbonate to carbonate)} \quad (1\text{-}4)$$

$$Ca^{2+} + CO_3^{2-} \leftrightarrow CaCO_3\ (s) \quad (1\text{-}5)$$

$$Ca^{2+} + 2HCO_3^- \leftrightarrow CaCO_3\ (s) + CO_2\ (g) + H_2O \quad (1\text{-}6)$$

The above reactions only occur in close proximity to the bacteria where the enzyme is released. The process described above is known as MICP through bio-augmentation since naturally-occurring native bacteria in the soil are supplemented prior to the first reaction with an externally-grown bacteria stock.

While the above urea hydrolysis reactions constitute the most commonly used method of bacteria-stimulated calcite precipitation, other methods may also be used including denitrification, iron reduction, photosynthesis (Ehrlich 1998; McConnaughey and Whelan 1997), or sulfate reduction (Castanier et al. 1999; Wright 1999). In concept, each of these techniques is similar in that they all increase pH and drive Equation 1-2 (please see below for a more in-depth discussion of pH). Figure 1-2 from DeJong et al. (2010) outlines each of these chemical processes.

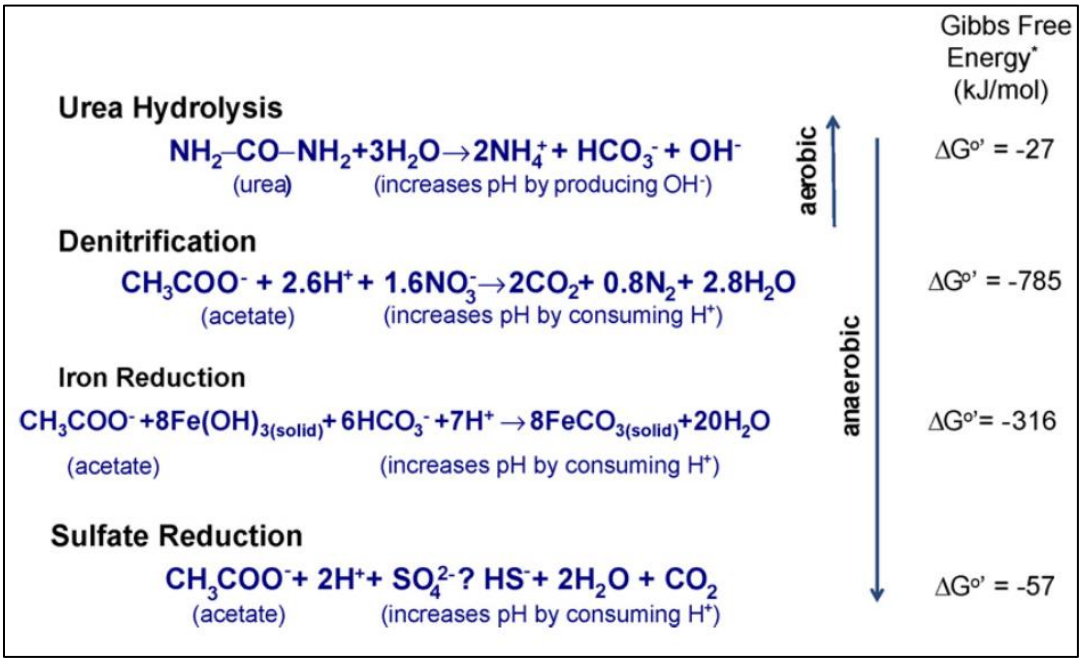

Figure 1-2. Alternative biomediated processes (from DeJong et al., 2010)

A study by van Paassen et al. (2010) concluded that urea hydrolysis was the most thermodynamically favored method, and it leads to the highest potential calcite conversion rate when compared with aerobic oxidation, denitrification, or sulfate reduction. Hence, it has become the most common MICP technique for soil improvement.

1.3.2 Controlling Factors of MICP

The chemical process of calcite precipitation is regulated by the following key elements: calcium concentration, concentration of dissolved inorganic carbon (DIC), pH (as mentioned above), availability of nucleation sites (e.g., bacterial cells), and urea in the case of ureolysis (Kile et al., 2000; Castanier et al., 1999; Whiffin et al., 2007; Hammes and Verstraete, 2002). These can collectively be termed "reagents." Additional environmental factors may play a role including salinity, temperature, and geometric compatibility of bacteria (i.e., soil particle grain type and size) (Nemati et al., 2005; Rivadeneyra et al., 2004; De Muynck et al., 2010b; Maier et al., 2009).

During the process of soil strengthening via MICP, specific methods applied may yield variability in results. Salifu et al. (2016) identified key important factors for cementation as bacterial aggregation, pore size distribution of media, application strategy of bacteria and salt, i.e., injection rate, and grouting technique. The time allowed for MICP to take place is an additional variable. A more in-depth discussion of some of these key components is presented below.

1.3.2.1 pH

The critical role of pH throughout the MICP process was discussed briefly above. With the exception of a small group of acid urease enzymes, microbial ureases generally possess an optimum pH of near neutrality (Mobley et al. 1995). For example, the commonly-used microbe *S. pasteurii* (Section 1.3.3 contains a complete discussion of microbes) has an optimum pH of 8 (Stocks-Fischer et al., 1999). When pH drops below 5, microbial urease can potentially be irreversibly denatured (Mobley et al., 1995). Studies of optimal pH ranges for different microbes are listed in Table 1-1 below. The production of ammonia from urea hydrolysis increases the medium pH during MICP, but bicarbonate from urea hydrolysis and microbial respiration acts as a buffer to the pH rise (Soon, 2013). The pH at which $CaCO_3$ will spontaneously occur is presented in Figure 1-3 while Table 1-1 outlines pH ranges for various calcite-inducing bacteria.

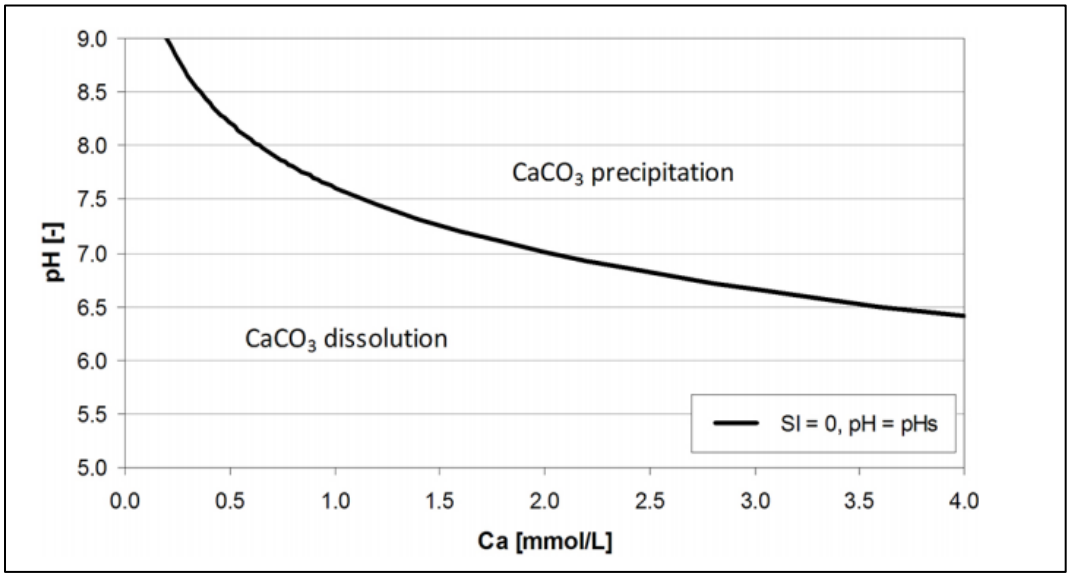

Figure 1-3. Calcium equilibrium or saturation with over- and under-saturation (i.e., calcium carbonate precipitation and dissolution from De Moel et al., 2013)

Table 1-1. Various bacterial pH optimizations

Bacteria Type	**pH Ranges**							
S. pasteurii	9 (Feng and Montoya, 2016)	Optimum: 8 Max: 9.5 (Stocks-Fischer et al., 1999)	Max: 9.3 (Ferris et al., 2003)	Max: 9.1 (Fujita et al., 2004)	8.7-9.5 (Dupraz et al., 2009)	Optimum: 8 (Arunachalam et al., 2010)	Range of 6-8, significant loss at pH 5 and 9 (van Elsas and Penido, 1982)	Range of 7-9 Peaked at 7 (Khan, 2011)
B. sphaericus	Peaked at 8 (Arunachalam et al., 2010)							
B. megaterium	Range of 6-8, significant loss at pH 5 and 9 (van Elsas and Penido, 1982)	Range of 7-9 Peaked at 7 (Khan, 2011)						

1.3.2.2 Bacteria Cell Concentration

A high concentration of bacterial cells increases the amount of calcite precipitation from MICP (Okwadha and Li, 2010). Urea hydrolysis production is directly correlated with bacterial cell concentration when provided sufficient reagent (Soon, 2013). Li et al. (2012) and Stocks-Fischer et al. (1999) both suggested that bacteria cell served as nucleation sites for calcite to precipitate in the biochemical reaction. Using SEM imaging, researchers have determined that the nucleation sites, a key necessity for calcite precipitation, are the cell walls of the bacteria (Lian et al., 2006; Knorre and Krumbein, 2000).

1.3.2.3 Provided Nutrients

Common nutrients used by bacteria during the MICP process include CO_2, N, P, K, Mg, Ca, Fe, etc. (Mitchell and Santamarina, 2005). The nutrient mixes are supplied to the bacteria during the culture and soil treatment stage (Soon, 2013). Several studies used 3 g/L of nutrient broth in the treatment solution to sustain growth and viability of urease producing bacteria (DeJong et al., 2006; Stocks-Fischer et al., 1999; Al Qabany et al., 2012). The purpose of the nutrients are to ensure the bacteria sustain long enough to support calcite precipitation (Soon, 2013).

Inagaki et al. (2011) varied the mol densities of urea and calcium chloride in their cementation solution, while keeping them equal to each other. Their tests include 0.25, 0.5, 0.75, 1, and 1.5

mol/L. They concluded that a concentration of 0.5 mol/L as the optimum; and at greater concentrations, the precipitation process is stagnated.

1.3.2.4 Temperature

Temperature is a crucial factor in the rate of MICP. Van Paassen et al. (2010) found that at temperatures below 5^{o}C, urease activity was negligible. Whiffin (2004), using *S. pasteurii*, found that urease activity increased proportionally between 25^{o}C and 60^{o}C, with an optimal temperature of 70^{o}C. By 80^{o}C, precipitation was reduced by approximately 50%. Since the manipulation of temperature is generally not feasible in the field, most experiments are conducted near room temperature, or 20-30^{o}C. However, because production appears to increase as a function of temperature, microbial treatment may be ideal in Florida at shallow depths during the summer when surface temperature often approaches 35^{o}C. Because soil is a thermal insulator, at greater depths, its effectiveness will decrease as temperature decreases thereby approaching room temperature conditions.

Other studies have been conducted on the optimal temperature of urease activity, including Sahrawat (1984), Liang et al. (2005), and Chen et al. (1996). However, it is more practical to study and select urease-producing bacteria that are optimal at typical soil temperatures, which vary depending on latitude, altitude, solar radiation, moisture content, conduction, soil type, depth, etc. (Doty and Turner, 2009).

1.3.3 Microbes

As alluded to in Section 1.3.2.1, much research in recent years has been aimed at determining which microbes can be used to induce MICP. The following is a more in-depth discussion of some of these microbes.

1.3.3.1 Microbe Types

Microbes used for MICP are divided into two categories: ureolytic (i.e., urea consuming) and non-ureolytic (i.e., non-urea consuming). In particular, *S. pasteurii*, a soil organism (mentioned in Section 1.3.4.1), is widely used due to its ability to produce carbon dioxide (CO_2) by respiration and decomposition of urea (Bachmeier et al., 2002; Cuthbert et al., 2013; DeJong et al., 2006; Feng and Montoya, 2016; Maleki et al., 2016; Stocks-Fischer et al., 1999; Whiffin et al., 2007). Common Gramm-positive ureolytic bacteria come from genera *Bacillus*, *Sporosarcina*, *Sporololoactobacillus*, *Clostridium*, and *Desulfotomaculum* (Kucharski et al., 2008). The genus Bacillus has been of particular interest in research due to its proven ability in MICP applications (Wong, 2015). Aerobic bacteria are preferable because they release CO_2 via cell respiration, which aids calcite production by increasing pH as a result of ammonium and hydroxide ion production (Soon, 2013). *S. pasteurii* is especially favorable because it does not aggregate, thus ensuring a high cell surface-to-volume ratio (DeJong et al., 2006).

Some researchers used methods of bacteria isolation from soil samples to isolate and identify new MICP candidate bacteria. In one such study, researchers isolated calcium carbonate precipitating strains from Beidaihe marine sediment (119°31’18.89” N and 39°50’11.90” E) (Wei et al., 2015). Strains were tested for solubilization capability (summarized in Appendix A) and quantified by

the diameter of the clear halo around the colony. Results showed that *B. diminuta* CP16, *S. Soli* CP23 and *B. Lentus* CP28 induced similar morphologies of crystals capable of MICP through ureolysis. Researchers also concluded that the production of carbonate polymorph was not specifically related to any bacterial species, but rather controlled by complicated environmental factors (Wei et al., 2015).

In another example, investigators collected surface scrapings and soil samples in Iran. The most promising isolate from their study was *B. licheniformis* AK01 which produced 1.33 g of calcium carbonate per liter in 7 days (18% more than the common *S. pasteurii*) (Vahabi et al., 2015). In another study *P. azotoformans* was isolated from an initial pool of 38 bacteria from soil and concrete (Nonakaran et al., 2015). The strain had the highest rate of urea hydrolysis, highest calcite precipitation, and was the most adhesive and insoluble. The investigators suggested that more research was needed to study the strain's potential for concrete crack repair.

Pseudomonas Stutzeri's ability to drive calcite production was investigated and shown to occur during NO_3^- reduction (Singh et al., 2015). Other microbes studied include *Escherichia Coli* HB101 (Bachmeier et al., 2002) and *Proteus Vulgaris* (Nemati et al., 2005). Bachmeier et al. (2002) found that low concentrations (5–100 μM) of nickel, the cofactor of urease, to the medium further enhanced calcite precipitation by *E. Coli* containing the plasmid pBU11, while calcite precipitation was inhibited by acetohydroxamic acid (AHA).

Other recently investigated bacteria and their bioengineering field of application include *B. Sphaericus* for repairing or improving the durability of concrete (De Muynck et al., 2008; Van Tittelboom et al., 2010); and *B. megaterium* for improvement of concrete strength and durability (Achal et al., 2011a; Siddique et al., 2008).

1.3.3.2 Geometric Compatibility

Soil microbes are transported through soil by way of pore openings between soil particles generally via passive diffusion. The pore opening is estimated as 20% of the soil particle diameter corresponding to the 10% passing particle size (Holtz and Kovacs, 1981). Hence, small pore size, relative to the size of the microbe used, can limit free passage (Soon, 2013). Maier et al. (2009) found that bacteria that are generally in the size range of 0.3 to 2 μm can move freely through sandy soil with particle sizes ranging from 0.05 to 2 mm. Intuitively, silts and clays tend to have a greater inhibitory effect on bacteria movement, and thus may limit homogenous distribution of bacteria in the soil. Rebata-Landa (2007) found that the optimum range of soil particle sizes for MICP reactions ranged between 50 to 400 μm. Figure 1-4 shows the generalized relation between microbe size and their effectiveness for treating soils of different grain sizes. The effects of organic matter on these size relationships are currently unknown.

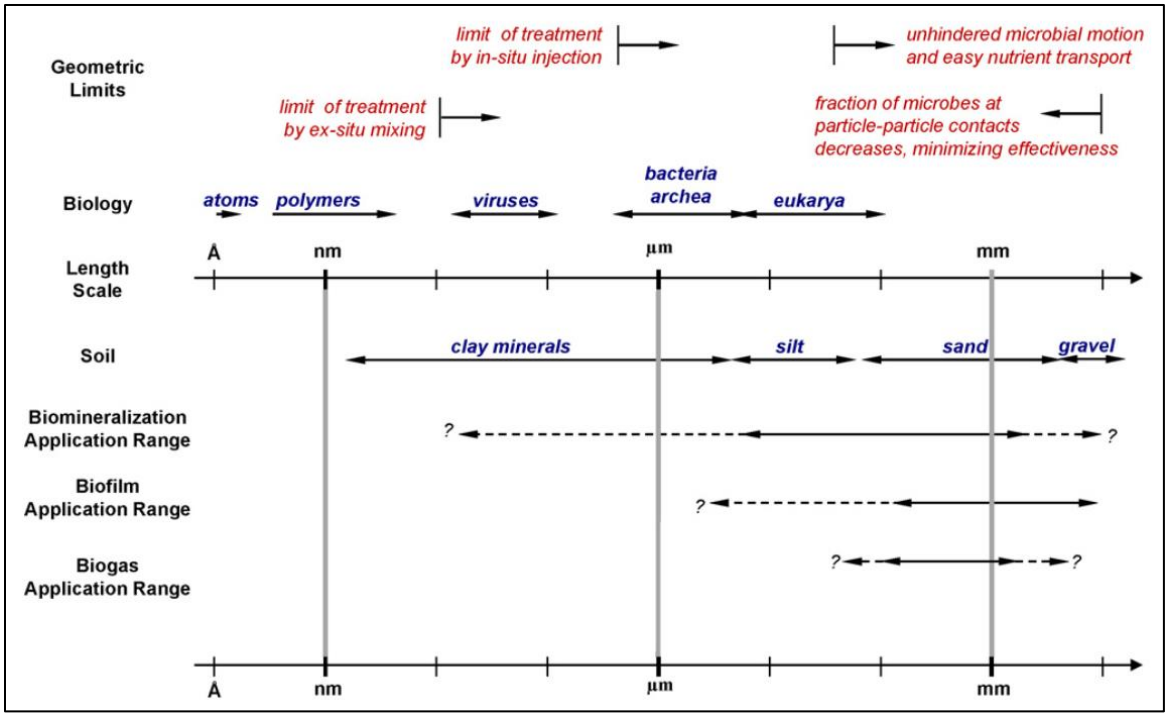

Figure 1-4. Comparison of typical sizes of soil particles and bacteria, geometric limitations, and approximate limits of various treatment methods (from DeJong et al., 2010)

1.3.4 MICP as a Geotechnical Improvement Technique

As mentioned above, MICP may be used for a number of ground improvement applications. In general, the goal with MICP treatment is to increase a geomaterial's strength via biocementation or decrease the geomaterial's hydraulic conductivity via bioclogging.

1.3.4.1 Biocementation as a Process

Soil strength improvement via MICP is attained by the calcite filling of interparticle pore spaces thereby decreasing the void volume. The distribution of calcite within the void space can range from "uniform" (the calcite coats the entire surface of a given particle evenly, which results in minimal shear strengthening) to "preferential" (the calcite only precipitates at the particle-to-particle contacts, which results in the maximum shear strengthening) to "actual" (precipitation activity falls somewhere in between "uniform" and "preferential", resulting in moderate soil property improvements) (Soon, 2013). These three cases are shown in Figure 1-5. The spatial distribution of precipitate is affected by biological behavior and filtering processes. Table 1-3 below, adapted from Ivanov and Chu (2008), lists other possible microbial processes that lead to biocementation.

Table 1-2. Biocementation from microbial processes

Physiological group of microorganisms	Mechanism of Biocementation	Essential conditions for Biocementation	Potential geotechnical applications
Sulfate-reducing bacteria	Production of undissolved sulfides of metals	Anaerobic conditions; presence of sulfate and carbon source in soil	Enhance stability for slopes and dams
Ammonifying bacteria	Formation of undissolved carbonates of metals in soil due to increase of pH and release of CO2	Presence of urea and dissolved metal salt	Mitigate liquefaction potential of sand. Enhance stability for retaining walls, embankments, and dams. Increase bearing capacity of foundations.
Iron-reducing bacteria	Production of ferrous solution and precipitation of undissolved ferrous and ferric salts and hydroxides in soil	Anaerobic conditions changed for aerobic conditions; presence of ferric minerals	Densify soil on reclaimed land sites and prevent soil avalanching. Reduce liquefaction potential of soil

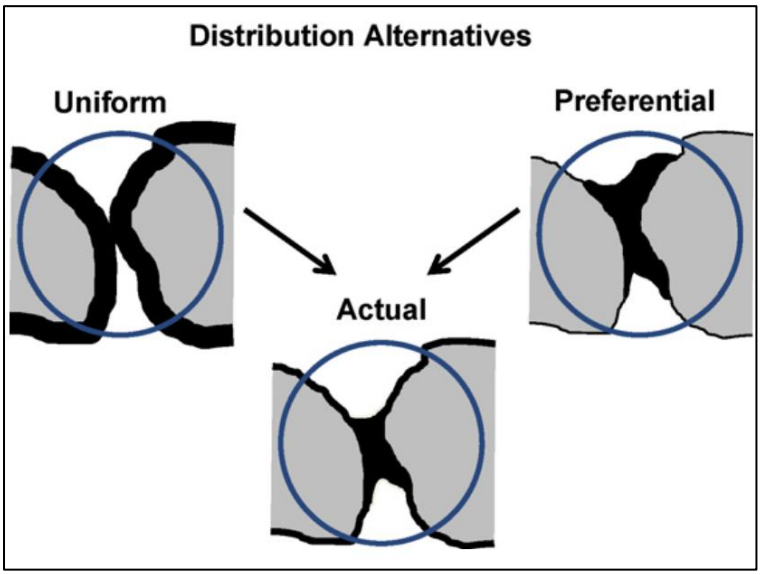

Figure 1-5. Calcite distribution alternatives (from DeJong et al., 2010)

1.3.4.2 Strength Improvements from Biocementation

The MICP biocementation process has been shown to be successful in a variety of sands; silica, calcite, iron, and beach sands. Often, an increase in shear wave velocity over time is used to demonstrate these improvements (DeJong et al., 2009; Mortensen et al., 2011). Numerous examples are available in the literature that illustrate these strength improvements. For example, DeJong et al. (2006) showed significant strength improvement for MICP-treated specimens via triaxial testing. Whiffin et al. (2007) studied a five-meter long sand tube. They showed that strength was increased between 1.8 and 3.4 times and that a minimum of 3.5% or 60 kg/m^3 of calcite was needed to improve compressive strength. Another study on MICP's effect on compressive strength concluded an improvement of 140% compared to untreated samples (Lu et al., 2010). Other studies where strength improvements were observed include Montoya et al. (2012), and Mortensen and DeJong (2011).

1.3.4.3 Bio-Clogging as a Process

Bioclogging is achieved through the same or similar processes as biocementation. It is the process by which soil voids are filled by the product of MICP, which restricts the water flow through the soil (Soon, 2013). Vandevivere and Baveye (1992) and Abdel Aal et al. (2010) found that hydraulic conductivity is significantly reduced by the accumulation of biomass and production of exopolymeric substances. However, these effects are not typically permanent. These results are attained similarly to the processes described in the biocementation section. Table 1-4 below, adapted from Ivanov and Chu (2008), describes possible non-MICP processes of bioclogging.

Table 1-3. Bioclogging processes

Physiological group of microorganisms	**Mechanism of bioclogging**	**Essential conditions for bioclogging**	**Potential geotechnical applications**
Algae and cyanobacteria	Formation of impermeable layer of biomass	Light penetration and presence of nutrients	Reduce of water infiltration into slopes and control seepage
Aerobic and facultative anaerobic heterotrophic slime-producing bacteria	Production of slime in soil	Presence of oxygen and medium with ratio of C:N > 20	Avoid cover for soil erosion control and slope
Oligotrophic microaerophilic bacteria	Production of slime in soil	Low concentration oxygen and medium with low concentration of carbon source	Reduce drain channel erosion and control seepage
Nitrifying bacteria	Production of slime in soil	Presence of ammonium and oxygen in soil	Reduce drain channel
Sulfate-reducing bacteria	Production of undissolved sulfides of metals	Anaerobic conditions; presence of sulfate and carbon source in soil	Form grout curtains to reduce the migration of heavy metals and organic pollutants
Ammonifying bacteria	Formation of undissolved carbonates of metals in soil	Presence of urea and dissolved metal salt	Prevent piping of earth dams and dikes

1.3.4.4 Hydraulic Conductivity Reduction from Geomicrobial Bioclogging

To study hydraulic conductivity reduction in sands, Nemati and Voordouw (2003) used a mix of coarse sand and glass beads as their study media. The urease enzyme was applied directly into the soil instead of using urease producing microorganisms. Upon treating the specimens multiple times, the investigators found that two injections produced hydraulic conductivity decreases of 92% and 72% sequentially. This resulted in a total reduction of 98% compared to untreated samples. Subsequent injections failed to produce measurable results, indicating that there is a limit in effectiveness of multiple injections.

Nemati et al. (2005) conducted a similar study using *Proteus Vulgaris* (urease-producing microorganism) to produce in situ calcite using urease enzyme. The reduction in hydraulic conductivities for specimens treated with biomass only, combination of biomass and reagent, and combination of urease enzyme (direct supply) and reagent were 52%, 65%, and 62%, respectfully. Researchers concluded bacterial and enzymatic treatments yielded similar results for pore plugging. However, the nondurable biomass plugging agent resulting from the biomass reagent combination did not produce a reliable long-term reduction in hydraulic conductivity.

1.3.4.5 Rock Repair

Stocks-Fisher et al. (1999) found MICP using *S. pasteurii* was optimally effective at remediating fissures in granite at an average width of 2.7 mm with a silica (10%) and sand (90%) mixture. Cuthbert et al. (2013) tested the upscaling potential of this application by applying MICP to reduce fractured rock hydraulic conductivity. Using borehole injections, researchers were able to precipitate approximately 750 grams of calcite over a large surface fissure (approximately 4 square meters) with 17 hours of treatment.

1.3.4.6 MICP in Organic Soils

Inagaki et al. (2011) compared different sands with peat samples by compacting 10 g of peat to 40 mL in 50-mL graduated cylinders and saturating these specimens with 25 mL of distilled water. The peat produced the greatest precipitation efficiency and did not vary with different injection frequencies. In addition, Canakci et al. (2015) showed some success in cementing organic-rich specimens using MICP. However, beyond these studies, MICP application in organics has been limited.

1.3.5 MICP Laboratory Testing

A number of laboratory-based MICP studies have been conducted in recent years. The following is a summary of the results of several of these studies that focuses on different sample preparation techniques, treatment options, monitoring techniques, and post-treatment testing.

1.3.5.1 Preparation/Incubation Techniques

While the chemical reactions that govern microbial calcite production are similar from study-to-study, researchers have attempted to optimize these reactions via varying sample preparation procedures. For example, Stocks-Fischer et al. (1999) mixed bacterial solutions with sand in 60 mL plastic syringe columns. Inagaki et al. (2011) used the same sample setup for testing the effects of varied initial microbe solution volumes and injection intervals. DeJong et al. (2006) treated their specimens in triaxial cells with 72 mm diameters and aspect ratios of 2:1 and 1:1. Mortensen et al. (2011) constructed 50 mm rigid cells with 1:1 and 2:1 aspect ratios equipped with bender elements for measuring shear wave velocity. Soil was poured in loosely and loaded with a confining stress of 100 KPa. Whiffin et al. (2007) scaled up the procedure by treating gravel specimens in five-meter long, 66 mm internal diameter PVC tubes. During these tests, downward (as opposed to upward) flow was used. Scouring pad filters were used as end caps during the procedure.

Salifu et al. (2016) studied MICP's effectiveness in treating slopes in a tidal environment by comparing untreated and treated sandy slopes using a cubic Perspex container (0.2 m sides). Water was pumped in and out of the box to simulate the tides (30 cycles) and slopes were tested at angles ranging from 35 to 53 degrees. Results showed significant stability improvements for treated specimens. Maleki et al. (2016) tested MICP treated soils against wind erosion by placing surface-treated specimens in wind tunnels. Again, results showed significant improvement for treated specimens.

Feng and Montoya (2016) studied the effects of confining pressures and sample treatment repetition. Like DeJong et al. (2006), specimens were treated in triaxial cells. Confining pressures of 100, 200, and 400 kPa were used during treatment. Treatment was repeated 10 times, 20 times, and 40 times, and calcite precipitation was monitored after each round. Results showed that precipitation significantly decreased after 6-8 repetitions.

Most MICP testing has been conducted using saturated samples, but recent studies have tested MICP in unsaturated conditions. This is an ongoing area of research.

1.3.5.2 MICP Treatment Techniques

Geomicrobial calcite precipitation is also affected by injection conditions. The injection method must be chosen in accordance with the soil conditions (Inagaki et al., 2011). Several researchers have studied various treatment techniques in order to quantify these effects.

Stocks-Fischer et al. (1999) prepared stock cultures by combining a 1:2 ratio of ammonium sulfate and yeast extract in a Tris-HCl buffer with a pH of 9.0. Individual ingredients were autoclaved separately and mixed afterward to avoid precipitation. The microbes were grown in an aerobic environment, typically in a shaker, then harvested with a centrifuge, and used to treat sand columns (Stocks-Fischer et al., 1999). This early study confirmed the validity of MICP and found a suitable pH range of 8-9.

DeJong et al. (2006) applied the bacterial solution to triaxial sand specimens at 20 mL/min for 20 minutes using a peristaltic pump. Specimens were allowed to set for 4 hours after treatment. Cementation solutions and filtered air were then pumped through samples at 4 mL/min until the desired cementation was reached (35% relative density). The urea solution was stirred prior to pumping until a pH of 7.5 was achieved in an effort to enhance alkalophilic bacterial activity. Specimen pH was maintained at 8.2 or greater.

During the Inagaki et al. (2011) study, researchers varied the amount of culture solution (5, 10, 20, 40, and 80 mL) and the number of nutrient injections per day (2, 4, and 8 times per day). Results showed that regardless of the amount of injected culture solution, the amount of calcium carbonate precipitate was proportional to the injection period. In addition, precipitation efficiency was higher for injection periods of two and four days than for one day. Finally, both quantity of calcium carbonate precipitate and calcium carbonate production efficiency were proportional to culture solution quantity.

In another study, researchers tested *S. pasteurii*'s MICP production alone and with a competing non-ureolytic bacteria, *B. subtilis* (Gat et al., 2011). The treatment with non-ureolytic bacteria

exhibited significantly higher growth rates than that with ureolytic bacteria alone. Although the chemical conditions deteriorated, the increase in nucleation sites ultimately accelerated calcite precipitation.

The effect of salinity on geomicrobial calcite development has also been studied. A high salinity solution encourages flocculation, and this promotes the adsorption of bacteria and retention in sand columns (Ritvo et al., 2003; Torkzaban et al., 2008). A low salinity solution or fresh water with a low ionic strength allows the bacteria to be transported over large distances and therefore inhibits precipitation (Harkes et al., 2010). Mortensen et al. (2011) tested bacterial growth at 0, 25, 50, 75 and 100 % saltwater concentrations and different freshwater formulations. Bacteria growth rate appeared to be independent of salinity levels. However, higher salinity concentrations showed an increase in calcite precipitation. This was explained by DeJong et al. (2010); higher salinity provides more cations to precipitate with microbially-generated carbonate.

1.3.5.3 MICP Monitoring Techniques

Monitoring refers to any data collected during the MICP treatment process, which includes geophysical, chemical, and biological measurements. Chemical and biological processes of MICP, which ultimately control the desired geophysical changes, are intimately linked (DeJong et al., 2010). While several typical monitoring techniques have been alluded to above, the following is a more in-depth discussion of these techniques.

Geophysical Monitoring

To date, the three primary methods of geophysical measurements used to monitor MICP are S-wave (shear wave velocity), P-wave (compression wave velocity), and resistivity mapping. Both S- and P-wave velocities can be easily measured in the laboratory with piezoelectric ceramic transducers, bender elements, or accelerometers. Ultrasonic devices can be used to measure compression wave velocities (DeJong et al., 2010).

Monitoring MICP by measuring S-waves is advantageous over P-wave measurements as shear waves do not propagate through fluids and there is a direct relationship between S-wave and the mass of precipitated calcium carbonate, void ratio, coordination number, and confining stress (DeJong et al., 2006). Because of the carbonate-dependency and the relative simple application of the bender element or accelerometers, this technique is an excellent monitoring tool during laboratory incubations. Using bender elements in MICP lab tests, DeJong et al. (2006) was able to show how treatment frequency, duration, and concentration affected the evolution of cementation of specimens.

More recently, researchers evaluated the shear strength and stiffness of sand subjected to drained and undrained shearing via triaxial tests of samples of varying degrees of cementation (Montoya and DeJong, 2015). Shear wave velocity was used to monitor the change in small strain stiffness during shearing. This confirmed previous results in that shear strength and stiffness were directly correlated with cementation. Testing indicated that the critical state stress ratio was not significantly affected by cementation, the peak shear strength increased with increased cementation levels, and as the cementation increased the stress-strain behavior transitioned from

strain hardening to strain softening. Also, the loading regime influenced the rate of stiffness reduction due to cementation degradation and softening (Montoya and DeJong, 2015).

Resistivity, in an electrical sense, measures the voltage potential gradient through a soil matrix and is dependent on the volume fractions comprised of particles versus voids, mineral composition, and the chemical composition of pore fluid (DeJong et al., 2010). These measurements are used to detect soil density variation and changes in pore fluid composition. These measurements can be used to monitor the hydrolysis of urea via the increase in ionic potential of the pore fluid (Mortensen et al., 2011). Li et al. (2005) used two- and three-dimensional arrays to track displacements and deformations within soils. Additionally, Whiffin et al. (2007) monitored urease activity by conductivity (used in the absence of calcium ions) and ammonium production rate (Nessler method). Calcium concentration was determined via UV absorption (LCK 327 – Hach Lange, Germany). Mortensen et al. (2011) followed a similar procedure. Researchers have also used water pressure transducers and fluid sampling ports to monitor hydraulic conductivity and regulate fluid in- and out-flow pumps (Whiffin et al., 2007).

Biological and Chemical

MICP's biological processes can be detected via measurements of microbial concentration, activity state, activity potential, biomass, and nutrient concentration (DeJong et al., 2010). The chemical processes are primarily captured via monitoring of pH, chemical concentrations, and conductivity. The invasive nature of the testing of these properties however make it almost impossible to gather real-time data on these variables except in the effluent of flow-through experiments. However, understanding them is very important to understanding biomediated processes (DeJong et al., 2010). Biological and chemical tests are thus usually conducted post-treatment.

An exception to the usual bio-chemical post treatment testing was the Salifu et al. (2016) study where samples were collected from the foot of the treated soil slopes using a 20-mL syringe at certain time intervals during treatment. The samples were frozen and tested for ammonium and calcium concentrations using colorimetric KONE analyzer and Inductively Coupled Plasma Optical Emission Spectrometry (ICP-OES).

1.3.5.4 MICP Treatment Post-Testing Techniques

A number of destructive and non-destructive tests have been performed on MICP specimens after treatment. Early research measured reductions in porosity and hydraulic conductivity (Kantzas et al., 1992). Whiffin et al. (2007) quantified the porosity and hydraulic conductivity of treated specimens using wet/dry density tests and constant head tests, respectively.

Before MICP was studied in soils, researchers used porous polyurethane foam as a testing medium (Bachmeier et al., 2002). A micro-penetrometer has been used to test the penetration resistance of treated and untreated samples (Maleki et al., 2016). X-ray diffraction (XRD) quantitative analysis has been used to detect the formations of new minerals (Stocks-Fischer et al., 1999). Similar testing was conducted by others to characterize precipitate (Nonakaran et al., 2015; Vahabi et al., 2015). Optical density measures have also been taken to analyze bacterial cell density, usually at a wavelength of 600 nm (Gat et al., 2011; Rong and Qian, 2014).

X-ray compositional mapping for the purpose of assessing surface modifications has been used in the past (DeJong et al., 2006; Maleki et al., 2016). Additionally, x-ray tomography has been used to follow the three dimensional deformation processes during triaxial compression tests (Tagliaferri et al., 2011).

Fourier-transform-infrared (FTIR) was used by Vahabi et al. (2015) to analyze precipitate from different isolates. Rong and Qian (2015) analyzed the bonding structure using transmission electron microscope, infrared spectra, x-ray photoelectron spectroscopy, and nuclear magnetic resonance.

Shear strength and triaxial testing after treatment are commonly used to quantify cementation effects. For example, Whiffin et al. (2007) used single-stage, confined, drained triaxial tests at a confining pressure of 50 kPa to determine compressive strength (q) and stiffness (E_{50}). Ng et al. (2012) used unconfined compression tests on 50-mm diameter saturated specimens. DeJong et al. (2006) conducted a number of direct shear tests on several specimens. Similarly, Feng and Montoya (2016) divided their triaxially-prepared specimens into six sub-specimens (similar to the proposed procedure for this project) and conducted a number of direct shear tests to show vertical variability during column treatment.

Scanning electron microscopy (SEM) has often been used to understand and visualize calcite precipitation on a micro-scale. Treated specimens were prepared by epoxy impregnation of polished surfaces. Images showed the soil particles, reduced pore space, and precipitated calcite phases (DeJong et al., 2010). Many researchers have used and continue to use this method for MICP understanding and validation (Bachmeier et al., 2002; DeJong et al., 2006; Maleki et al., 2016; Ng et al., 2012; Stocks-Fischer et al., 1999). Stocks-Fischer (1999) carbon-coated fractured samples and viewed them at using SEM imaging and back-scattering electron imaging at accelerating voltages from 30 to 35 kV.

SEM has shown that during destructive (i.e., compression, triaxial, and direct shear) testing, treated specimens fail because the precipitate fails. In other words, a layer of calcite is usually left on specimens' failure planes (DeJong et al., 2010). Using concrete-sealant as an analogy, this is similar to a cohesive (as opposed to an adhesive) failure mechanism.

Salifu et al. (2016) measured the mass of calcite precipitation by oven-drying samples, then weighing them before and after being washed with a 10% HCl solution. This method is widely used for understanding coverage (Feng and Montoya, 2016; Whiffin et al., 2007). Another common method for quantifying the amount of solid formations is by direct measurement of Ca^{2+} ions (Bachmeier et al., 2002; Stocks-Fischer et al., 1999). During the Montoya et al. (2013) study, researchers followed ASTM D4373, *Standard Test method for Rapid Determination of Carbonate Content in Soils* to quantify cementation.

1.3.6 MICP Field Studies

In the past five years, much MICP research has moved from the laboratory to the field. As should be expected, the major issue associated with scaling up the technology is coverage. Variables associated with this include cost, scale, required treatment resolution, and application method.

1.3.6.1 Bio-Augmentation versus Bio-Stimulation

On average, more than 10^9 microbial cells per gram of soil exist in the top meter of soil. At a depth of 30 m, geomicrobe concentration drops to approximately 10^6 cells per gram of soil. (DeJong et al., 2010). Based upon these concentrations, it would appear that coverage to 30 m may be possible via bio-stimulation with the proper field technique. In cases where appropriate calcite-producing microbes are unavailable, it may be possible to augment via injection (DeJong et al., 2009).

1.3.6.2 Medium-Scale Testing

In the late 2000s and early 2010s, several medium-scale studies were conducted to assess the feasibility of upscaling MICP. For example, Martinez and DeJong (2009) conducted a model shallow foundation load test on soil improved by MICP, which yielded a five-fold settlement reduction. However, differential settlement was observed and attributed to variability in cementation.

Weil et al. (2012) proposed the use of incrementally spaced boreholes to conduct cross-hole monitoring of shear wave velocity, compression wave velocity, and electrical resistivity during treatment. These three measures can be grouped at different depth intervals which would have the potential to provide three-dimensional understanding of the MICP process during large scale field application.

During the Whiffin et al. (2007) five-meter sand column experiment with top-down treatment, some calcite precipitation was observed near the bottom of the specimen which would appear to indicate that augmentation is at least somewhat effective at depth.

1.3.6.3 Larger-Scale Testing

In recent years, researchers have begun larger-scale testing with MICP. Cuthbert et al. (2013) drilled four 100 mm diameter borehole wells to a depth of approximately 27 meters. Initial hydraulic conductivity of the rock was measured at each of these locations. During treatment, a bio-augmented solution was injected, and some boreholes were monitored to quantify coverage immediately thereafter. Twelve weeks later, these boreholes were examined via hydraulic conductivity tests to determine if the calcite reactions continued after being induced. Results showed a decrease in hydraulic conductivity.

DeJong et al. (2013) identified two more field applications. The first was a bio-augmented study where the contractor Visser & Smit Hanab applied MICP treatment to gravel to enable horizontal directional drilling for a gas pipeline in the Netherlands in 2010 by treating a 100 m^3 volume between depths of 3 and 20 meters. Using bacterial (200 m^3) and cementation (two injections between 300 and 600 m^3) treatments, this study was deemed successful as they were able to drill without instability issues in the loose gravel deposit. The second was a bio-stimulation study where the co-precipitation of heavy metals (strontium-90) with calcium carbonate (to immobilize the heavy metals) was initiated at the Vadose Zone Research Park (VZRP) at the Idaho National Laboratory (INL). This study is ongoing at the US Department of Energy site in Rifle, Colorado (Fujita et al., 2010). By injecting dissolved molasses and urea, researchers are noting slow but quantifiable calcite precipitation (DeJong et al., 2013).

1.3.6.4 Potential Issues

While the MICP technique is showing promise, issues associated with its field applicability have been identified. Some of these issues include limited injection depth (on the order of centimeters) due to relatively low hydraulic conductivity and clogging of the injection systems (Whiffin et al., 2007).

Another concern with up-scaling to the field is the environmental conditions of the soil. However, previous research indicates that these issues may be less critical. Mortensen et al. (2011) conducted a comprehensive study of environmental factors. Results show that ureolytic bacteria are able to grow in a wide range of groundwater environments (different types of freshwater and levels of salinity); are not affected by high ammonium concentrations; are able to survive in anoxic conditions; treatment uniformity is increased as injection rate decreases; reducing nutrient concentration reduces affluent ammonium concentrations while maintaining uniform treatment; precipitation rate increases with increased salinity; and that MICP is possible in a wide range of soil mineralogies and particle sizes.

1.3.6.5 Coverage Uniformity

Coverage uniformity is an ongoing topic of research. Obviously, soil is a heterogenic, anisotropic material. Intuitively, then, calcite concentration decreases as the distance from the injection point increases (Whiffin et al., 2007). Near the injection point (i.e.,, spatial distances between 0.1 and 1.2 meters), calcite content ranges between 85-105 kg/m^3. As distance from the injection point increases to 2.5-5 m, calcite content decreases to 2-30 kg/m^3. However, as research continues, progress is being made to improve coverage. DeJong et al. (2010) suggested that a push-pull injection process, gridded injection/extraction, and chemical optimization of treatment media may all increase coverage area. More recently, the treatment procedures used by Feng and Montoya (2016) and DeJong et al. (2006), show positive coverage during laboratory scale tests. It is believed that these techniques will translate well to the field.

Directional-dependent hydraulic conductivity effect on coverage has been discussed in the literature to some extent. Some (for example, DeJong et al., 2009) have argued that higher hydraulic conductivity horizontal flow paths may lead to a decrease in uniformity during treatment. However, others (for example, Martinez, 2012) have argued that geomicrobial calcite production is self-equilibrating in that preferential paths become increasing “less preferential” during treatment because of the calcite precipitation. Determining the dominant case is an ongoing area of research.

1.3.6.6 Coverage Permanence

MICP treatment in engineering applications must have permanence over a realistic design life to be useful. Therefore, treatment areas where calcite is already stable are most favorable because most of the calcite remains post-treatment (once normal geochemical conditions return) (DeJong et al., 2009). Some research indicates that geomicrobially-treated soil’s strengthening properties can be effective for up to 50 years (DeJong et al., 2009). As this aspect of MICP remains understudied to date, economic and risk assessments are required to understand the groundwater-

precipitate interaction, performance monitoring requirements, and the ability/intervals for retreatment (DeJong et al., 2013).

1.3.6.7 Methods of Injection

Usually, bio-augmented MICP solution is injected using similar methods that would be used for injection of any geo-strengthening material (Soon, 2013). A two-phase injection procedure where *S. pasteurii* suspensions were injected followed by a high salt content fixation fluid successfully retained 100% of urease activity in a sand column (Harkes et al., 2010). A recent field study injected this solution into 27 meter deep boreholes (Cuthbert et al., 2013).

Stopped-flow injection (injection of 1.5 pore volume of reagent, followed by 2.5 hours of rest period) offered better uniform concentration than continuous injection (Martinez et al., 2011). This technique yielded abundant calcite precipitation near the injection point, but calcification decreased with the distance from the injection point. A numerical model by (Barkouki et al., 2011) obtained similar findings. Stopped-flow injection has been shown to distribute cementation fluid evenly in a sample before the composition of calcite (Soon, 2013).

Repeated injection of reagent to the soil increases the composition of calcite. Effectively, this is very similar to stopped-flow injection. Studies on repeated injection for carbonate precipitation in limestone and loss of hydraulic conductivity found that for second and third treatments there was weight gains of 36% and 33%, respectively (De Muynck et al., 2010b). Hydraulic conductively reduced 65%, 12%, and insignificantly for the first, second, and third treatments (Nemati et al., 2005). The introduction of urease enzyme directly into the sand produced a greater reduction in hydraulic conductivity for the second and third treatments.

Inagaki et al. (2011) concluded that precipitation is optimized when the bacterial solution volume is equal to the void volume of the soil as it is able to replace any other fluid or gases. Rather intuitively, higher injection rates (on the order of 10 mL/min) produce higher cementation rates, but less uniformity (Mortensen et al., 2011).

The injection methods previously discussed refer to injections into saturated samples. When dealing with larger-scale field applications, these pretreatment conditions can be difficult to attain. An alternative method of surface percolation in unsaturated specimens has been studied (Cheng and Cord-Ruwisch, 2012). The procedure used was: (1) percolate 50% of the water retention capacity of the sample of bacterial solution, (2) percolate an equal amount of cementation solution, (3) incubate for 12 hours at 25^{o}C, and (4) repeat. The results indicated that bacteria can be immobilized over 1 m column height by alternating layers of solutions. This technique appears to reach a reasonable amount of homogeneity with crust formation. The percolation test produced about 3 times higher local strength per mass of calcite compared to the saturated method (Cheng and Cord-Ruwisch, 2012).

1.4 Summary

This discussion shows that MICP has been gaining traction as a soil improvement technique in recent years. Research thus far has focused on identification of controlling variables. However, with the exception of the Inagaki et al. (2011) study, its application to organic matter-rich materials

has been limited. In principle, the methods that have been developed to treat cohesionless sediments should be applicable to high-OM soils with sufficient hydraulic conductivities.

CHAPTER 2
TREATMENT OF OTTAWA SANDS USING AN INJECTION METHOD

2.1 Introduction

Beyond a literature review, the first task associated with this research was to recreate the DeJong et al. (2010) treatment procedures, utilize these procedures to treat Ottawa sand, and subject the treated specimens to direct shear and consolidation testing to determine engineering property improvement.

2.2 Materials and Methods

2.2.1 Initial Soil

50-70 Ottawa sand was used throughout most of this task (Figure 2-1; Figure 2-2; Table 2-1).

Figure 2-1. Ottawa 50-70 silica sand

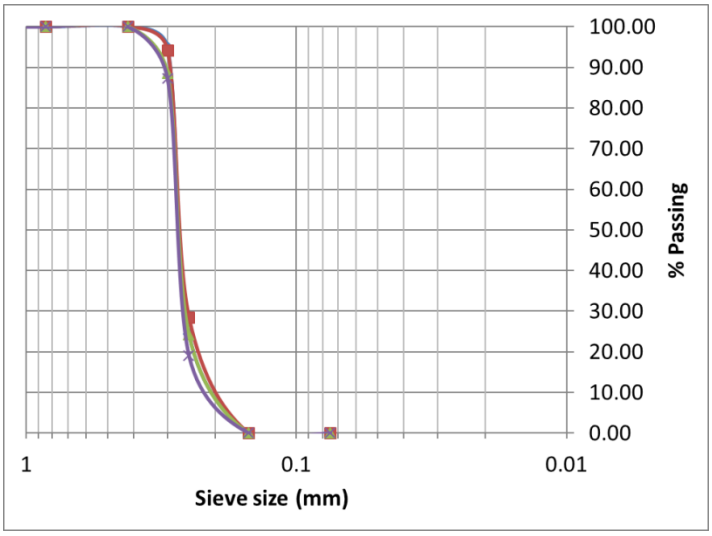

Figure 2-2. Ottawa 50-70 sieve analysis

Table 2-1. Ottawa 50-70 sand properties

Properties	Current Research	Simpson (2014)	Feng and Montoya (2016)	Lin et al. (2015)
Gs	2.64	2.65	2.65	2.65
D10(mm)	0.21	0.248	n/a	0.26
D30(mm)	0.25	0.259	n/a	0.31
D50(mm)	0.27	0.264	0.22	0.33
D60(mm)	0.28	0.266	n/a	0.37
Cu	1.37	1.07	1.4	1.43
Cc	1.07	1.02	0.9	1.01

2.2.2 Soil pH Adjustment

The initial, during treatment, and final pH of the pore fluid is known to play a role in MICP-treated soil calcification. Therefore, soils were adjusted to initial pH values of 5 and 7 prior to treatment to further understand these factors. Ottawa 50-70 sand has a natural pH of approximately 7 while the organic soil has a natural pH of approximately 5. Chemical adjustment was used to generate soils with an initial pH of 5. Adjustment consisted of adding 0.0075 to 0.0085 M HCl to the soil matrix. This molarity range was found using a trial-and-error process. Between each adjustment, it was important to ensure that equilibrium conditions had been achieved. Tests (Figure 2-3) showed that it took approximately 100 minutes to reach equilibrium after each HCl addition. Note that pH was determined following the standard procedures of ASTM D4972.

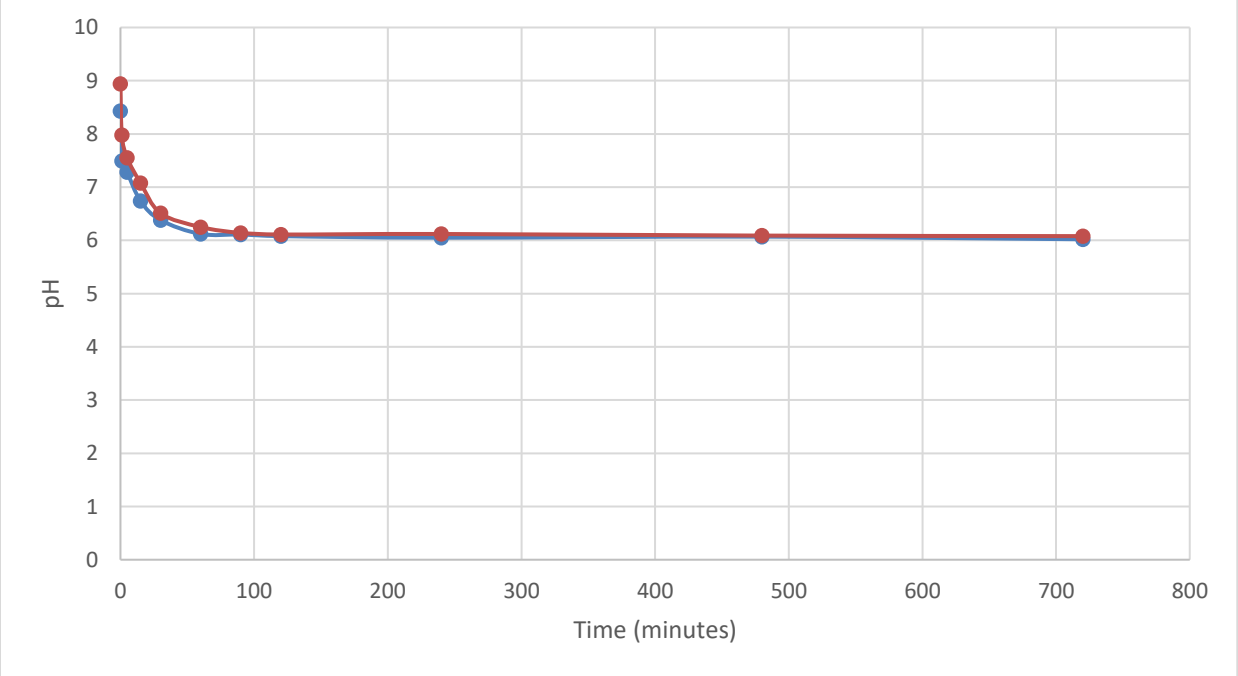

Figure 2-3. pH versus time for 50% organic content specimen

2.2.3 Sporosarcina Pasteurii

S. pasteurii has consistently proven to be the most successful bacterial species utilized for MICP. Therefore, it was used throughout this study. As discussed in Chapter 1, calcite from MICP is supposed to cement soil particles together. However, it is important to note, that calcification can occur without true cementation. Cementation only occurs when the precipitated calcite forms bonds between the soil particles. This is known to be dependent on the formation of a "biofilm" which allows the bacteria to evenly distribute around the soil matrix, hold themselves in place, and pass nutrients among themselves. The "biofilm" was further-explored as part of this study. As will be shown in Chapter 5, it is believed that the "biofilm" is a result of exopolysaccharide (EPS) formation.

2.2.4 Ottawa Sand Treatment Procedure

The traditional percolation treatment method involves percolating bacteria/feed stock through a chamber-enclosed soil at a specified rate. During this study, the treatment chambers (Figure 2-4), were designed to generate soil columns with diameters appropriate for triaxial, consolidation, and direct shear tests. The acrylic chamber was made of a split cylinder and square caps on either end with small, centered inlet/outlet holes. The split cylinders were held together with two metal worm gear hose clamps, and their end caps were held in place with threaded metal rods fastened with bolts. All seams were sealed with rubber gasket material. The dimensions of the treatment volumes were 2.8 inches in diameter and 7 inches in length. These cells were filled with soil that was air pluviated without compaction.

Figure 2-4. Traditional treatment chamber filled with Ottawa 50-70 sand

A 600-mL solution containing *S. pasteurii* was injected into the bottom of the soil columns via a peristaltic pump and allowed to freely flow out the columns' top outlet. The solution (Figure 2-5) sat for 12 hours to give the bacteria time to attach to the soil particles. The bacteria were then fed every 6 hours with a solution containing a mixture of urea and calcium chloride at a flow rate of 3 mL/minute using the peristaltic pump over a total period of 48 hours. The full treatment setup for multiple soil columns is shown in Figure 2-6. This treatment was conducted on twelve soil columns with an initial pH of 5 or 7.

Figure 2-5. *S, pasteurii* bacterial solution

Figure 2-6. Full percolation treatment setup

2.2.5 Direct Shear Testing

Both treated and untreated specimens were subjected to Direct Shear Testing (DST) in accordance with ASTM D3080 at a strain rate of 0.05 in/min. DST was performed on the DST apparatus shown in Figure 2-7 with soil specimens loaded into the shear boxes as shown in Figure 2-8. For lower normal stresses, the polyvinyl chloride (PVC) shear box-top was used. Horizontal deflections were measured using strain gauges while a load cell was used to measure shear force during testing. Data quality was judged by running multiple tests at the same vertical load (stress) and comparing consistent horizontal (shear) stresses.

Figure 2-7. DST apparatus

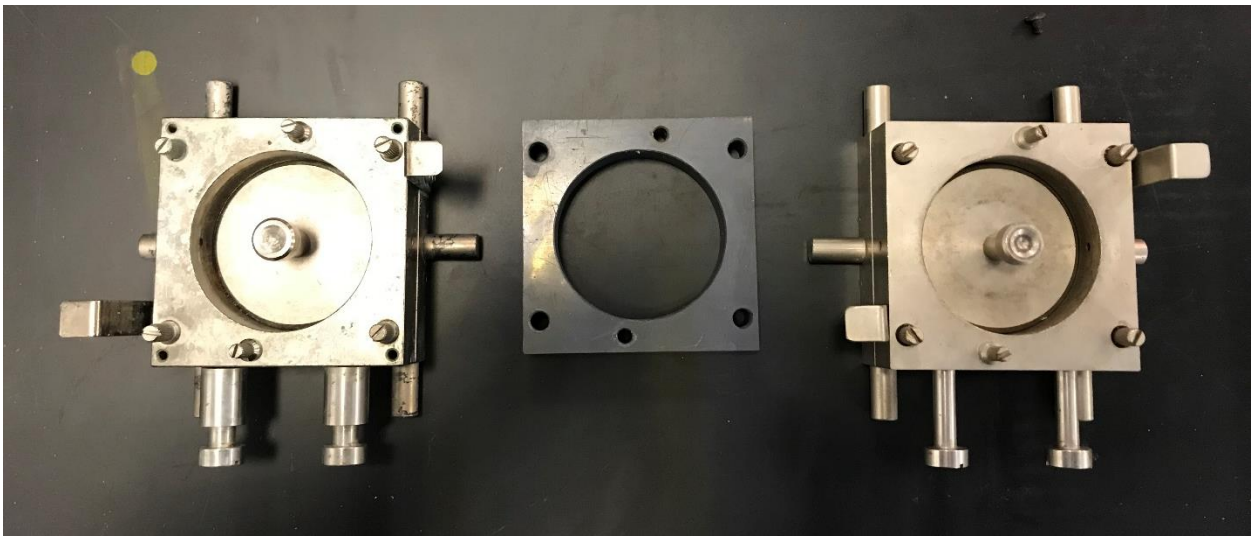

Figure 2-8. DST shear boxes (PVC box-top in center)

2.2.5.1 Control DST

A series of control tests was conducted on several untreated specimens so that these results could be compared with treated data. These tests were run in triplicate at the normal stresses of 1, 4, 7, and 14 psi. The soil was compacted in the DST box, shown in Figure 2-9, using three lifts. The specimens were then allowed to fully saturate under the maximum normal stress of 14 psi for 24 hours before testing began which served as the compaction process for consolidation. The sand initial total unit weight was approximately 107 pcf for all tests. For the organic soil, the initial total unit weights were 100 pcf, 78 pcf, and 57 pcf for organic contents of 10%, 30%, and 50%, respectively.

2.2.5.2 Treated DST

The MICP treated soil specimens were run at the same conditions as the control group, except the initial compaction was not necessary and the 4 psi normal stress was not used. Each treated soil column was sliced at one-inch intervals to create several test samples for the DST. These individual samples were trimmed and sanded to achieve uniform shape and heights between 0.9 and 0.98 inches. Some of these final samples were not perfectly uniform (Figure 2-9). Therefore, the loose sand which came off the samples during processing was used to fill any surface voids when placed in the DST box.

Figure 2-9. Treated percolation-treated sand samples prepared for DST

2.2.6 DST Data Analysis

Each DST provides horizontal displacement, vertical displacement, and horizontal load for a soil specimen at a given vertical (normal) loading. Shear stress was obtained by dividing the horizontal load by the shear box's area. The resulting shear stress was plotted as a function of horizontal displacement. These plots were used for data analysis.

2.2.7 Calcite Precipitation Distribution

2.2.7.1 Overview

The distribution of precipitated calcite along the height of a treated soil column using the percolation method is relatively well understood from previous research. This analysis is included in this research to further contribute to this body of data and to demonstrate that the percolation procedure used during this study produced specimens with similar post treatment properties as those reported in the literature.

2.2.7.2 Acid Wash Testing Procedure

Small pieces of treated soil samples were taken at certain intervals from the injection point from the fully cemented sand columns after treatment. These samples were then washed with HCl to dissolve the precipitated calcite. The percent mass of calcite at each increment was then calculated from the difference of mass in the soil before and after acid washing.

2.2.8 Consolidation Testing

2.2.8.1 Overview

Consolidation tests were performed using a fixed-ring oedometer (Figure 2-10) and followed procedures outlined in ASTM D2435. All consolidation tests were conducted at the FDOT State Materials Office (SMO) in Gainesville, FL. Initial tests used a load increment ratio (LIR) of one, and the loading schedule (in tons per square-foot or tsf) was 0.0625, 0.125, 0.25, 0.5, 1, 2, 4, 8, 16, 4, 1, 0.25, 0.0625, and 0. A few tests used a LIR of 0.5 to investigate yielding of cementation under increased vertical effective stress. In these cases, the loading schedule (in tsf) was 0.0625, 0.09375, 0.125, 0.1875, 0.25, 0.375, 0.5, 0.75, 1, 1.5, 2, 3, 4, 6, 8, 12, 16, 4, 1, 0.25, 0.0625, and 0. The loads were applied using calibrated masses, and the sample displacements were captured using a calibrated linear variable differential transformer (LVDT).

Figure 2-10. Fixed ring oedometer at SMO

2.2.8.2 Untreated Soil Preparation

The Ottawa sand and organic soil were placed in the oedometer rings at specific dry densities. The samples were saturated under the seating load followed by the application of the first load (1/16 tsf). For the sand, the LIR was 1 and each applied load was held for 24 hours because of sand's relatively high hydraulic conductivity. For the organic soil, LIRs of 0.5 and 1 were used with load durations of 72 hours.

2.2.8.3 Treated Soil Preparation

Treatment of the Ottawa sand and organic soil resulted in 2.8-inch diameter and 3- to 6-inch-long specimens that required careful trimming to fit into the ring (Figure 2-11). The number of samples obtained from each specimen ranged from one to three depending on the degree of calcification. Once fit into the ring (Figure 2-12) the sample was placed into the oedometer and the prescribed loading schedule was followed.

Figure 2-11. Careful trimming of calcified sand into oedometer ring

Figure 2-12. Calcified sand in ring after trimming

2.3 Results

2.3.1 DST Control Data

Figure 2-13 through Figure 2-15 display the shear stress versus horizontal displacement and the maximum shear stress versus normal stress obtained from the DST of untreated (i.e., control) Ottawa 50-70 sand.

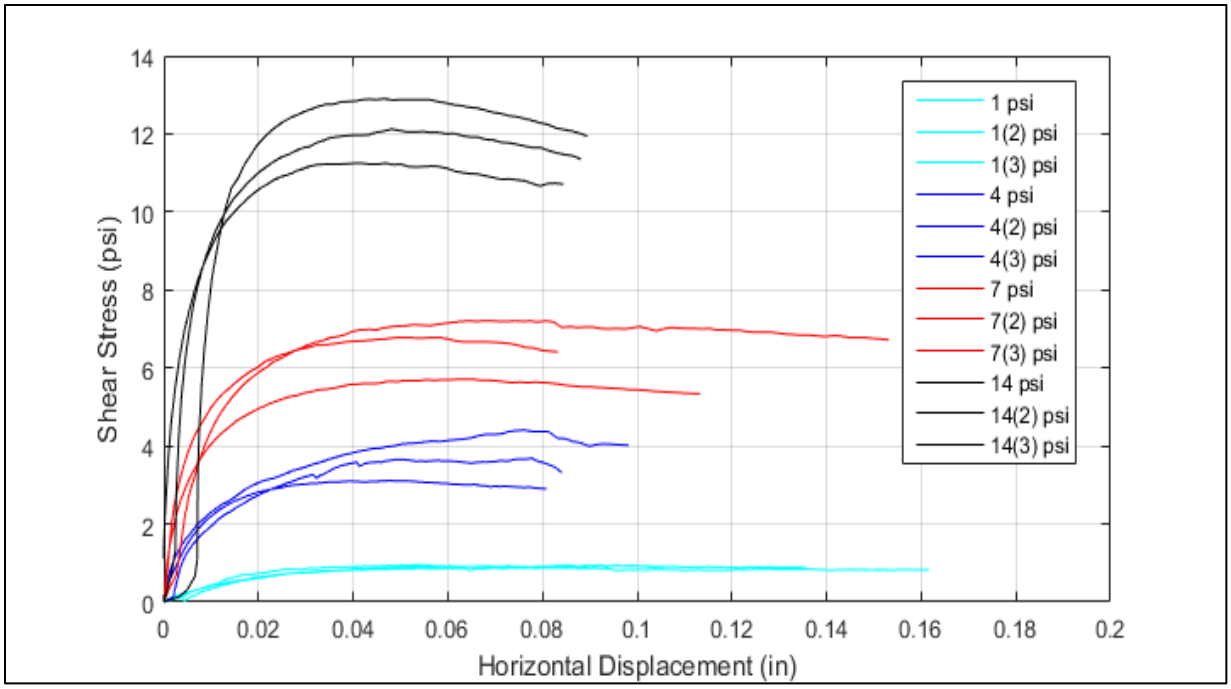

Figure 2-13. Control test pH 5 horizontal displacement vs. shear stress

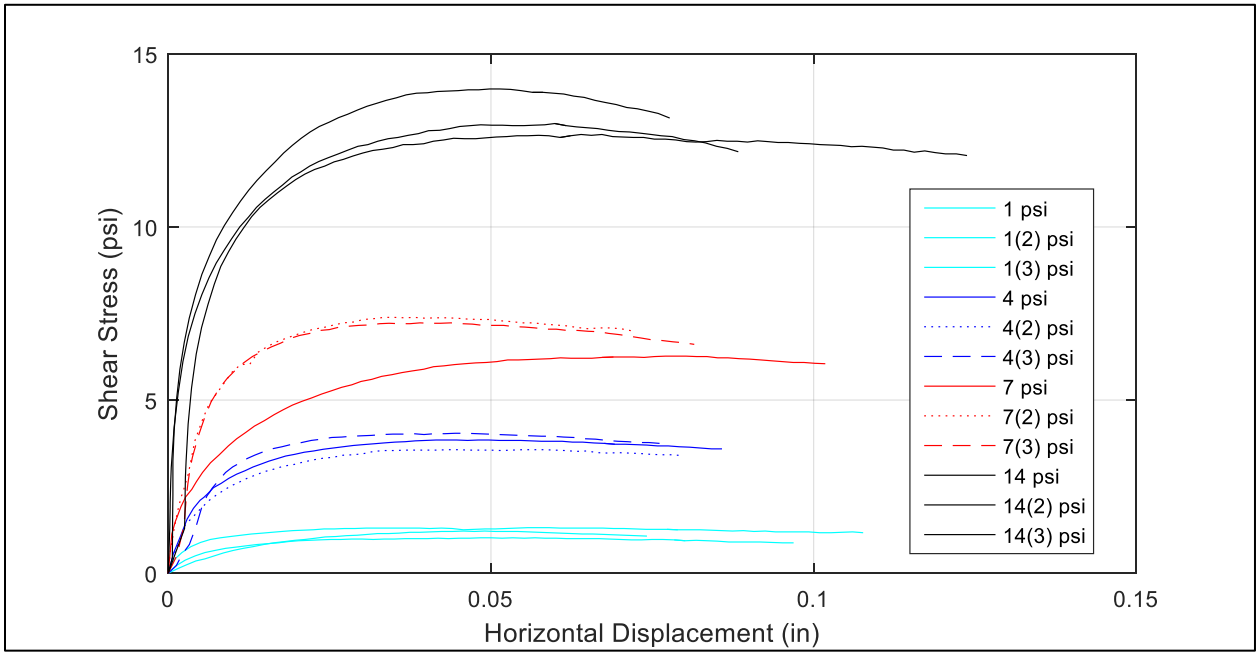

Figure 2-14. Control test pH 7 horizontal displacement vs. shear stress

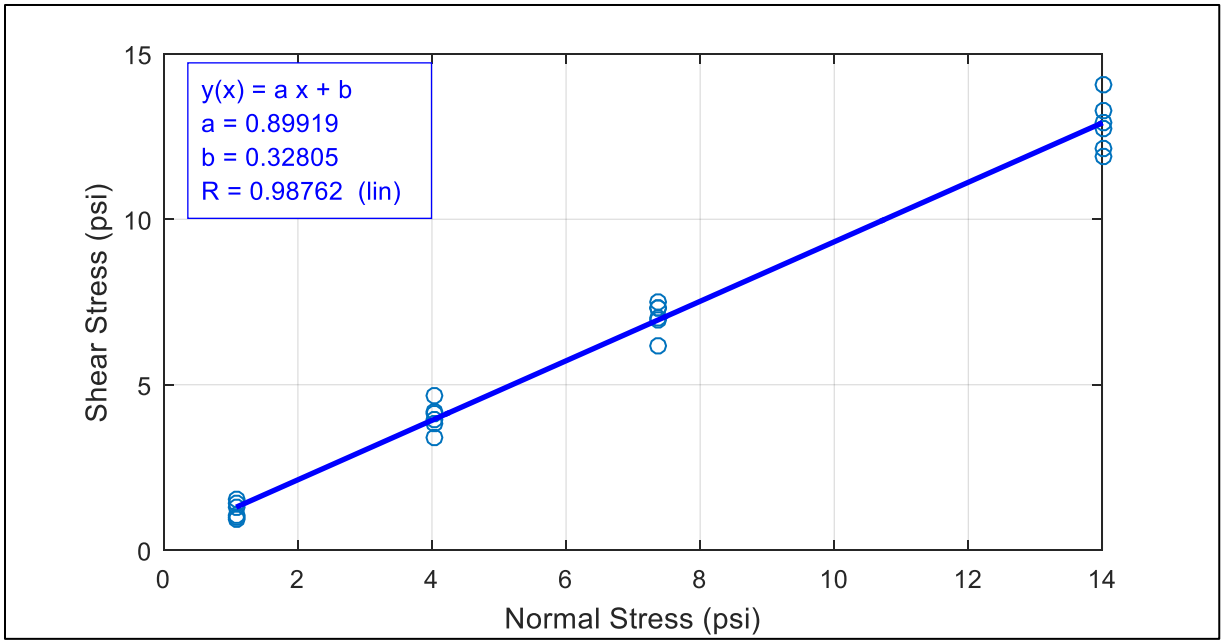

Figure 2-15. Control test normal stress vs. shear stress (combined pH 5 and pH 7 results)

2.3.2 Calcium Carbonate Precipitation Distribution

A summary of acid wash testing conditions is summarized in Table 2-2 while results are shown in Figure 2-16 for several sand specimens.

Table 2-2. Treated specimen characteristics (X indicates no cemented material present)

Specimen Name	Initial pH	Height of Cemented Material (inches)
J14-0	7	3.0
J14-1	5	X
J14-2	5	5.0
J14-3	7	X
J14-4	5	3.5
J14-X	7	2.0
J15-0	7	1.5
J15-1	7	2.0
J15-2	5	4.0
J15-3	5	X
J15-4	5	3.0
J15-X	5	2.0

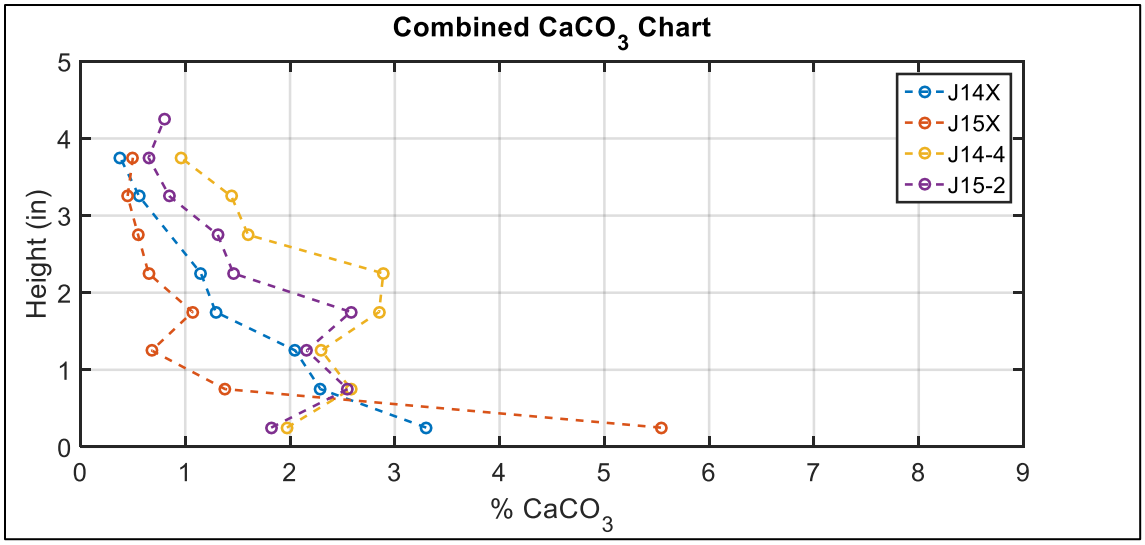

Figure 2-16. Calcium carbonate percentage vs. height for several sand specimens

2.3.3 Treated Specimen DST Data

2.3.3.1 General Results

Figure 2-17 shows an example of a treated soil column before processing. As discussed above, treated specimens were trimmed into samples for the DST. The individual samples were trimmed at intervals of one inch from the bottom of the specimen (i.e., 0-1", 1-2", 2-3" from the bottom). Figure 2-18 shows an example of these specimens.


Figure 2-17. Example of fully cemented soil column

Figure 2-18. DST samples from varied height intervals from the bottom of the specimen

Many of these specimens failed with distinctive failure planes that left several still well-cemented pieces of soil, (Figure 2-19). This type of failure was frequently displayed for the bottom one-inch specimens. Other specimens failed in a manner where the soil mostly returned to its pre-treatment granular state with scattered small pieces of cemented soil (Figure 2-20 and Figure 2-21). This type of failure was most common in samples from the top of the soil columns.

Figure 2-19. Post DST specimen of 0-1" sample

Figure 2-20. Post DST specimen of 1-2" sample

Figure 2-21. Post DST specimen of 2-3" sample

2.3.3.2 Initial pH 5 Results

Table 2-3 lists the total unit weights for each pH = 5 sample tested. Figure 2-22 displays plots of shear stress vs. horizontal displacement. Shear stress vs. normal stress was obtained by plotting the maximum shear stress from each test and the corresponding normal stress used during that test (Figure 2-23 and Figure 2-24).

Table 2-3. DST specimen total unit weights (pcf) for pH = 5

Normal Stress (psi)	Sample Location (in)	Total Unit Weight(pcf)
1	0-1"	103.7
1	1-2"	92.5
1	2-3"	87.3
7	0-1"	118.1
7	1-2"	106.3
7	2-3"	89.8
14	0-1"	115.1
14	1-2"	98.8
14	2-3"	92.4

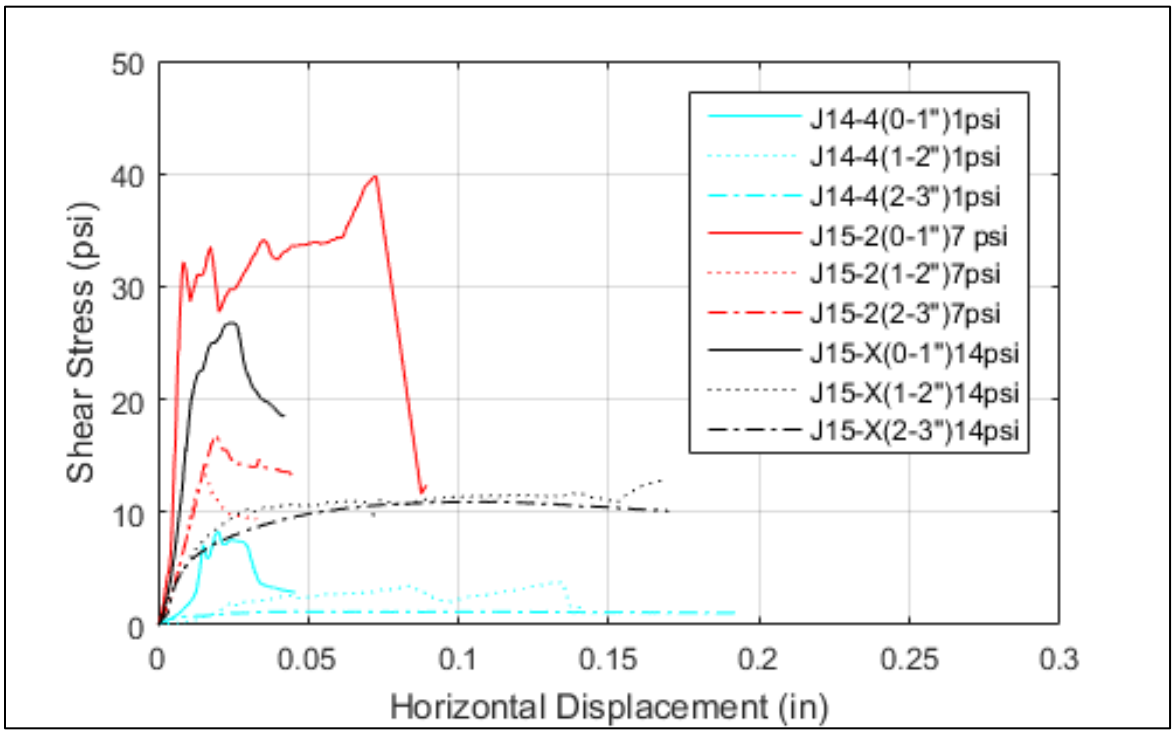

Figure 2-22. DST shear stress vs. horizontal displacement for pH = 5 sand specimens

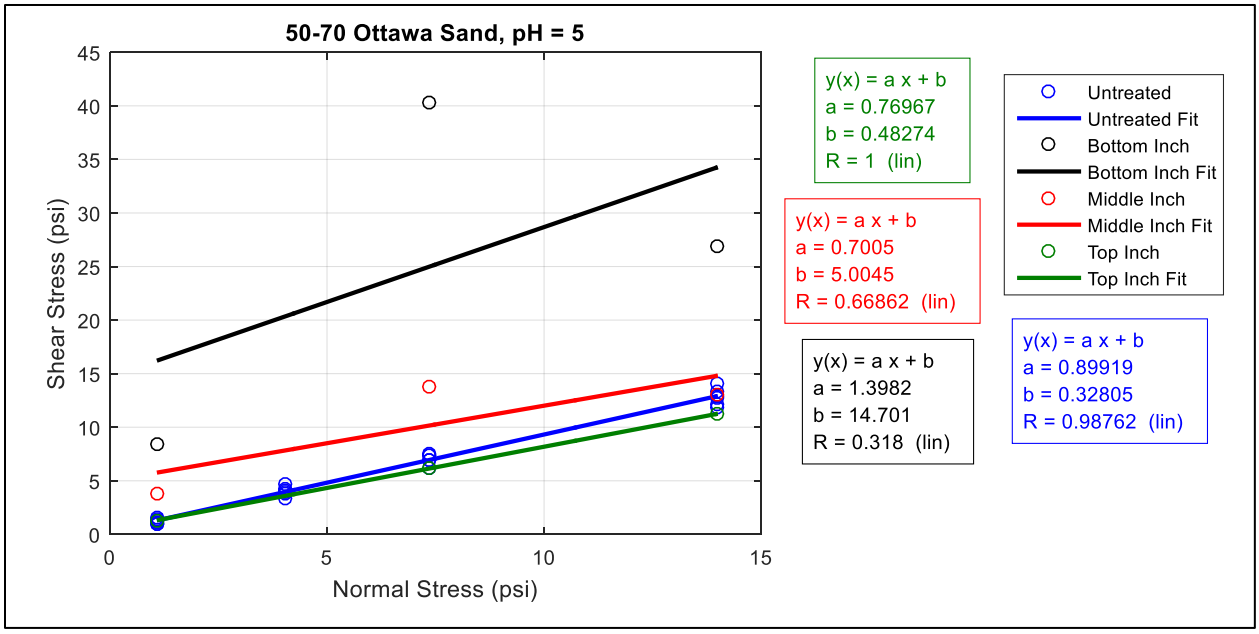

Figure 2-23. DST shear stress vs. normal stress for pH = 5 sand specimens

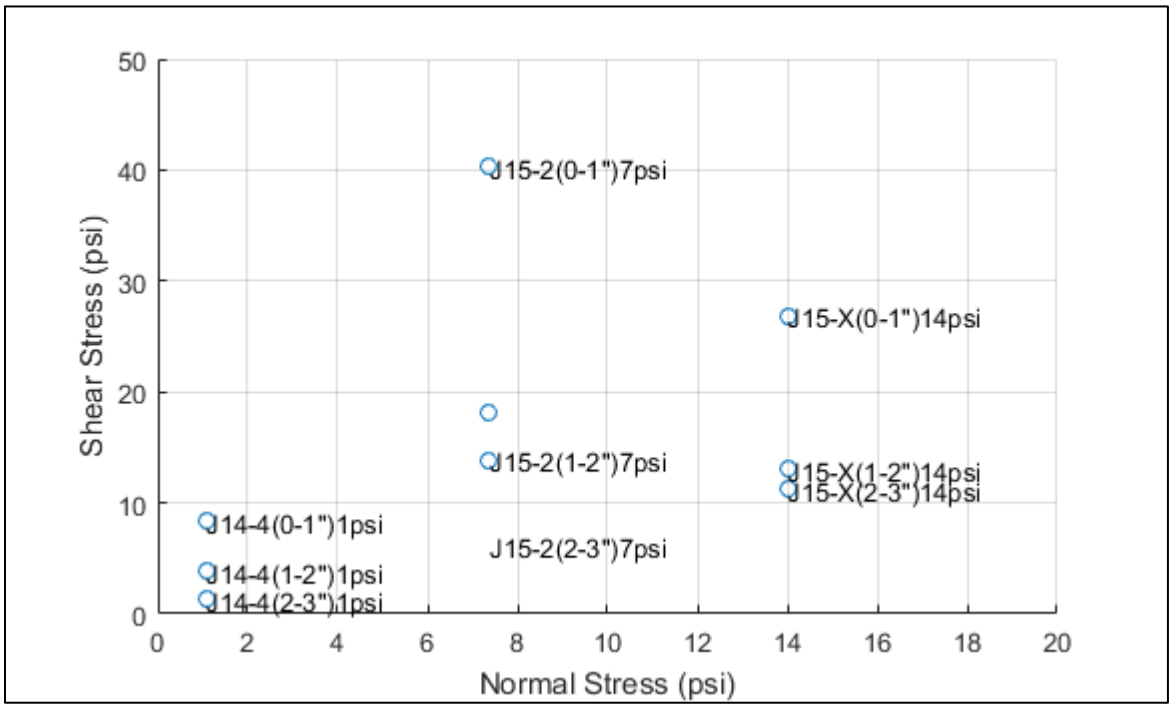

Figure 2-24. DST shear stress vs. normal stress for pH = 5 sand specimens with labels

2.3.3.3 Initial pH 7 Results

Table 2-4 lists the total unit weights for each pH = 7 sample tested. Figure 2-25 displays plots of shear stress vs. horizontal displacement. Shear stress vs. normal stress was obtained by plotting the maximum shear stress from each test and the corresponding normal stress used during that test (Figure 2-26 and Figure 2-27).

Table 2-4. DST specimen total unit weights (pcf) for pH = 7

Normal Stress (psi)	Sample Location (in)	Total Unit Weight (pcf)
1	0-1"	102
1	1-2"	103.6
1	2-3"	99.8
7	0-1"	115.8
7	1-2"	107.8
7	2-3"	106.6
14	0-1"	111.9
14	1-2"	109.3
14	2-3"	101.5

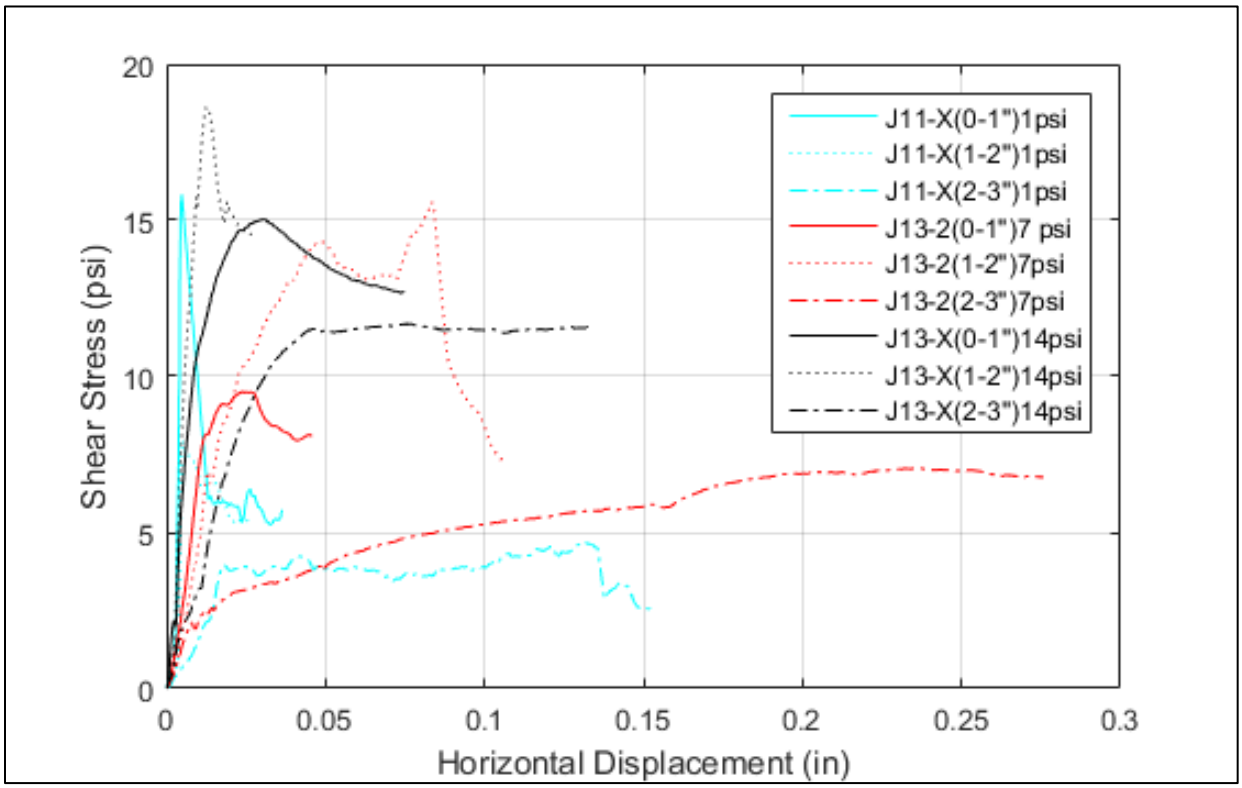

Figure 2-25. DST shear stress vs. horizontal displacement for pH = 7 sand specimens

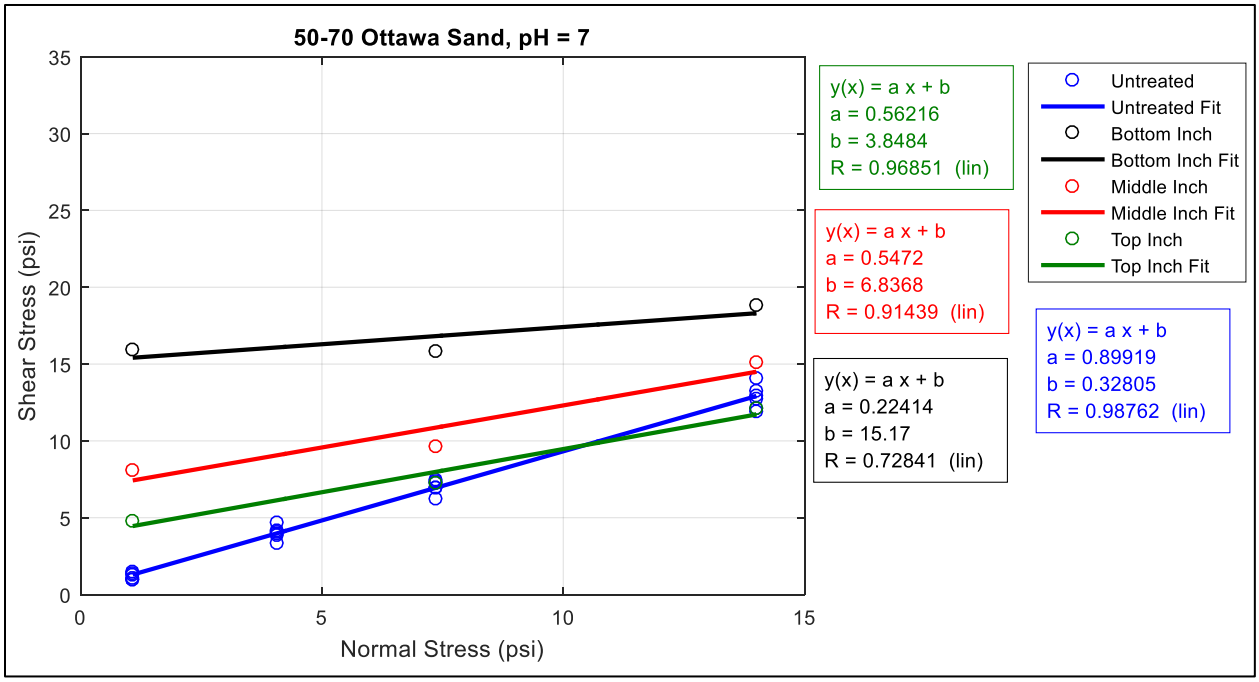

Figure 2-26. DST shear stress vs. normal stress for pH = 7 sand specimens

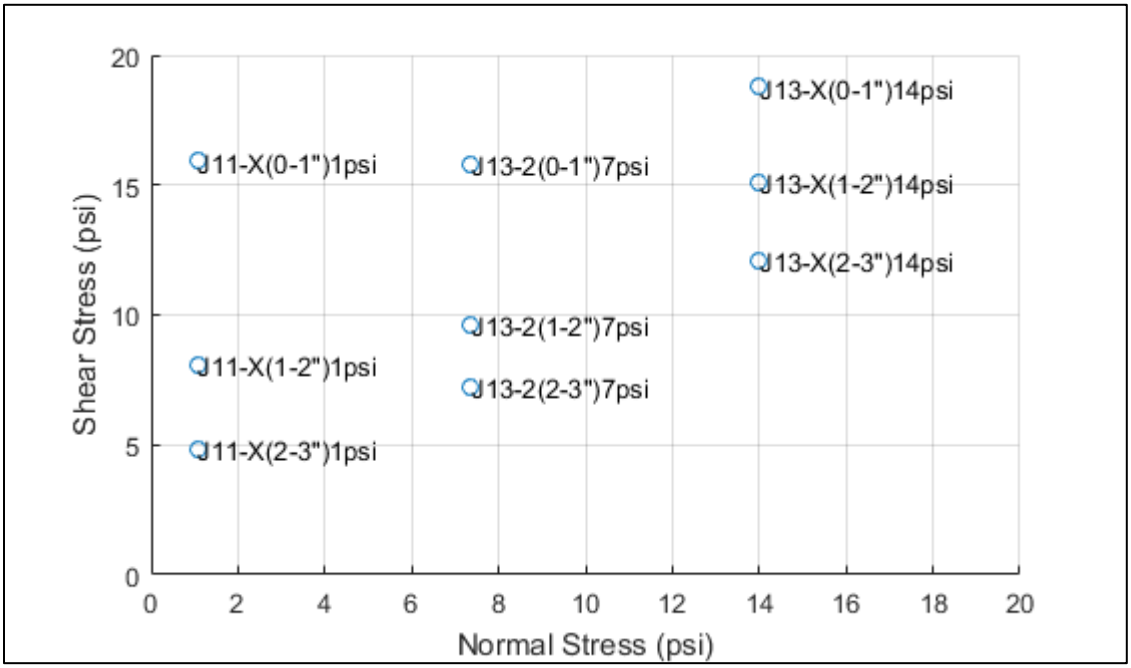

Figure 2-27. DST shear stress vs. normal stress for pH = 7 sand specimens with labels

2.3.3.4 Sand DST Results Summary

Table 2-5 summarizes the cohesion and angle of internal friction (phi) results from the DST data.

Table 2-5. Resulting properties for soils from DST.

		Cohesion (psi)	Angle of Internal Friction (degrees)
pH 7	Untreated	-	44
	2-3" Treated	3.8	29
	1-2" Treated	6.8	29
	0-1" Treated	15.2	12
pH 5	Untreated	-	42
	2-3" Treated	0.5	38
	1-2" Treated	5.0	35
	0-1" Treated	14.7	54

2.3.3.5 DST Data Reanalysis

All previous normal stress vs. shear stress relationships were obtained using the maximum DST failure point. However, Figure 2-22 and Figure 2-25 showed that specimens J15-2 (0-1”), J14-4 (0-1”), and J13-2 (1-2”) reached their maximum shear stresses after the first sign of failure occurred. Figure 2-28 and Figure 2-29 display maximum shear stress vs. normal stress results using only points of first sign of failure. Table 2-6 summarizes this reanalysis.

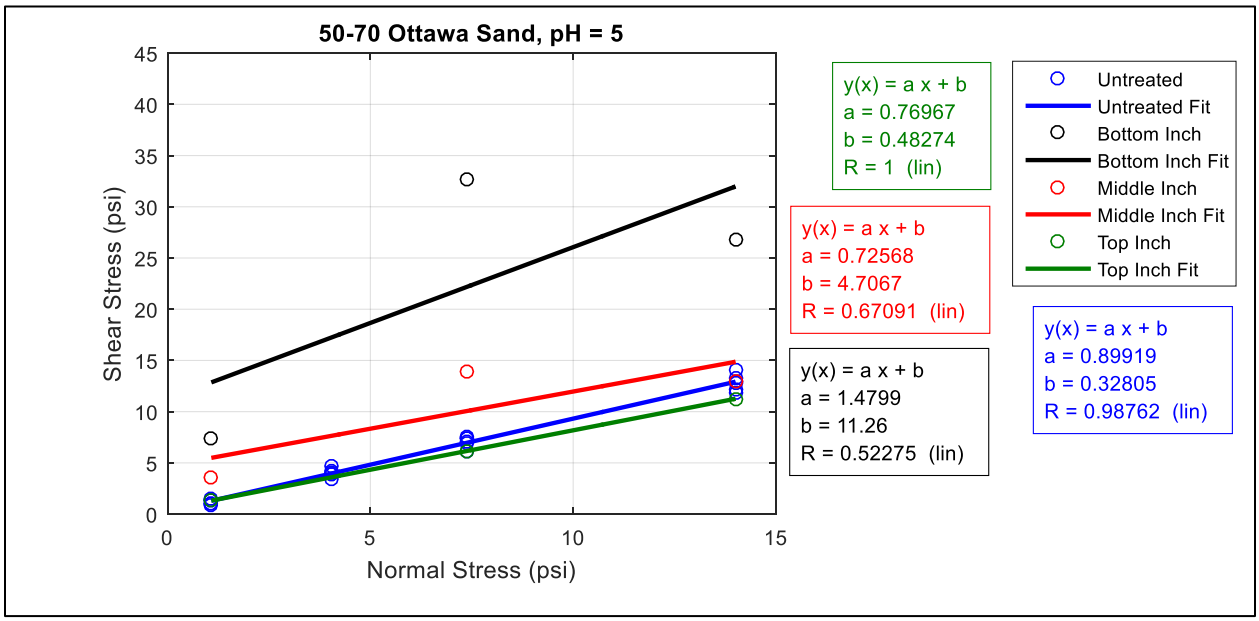

Figure 2-28. DST shear stress vs. normal stress for pH = 5 sand specimens (first failure data)

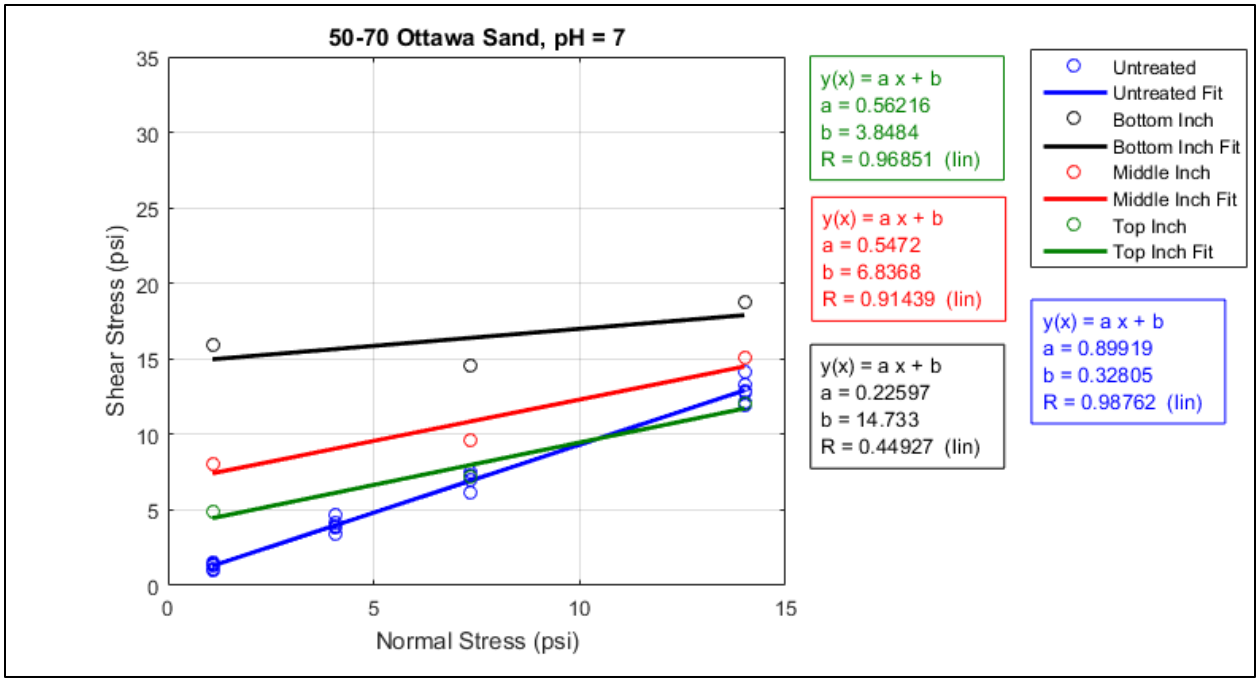

Figure 2-29. DST shear stress vs. normal stress for pH = 7 sand specimens (first failure data)

Table 2-6. Average soil property values of treated soil at varied distances from injection point (first failure data)

		Number of Specimens	Cohesion (psi)	Angle of Internal Friction (degrees)
pH 7	Untreated	15	-	43
	2-3" treated	3	3.9	29
	1-2" treated	3	6.8	29
	0-1" treated	3	14.7	13
pH 5	Untreated	15	-	43
	2-3" treated	3	0.5	38
	1-2" treated	3	4.7	29
	0-1" treated	3	11.3	24

2.3.4 Calcification Results

Figure 2-30 displays a plot of percent calcite vs. maximum shear stress (psi) divided by the normal stress. Table 2-7 shows the properties of pH = 5 soils at the different distances from the injection point. The same data for pH = 7 were not available because a calcite distribution analysis was not conducted on all treated columns.

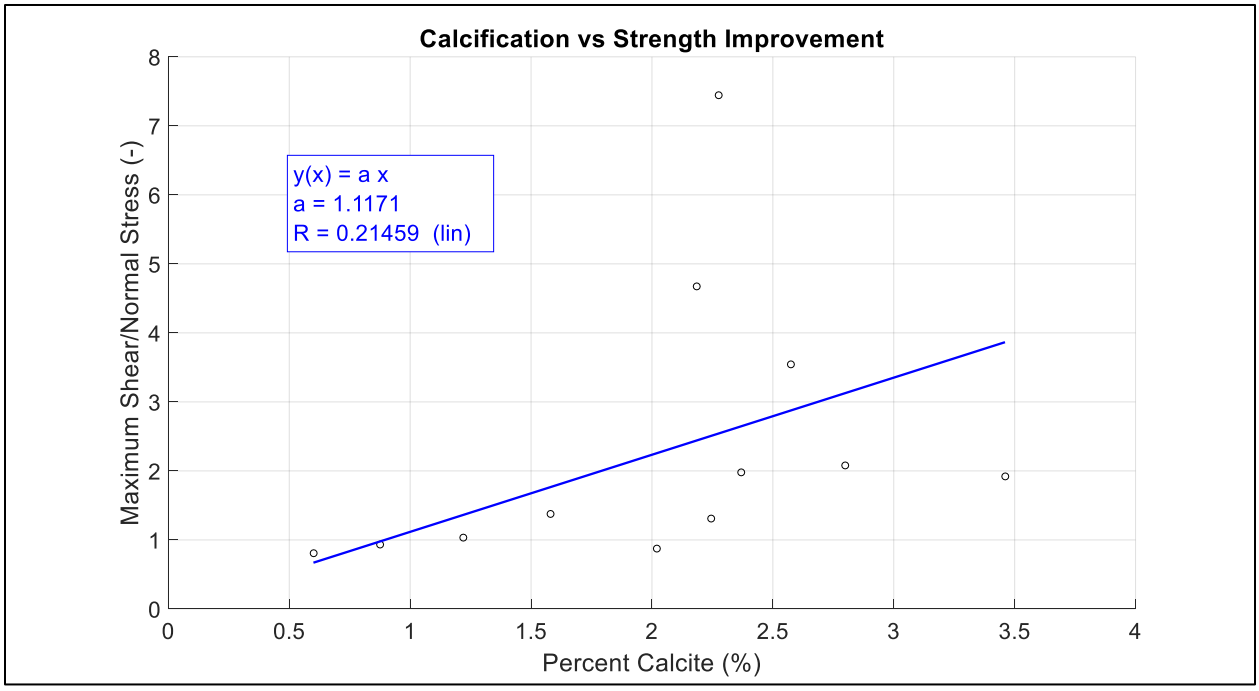

Figure 2-30. Calcite vs max shear/normal stress

Table 2-7. Average properties of pH = 5 soils at different heights

Distance from Injection Point (inches)	Average Calcite (%)	Cohesion (psi)	Angle of Internal Friction (degrees)
0-1"	2.64	11.26	24
1-2"	1.94	4.71	29
2-3"	1.62	0.48	38

2.3.5 Consolidation Results

Results from the consolidation tests are presented in Figure 2-31 through Figure 2-37, with sample properties and consolidation parameters summarized in Table 2-8. Initial consolidation tests (Figure 2-31) were performed on untreated sands, prepared medium dense to dense, based on the maximum and minimum void ratios. The series of tests performed on treated sand with pH of 5 and 7 (Figure 2-32 and Figure 2-33) had unit weights less than the untreated sands. This was a result of the specimen preparation in the treatment method. Figure 2-34 and Figure 2-35 show the results of of tests on treated sand using LIR of 0.5 for the purpose of investigating the compression and yielding of the $CaCO_3$ bonds in the cemented material. At the conclusion of the J21 and J23 series tests, additional tests on untreated sands (U1 in 2-36 and U2 Figure 2-37) were performed. These samples were prepared with unit weights similar to the J21 and J23 tests to isolate the influence of the $CaCO_3$ on the compression behavior.

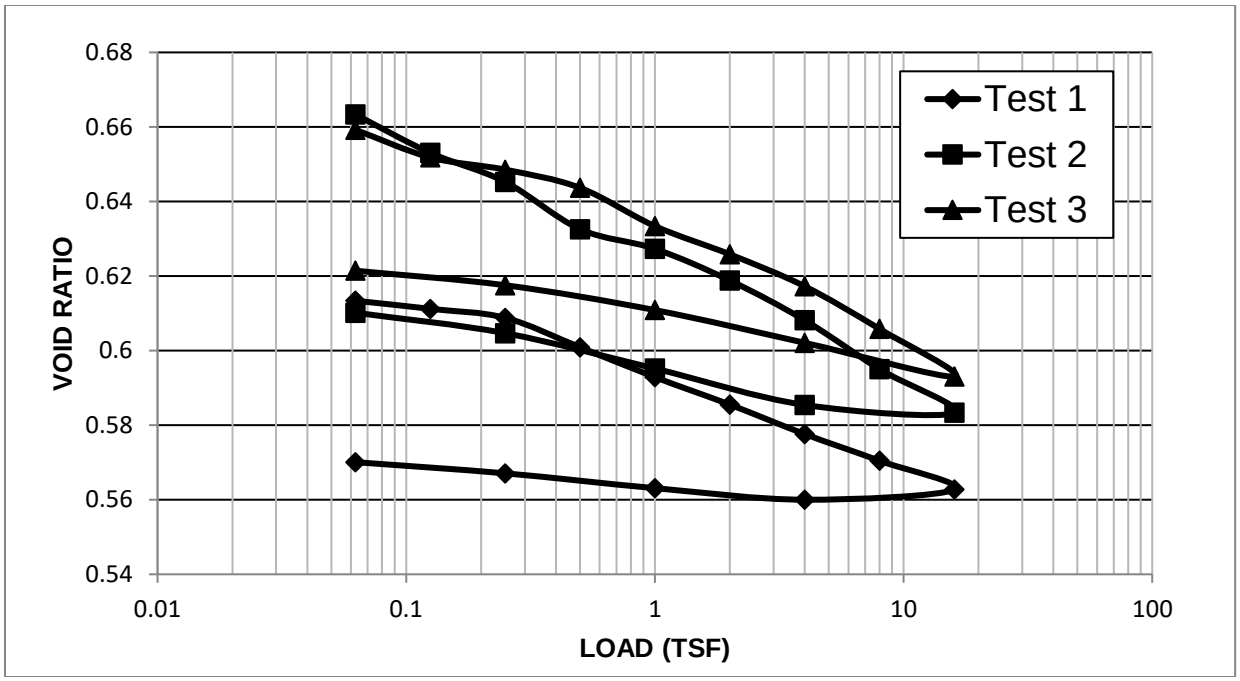

Figure 2-31. Void ratio vs. load for initial untreated sand samples

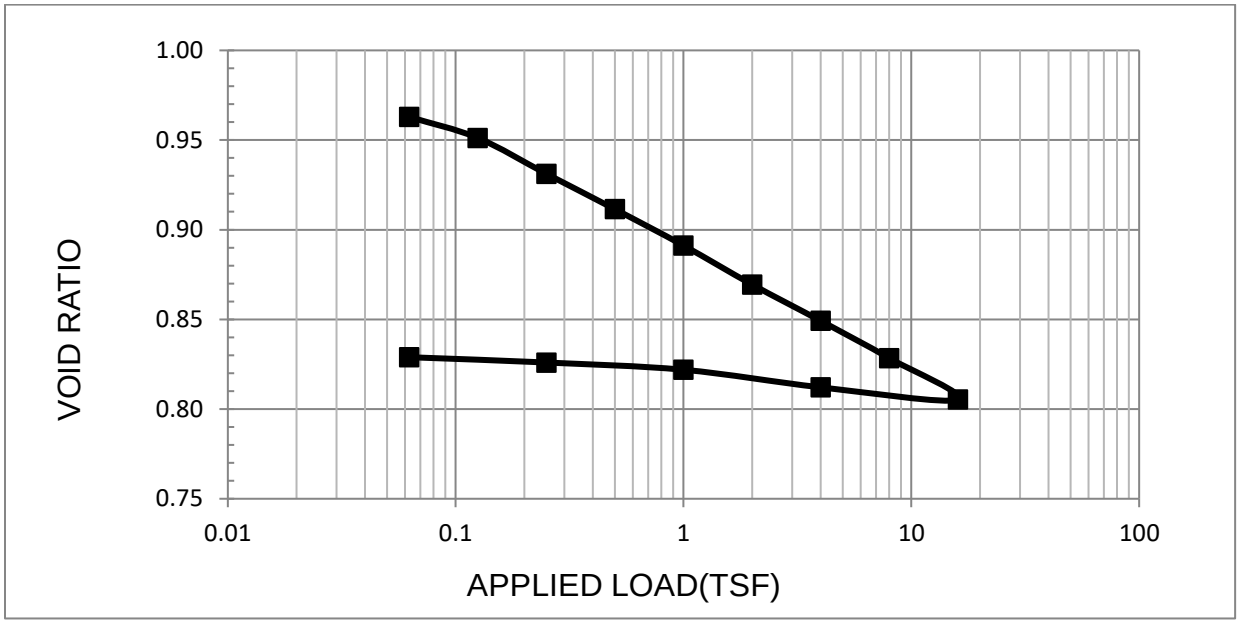

Figure 2-32. Void ratio vs. applied load for U1 untreated sand

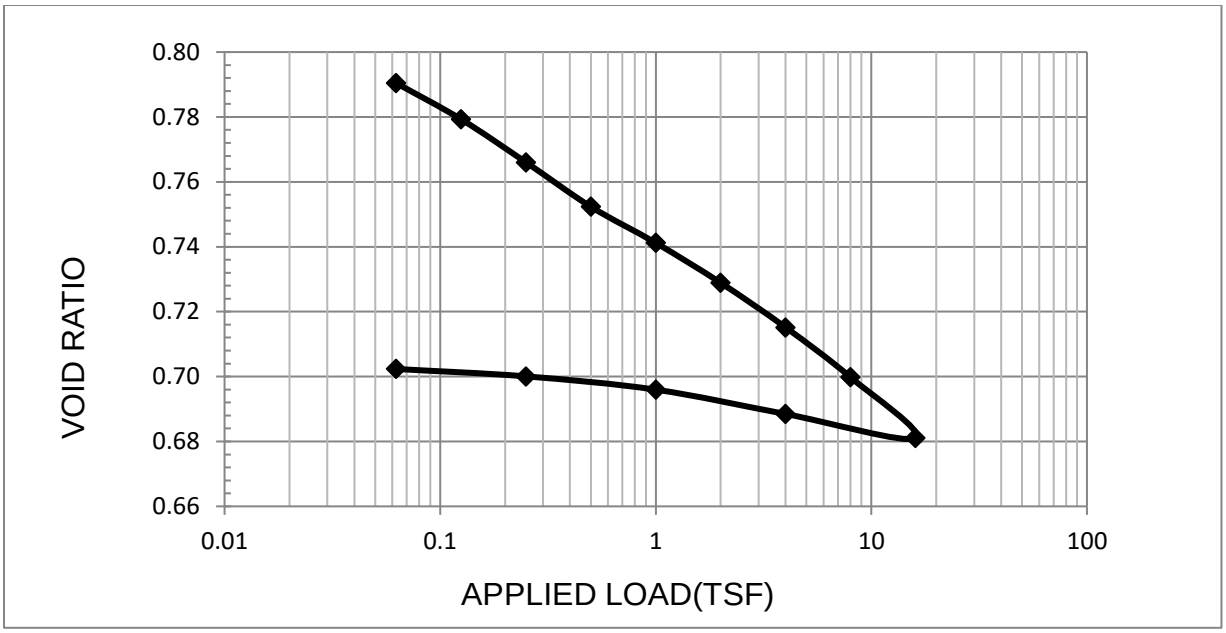

Figure 2-33. Void ratio vs. applied load for U2 untreated sand

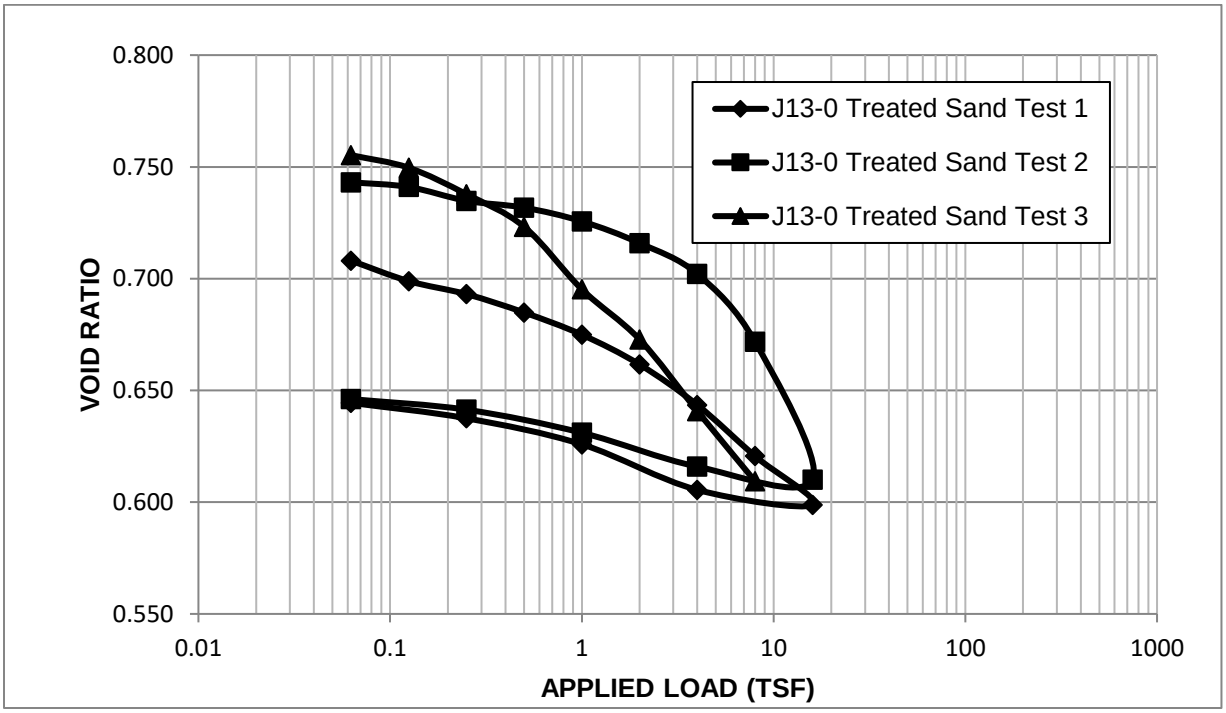

Figure 2-34. Void ratio vs. load for J13-0 treated sand with initial pH of 5

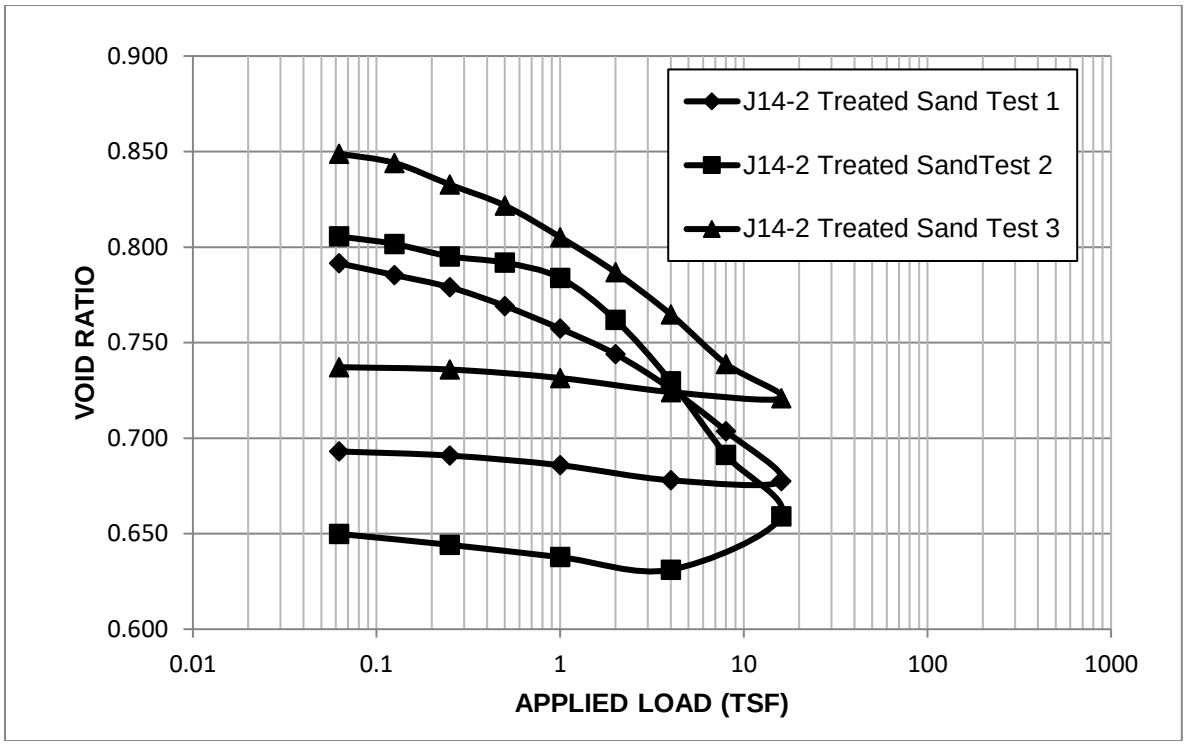

Figure 2-35. Void ratio vs. load for J14-2 treated sand with initial pH of 7

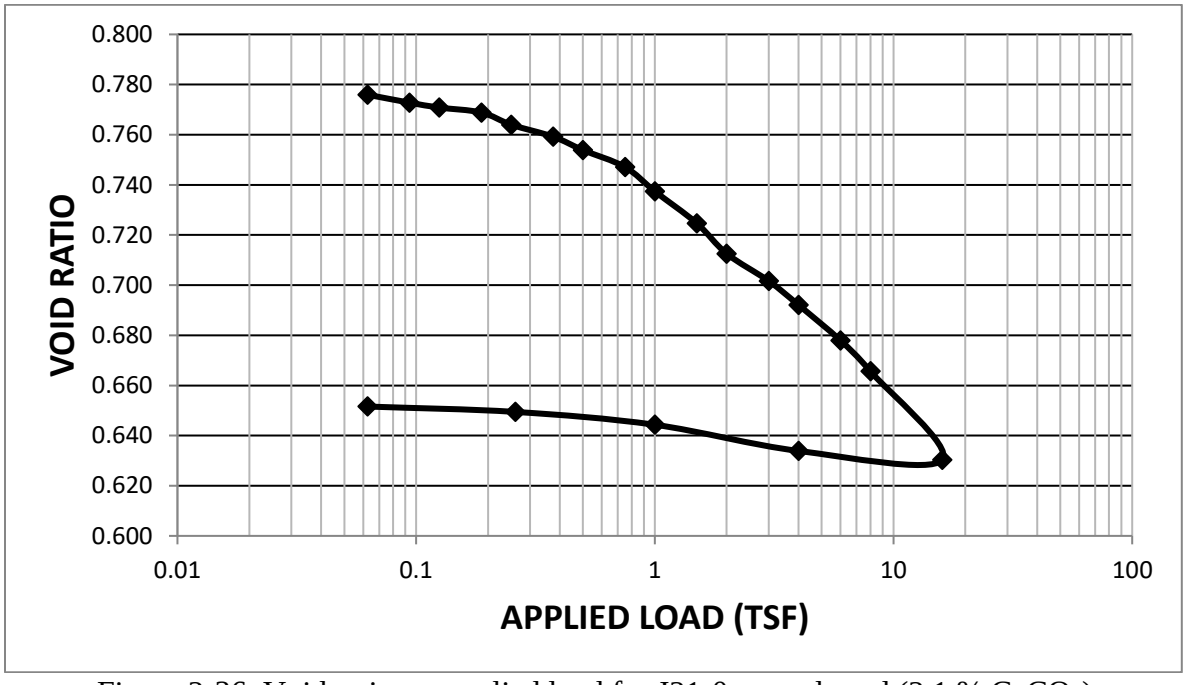

Figure 2-36. Void ratio vs. applied load for J21-0 treated sand (2.1 % $CaCO_3$)

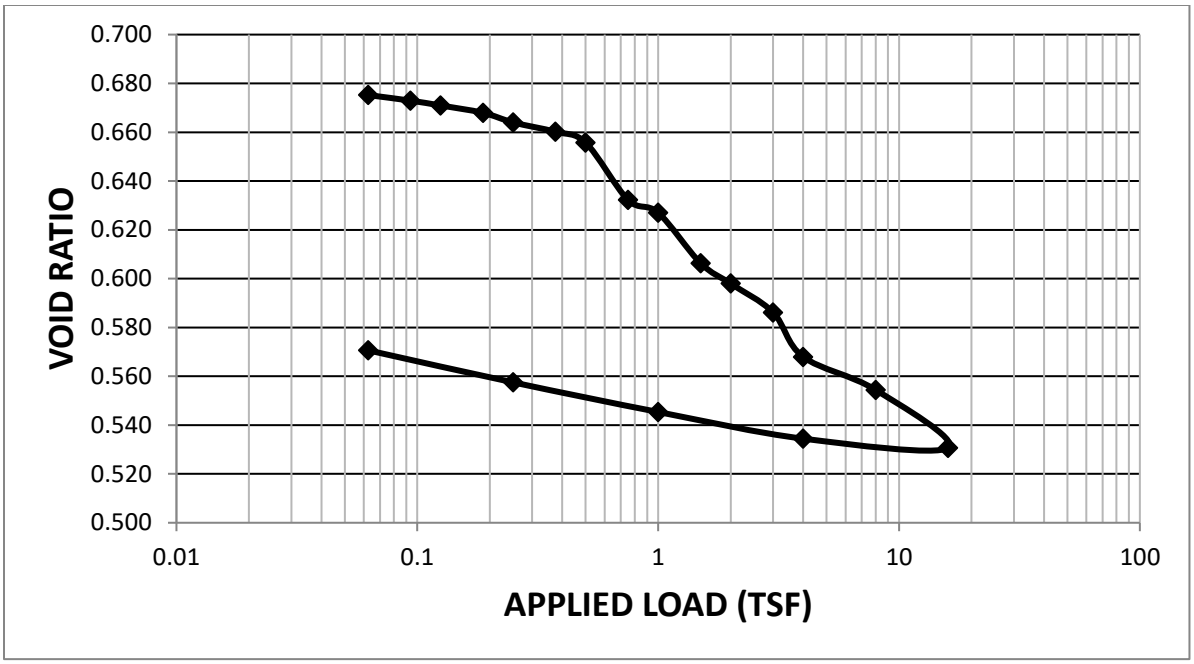

Figure 2-37. Void ratio vs. applied load for J23-0 treated sand (2.9 % $CaCO_3$)

Table 2-8. Summary of untreated and treated sand specimen properties and consolidation results

PARAMETERS	UNTREATED SANDS					TREATED SANDS							
						J13-0			J14-2			J21-0	J23-0
	Test 1	Test 2	Test 3	U1	U2	Test 1	Test 2	Test 3	Test 1	Test 2	Test 3		
Specific gravity, G_s	2.64					2.66			2.68			2.65	2.65
pH	7					8.52†			8.1†			9.06†	9.16†
Initial void ratio, e_o	0.61	0.67	0.68	1.03	0.79	0.72	0.75	0.76	0.79	0.81	0.85	0.78	0.68
Initial moisture content, w (%)	9.2	9.7	10.1	7.9	8.1	0.45	0.45	0.45	0.75	0.75	0.75	0	0
Wet unit weight, γ (pcf)	111.5	109.7	108.1	88.0	99.8	96.2	95.0	94.0	92.6	91.9	89.8	93.1	82.3
Dry unit weight, γ_d (pcf)	102.1	100.0	98.2	81.6	92.4	95.7	94.5	93.7	91.9	91.2	89.1	93.1	82.3
$CaCO_3$ (%)	0	0	0	0	0	2.4 to 2.53‡	1.1 to 2.4‡	0.8 to 1.1‡	1.97 to 3.3‡	1 to 3‡	0.5 to 3‡	2.9	2.1
Preconsolidation Pressure, P_c (tsf)	0.3	NA	NA	NA	NA	1	2	0.5	1	1	0.5	1	0.75
Compression index, C_{ci} (before P_c)	0.0076	NA	NA	NA	NA	0.0233	0.0153	0.044	0.0265	0.0152	0.0365	0.0269	0.021
Compression index, C_c (after P_c)	0.0252	0.0398	0.039	0.07	0.05	0.081	0.156	0.103	0.0664	0.116	0.078	0.088	0.0974
Recompression index, C_r	0.007	0.017	0.015	0.014	0.0125	0.022	0.0216	0.02	0.0133	0.011	0.022	0.017	0.015

† pH of effluent at end of MICP treatment
‡ Assumed range of $CaCO_3$ based on measured % from other specimens in same treatment series
NA = not applicable

2.4 Sand Discussion

2.4.1 Untreated Sand DST

DST results confirmed previous shear strength results for untreated specimens. Additionally, the shear vs. horizontal displacement resulted in smooth plots with clearly defined failures.

2.4.2 Treated Sand DST

2.4.2.1 Shear Behavior

DST results were more erratic than the untreated results, and specimens taken from the bottom of the soil columns were the most erratic. Untreated soil derives its strength from friction between the soil particles as they slide and roll past one another. Treated specimens derive their initial strengths primarily from calcification – similar to a soft rock such as limestone. The shear stress vs. horizontal displacement data displayed steep initial plots that quickly reach their highest maximum stress at relatively small horizontal displacements. When failure occurs, the shear stress will typically decrease and then increase as the failure mechanism moves from breaking the bonds between particles toward a friction failure mechanism. These processes are illustrated in Figure 2-38.

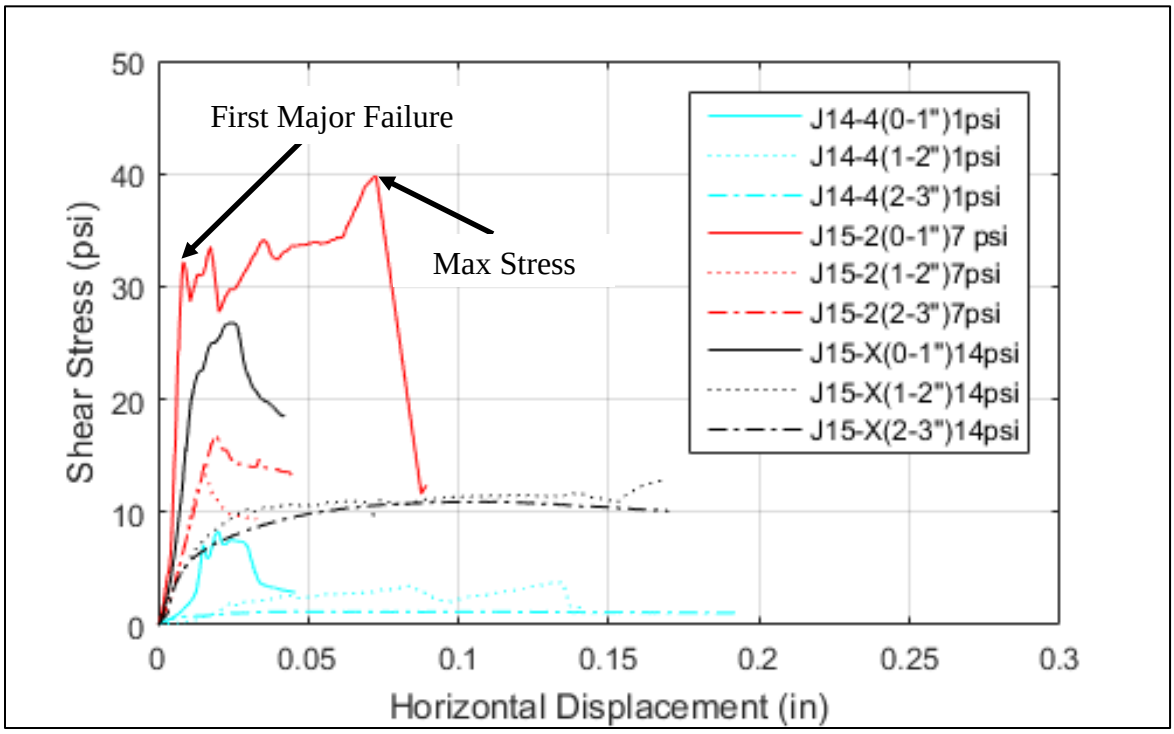

Figure 2-38. Difference between first major failure and maximum shear stress

Specimens close to the injection point showed these types of double-failure behavior. Further from the injection point, specimens behaved more like typical granular material. These results

confirmed previous ones indicating that calcification decreases as a function of distance from the injection point.

In specimens with this sort of double-failure behavior, the first major failure was typically the maximum shear stress (i.e., the highest shear stress value achieved during testing and, subsequently, the value used for the shear stress vs. normal stress plot). However, in tests J15-2 (0-1"), J14-4 (0-1"), and J13-2 (1-2"), the maximum shear stress occurred after the first major failure. The reanalysis (where first failure, instead of maximum stress, was used) showed a slight decrease in cohesion and internal friction angle for the 0-1" samples for both pHs. However, it did not seem to change the overall variability of the results significantly. The first failure equates to a detrimental failure (excessive movement) of the roadway or structure the treated soil is meant to support. Therefore, this value should be considered as the maximum shear stress of the soil at the tested normal stress for design purposes when applying MICP treatments.

It should also be noted that between the first failure and second failure, the soil particles behave very differently. Results showed that this soil exhibited properties from both untreated and treated sand as its cemented bonds are broken. However, it still contained some cemented sand pieces and therefore had a different grain size distribution compared to the untreated sand. For these soils, as with the untreated soil, their maximum strengths were due to friction only.

2.4.2.2 Strength Variability

All specimens from both initial pH groups showed some increase in cohesion when compared to the untreated sands. However, there was a clear inverse relationship between strength improvements and distance from the injection point. There was a small amount of variation between specimens treated with initial pH values of 5 and 7, but no significant statistical differences were observed. This may be due to a flushing effect whereby the initial HCl in the voids may have been flushed out of the specimens when the bacteria broth was introduced. In the future, it may be better to adjust initial pH using another mechanism.

2.4.2.3 New Analysis Technique

Because of the variability shown in the treated specimens' data, a new analysis technique was used to better understand the relationship between precipitated calcite and strength improvements. Maximum shear stress data was divided by their respective normal stresses and plotted against percent of precipitated calcite. These results appeared to show a direct relationship between mass of precipitated calcite and strength improvement. Additionally, these data showed that while there was some strength improvement at calcite percentages up to two percent, the significant improvement of the soil was only realized at calcite concentrations of 2% or greater. These results are supported by similar analyses in Whiffin et al. (2007), which showed that a similar minimum calcite concentration was needed for measurable strength improvement.

Calcite levels greater than the 2% threshold were only seen consistently for samples closest to the injection point (0-1"). Methods to increase calcification in the rest of the soil column and achieve better cementation uniformity are currently only feasible at the bench scale of treatment. In the field, implementation of these techniques would be difficult to implement.

2.4.3 Consolidation Tests

2.4.3.1 Void Ratio vs. Effective Stress

Generally, two slopes were observed for the void ratio vs. effective stress plots for the treated sands; whereas, one slope was generally observed for the untreated sands (Figure 2-36 through Figure 2-37). Typically, the two slopes are a result of the applied stress exceeding preconsolidation pressure, P_c. Preconsolidation pressure is a result of a maximum past pressure experienced by the sample. Since the samples used for this study were all reconstituted samples, there was no true preconsolidation pressure. In the case of the treated sand, this was due to the cementation of the sand particles which locked in a stress within the soil matrix (Bjerrum, 1967). While this effect is the goal of MICP treatment, the benefit appears to be limited to low pressures when the bond strength is mobilized and the limit is the apparent P_c. Evidence of this can be seen in the initial slopes of 2-41 and 2-42. Compression behavior under greater pressures is controlled by the decreased permeability and redistribution of internal stresses in the treated soil, which is still particulate but comprises silica sand and $CaCO_3$. When interpreting the consolidation behavior of MICP treated soils, consideration of this limit is paramount as pressures exceeding it result in settlements more like the untreated soil. The P_c of the treated sands ranged between 0.5 tsf and 2 tsf; therefore, loads exceeding these pressures led to higher deformation rates (2 to 10 times greater) of the treated sands (Table 2-8). Lee et al. (2013) observed identical rates between untreated and treated Ottawa sand when the loading exceeded the P_c.

In Figure 2-38 through Figure 2-40, the initial slopes (occurring before P_c) represent the compression of the cemented sand which are included in Table 2-8 as C_{ci}. These are followed by the higher C_c (occurring after P_c) of the steeper second slope indicating yielding of the $CaCO_3$ bonds had occurred and the particulate matrix of sand and $CaCO_3$ is now carrying the applied pressure. It is expected that this analysis can be applied to the treated organic soil. For in situ treatment, organic soil that has consolidated and is in its creep phase of compression, cementation would expectedly have the same effect as shown in the sands and decrease secondary compression.

It was expected that specimens closest to the injection point (bottom of the soil column) would have resulted in an indirect correlation between C_c and specimen height (similar to the DST results) due to the indirect relationship between $CaCO_3$ content and specimen height. However, C_{ci} results did not appear to show this trend. Instead, C_{ci} was highest for Test 2 – the middle of the specimen. This could be attributed to the non-uniform distribution of the nutrients injected in the sand. The flow rate used was 3 mL/min which is slower than 10 mL/min used in Lin et al. (2015) and 6 mL/min (0.35 L/h) reported in Whiffin et al. (2007). In addition, Whiffin et al. (2007) concluded that to achieve strengthening through $CaCO_3$ precipitation at desired locations, there should be a balance between the rate of urea hydrolysis with the flow rate delivery of reactants. If these two parameters are not balanced, $CaCO_3$ precipitate in the soil will be nonhomogeneous. In addition, Lee et al. (2013) showed poor correlation between C_c and $CaCO_3$. However, low flow injection pressures at 0.2 bar gave the best stiffness results in the treated samples due to homogenous distribution of nutrients.

Holistically, these results and related literature show that the primary compression index does not adequately describe compressibility of the treated soil. This can be seen from the results by an increase in C_c of the treated sands from 0.05 to 0.09 at 81 pcf dry density and 0.07 to 0.08 for 92

pcf dry density. Although Lin et al. (2016) showed a reduction in compression of Ottawa sand with increasing $CaCO_3$ contents at 1.4% and 2.6%, it is unclear from the plots where the slopes for the compression index were selected. Feng and Montoya (2016) showed that as little as 0.2% calcite content, there was a reduction in initial void ratio from 0.751 to 0.745 of the untreated and treated sands respectively at the same dry densities. In the current study, at approximately 82 pcf dry density, calcification appeared to reduce initial void ratio from 1.03 to 0.68; and at approximately 92 pcf, calcification reduced initial void ratio from 0.79 to 0.78.

2.4.3.2 Deformation vs. Time

A second series of tests on untreated sand with the same density as the treated sand was performed to further investigate the compression index relationship with $CaCO_3$. The comparisons between untreated and treated sands at similar densities are: U1 (untreated) and J23-0 (treated), each with dry densities of approximately 81 pcf, and U2 (untreated) and J21-0 (treated), each with dry densities of approximately 92 pcf.

Comparisons between specimen J23-0 and U1 show lower total deformations for J23-0 compared to U1 as effective stress increases from 0.0625 tsf to 4 tsf (Figure B-1through Figure B-9 in Appendix B). The $CaCO_3$ content for J23-0 was 2.1%. At 8 tsf, the magnitude of total deformations was greater than the untreated sand. This may be attributed to the continued $CaCO_3$ bond yielding, compression of the $CaCO_3$, and more effective stress having to be carried by the silica sand particles. J21-0, with 2.9% $CaCO_3$, experienced total deformations comparable to U2 between 0.0625 tsf and 0.25 tsf, with greater deformations occurring at higher stresses (Figure A-10 through Figure A-18). Table 2-9 and Table 2-10 summarize the results based on the end of primary (EOP) consolidation using Taylor's method. Interestingly, the EOP values did not always support the conclusion that the $CaCO_3$ affected the stiffness up to the P_c based on the total deformations.

Table 2-9. Summary table showing decreasing sample height, end of primary time and void ratio with increasing applied effective stresses for U1 and J23-0.

Load (tsf)	U1			J23-0			EOP_{J23-0}/EOP_{U1}
	Height of sample (in)	EOP time, tp (mins)	void ratio	Height of sample (in)	EOP time, tp (mins)	void ratio	
0	1.001	0	1.028	1.033	0	0.6775	-
0.0625	0.969	0.5	0.963	1.032	4	0.675	8
0.125	0.964	2	0.951	1.029	8	0.671	4
0.25	0.954	15	0.931	1.025	4	0.664	0.267
0.5	0.944	8	0.911	1.019	4	0.656	0.5
1	0.934	2	0.891	1.002	2	0.627	1
2	0.923	2	0.869	0.984	1	0.598	0.5
4	0.913	4	0.849	0.966	15	0.568	3.75
8	0.903	4	0.828	0.957	2	0.554	0.5
16	0.892	2	0.805	0.943	2	0.531	1

Table 2-10. Summary table showing decreasing sample height, end of primary time and void ratio with increasing applied effective stresses for U2 and J21-0.

Load (tsf)	U2			J21-0			EOP_{J21-0}/EOP_{U2}
	Height of sample (in)	EOP time, tp (mins)	void ratio	Height of sample (in)	EOP time, tp (mins)	void ratio	
0	1.001	0	0.791	1.000	0	0.777	-
0.0625	1.001	2	0.790	0.999	4	0.776	2
0.125	0.995	2	0.779	0.996	--	0.771	392
0.25	0.987	2	0.766	0.992	8	0.764	4
0.5	0.979	4	0.752	0.987	15	0.754	3.75
1	0.973	8	0.741	0.977	4	0.737	0.5
2	0.966	2	0.729	0.963	30	0.713	15
4	0.959	4	0.715	0.952	8	0.692	2
8	0.950	4	0.700	0.937	4	0.666	1
16	0.940	2	0.681	0.9171	2	0.630	1

CHAPTER 3
TREATMENT OF ORGANIC-RICH SOIL SPECIMENS USING A PERCOLATION METHOD

3.1 Control Testing

The first step in treating organic-rich specimens was to perform several control tests on untreated specimens so that they may be used as a basis for comparison.

3.1.1 Material and Methods

Organic-rich soil from Polk County, FL with an in situ organic content of approximately 50% was also obtained from FDOT. This soil was mixed with quantities of 50/70 Ottawa sand to produce soils with different fractions of organic content. Grain size distributions for theses organic soils are presented in Figure 3-1.

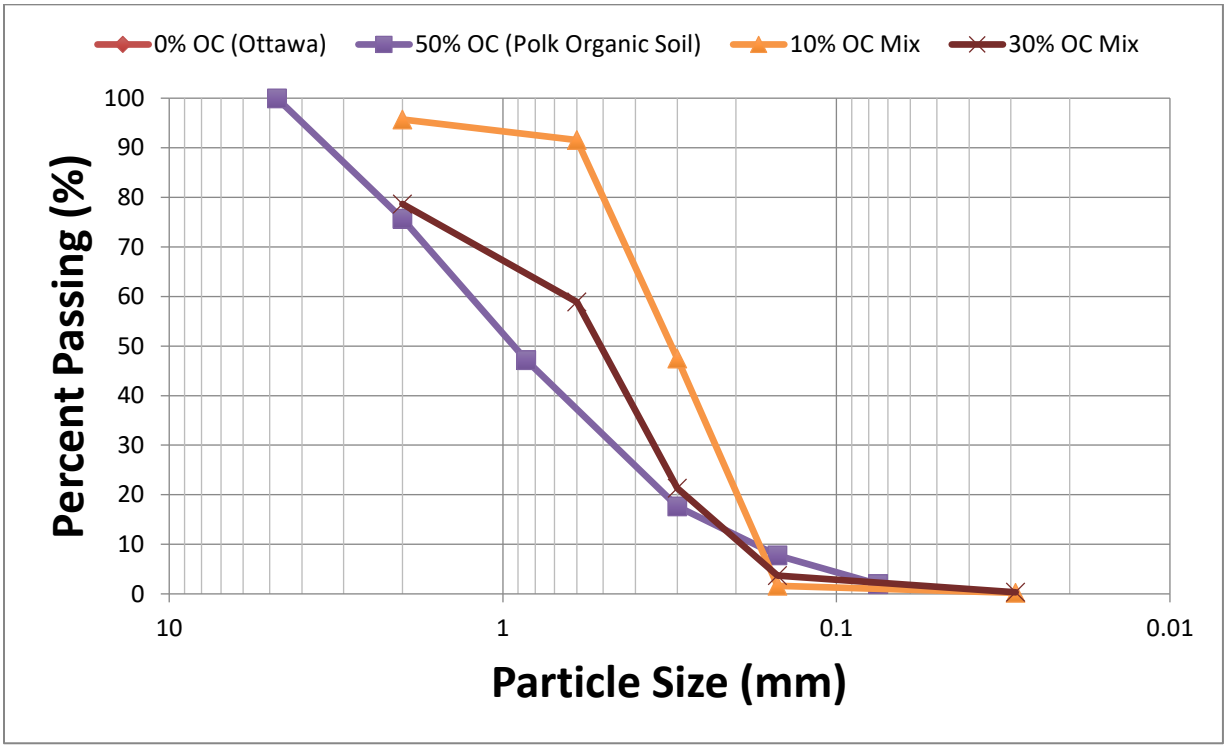

Figure 3-1. Sieve analyses for organic soils

3.1.2 DST Control Data

Once the soil had been obtained, specimens were subjected to DST. Figure 3-2 through Figure 3-XX display the shear stress vs. horizontal displacement and the maximum shear stress vs. normal stress obtained from the DST of untreated (i.e., control) specimens. Results are summarized in Table 3-1.

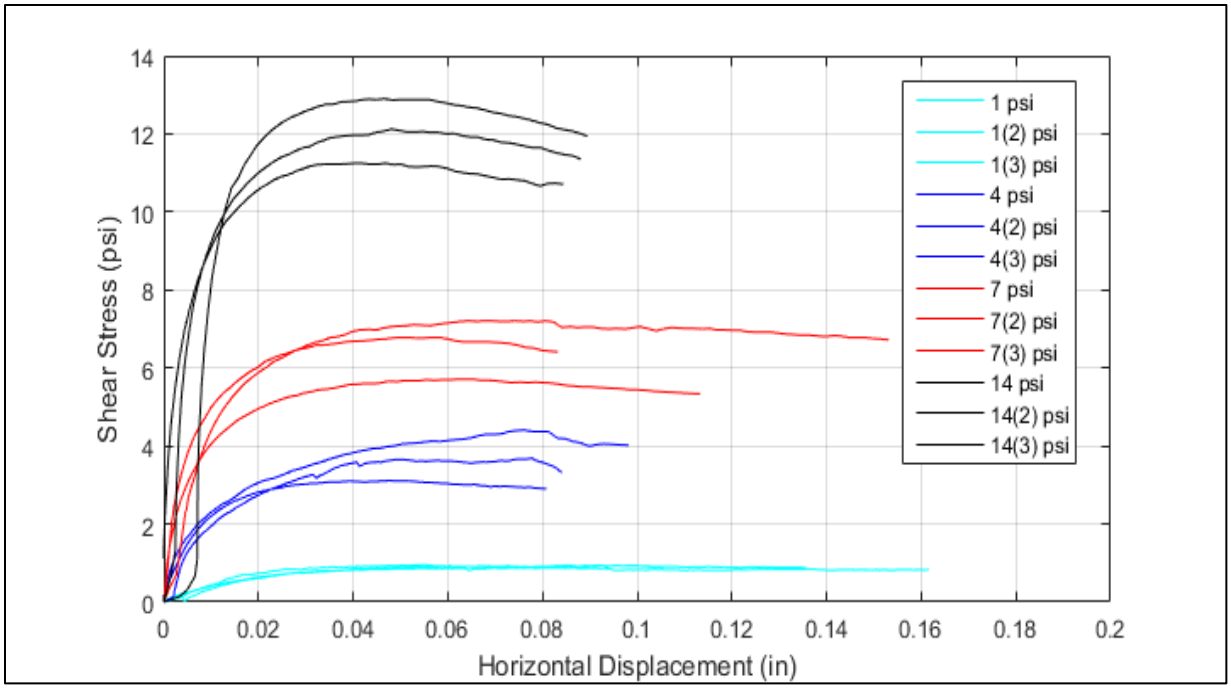

Figure 3-2. Horizontal displacement vs. shear stress: 0% organic content, pH 5

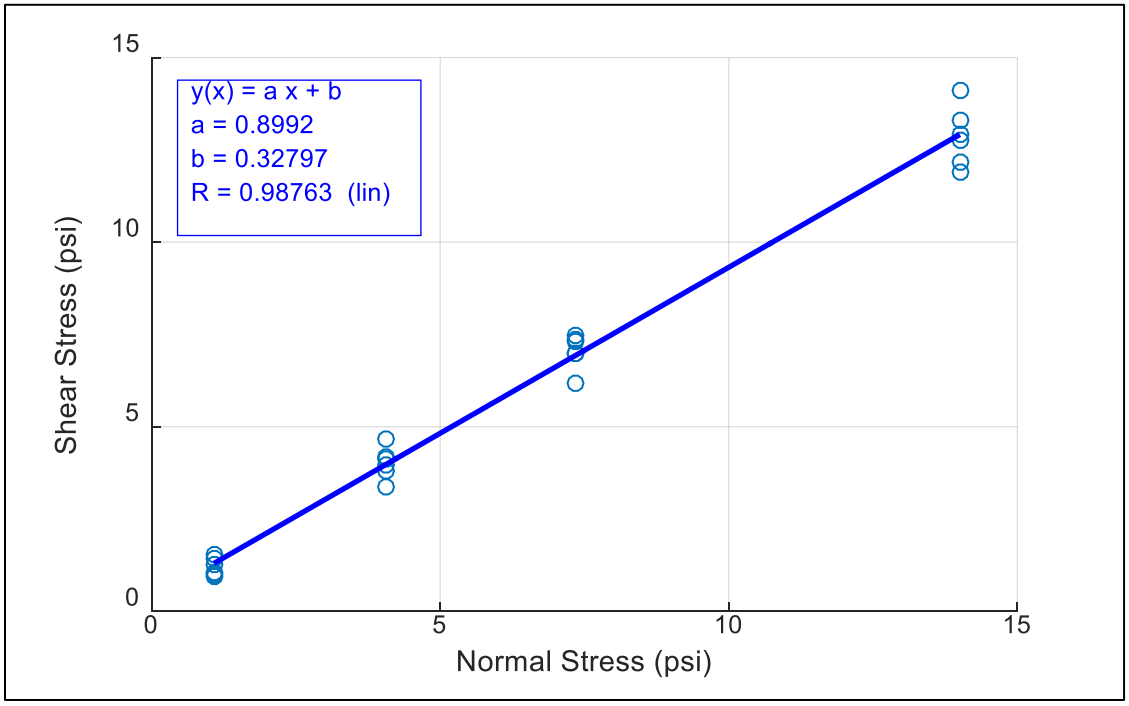

Figure 3-3. Shear stress vs. normal stress: 0% organic content, pH 5

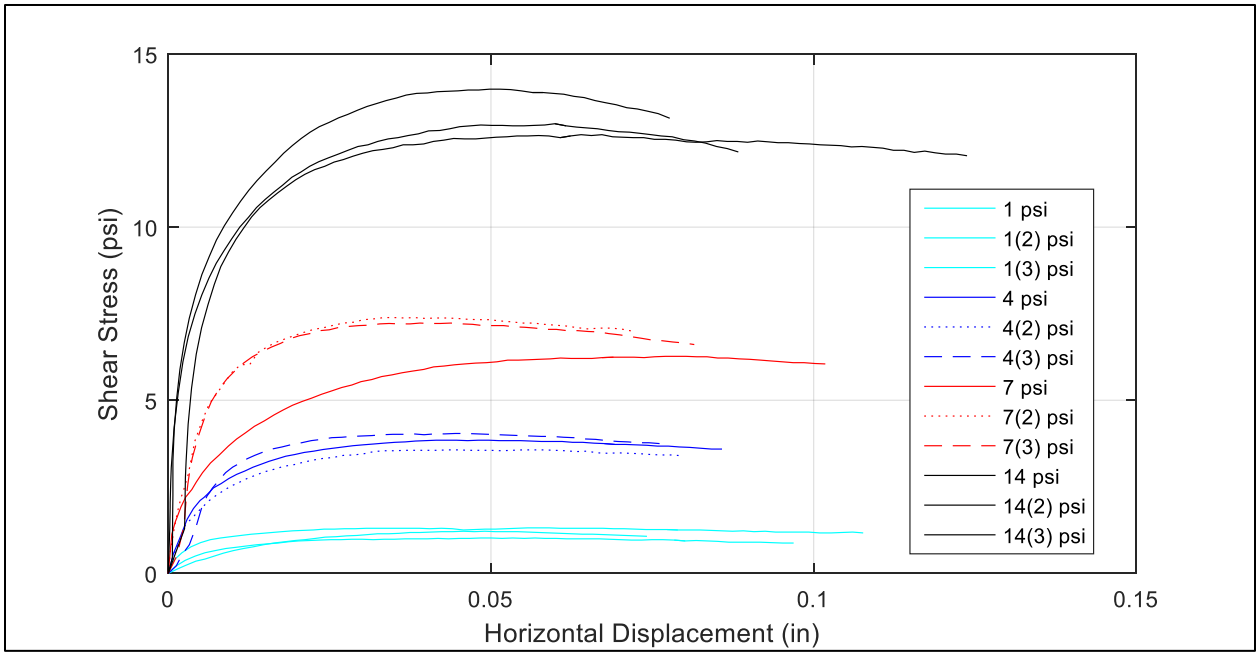

Figure 3-4. Horizontal displacement vs. shear stress: 0% organic content, pH 7

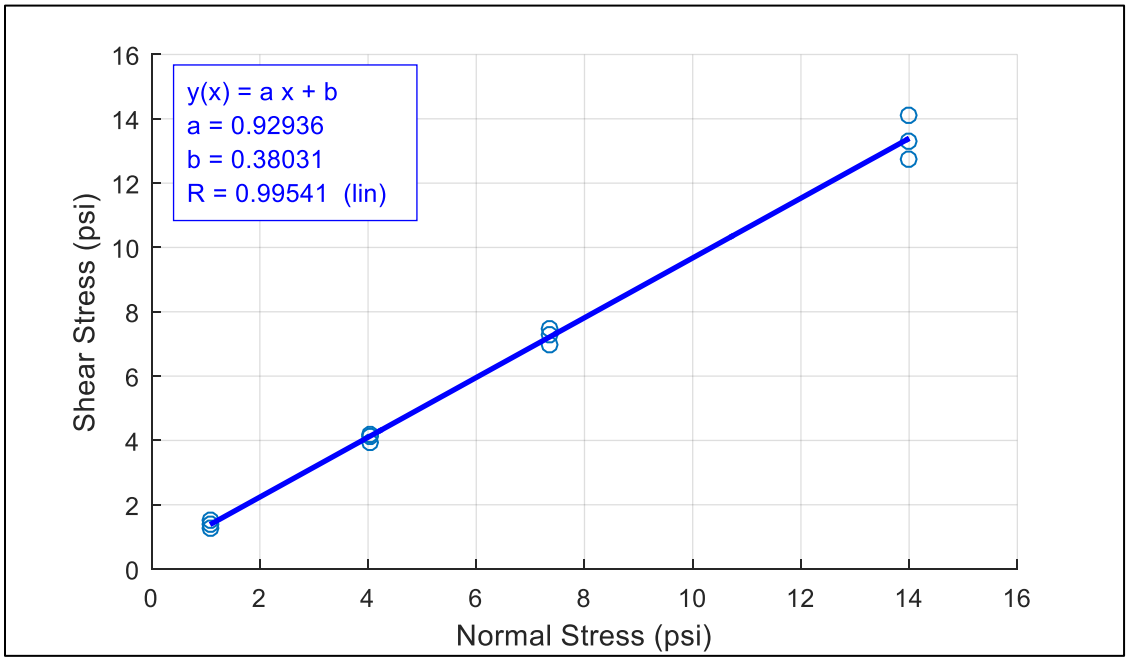

Figure 3-5. Shear stress vs. normal stress: 0% organic content, pH 7

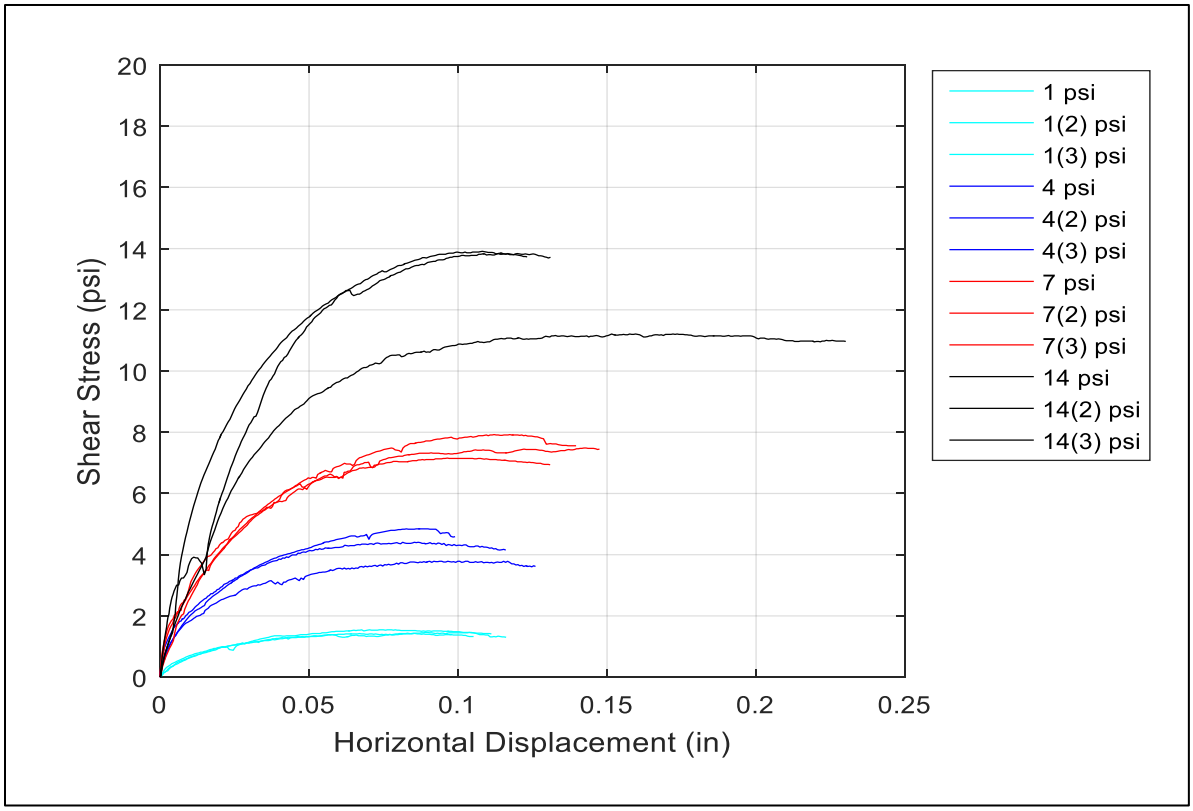

Figure 3-6. Horizontal displacement vs. shear stress: 10% organic content, pH 5

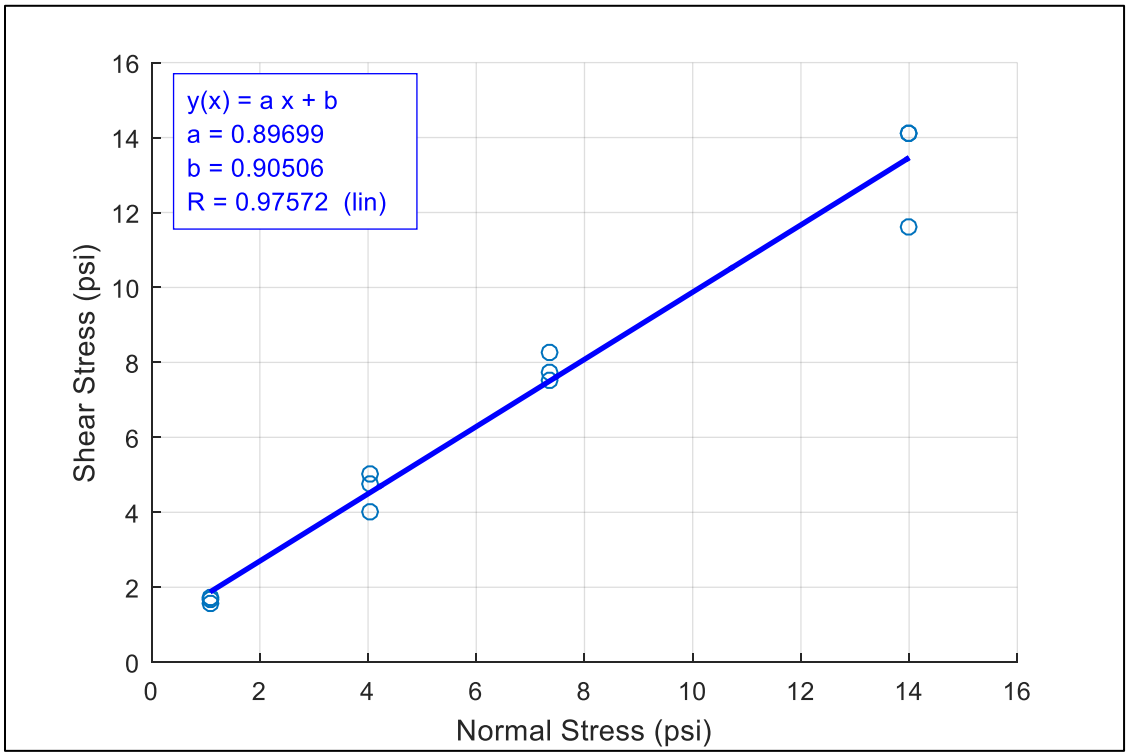

Figure 3-7. Shear stress vs. normal stress: 10% organic content, pH 5

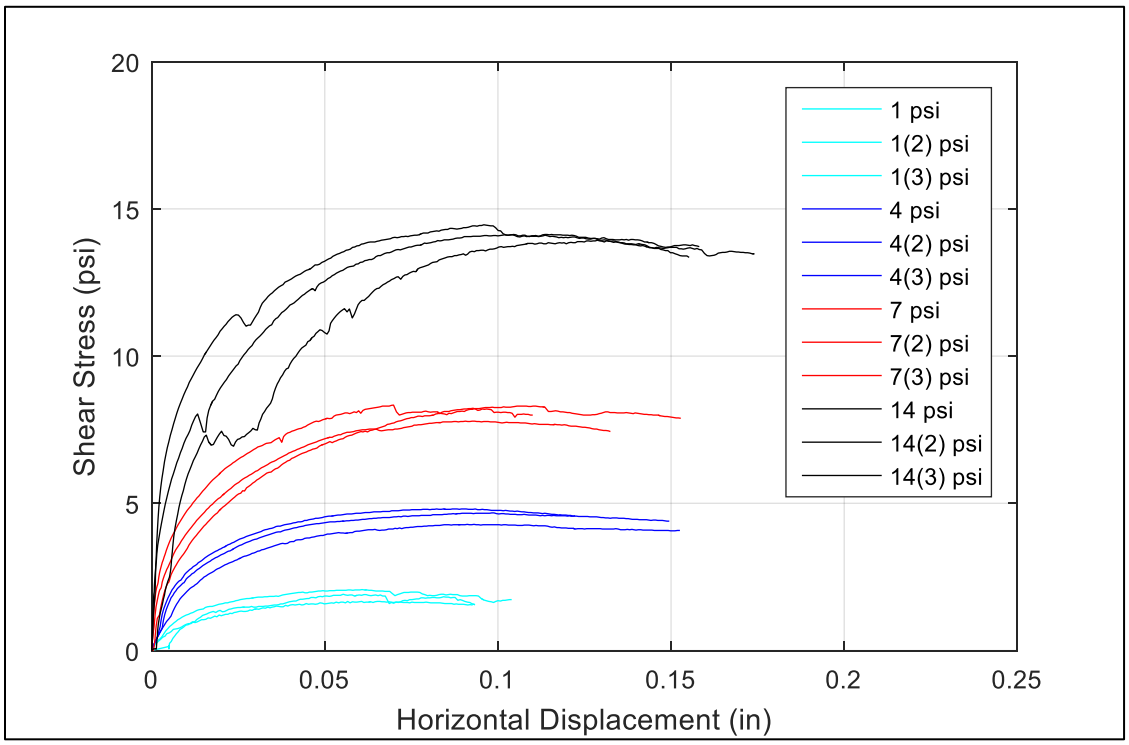

Figure 3-8. Horizontal displacement vs. shear stress: 10% organic content, pH 7

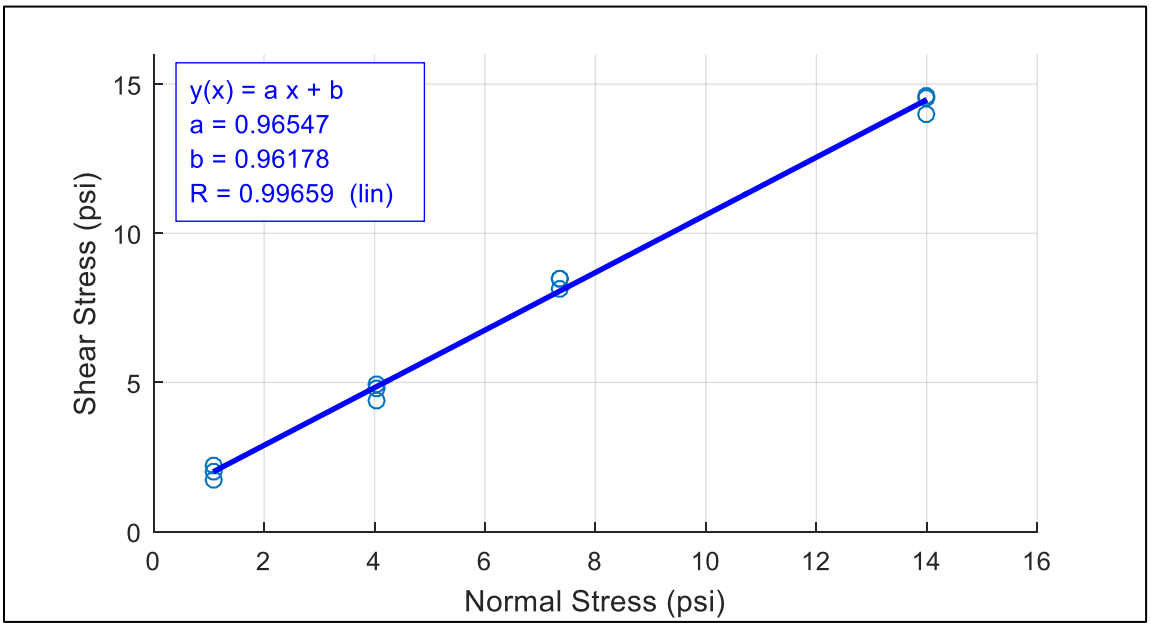

Figure 3-9. Shear stress vs. normal stress: 10% organic content, pH 7

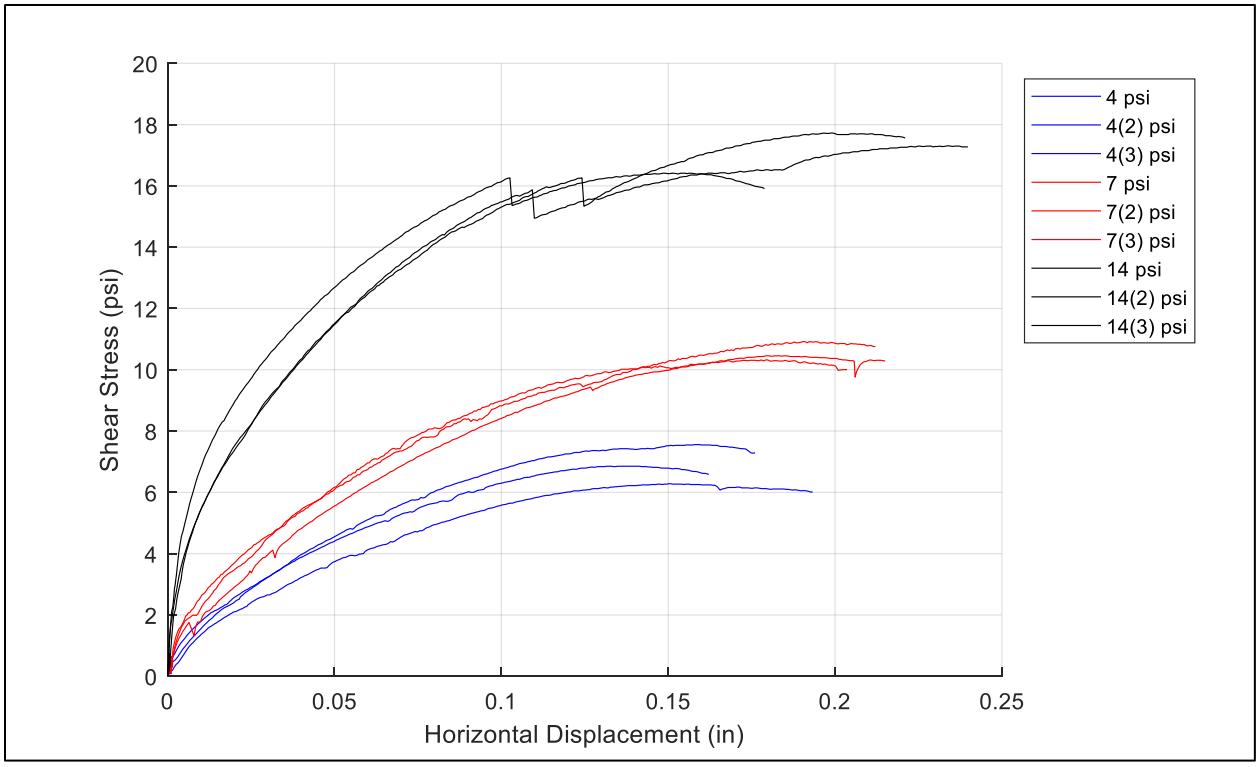

Figure 3-10. Horizontal displacement vs. shear stress: 30% organic content, pH 5

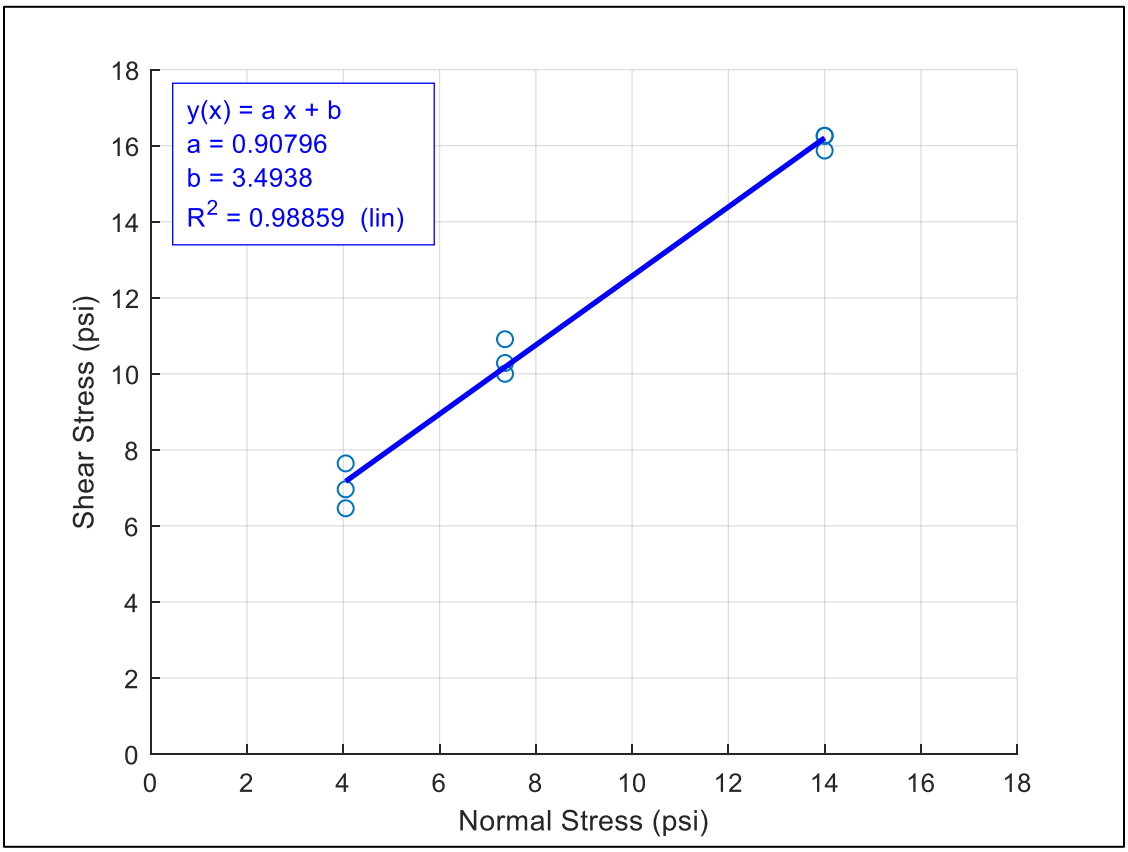

Figure 3-11. Shear stress vs. normal stress: 30% organic content, pH 5

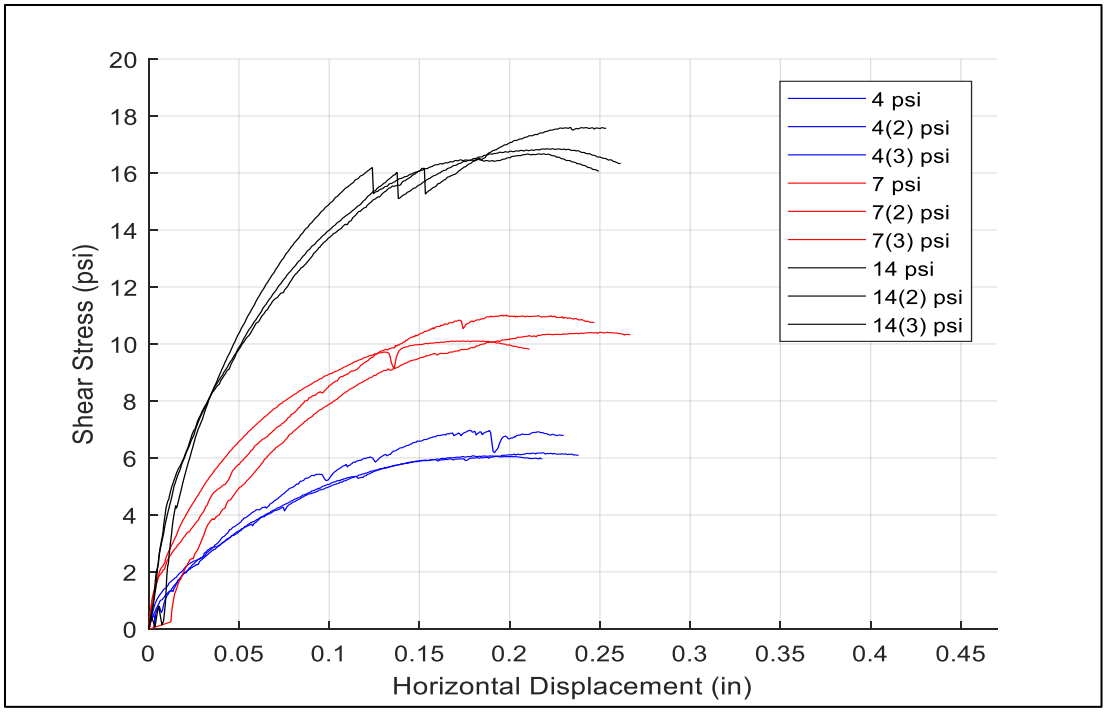

Figure 3-12. Horizontal displacement vs. shear stress: 30% organic content, pH 7

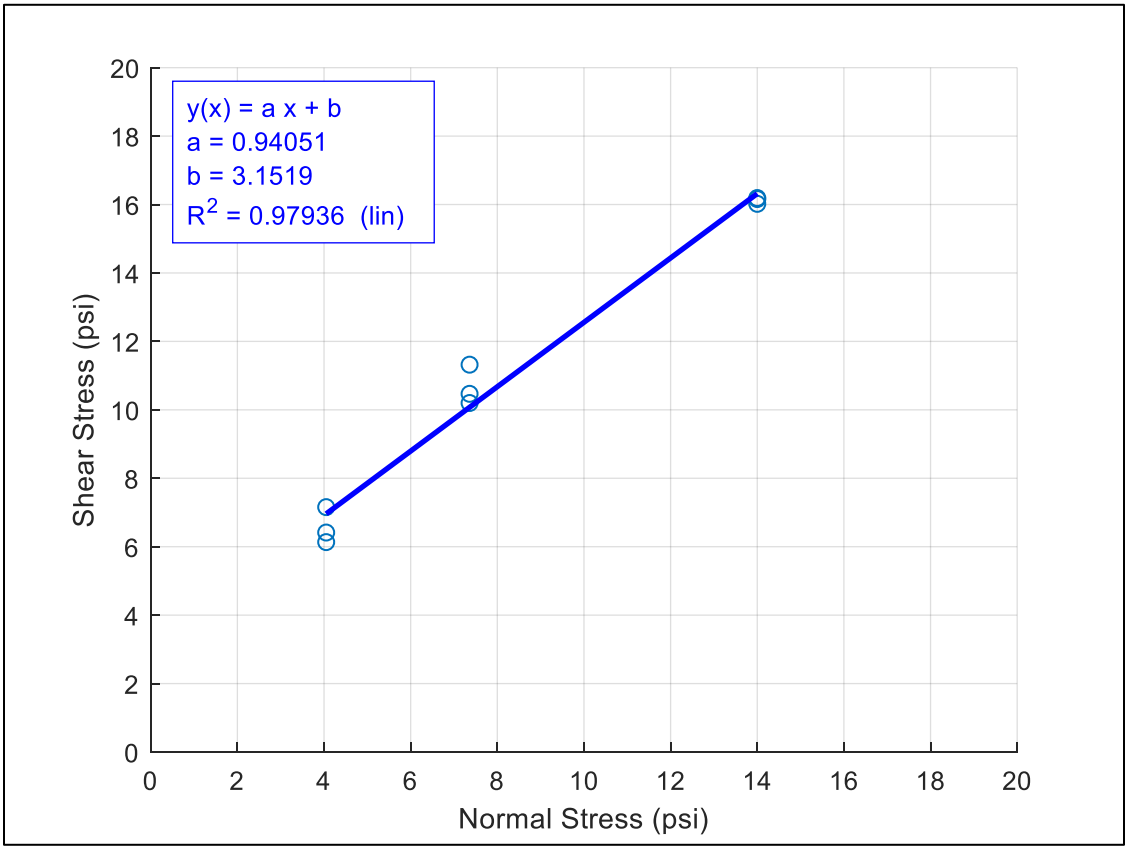

Figure 3-13. Shear stress vs. normal stress: 30% organic content, pH 7

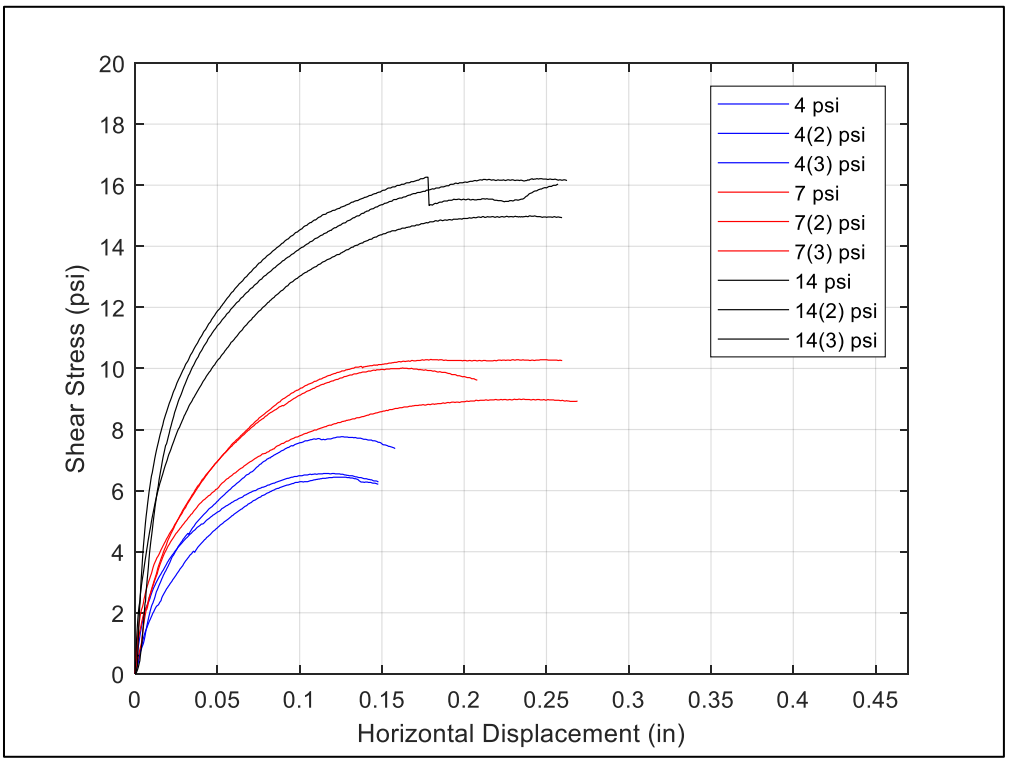

Figure 3-14. Horizontal displacement vs. shear stress: 50% organic content, pH 5

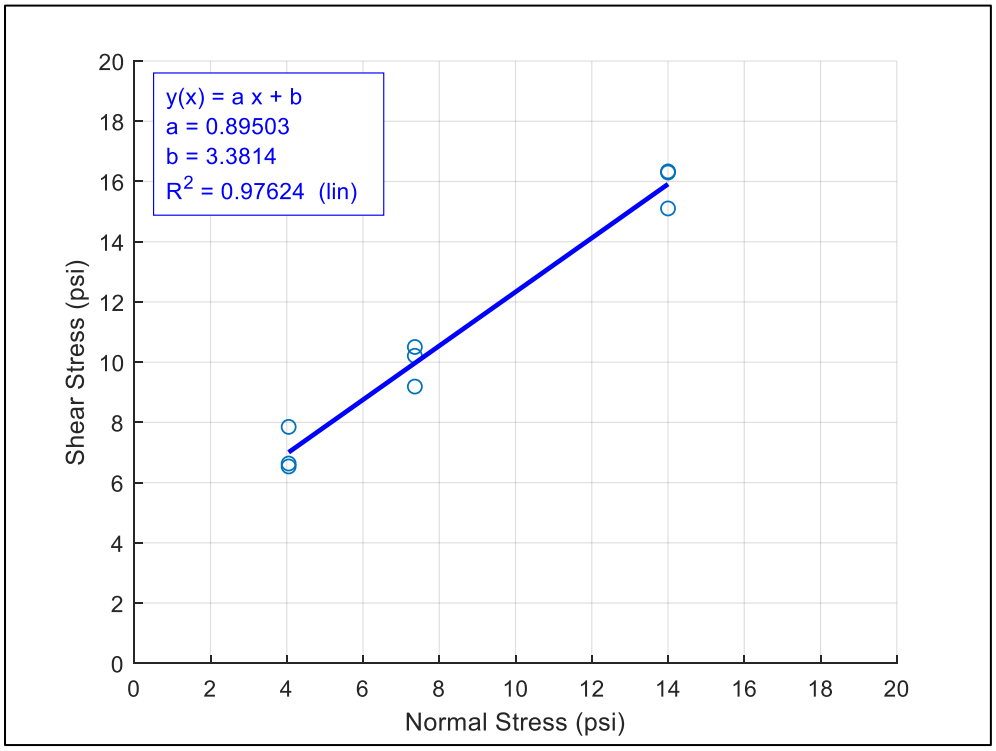

Figure 3-15. Shear stress vs. normal stress: 30% organic content, pH 5

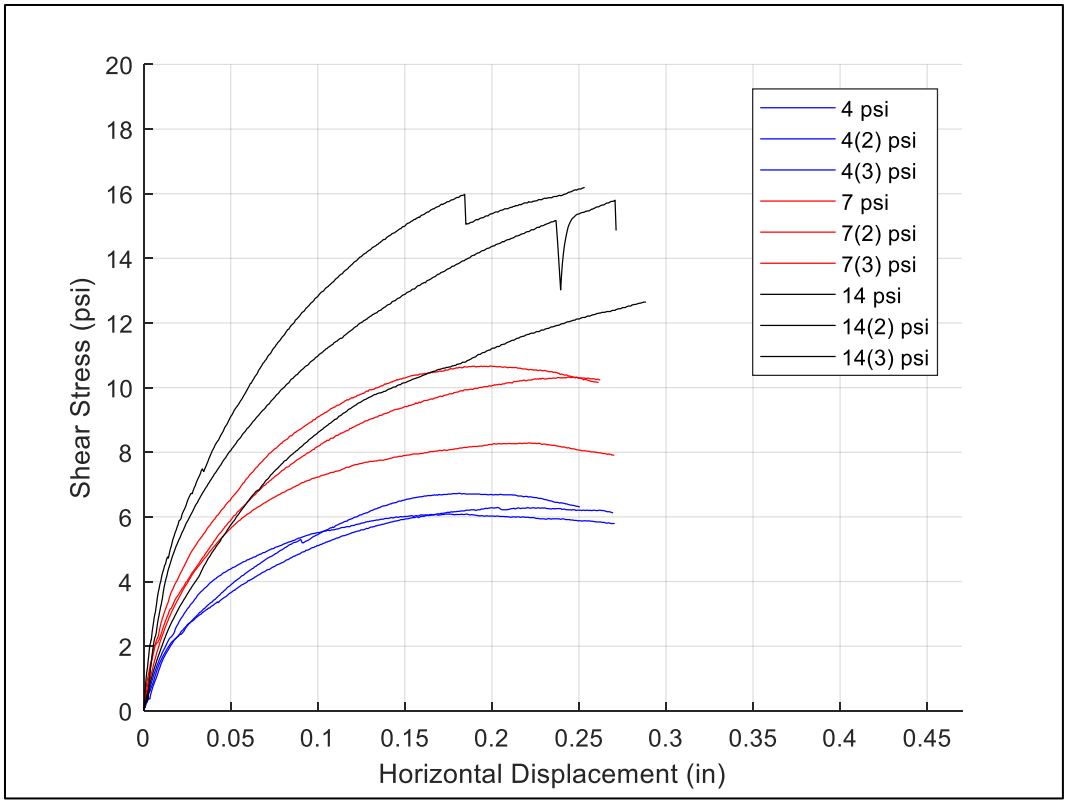

Figure 3-16. Horizontal displacement vs. shear stress: 50% organic content, pH 7

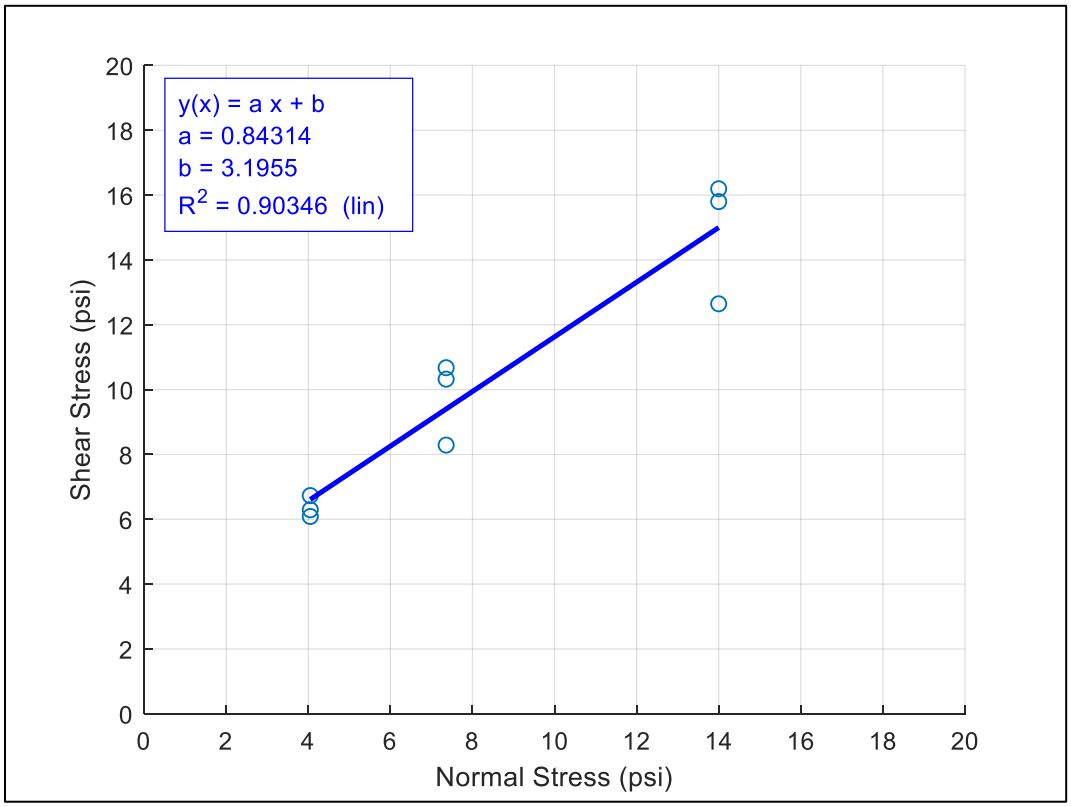

Figure 3-17. Shear stress vs. normal stress: 50% organic content, pH 7

Table 3-1. Untreated, saturated direct shear test results

Soil	pH	Angle of Internal Friction (deg)	Cohesion(psi)	Initial Total Unit Weight (pcf)
0% OC	5	42.0	0.33	107
	7	42.9	0.38	107
10% OC	5	41.9	0.91	100
	7	44.0	0.97	100
30% OC	5	42.2	3.5	78
	7	43.2	3.2	78
50% OC	5	41.8	3.4	57
	7	40.1	3.2	57

3.2 Organic Column Treatments

In parallel with control testing, several organic-rich soil columns were treated using the same technique referenced in Chapter 2. These data are summarized below in Table 3-2.

Table 3-2. Organic column treatment summary table (X means very small cementation volume)

Specimen	**Percent Organic Content**	**Height Affected (inches)**	**Stiffened or Cemented?**
J19-X	30	2.25	Cemented
J19-2	10	1.5	Cemented
J20-0	10	X	X
J20-1	10	X	X
J20-2	10	X	X
J20-3	30	X	X
J20-4	30	X	X
J20-X	30	X	X
J21-1	10	3.5	Stiffened
J21-2	10	1	Stiffened
J21-3	30	X	X
J21-4	30	2	Stiffened
J21-X	50	X	X
J22-1	10	X	X
J22-2	10	X	X
J22-3	30	X	X
J22-4	30	X	X
J22-X	50	X	X

In Table 3-2, “cemented” means that specimens were cemented together enough to cut a specimen for physical property testing. “Stiffened” means that some calcite precipitation was observed, but in small amounts that would not allow the organic soil matrix to cement together enough to cut

specimens for physical property testing. As shown, after 18 treatments, only two organic specimens were sufficiently cemented to allow for a physical property test sample and neither was at a high (i.e., 50%) organic content. Clearly, insufficient specimens were produced to conduct a DST analysis. A photograph of a typical post-percolation treated organic-rich specimen in presented below in Figure 3-18.

Figure 3-18. Typical organic-rich specimen after MICP treatment using the percolation method showing we specimen immediately after extraction (left) and specimen after drying (right)

3.3 Consolidation Testing

Since treatment success was so limited, it was not possible to conduct a full suite of consolidation tests on treated specimens. Consolidation testing was conducted on specimen J19-X to characterize its behavior. Results (Figure 3-19 through 3-29; Table 3-3Table through Table 3-7) showed some consolidation improvement compared to the untreated 30% organic content soil results. In addition, results indicated that this organic specimen behaved similarly under loading as the treated sand specimens. Compression under loading appeared to occur until the $CaCO_3$ bonds yield resulting in a higher rate of compression (steeper secondary slope). The most significant improvement appears to occur during primary consolidation, while there appears to be negligible improvement during secondary compression. It is believed this occurred because the calcite bonded to the silica particles from the Ottawa sand, but it failed to bond to the organic soil particles. This mechanism will be explained in much more depth in Chapter 4.

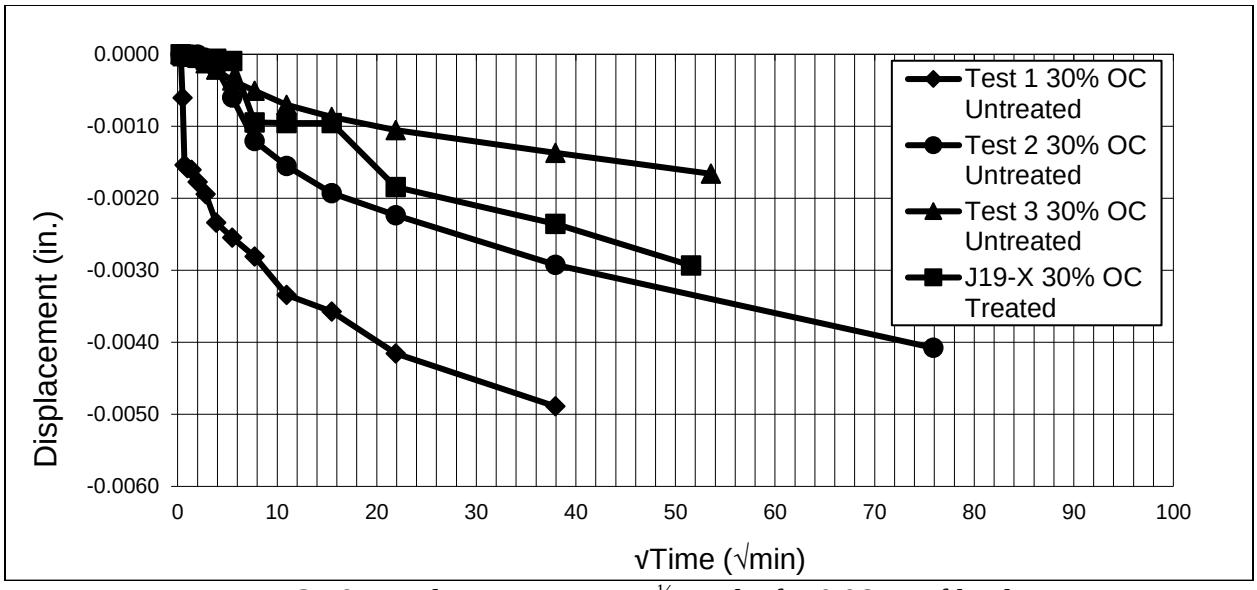

Figure 3-19. Displacement vs. time^{½} results for 0.0625-tsf loading

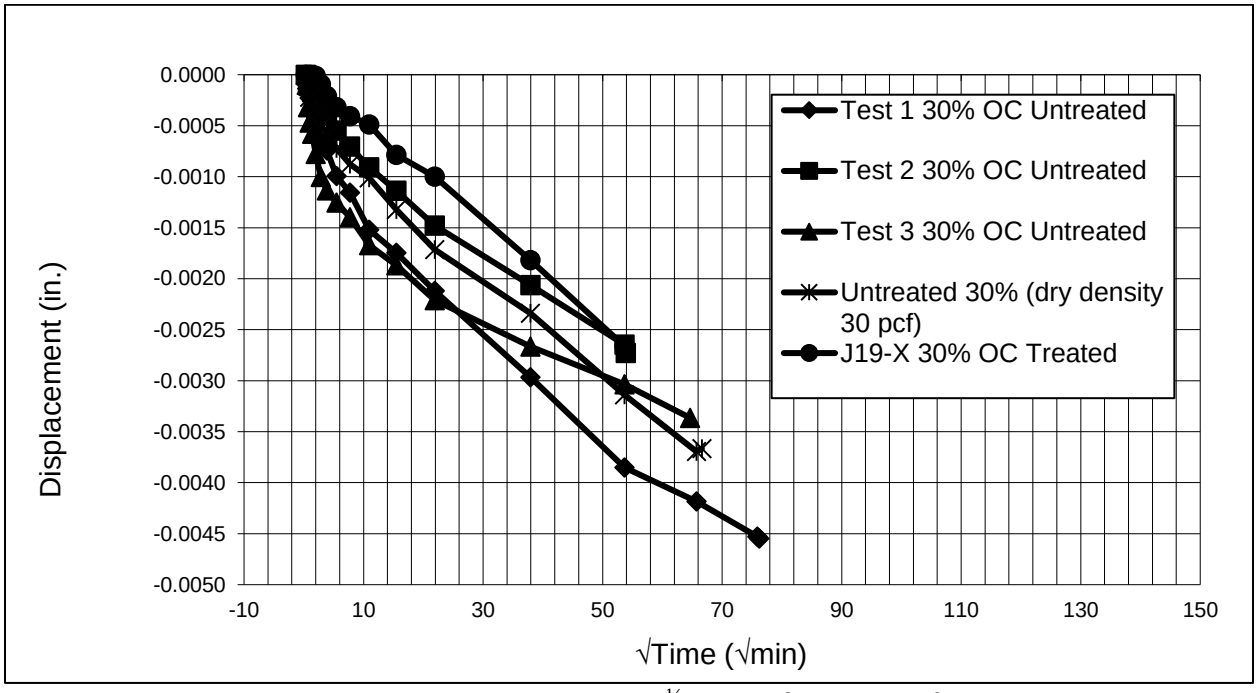

Figure 3-20. Displacement vs. time^{½} results for 0.125-tsf loading

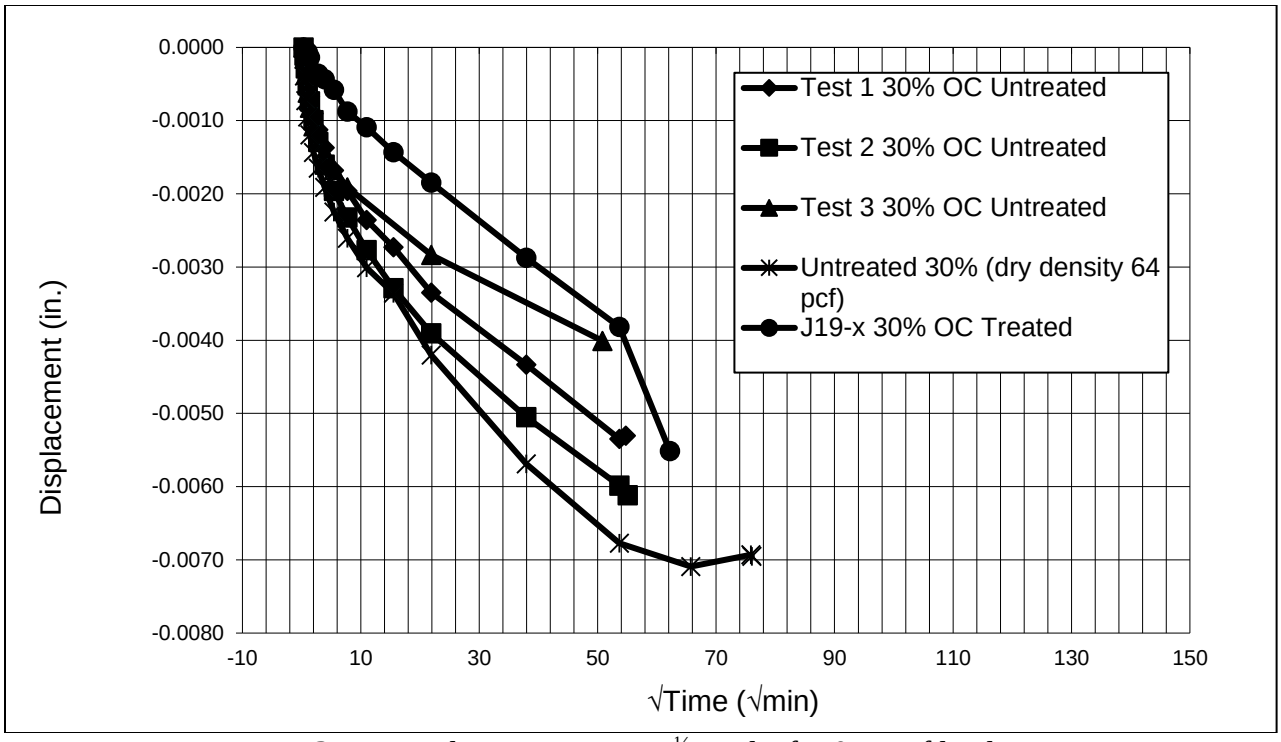

Figure 3-21. Displacement vs. time^{½} results for 0.25-tsf loading

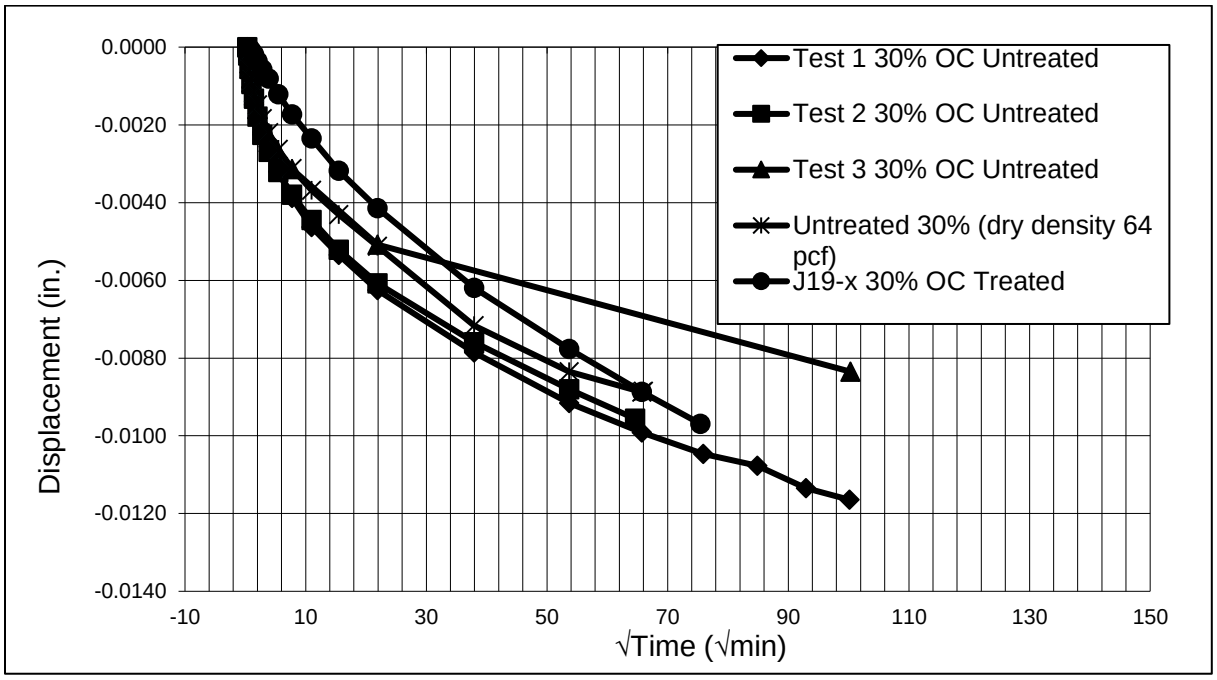

Figure 3-22. Displacement vs. time^{½} results for 0.5-tsf loading

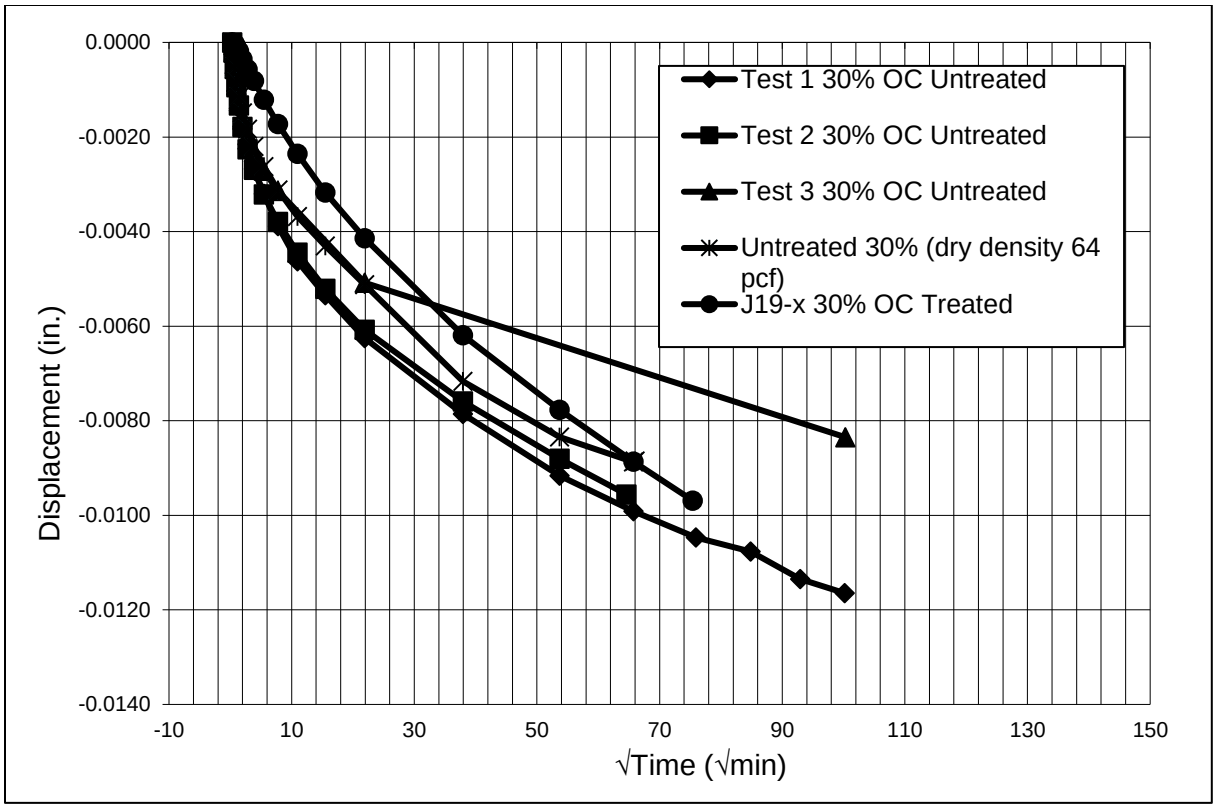

Figure 3-23. Displacement vs. time^{½} results for 1-tsf loading

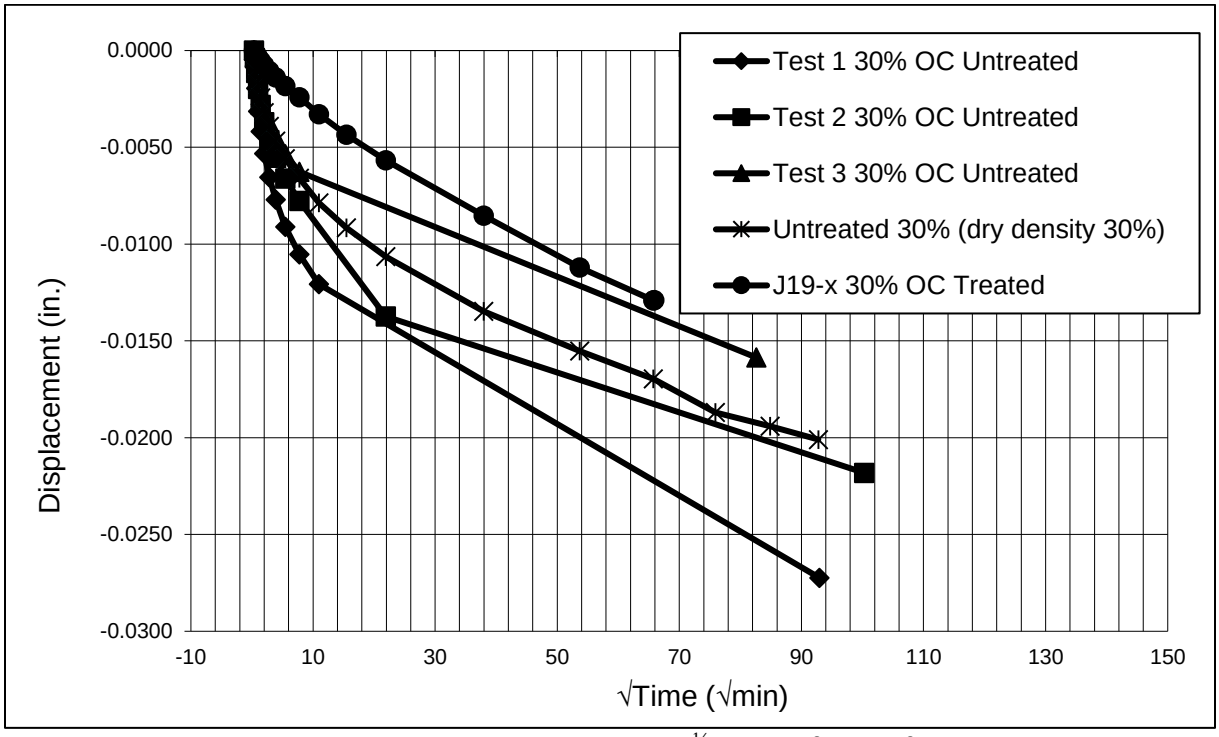

Figure 3-24. Displacement vs. time^{½} results for 2-tsf loading

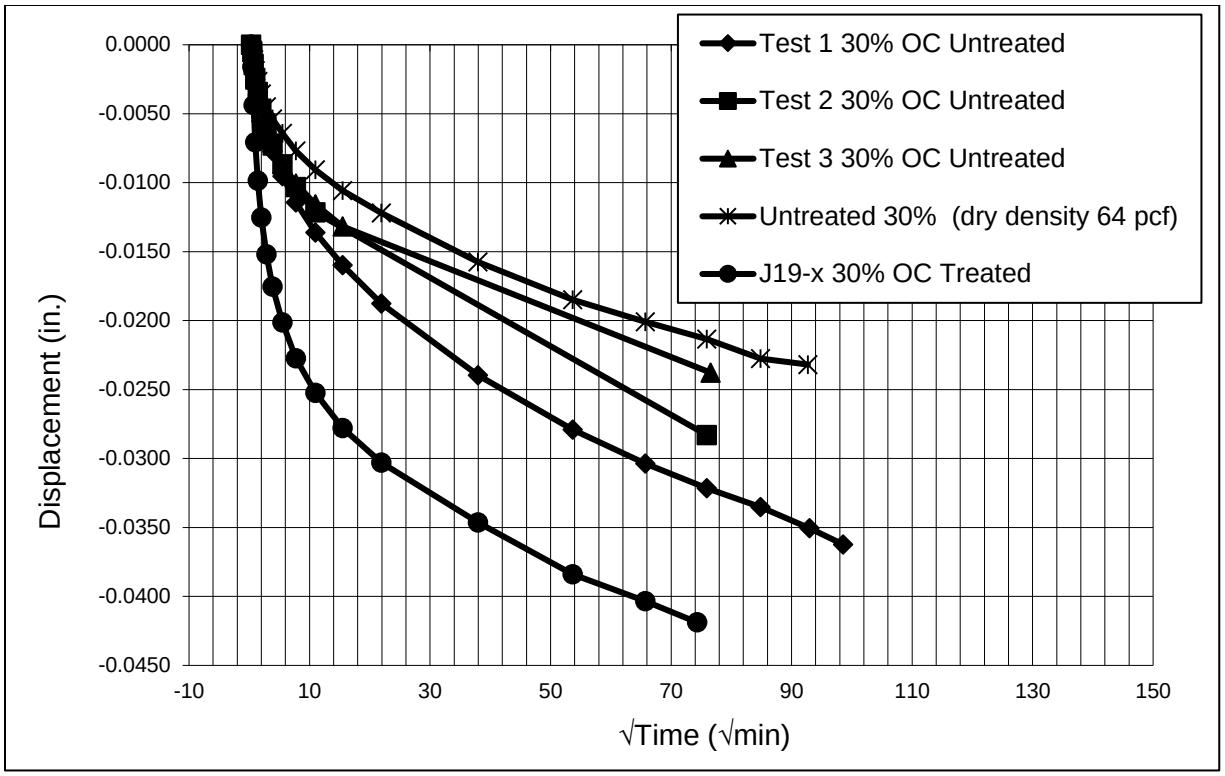

Figure 3-25. Displacement vs. time^{½} results for 4-tsf loading

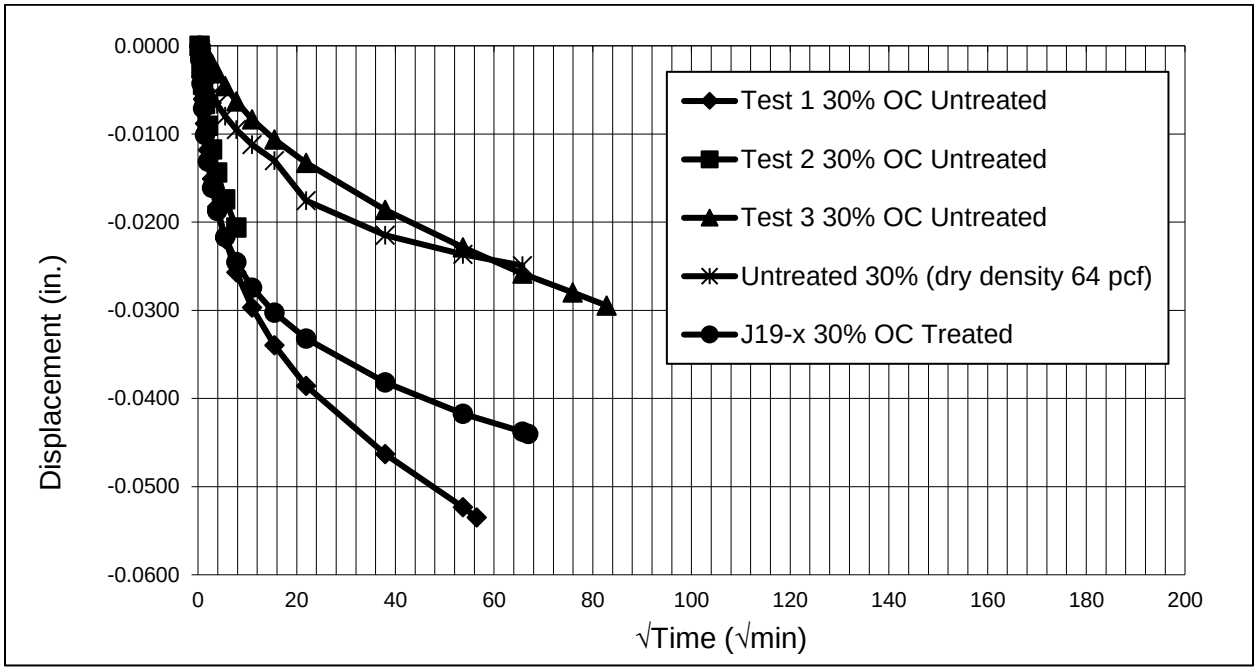

Figure 3-26. Displacement vs. time^{½} results for 8-tsf loading

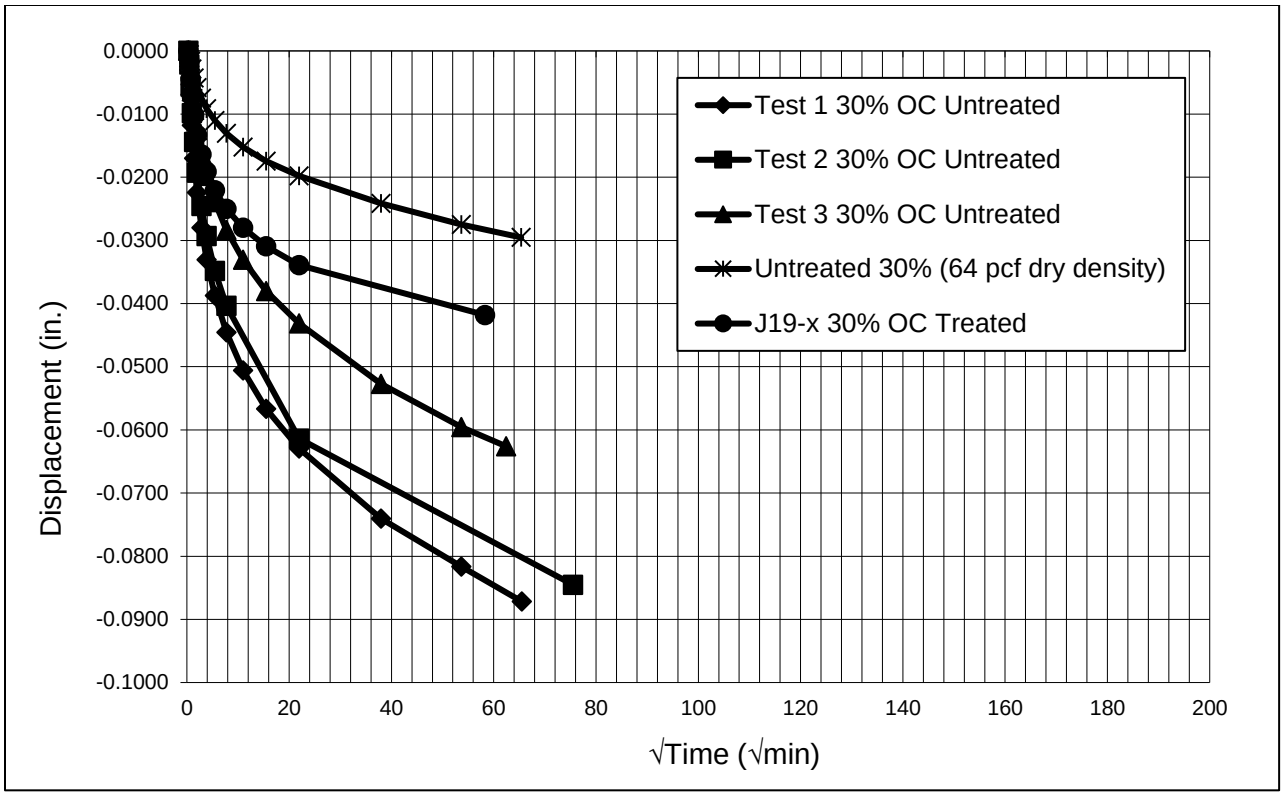

Figure 3-27. Deformation vs. time^{½} results for 16-tsf loading

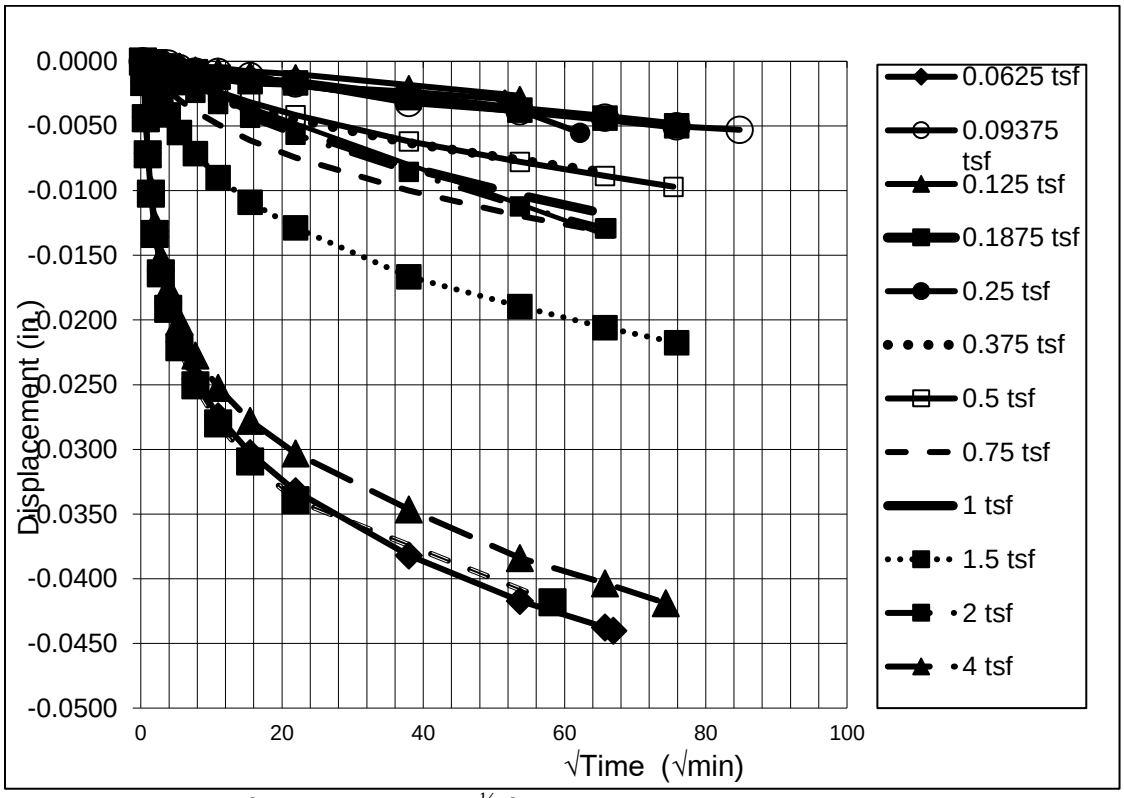

Figure 3-28. Deformation vs. time^{½} for treated 30% organic content soil with 3.24% $CaCO_3$

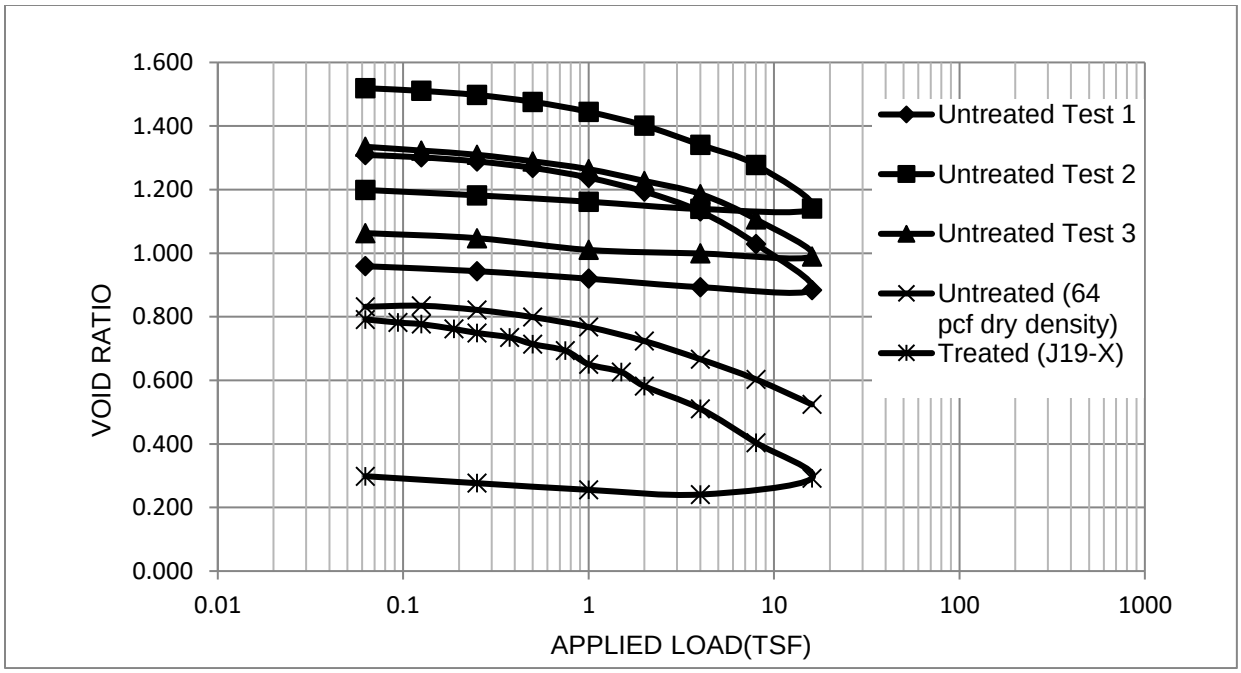

Figure 3-29. Consolidation curves for untreated and treated 30% organic content soil

Table 3-3. Summary of end of primary consolidation for untreated and treated 30% organic content soil

End of primary consolidation using Taylor's method (mins)					
30%	UNTREATED				TREATED
Load (tsf)	Test 1	Test 2	Test 3	64 pcf dry density	J19-X
0.0625	15	15	120	1	729
0.125	8	8	4	2	41
0.25	4	6.25	4	1	169
0.5	4	4	2	2	250
1	2.25	5	2	2	676
2	2.56	4	4	2	15
4	4	2	8	4	4
8	4.4	8	144	2	4
16	8	4	4	4	4

Table 3-4. Summary of coefficient of consolidation for untreated and treated 30% organic content soil

Coefficient of consolidation, C_v (m^2/yr)					
30%	UNTREATED				TREATED
Load (tsf)	Test 1	Test 2	Test 3	64 pcf dry density	J19-X
0.0625	157.26	160.06	18.73	817.20	1.08
0.125	294.93	300.10	561.88	408.60	19.59
0.25	589.86	384.16	561.88	817.20	4.74
0.5	589.86	600.30	1123.75	408.60	3.23
1	1048.62	480.18	1123.75	408.60	1.18
2	921.61	600.30	561.88	408.60	53.50
4	589.86	1200.50	280.94	204.30	200.53
8	536.15	300.10	15.61	408.60	200.53
16	294.93	600.30	561.88	204.30	200.53

Table 3-5. Summary of permeability for untreated and treated 30% organic content soil

Permeability, k (cm/s)					
30%	UNTREATED				TREATED
Load (tsf)	Test 1	Test 2	Test 3	64 pcf dry density	J19-X
0.0625	5.56E-07	1.37E-07	1.60E-08	1.56E-06	1.04E-11
0.125	5.31E-07	5.65E-07	1.19E-06	3.46E-07	5.43E-10
0.25	6.78E-07	3.72E-07	6.49E-07	1.42E-06	1.65E-10
0.5	4.59E-07	5.36E-07	9.76E-07	6.22E-07	9.63E-11
1	8.44E-07	3.42E-07	7.22E-07	4.35E-07	3.70E-11
2	3.94E-07	2.71E-07	2.61E-07	3.15E-07	9.13E-10
4	2.39E-07	3.63E-07	7.75E-08	1.05E-07	1.42E-09
8	1.55E-07	7.62E-08	4.16E-09	1.22E-07	1.15E-09
16	6.87E-08	1.48E-07	1.29E-07	3.97E-08	6.54E-10

Table 3-6. Summary of sample properties and consolidation parameters for untreated and treated 30% organic content soil

30% OC	Untreated			Treated J19-X
	Test 1	Test 2	Test 3	
Primary compression index, C_{ci} (before P_c)	0.35	0.382	0.344	0.0872
Compression index, Cc (after P_c)	N/A	N/A	N/A	0.3062
Primary recompression index, Cr	0.041	0.034	0.032	0.0319
Initial void ratio	1.33	1.53	1.34	0.795
pH	5.39			7.47
$CaCO_3$ (%)	0	0	0	3.24
Initial moisture content(%)	67.8	67	68.9	--
Wet density(pcf)	84.0	78.1	84.2	65.03
Dry density(pcf)	50.1	46.8	49.9	65.03

Table 3-7. Summary of secondary compression for untreated and treated 30% organic content soil

30%	**Untreated**			**Treated**
	Test 1	**Test 2**	**Test 3**	**J19-X**
Load (tsf)	**Secondary compression index (C_α)**			
0.0625	0.00117	0.00144	0.00084	0.00190
0.09375	N/A	N/A	N/A	0.00495
0.125	0.00237	0.00098	0.00066	0.00303
0.1875	N/A	N/A	N/A	0.00554
0.25	0.00164	0.00171	0.00108	0.00380
0.375	N/A	N/A	N/A	0.00781
0.5	0.00401	0.00248	0.00180	0.01101
0.75	N/A	N/A	N/A	0.01237
1	0.00270	0.00352	0.00264	0.01440
1.5	N/A	N/A	N/A	0.01620
2	0.00565	0.00549	0.00396	0.01569
4	0.00968	0.00714	0.00683	0.01969
8	0.01633	0.01524	0.01203	0.01839
16	0.02493	0.02614	0.02009	0.01636

3.4 Discussion

While consolidation data showed some positive signs for treating organic-rich soil via MICP, Table 3-2 shows that the method used throughout this chapter was mostly ineffective. It was concluded that a better method was needed to treat organic-rich soils.

CHAPTER 4
TREATMENT OF ORGANIC-RICH SOIL SPECIMENS USING A PRE-MIXING METHOD AND SODIUM DODECYL SULFATE

4.1 Introduction

While this project was ongoing, Mujah et al. (2016) published a paper that discussed various methods in which MICP treatment may be initiated. While the percolation method described throughout Chapter 2 and Chapter 3 is the most-studied treatment method, its drawback is non-uniform calcium carbonate distribution – very similar to the results described throughout Chapter 2. This non-uniform calcite distribution is thought to be the result of pore-clogging, and it may lead to variations both in terms of strength and hydraulic conductivity in treated specimens. Currently, active research is being conducted by others to enhance the percolation treatment method using micro-dosing whereby bacteria and feed stock are introduced alternately and repeatedly into the specimen undergoing treatment. Ultimately, this method may be optimized. In addition, results presented in Chapter 3 indicated that the percolation treatment methodology was ineffective for organic-rich soil. Results from Chapter 2 and Chapter 3 indicated that a change in approach was warranted.

Mujah et al. (2016) discussed an alternative to the pre-mixing treatment method whereby bacteria, urea, and calcium chloride are introduced to the soil in high concentrations. These constituents are mixed with the soil until near homogeneity is achieved. Then, the specimens are allowed to cure. Yasuhara et al. (2012) and Zhao et al. (2014a) reported significant increases in unconfined compressive strength (UCS) when compared with untreated specimens using such a method. Zhao et al. (2014b) reported a pre-mixing method whereby bacteria and sand were submerged in a calcium chloride/urea bath. However, Mujah et al. (2016) point out that the mixing method may have its issues in terms of disturbing soil from its in situ stress state.

After numerous discussions with this project's project manager (PM), all parties agreed that despite these possible drawbacks to the pre-mixing method, pre-mixing gave investigators the greatest chance to produce nearly uniform specimens. If the issues associated with MICP calcification discussed in Chapter 3 were the result of heterogenous bacteria/urea/calcium chloride distribution, the pre-mixing method would solve these issues. As a result, all parties agreed to conduct a series of experiments using pre-mixed specimens. If successful, field implementation would be similar to grout-mixing.

4.2 Pre-Mixing Methodology and Preliminary Results

Specifics of the pre-mixing method are as follows:

- Soils were pluviated into two-inch by four-inch plastic cylinder molds until the molds were approximately 75% full.
- A bacterial solution of *Sporosarcina* cultured to an optical density (OD) greater than 2.0 was added to the soil and hand mixed using a spatula.

- A 2.5M urea/2.5M calcium chloride solution was added to the soil/bacterial mixture. The urea/calcium chloride/bacteria/soil was hand-mixed using a spatula until near-homogeneity was achieved.

- The specimens were allowed to cure for a minimum for 48 hours.

- After curing, the molds were opened using a Dremel® tool and the specimens were extracted.

The above technique was first tested using 50/70 Ottawa sand, and significant calcification was observed. Ottawa 50/70 specimen cementation was nearly homogeneous (Figure 4-1).

Figure 4-1. Example of fully-cemented 50/70 Ottawa sand specimen

When the procedure above was repeated using the organic-rich soil, significant cementation was observed when organic content was 10%. When organic content increased to 30%, less cementation was observed. At 50% organic content, no significant cementation was observed (Figure 4-2).

Figure 4-2. Typical results using pre-mixing MICP treatment in organic-rich specimens from Polk County, FL

These results appeared to confirm that the bacteria were effectively releasing urease and that the urease was driving calcium carbonate formation. However, as hypothesized, the calcium carbonate was not adhering to the organic particles as effectively as it adhered to the silica particles from the Ottawa sand.

4.3 Soil Particle Geochemistry and the Rationale for Use of a Surfactant

In general, Florida organic-rich soils are usually created by the decomposition of living matter (plant, animal, and insect remains). Water soluble compounds tend to be dissolved and removed leaving behind the aliphatic organic compounds. The aliphatic organic compounds are typically composed of carbohydrates, fats, lignins, and proteins. As decomposition occurs, aliphatic organics are broken down into simple water insoluble compounds. What remains is a plethora of medium to large sized compounds composed mainly of carbon, hydrogen, and oxygen. These particles tend to be nonpolar due to the small differences in electronegativity between hydrogen and carbon, as shown in Figure 4-3. These compounds have neither diploes nor the ability to hydrogen bond and are repelled by polar substances.

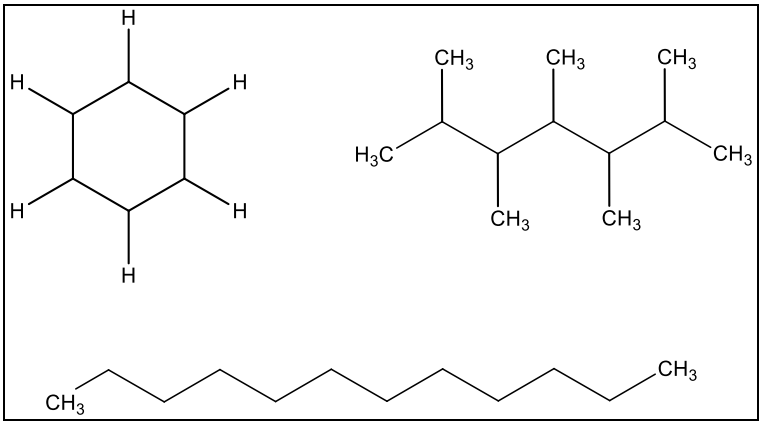

Figure 4-3. Typical molecular structure of aliphatic organic compounds; top-right is cyclohexane; top-left is 2,3,4,5,6-methylheptane; bottom is decane

Figure 4-3 shows organic materials lacking oxygen content; as such, they are completely hydrophobic. When organic material contains oxygen or other heteroatoms, which can be hydrophilic, the degree of hydrophobicity depends upon the length of the carbon chain and/or total carbon content (in the case of cyclic compounds). In general for organic-rich soils, oxygen content and subsequently hydrophobicity prevails. Hydrophobicity implies that in general, organic-rich soils are nonpolar because these soils do not hydrogen bond with water.

Of course, clay, absorbed water, quartz, etc. are polar compounds that are present in organic-rich soils. These continents may absorb cations such as Na^+, K^+, Ca^{2+}, Mg^{2+}, etc. The presence of inorganic compounds varies from 10% to 90% globally and affects the cation exchange capacity (CEC) of the bulk soil overall. But, without the presence of significant ionic solutes, an organic-rich soil will tend to have a net-zero surface polarity (Manahan, 2010). The soil in this study appeared to be hydrophobic based upon several water-solubility tests that were conducted prior to treatment.

On the other hand, much like water molecules, quartz sand tends to be mostly polar. While the structure of quartz (Figure 4-4) does not strictly have a negative charge, it is similar to water in that the peripheral surface oxygen have a partial negative charge resulting from the dipole created by the uneven distribution of electron density around the oxygens.

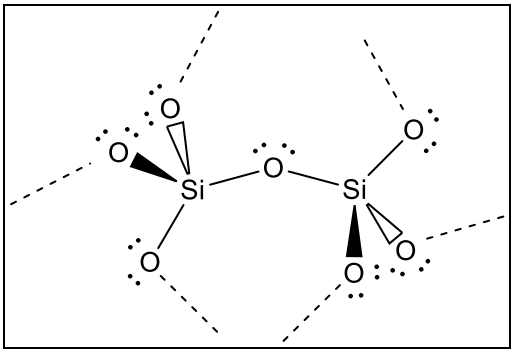

Figure 4-4. Molecular structure of quartz sand

Investigators hypothesized that the reason MICP was effective when silica particles were present and ineffective in the organic-rich soil from Polk County may be due to these sorts of polarity differences between relatively nonpolar organic surfaces and relatively polar quartz surfaces. During quartz sand treatment, the bacteria should first form calcite around the quartz particles followed by bridging between particles to create a meshed calcite network resulting in strong physical bonds between particles. When organic-rich material is used as a substrate instead, preliminary results appeared to indicate that this sort of bridging did not occur. To overcome this apparent bridging issue, a surfactant was chosen as a wetting agent. Investigators hypothesized that the surfactant should aid in calcification/cementation via two mechanisms:

1. A surfactant should serve as a wetting agent to solubilize OC-soil

2. Based upon results in quartz sand, *Sporosarcina* have demonstrated that some surface property associated with quartz sand aids in cementation. Investigators hypothesized that perhaps the bacteria were attracted to partial negative charge of the oxygen atoms. Some surfactants' chemical composition is similar to quartz sand in terms of surface polarity of the head. The "correct" surfactant may be able to mimic quartz sand surface polarity.

Sodium Dodecyl Sulfate (SDS; Figure 4-5) contains a linear twelve-carbon chain tail and polar sulfate head. From a charge perspective, the polar sulfate head mimics the surface polarity of the oxygen atoms present along quartz particles surfaces.

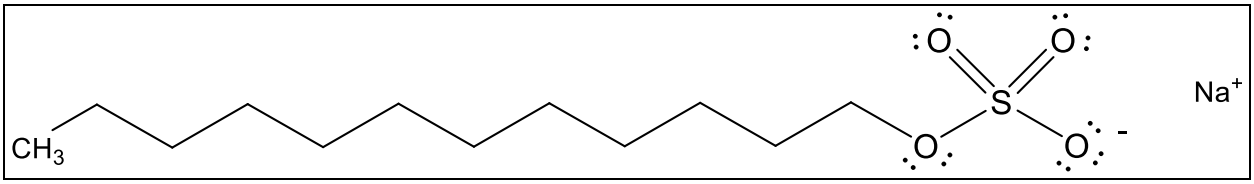

Figure 4-5. Sodium dodecyl sulfate (SDS)

4.4 Treatments and Testing using SDS

4.4.1 Methodology

Based upon these hypotheses, investigators mixed powdered SDS with organic-rich soil pre-treatment using a spatula. Various soil-dry SDS ratios (by weight) were treated via the mixing method discussed above in which bacteria, urea, and calcium chloride were added to the soil/SDS; stirred until near-homogeneity was achieved; and allowed to cure in 2-inch by 4-inch concrete cylinders for a minimum of 48 hours. Then, unconfined compressive strength (UCS) tests were conducted on the treated specimens (ASTM D2166). UCS was plotted as a function of % SDS, and best-fit regression curves were fit to the data. In addition, unconsolidated undrained (UU) triaxial (ASTM D4767) and consolidation testing (ASTM D2435) were conducted on several treated specimens at the FDOT State Materials Office (SMO) in Gainesville, FL.

4.4.2 Initial Results

Results from these UCS tests are presented below in Figure 4-6.

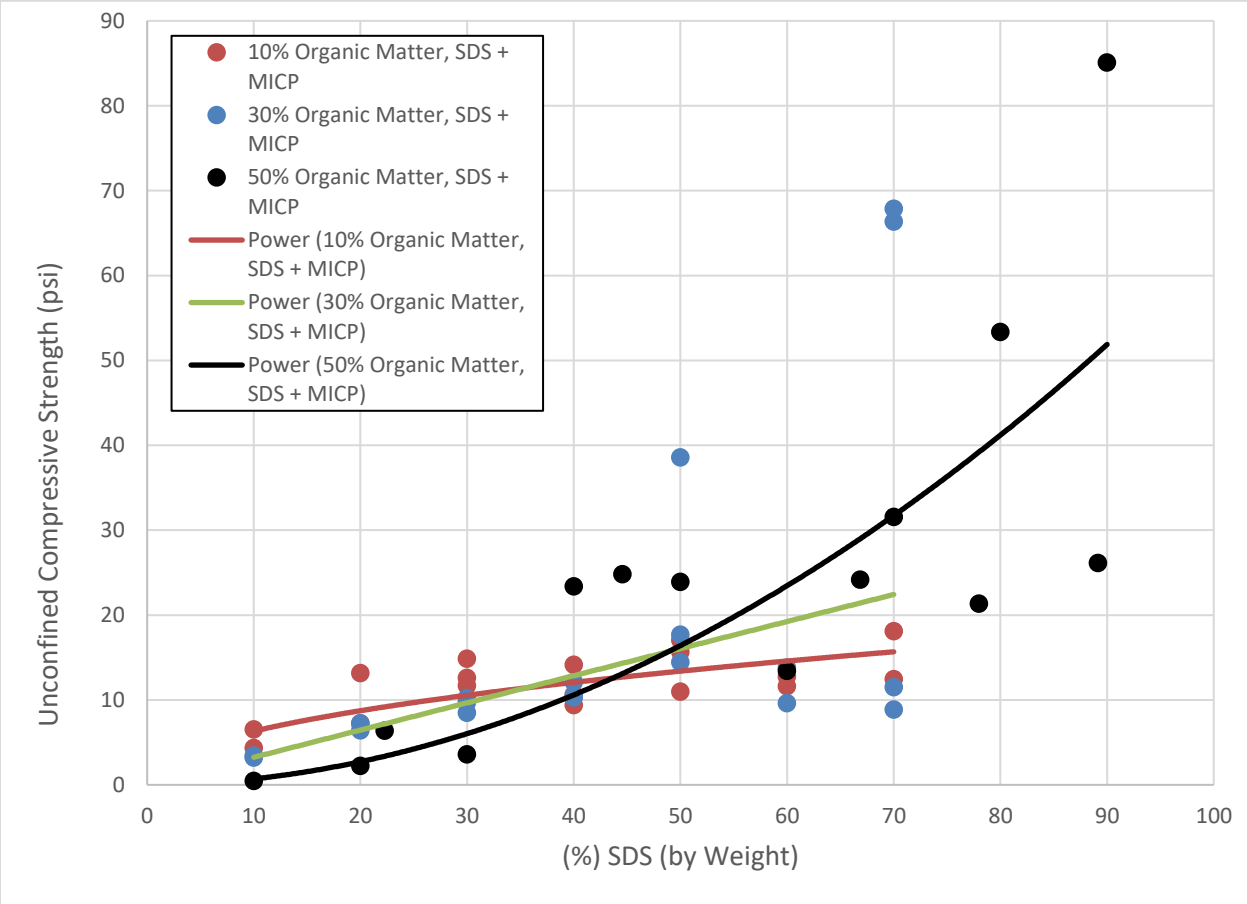

Figure 4-6. UCS testing results

In addition, several treated specimens were photographed (Figure 4-7). Visually, results were encouraging in that they indicated that cementation had been achieved and the SDS was functioning as anticipated. In addition, results indicated that in general, a direct relationship existed between SDS quantity and strength.

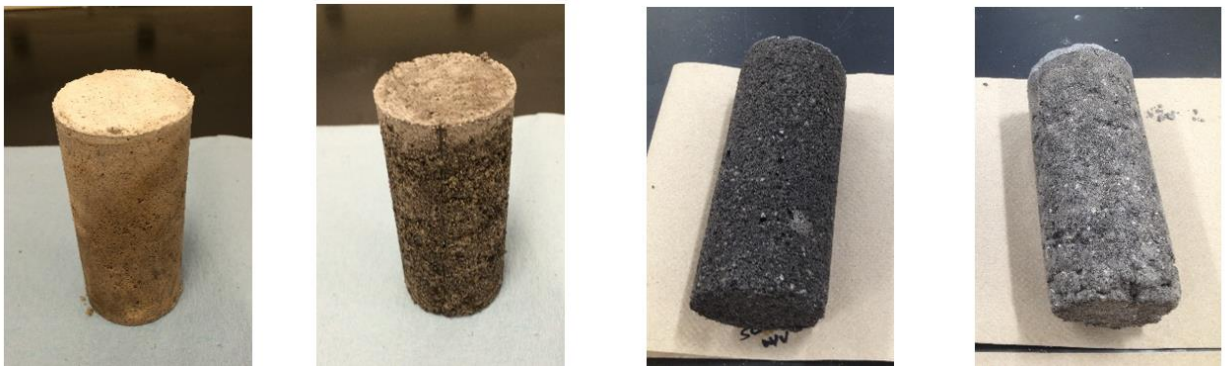

Figure 4-7. Typical SDS-MICP specimens after treatment showing (from left-to-right) soil with 10% organic content; soil with 30% organic content; soil with 50% organic content and 50% SDS; and soil with 50% organic content and 80% SDS

4.4.3 Preparation of Larger Specimens

These results were discussed with the Project Manager, and all parties agreed that data appeared promising. As a result, several larger specimens were prepared for triaxial and consolidation testing. The following SDS/soil ratios were used for the larger specimens:

- For the soil with 10% organic content, SDS percentages were 30% and 50%
- For the soil with 30% organic content, SDS percentages were 40% and 60%
- For the soil with 50% organic content, SDS percentages were 50% and 80%

4.4.4 Consolidation Testing Results and Discussion

4.4.4.1 Treated Soil Specimen Preparation

Treated 50% organic content soil specimens are shown in Figures 4-8 through 4-11 and general information for specimen each is listed in Table 4-1. Each of the treated specimens listed in Table 4-1 was carefully trimmed (Figure 4-12Figure) into multiple samples for consolidation testing. Specimens 22 and XY each had 3 samples placed into 2.5-inch diameter by 1-inch tall oedometer rings (Figure 4-13). Specimens MD102 and MD202 each had 2 samples placed into 2.8-inch diameter by 1.8-inch tall oedometer rings (Figure 4-14)Figure. The soils were fully saturated and seating loads were immediately placed at the time of 0 minutes with a load increment ratio of 1. The duration for each load step lasted between 72 to 120 hours.

Table 4-1. Treated soil measurements

Sample	Diameter (mm)	Length (mm)	Mass (g)	% surfactant (SDS)
22	62.3	160	237.4	50
XY	61	152.6	224.4	50
MD102	70	141	374.11	50
MD202	70	159	369.3	80

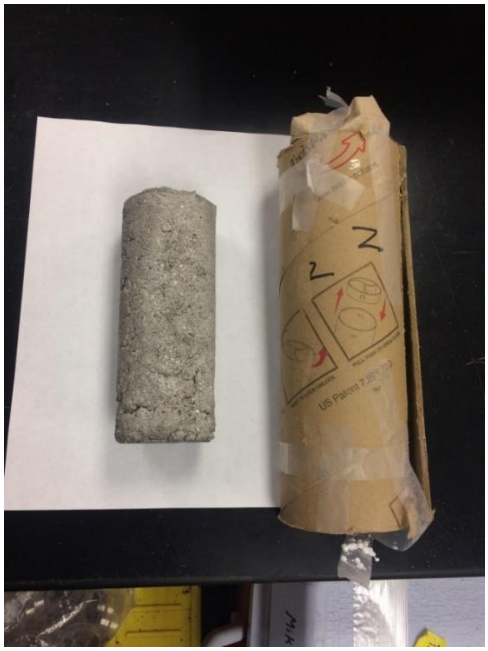

Figure 4-8. Sample 22

Figure 4-9. Sample XY

Figure 4-10. Sample MD102

Figure 4-11. Sample MD202

Figure 4-12. Careful trimming of sample into oedometer ring using a saw

Figure 4-13. Specimen placed in ring after trimming

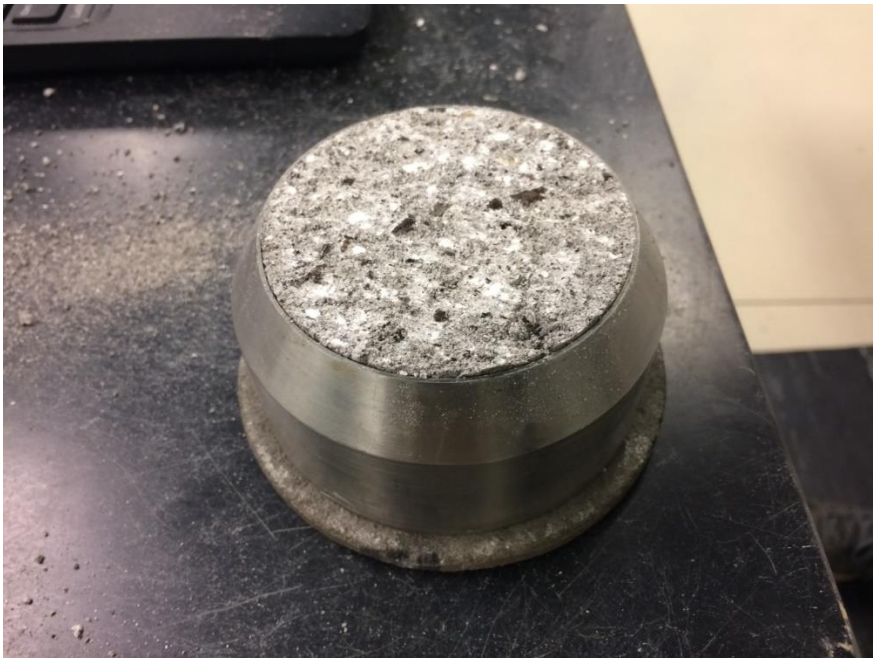

Figure 4-14. 2.8-inch diameter oedometer ring filled with treated soil

4.4.4.2 Consolidation Results

Deformation Versus Time for 0.0625 tsf

Though the untreated specimens were not directly comparable with the treated specimens, certain distinct observations of their consolidation behaviors can be made from the deformation vs. square root of time graphs for each specimen. The initial load of 0.0625 tsf of the 50% SDS samples, 22 (Figure 4-15), XY (Figure 4-16), and MD102 (Figure 4-17) generally showed a sudden deformation within 0 and 2 minutes, followed by a very gradual deformation over a long period of time after 2 minutes. This behavior can be attributed to the effect of the surfactant and $CaCO_3$. They are both soluble and cause changes in the soil densities which cause a collapse under small loads. It could also be that the initial loads are carried by the surfactant and $CaCO_3$ structure, which is weak, leading to the collapse. This deformation behavior is similar or a bit steeper in the untreated soil (Figure 4-18). However, in Figure 4-19, the 80% SDS sample continues to deform at the same rate. This may be a result of the apparent formation (optical and mapping evidence are presented in the next section) of structures of sodium chloride crystals or gypsum (calcium sulfate dihydrate) and not $CaCO_3$, for which there was little evidence.

Deformation Versus Time from 0.125 tsf to 16 tsf Loading

The untreated soil (Figure C-1 through Figure C-8) showed similar deformation characteristics with the 50% SDS samples. Beyond 0.0625 tsf, all 50% SDS samples, 22 (Figure C-9 to Figure C-16), XY (Figure C-17 to Figure C-24) and MD102 (Figure C-25 to Figure C-32), deformed similarly with time in that they appeared to have a gently curved shape showing gradual deformation possibly due to the relatively high amounts of Ca compared to Na. The 80% SDS sample (MD202) differed in deformation as it appears to be almost a straight line as seen in Figure C-33 to Figure C-40 and appeared to be similar to 0.0625 tsf (Figure 4-16). Taken together, these data suggested that the surfactants were more controlling than the $CaCO_3$ causing further deformation with time.

Void Ratio Versus Log Stress Plots

In examining the e-logP plots, the shape of the curve of the untreated soil (Figure 4-20) shows little gradient change from 0.0625 tsf to 16 tsf with a preconsolidation pressure at 1 tsf. This contrasts with the treated specimens. For 50% SDS, sample 22 (Figure 4-21) shows a steep gradient from 0.0625 tsf and 0.125 tsf and then some cementation occurs from 0.0625 tsf to 1 tsf. Sample XY (Figure 4-22) generally shows a steep gradient from 0.0625 tsf to 0.125 tsf beyond which has a relatively gentle slope. Sample MD102 (Figure 4-23) shows similar behavior between 0.0625 tsf and 0.25 tsf. 80% SDS (Figure 2-18) shows a steeper slope between the loads of 0.0625 tsf and 2 tsf. This range is higher than the 50% SDS samples and shows it is highly compressible. As a result of these behaviors of the treated soils, two C_c are seen: the first one $C_{c(1)}$ for the steeper slope followed by $C_{c(2)}$ for the gentler slope. From Table 4-2, the C_c ranges from 0.5 to about 0.7 for the untreated soils. Table 4-3 shows all of the C_c values with 80% SDS showing a lower $C_{c(2)}$ ranging from 0.45 to 0.47. This could be attributed to the rearrangement of soil grains coupled with filling of the voids with the surfactant and $CaCO_3$ causing reduction in void ratio with further loading. In general, the e-logP for the treated soils (Figure 4-21, Figure 4-22, Figure 4-23 and Figure 4-24) show a greater change in void structure with time as opposed to the untreated soil (Figure 4-20) which could be the result of the MICP mixing causing an expulsion of CO_2 which lifts the organic particles resulting in a higher void ratio specimen. The compressibility at the beginning of load application indicates that the SDS+$CaCO_3$ is water soluble, which is a significant disadvantage to the objective of reducing compressibility. Also, it is possible that an imperfect mixture can occur and lead to variable biocementation throughout the specimen.

Figure 4-25 shows the C_v of the untreated samples. Generally, the initial loads have very high values of about 2500 ft^2/yr and reduces to 200 to 500 ft^2/yr with increasing loading. In Figure 2-20, the initial load of 0.0625 tsf of 50% SDS specimens also has almost 2500 ft^2/yr; however, they generally remain constant with further loading. Figure 4-27 shows a similar initial C_v of 2500 ft^2/yr; however, the C_v do not remain constant with time but varies but is higher than the 50% SDS soils. In general, the average C_v for all loads in the 50% SDS is between 150 to 600 ft^2/yr which is lower than the 80% SDS soil with an average value of about 700 ft^2/yr. The higher C_v of the 80% SDS agrees with the void ratio changes seen in its e-logP (Figure 4-24). According to Whitman and Lambe (1959), the estimation of C_v varies with load and for different materials.

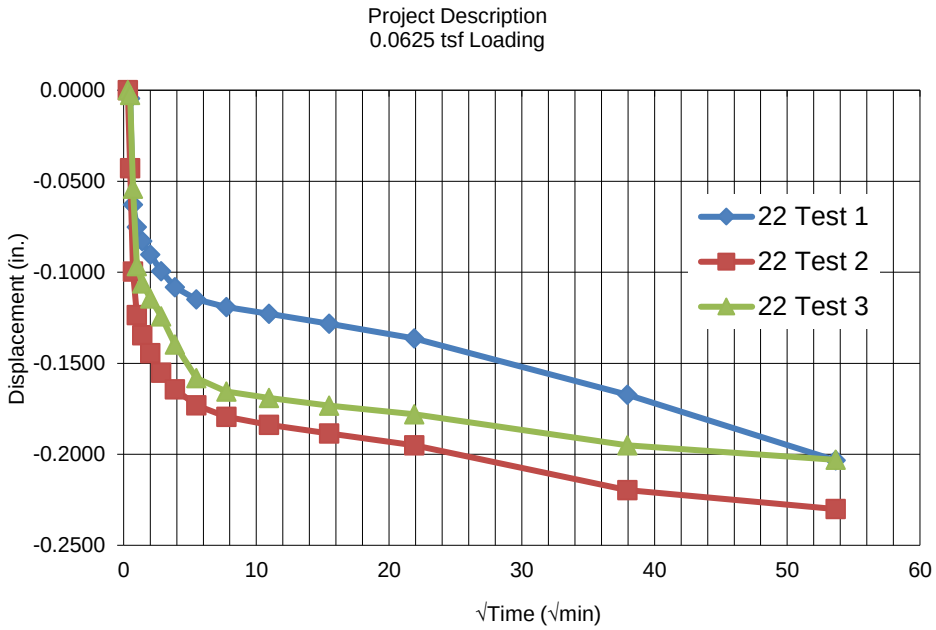

Figure 4-15. Deformation vs. time^{½} for sample 22 at 0.0625 tsf

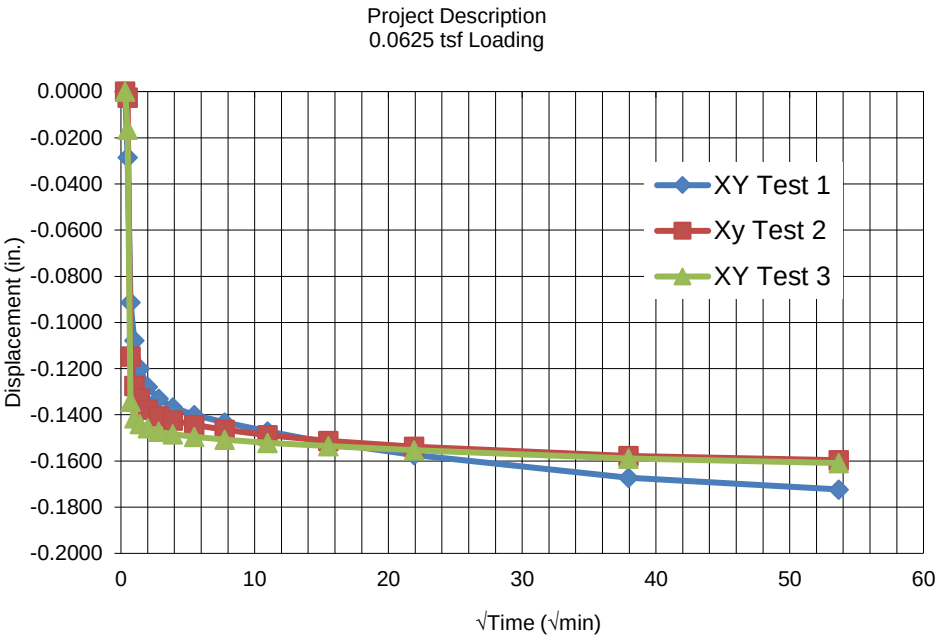

Figure 4-16. Deformation vs. time^{½} for sample XY at 0.0625 tsf

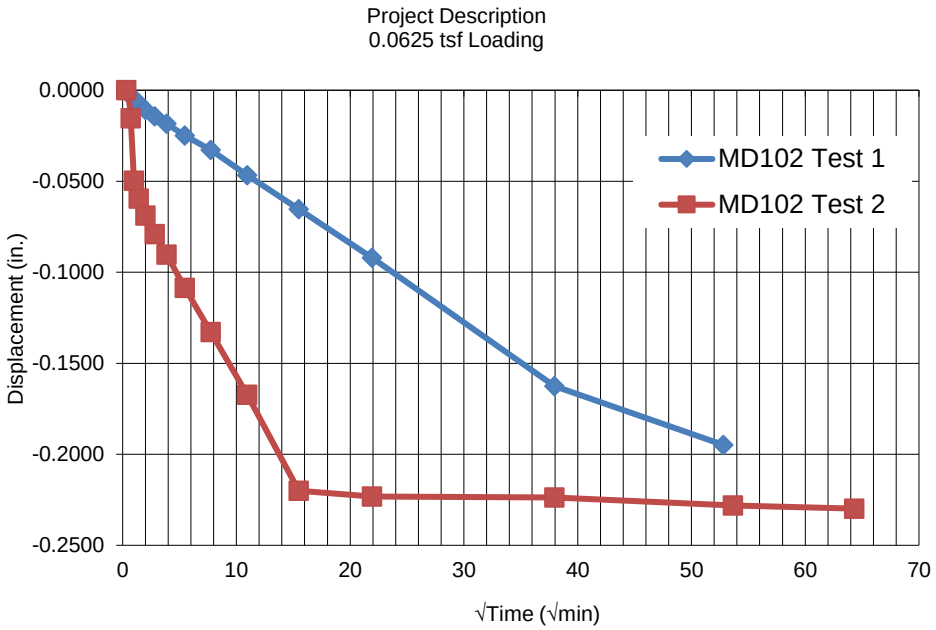

Figure 4-17. Deformation vs. time^{½} for sample MD102 at 0.0625 tsf

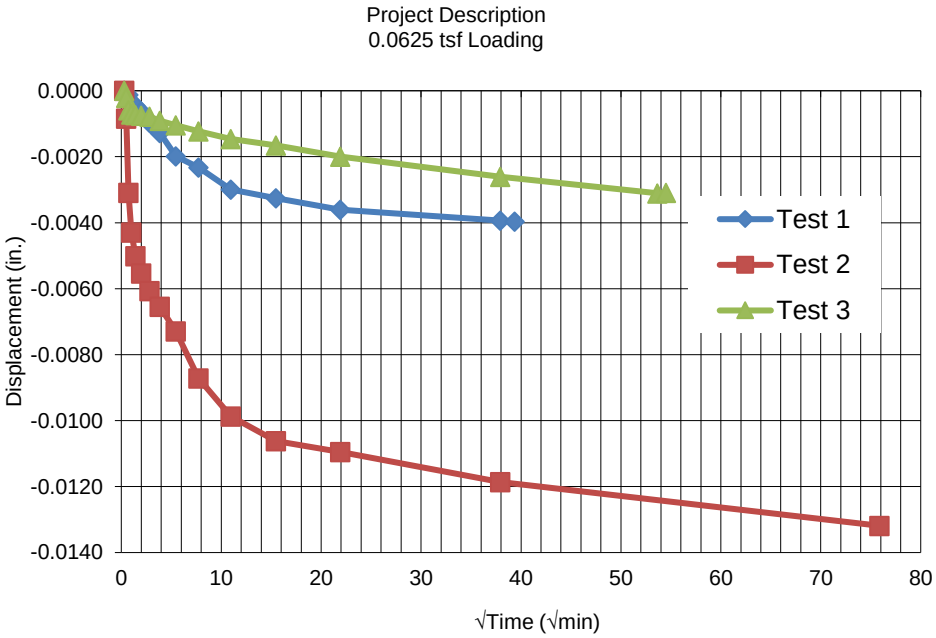

Figure 4-18. Deformation vs. time^{½} for untreated soil at 0.0625 tsf

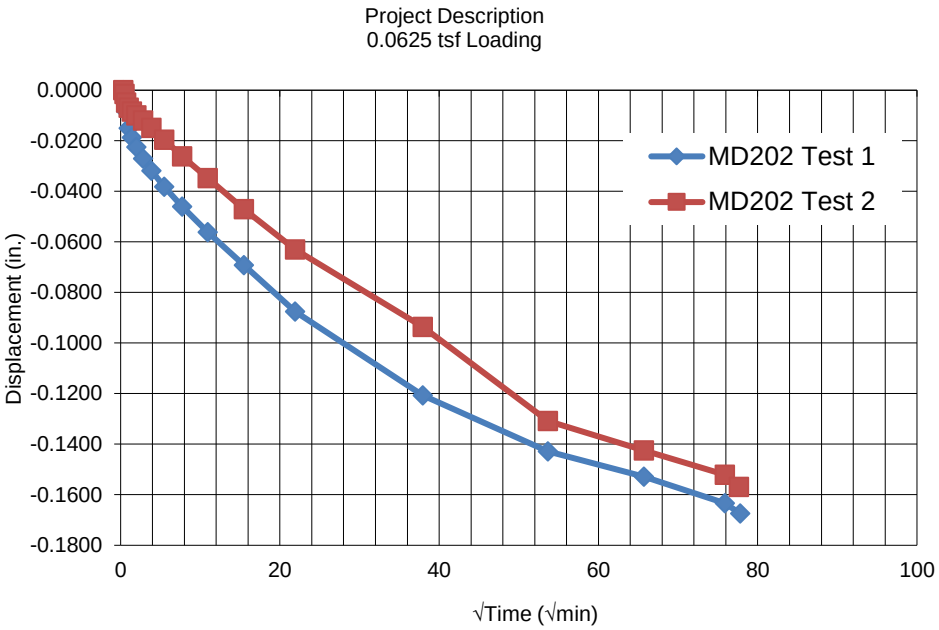

Figure 4-19. Deformation vs. time^{½} for sample MD202 at 0.0625 tsf

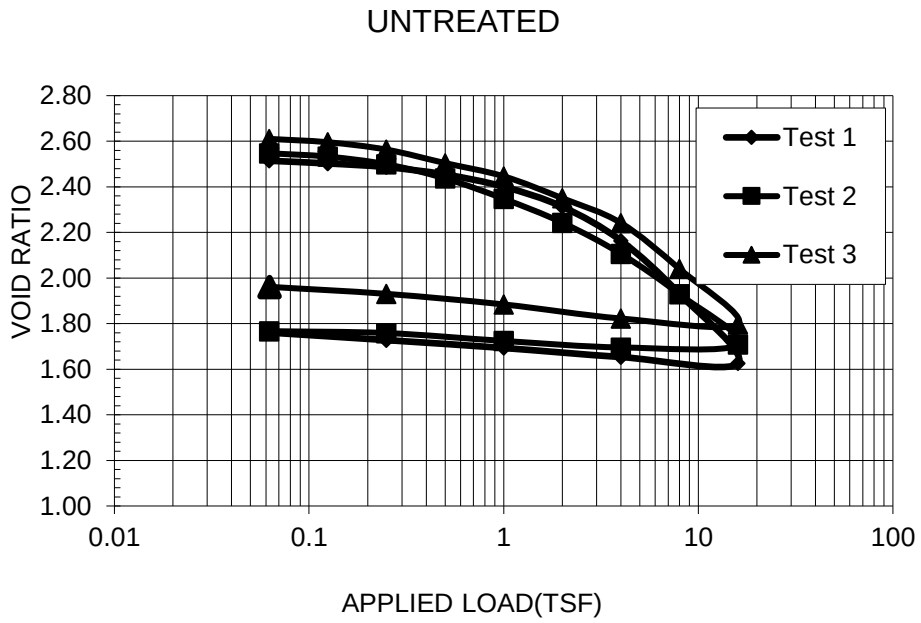

Figure 4-20. e-logP plot for untreated samples

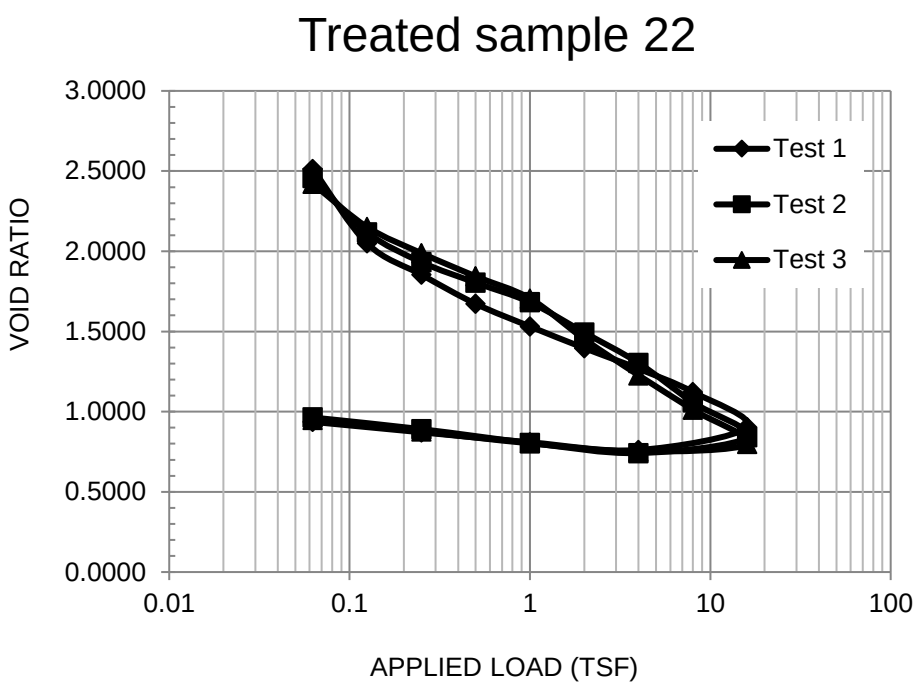

Figure 4-21. e-logP plot for treated sample 22

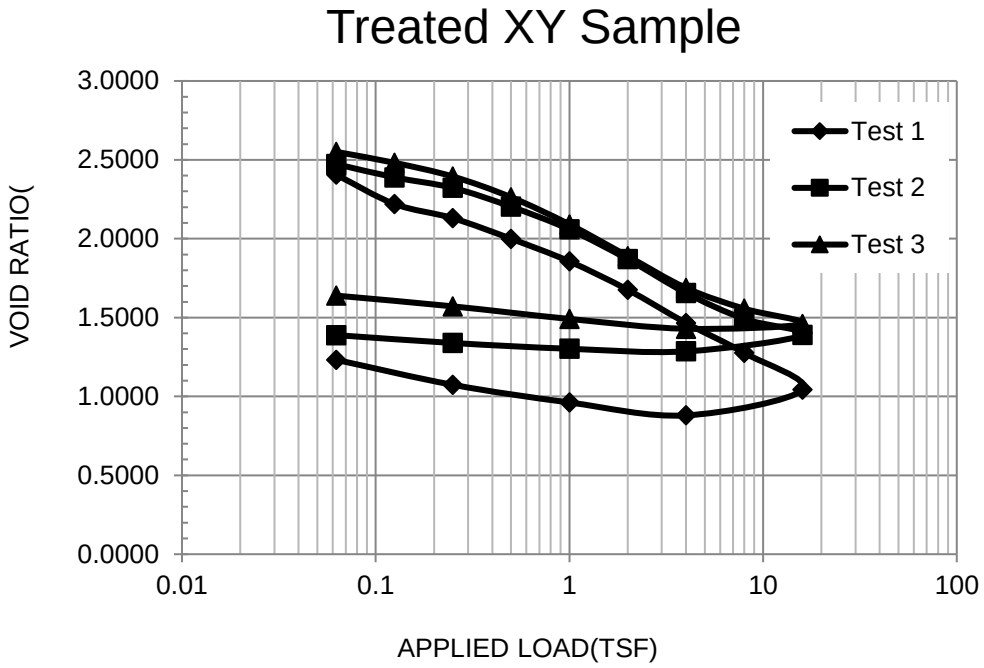

Figure 4-22. e-logP plot for treated sample XY

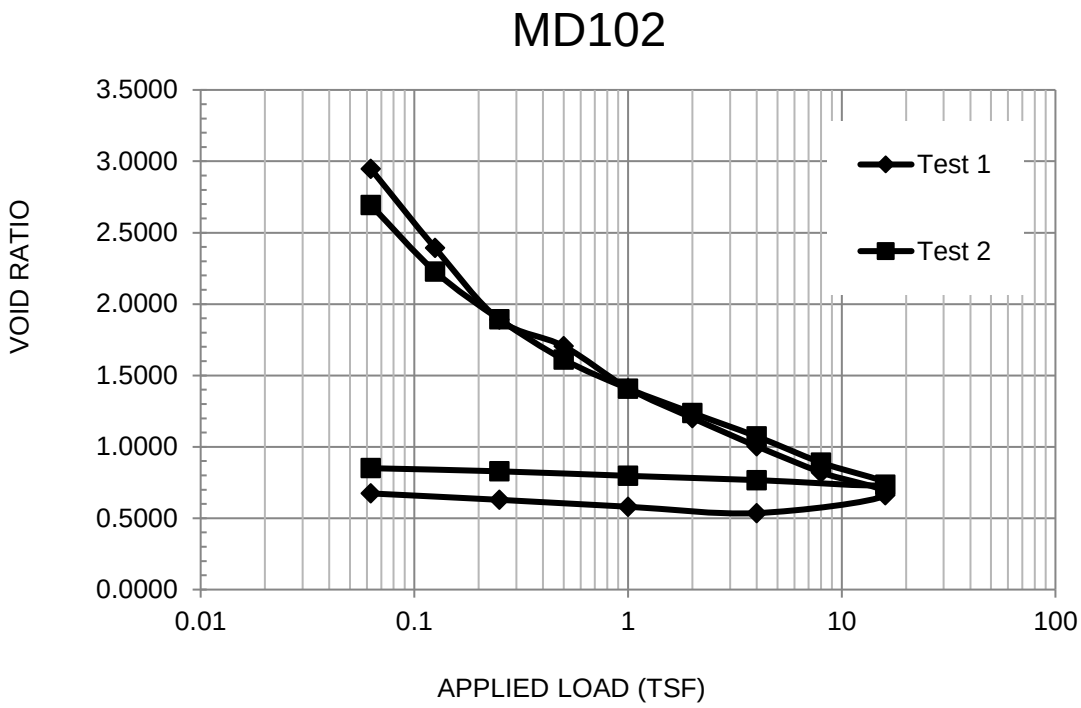

Figure 4-23. e-logP plot for treated sample MD102

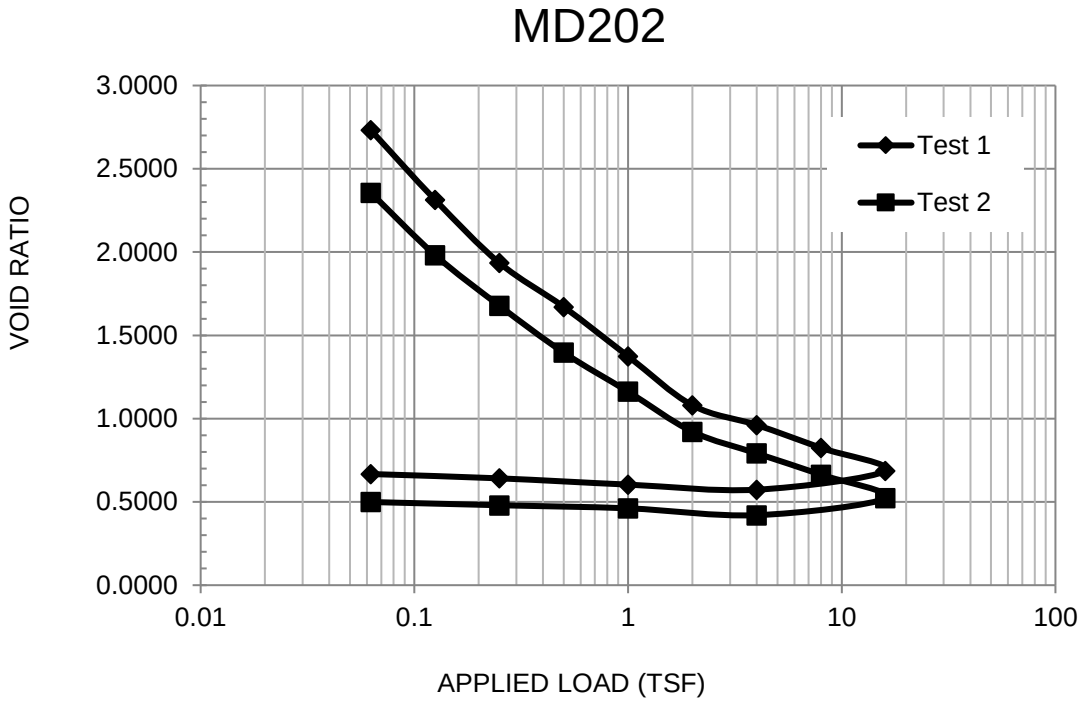

Figure 4-24. e-logP plot for treated sample MD202

Table 4-2. Summary of untreated soil

PARAMETERS	Test 1	Test 2	Test 3
Specific gravity, G_s	1.71	1.71	1.71
Initial void ratio, e_o	2.52	2.58	2.62
Initial moisture content, w (%)	88.9	87.8	89.3
Wet density, γ (pcf)	57.2	56.0	56.1
Dry density, γ_d (pcf)	30.3	29.8	29.6
% Ca from EDS		4.75	
Compression index, C_c	0.548	0.62	0.649
Recompression index, C_r	0.06	0.05	0.08

Table 4-3. Summary on treated soils

PARAMETERS	22			XY			MD102		MD202	
	Test 1	Test 2	Test 3	Test 1	Test 2	Test 3	Test 1	Test 2	Test 1	Test 2
Specific gravity, G_s	1.67	1.70	1.66	1.71	1.69	1.70	1.60	1.60	1.63	1.63
% Surfactant (by weight)	50	50	50	50	50	50	50	50	80	80
Initial void ratio, e_o	2.84	3.16	2.95	2.93	3.00	3.16	2.96	2.80	2.77	2.37
Initial moisture content, w (%)	11.2	11.2	11.2	15.1	15.1	15.1	31.9	15.9	34.3	25.0
Wet density, □ (pcf)	30.1	28.3	29.2	31.2	30.4	29.3	35.5	30.4	36.2	37.6
Dry density, □$_d$ (pcf)	27.1	25.5	26.3	27.1	26.4	25.4	27.0	26.3	26.9	30.1
% Ca from SDS	4.4	4.4	4.4	-	-	-	10.8	10.8	12.4	12.4
Compression index, $C_{c\,(1)}$	1.154	1.123	0.894	0.458	0.249	0.266	1.757	1.332	1.0982	1.003
Compression index, $C_{c\,(2)}$	0.544	0.607	0.642	0.602	0.517	0.676	0.681	0.622	0.458	0.466
Recompression index, C_r	0.097	0.123	0.11	0.195	0.057	0.116	0.076	0.055	0.0548	0.04

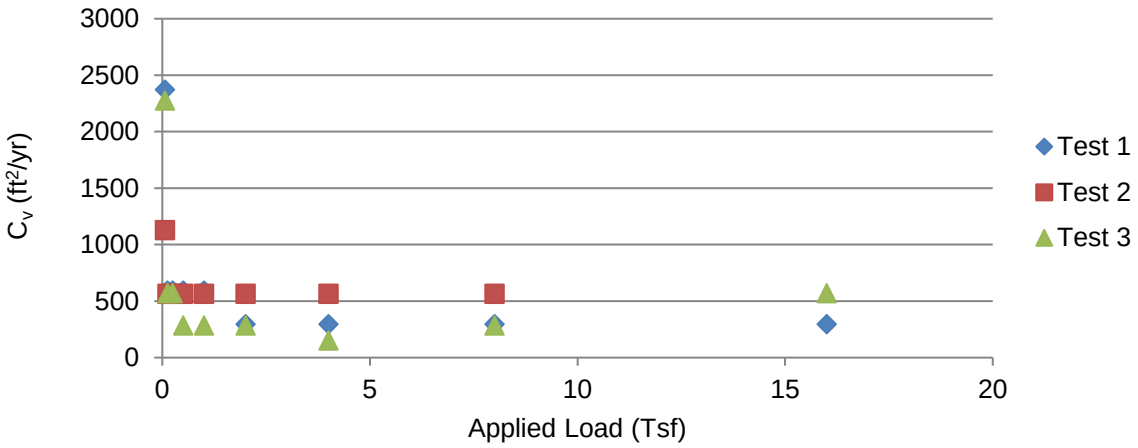

Figure 4-25. Coefficient of consolidation, c_v (ft^2/yr) of untreated soils

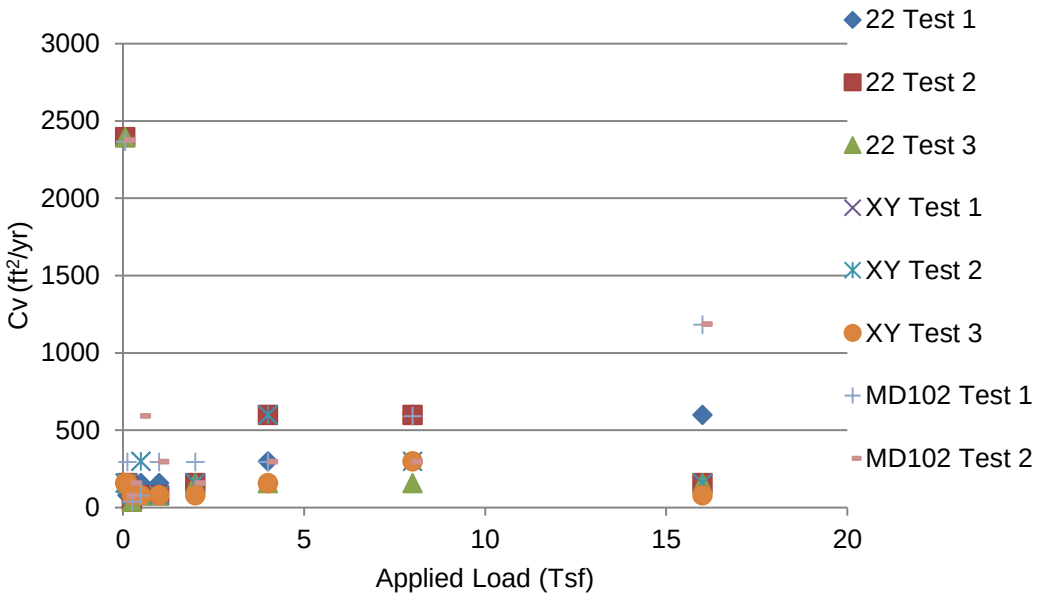

Figure 4-26. Coefficient of consolidation values, c_v (ft^2/yr) of 50% SDS soils

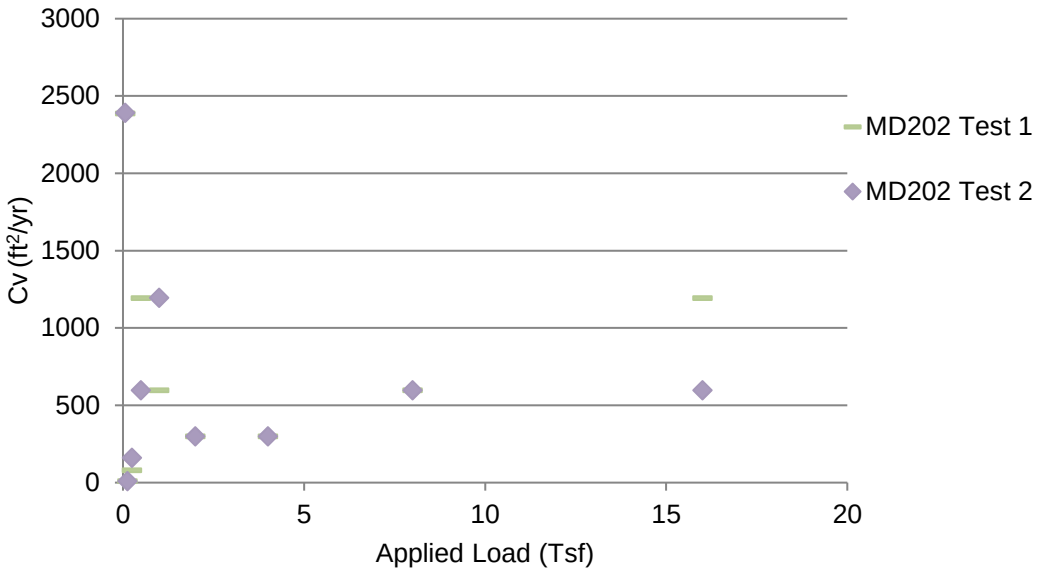

Figure 4-27. Coefficient of consolidation values, c_v (ft^2/yr) of 80% SDS (MD202) soils

4.4.5 Triaxial Testing Results and Discussion

UU triaxial tests were run on treated 50% organic content soil with 50% SDS and 80% SDS. Table 4-4 lists the properties of the specimens tested. Note, only two specimens of the 50% organic content + 80% SDS were available to be tested. Similar to the consolidation results, the treated organic content soil showed undesirable behavior under axial loading with increased confining pressure. Figure 4-28 is the triaxial stress-strain results for 5 psi, 10 psi, and 15 psi confining pressures. Evident is the decreasing maximum shear with increasing confining pressure, which is uncharacteristic of engineered materials and disadvantageous as a load carrying material. The p-q diagram in Figure 4-29 shows the characteristic stress path for axial loading with constant confining pressure for each specimen; however, the direction of the failure envelope indicates the significantly reduced axial capacity with increased horizontal stress. This represents an unsafe condition of modified soil. The same behavior was observed in the triaxial results of the 50% organic content + 80% SDS specimens.

Table 4-4. Summary of UU triaxial test specimens

PARAMETERS	50% organic content + 50% SDS			50% organic content + 80% SDS	
	Test 1	Test 2	Test 3	Test 1	Test 2
Specific gravity, G_s	1.66	1.66	1.66	1.62	1.62
Moisture content, w (%)	14.0	20.6	15.0	23.3	27.8
Wet density, γ (pcf)	36.5	32.0	31.5	41.8	42.8
Dry density, γ_d (pcf)	32.0	26.5	27.4	33.9	33.5

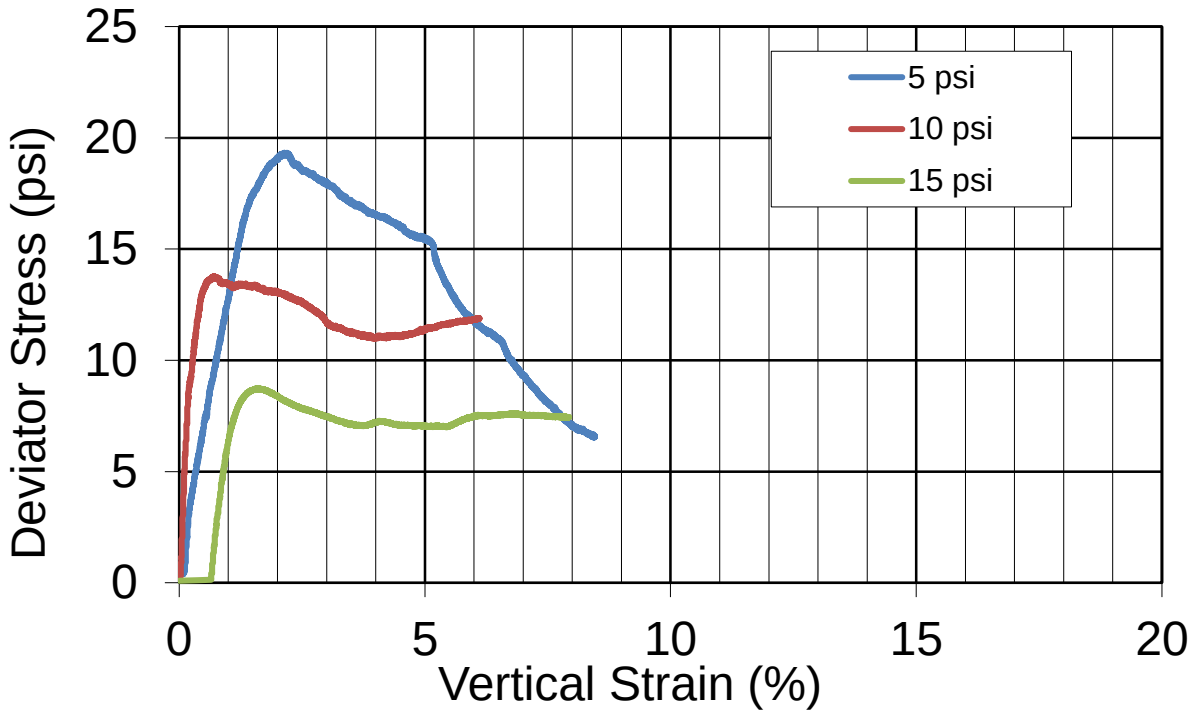

Figure 4-28. Triaxial stress strain for confining stress of 5 psi, 10 psi, and 15 psi on 50% organic content + 50% SDS

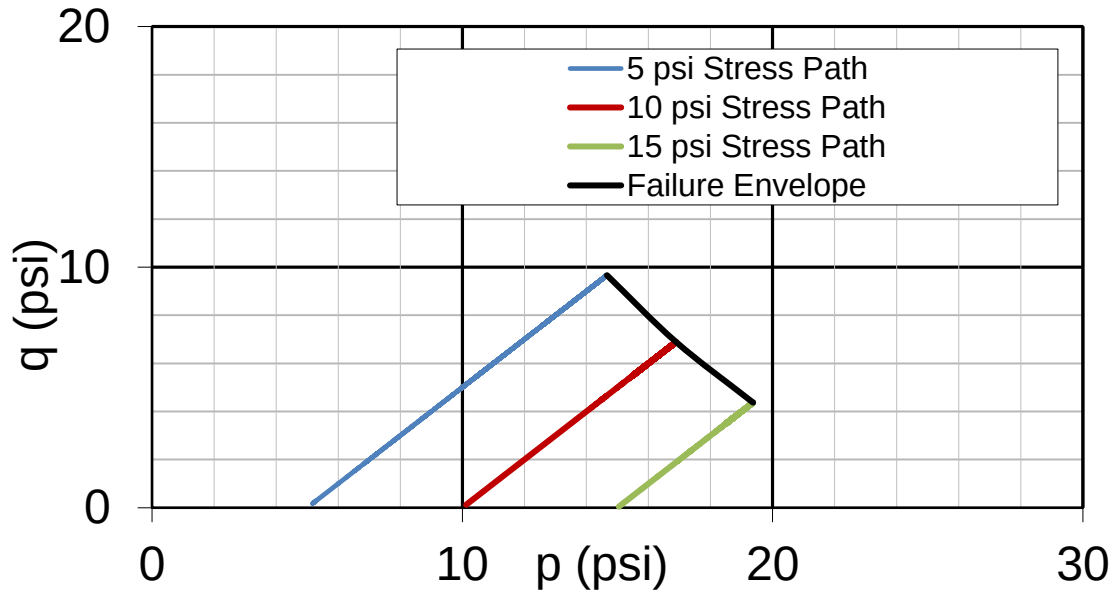

Figure 4-29. Triaxial p-q for confining stress of 5 psi, 10 psi, and 15 psi on 50% organic content + 50% SDS

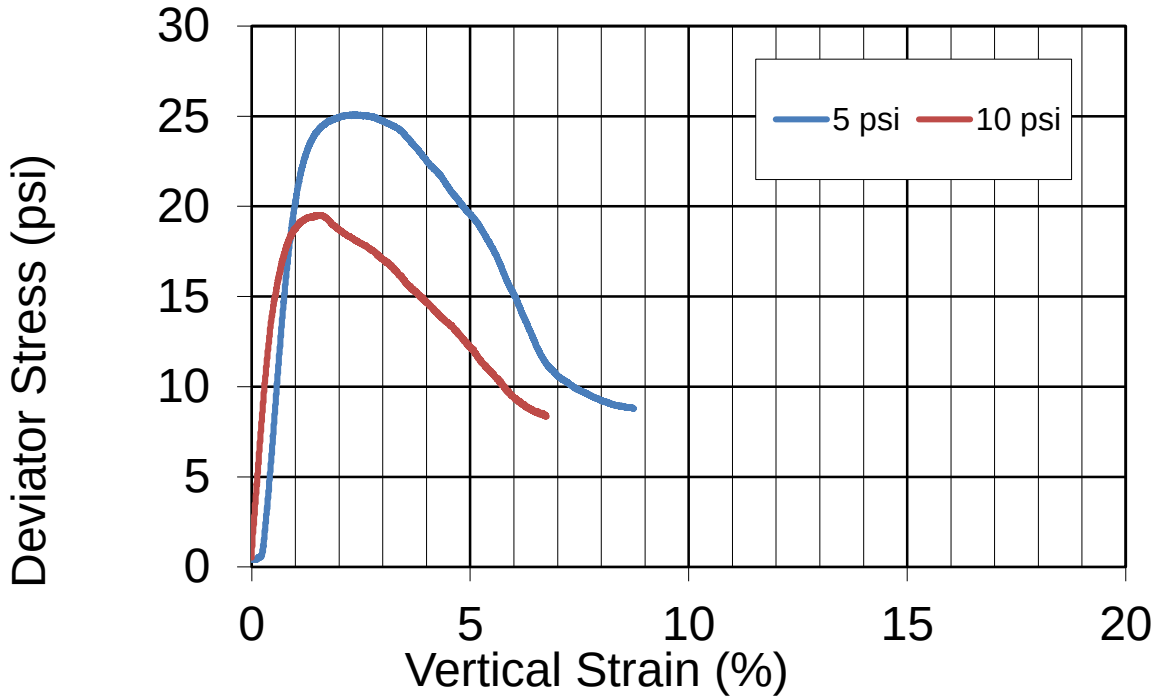

Figure 4-30. Triaxial stress strain for confining stress of 5 psi and 10 psi on 50% organic content + 80% SDS

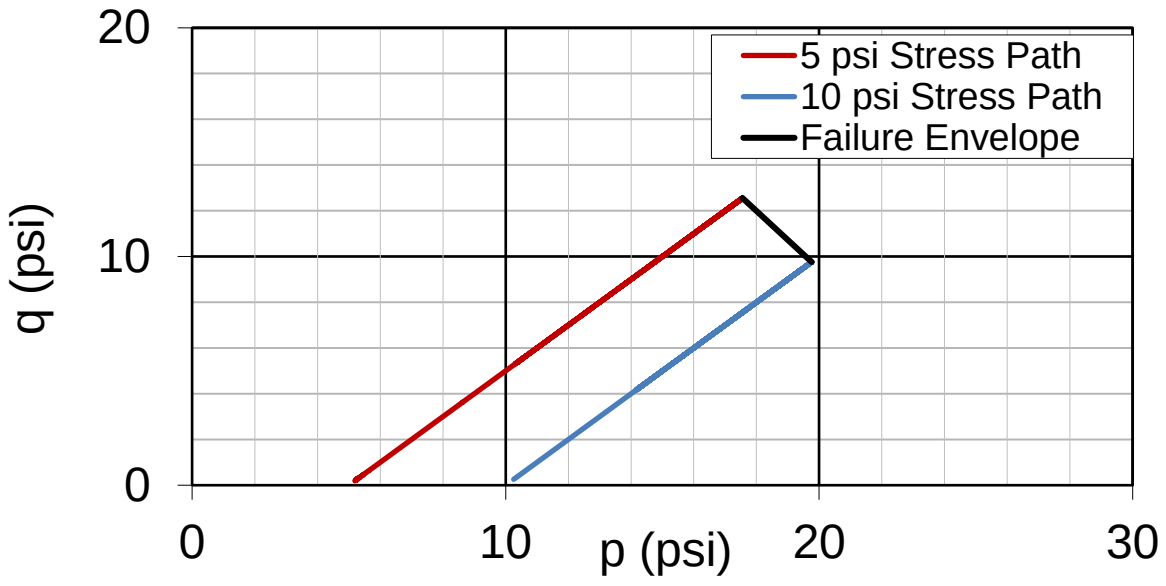

Figure 4-31. Triaxial p-q for confining stress of 5 psi and 10 psi on 50% organic content + 80% SDS

4.5 Development of Surfactant-Induced Soil Strengthening (SISS)

Results from the consolidation and triaxial testing clearly show that calcium carbonate stabilization had not been achieved. Rather, they showed that the mechanism that appeared to be cementing the soil matrix together was dissolvable. Calcium carbonate is relatively insoluble. Therefore, the results indicate that another mechanism must have been responsible for the apparent soil improvements discussed in Section 4.4.2. Concurrent with the triaxial/consolidation testing, the research team held some internal discussions to further analyze results. Some skepticism was raised about the apparent strength improvements shown during UCS testing, and it was suggested that some control specimens be analyzed to ensure that strength improvements were caused by calcium carbonate formation and not another mechanism.

4.5.1 Control Testing

The first "control" test involved mixing soil with 50% organic content with SDS and water to ensure that the SDS was not causing any unexpected bonds to form between the soil particles and/or between the soil particles and the SDS. Two specimens with 50% organic content were mixed with SDS (in a 1:2 ratio). Then, 80-mL of water was added to the SDS/soil and the specimens were allowed to cure in 2-inch by 4-inch concrete cylinders for 48 hours. Both specimens resulted in watery, semi-viscous mixtures that failed under their own weight and therefore could not be subjected to UCS testing. Thus, researchers concluded that the SDS was not solely responsible for strength improvements.

The second "control" test involved using all MICP constituents except for the microbes – i.e., SDS, urea, and calcium chloride were mixed with 50% organic content soil. Once again, SDS-soil percentage was 50% by weight. Two specimens were prepared using this method and two additional specimens were prepared that included the microbes. Results from this test were very unexpected in that the specimens without the microbes appeared to be "cemented." One non-microbe specimen and one with-microbe specimen were subjected to UCS testing. Results showed similar strength between the two specimens. The remaining two specimens were placed underwater for 48 hours. The specimen with microbes dissolved rather quickly (within 24 hours). The specimen without microbes still appeared to dissolve, but dissolution was much slower.

The goal of the third "control" test was to obtain results to characterize the observations made during control test 1 and control test 2. Specifically, a testing matrix was designed as follows:

Table 4-5. Third control test matrix

Test C3-1A – 30% SDS, microbes, calcium chloride, urea	Test C3-2A – 30% SDS, no microbes, calcium chloride, urea	Test C3-3A – 30% SDS, no microbes, calcium chloride, no urea
Test C3-1B – 60% SDS, microbes, calcium chloride, urea	Test C3-2B – 60% SDS, no microbes, calcium chloride, urea	Test C3-3B – 60% SDS, no microbes, calcium chloride no urea
Test C3-1C – 90% SDS, microbes, calcium chloride, urea	Test C3-2C – 90% SDS, no microbes, calcium chloride, urea	Test C3-3C – 90% SDS, no microbes, calcium chloride, no urea

Each of these specimens was prepared using 50% organic content soil. After curing for 48 hours, each of these specimens was placed in deionized water for two weeks. Results are shown below in Figure 4-32.

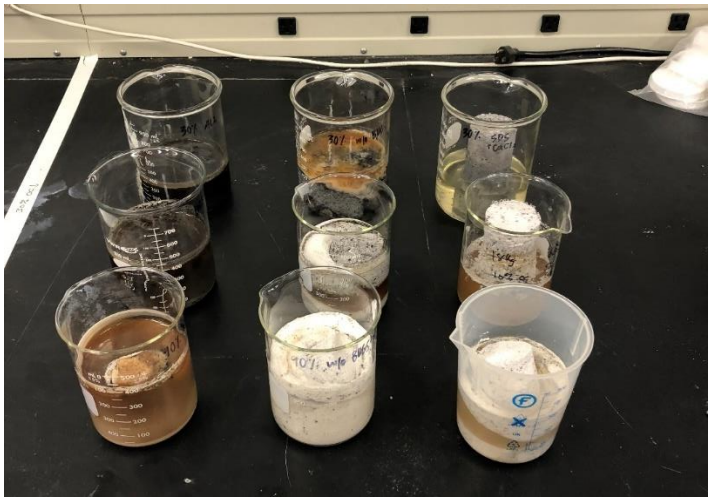

Figure 4-32. Results from Control Test 3; far-left column are with microbes; middle column is without microbes; far-right column are without microbes and urea; top row is 30% SDS; middle row is 60% SDS; bottom row is 90% SDS

As shown, the specimens with the microbes dissolved relatively quickly. The specimens without microbes and with urea also dissolved to some extent, although not nearly as quickly or as much as the specimens with microbes. The specimens that only contained calcium chloride and SDS performed the best in terms of dissolution. The specimen that dissolved the least was the 30% SDS specimen with only calcium chloride – i.e., the specimen at the top-right of Figure 4-32. This specimen is shown in more detail in Figure 4-33 below.

Figure 4-33. Close-up of Test C3-3A

4.5.2 XRD and SEM Analysis of Control Specimens

Results from these control tests were very unexpected, although as stated above, when compared to the results from triaxial and consolidation testing, they are consistent (at the time, consolidation and triaxial data were not yet available). SEM and XRD analyses were conducted to develop some better ideas about the chemical mechanisms that were occurring during treatment. Results from these tests are presented below from Figure 4-34 through Figure 4-47. Taken holistically, results appear to show the following:

1. Significant calcium carbonate precipitation was not observed during any of the treatments. If significant calcium carbonate had precipitated, small round crystalline deposits would have been observed in the SEM images.

2. Sodium chloride crystalline formation was suggested – particularly on specimens from Test C3-3A. Sodium chloride crystals are small needle-like projections. Presence of sodium chloride appeared to be confirmed with the XRD analysis.

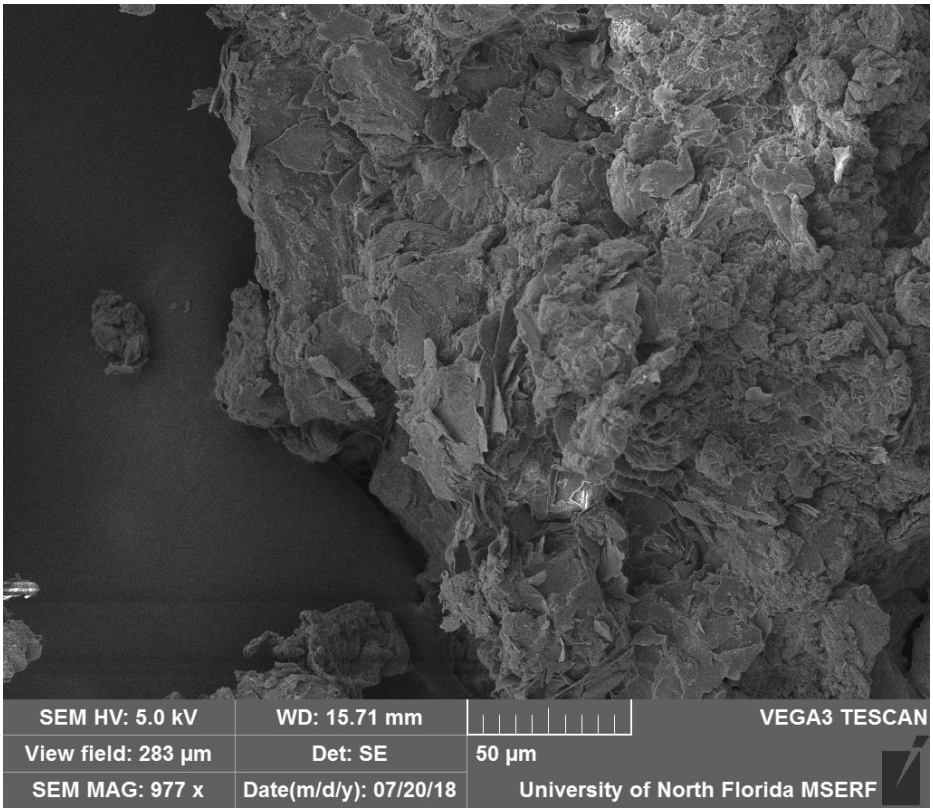

Figure 4-34. SEM image from test C3-1A

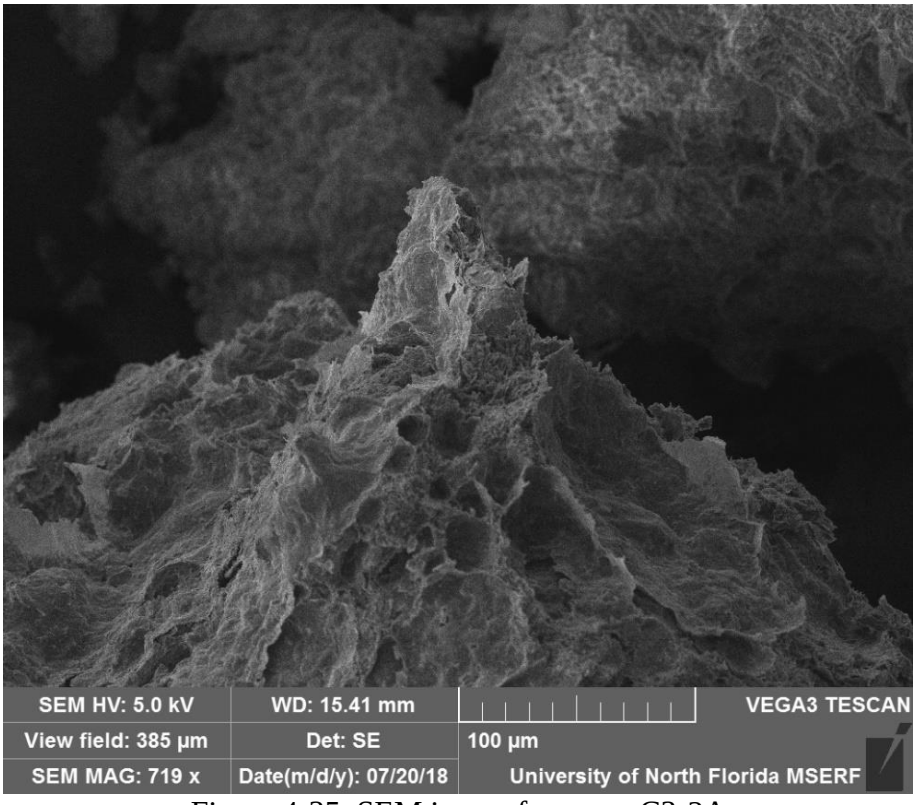

Figure 4-35. SEM image from test C3-2A

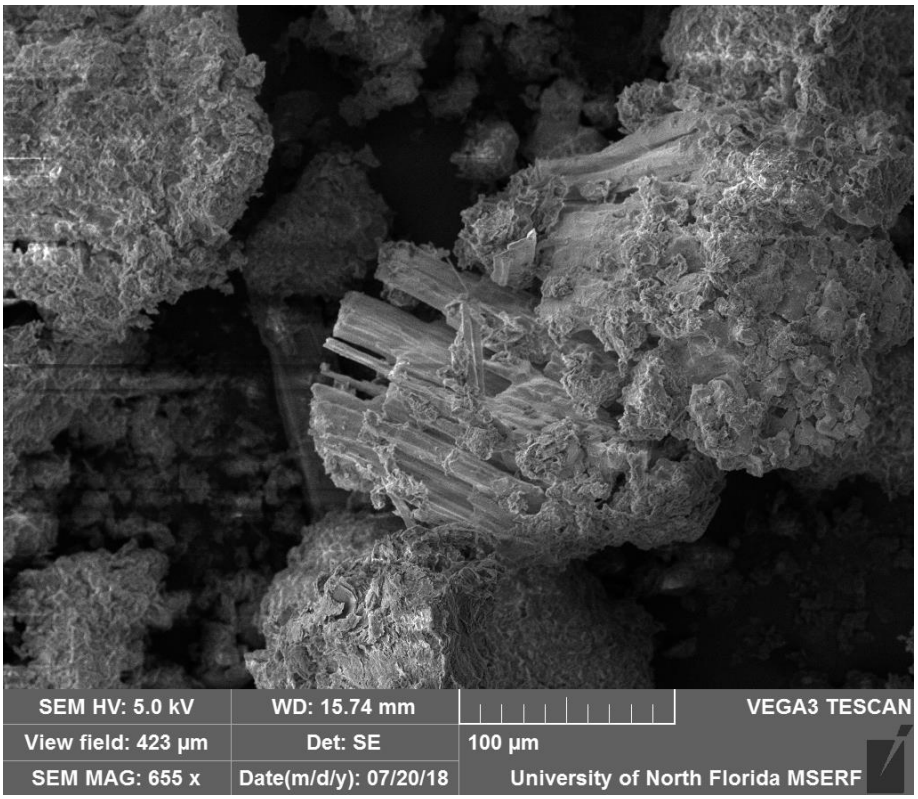

Figure 4-36. SEM image from test C3-3A

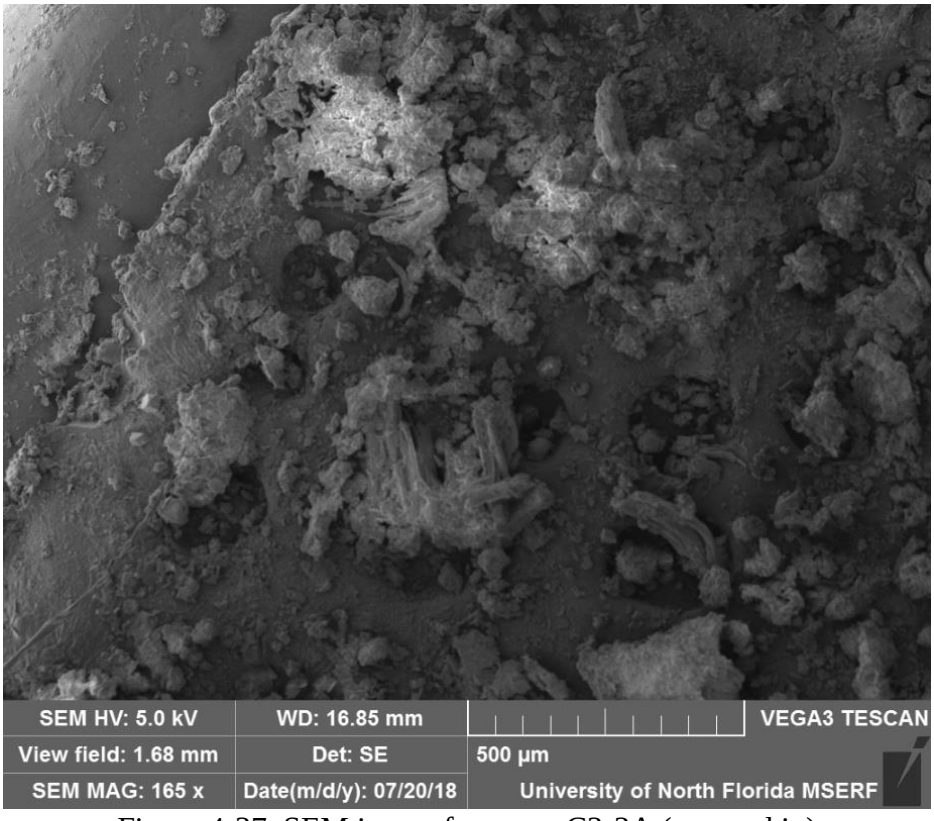

Figure 4-37. SEM image from test C3-3A (zoomed in)

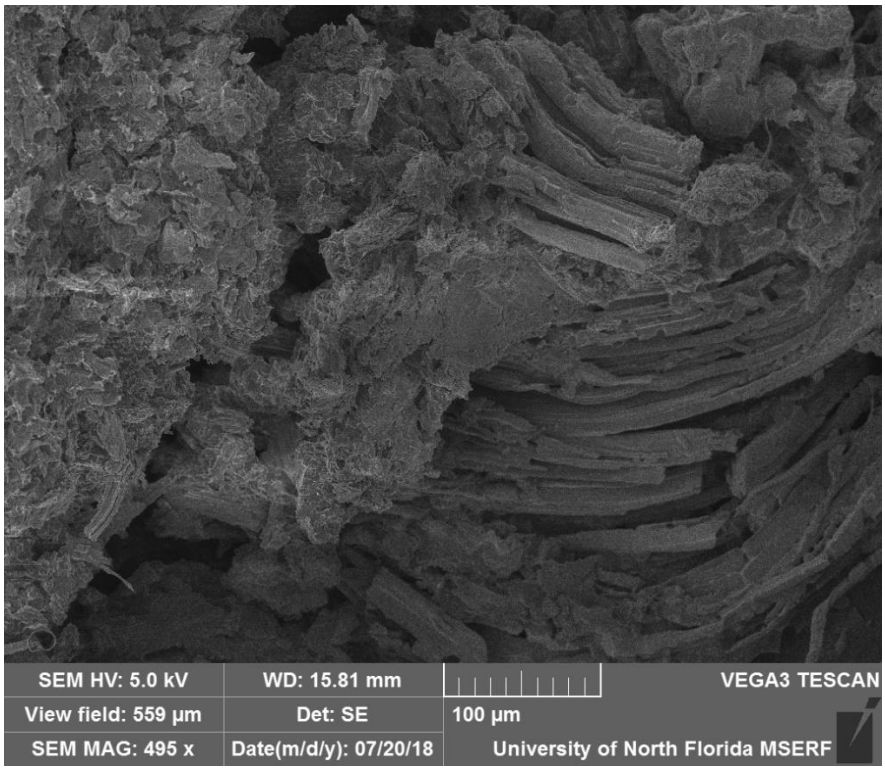

Figure 4-38. SEM image from test C3-1B

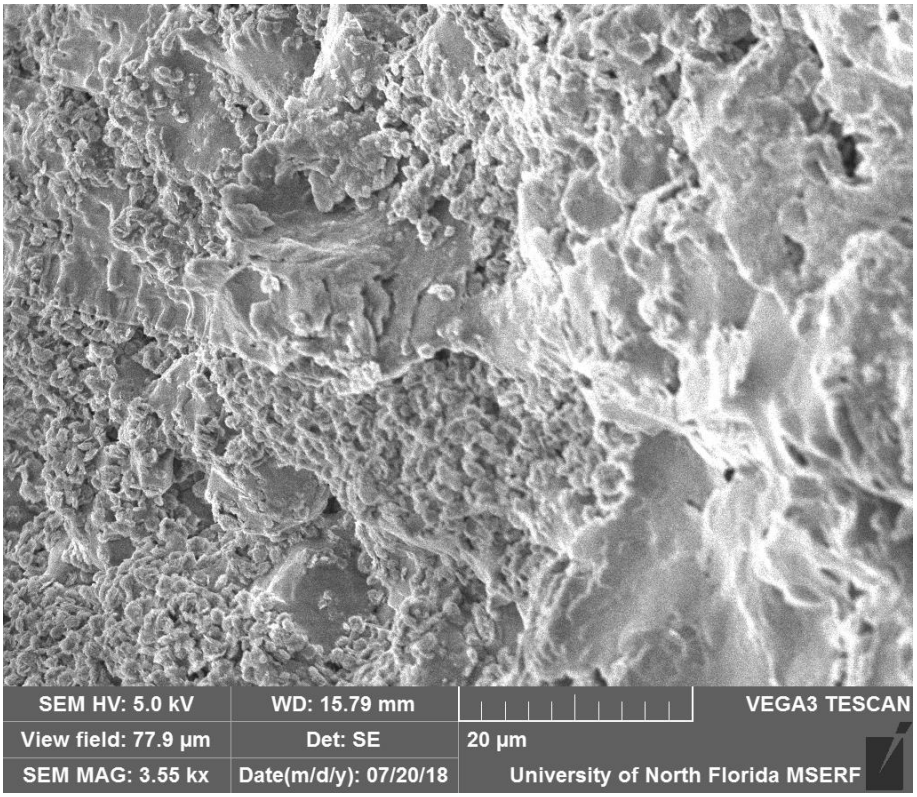

Figure 4-39. SEM image from test C3-1B (zoomed out)

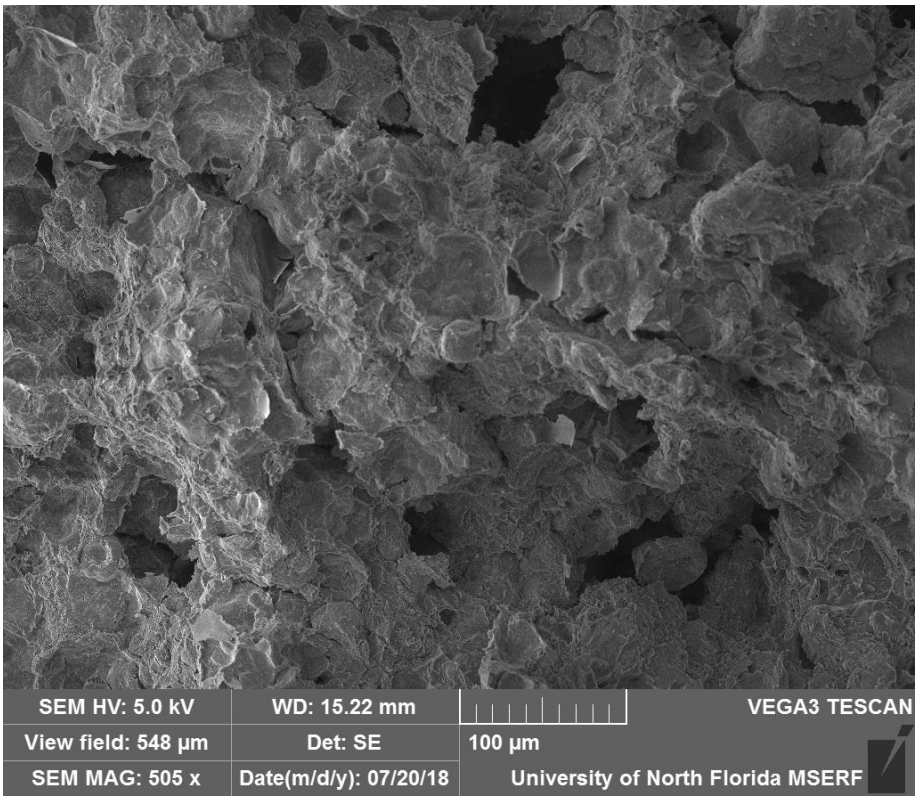

Figure 4-40. SEM image from test C3-2B

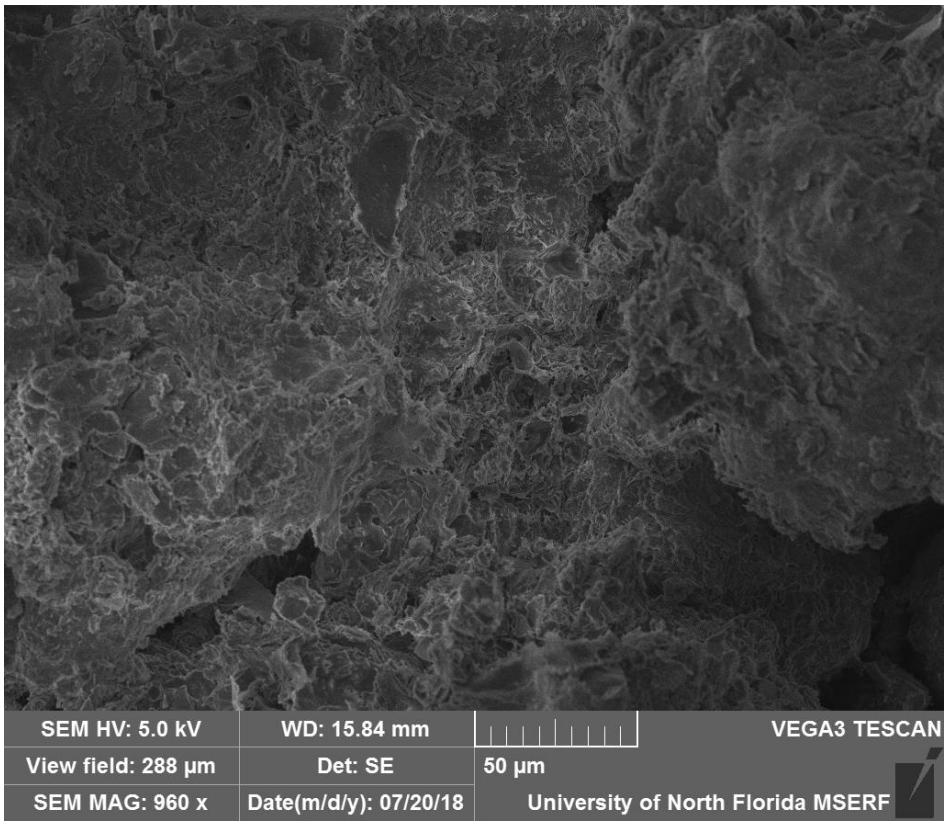

Figure 4-41. SEM image from test C3-3B

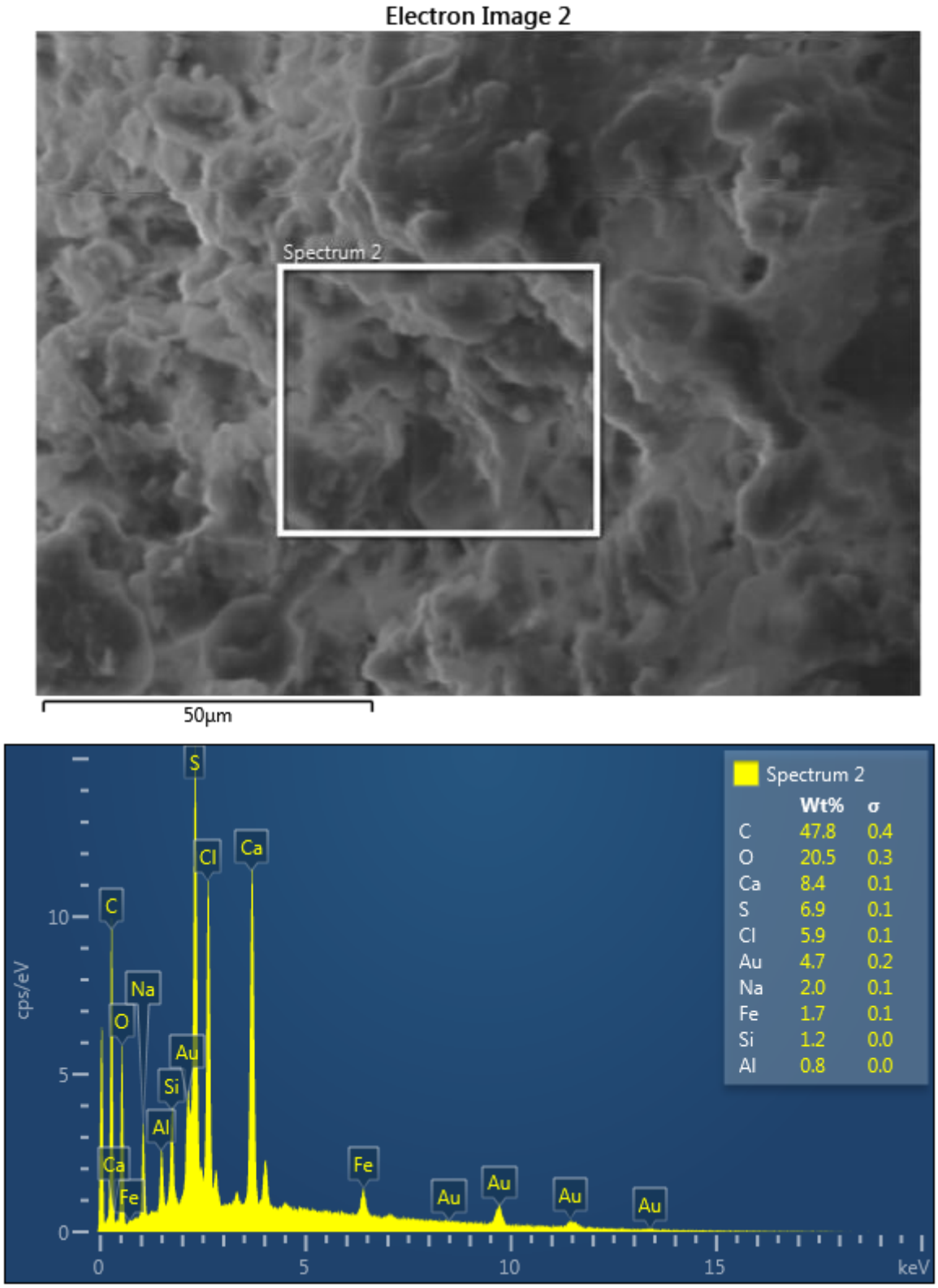

Figure 4-42. XRD results from test C3-1A

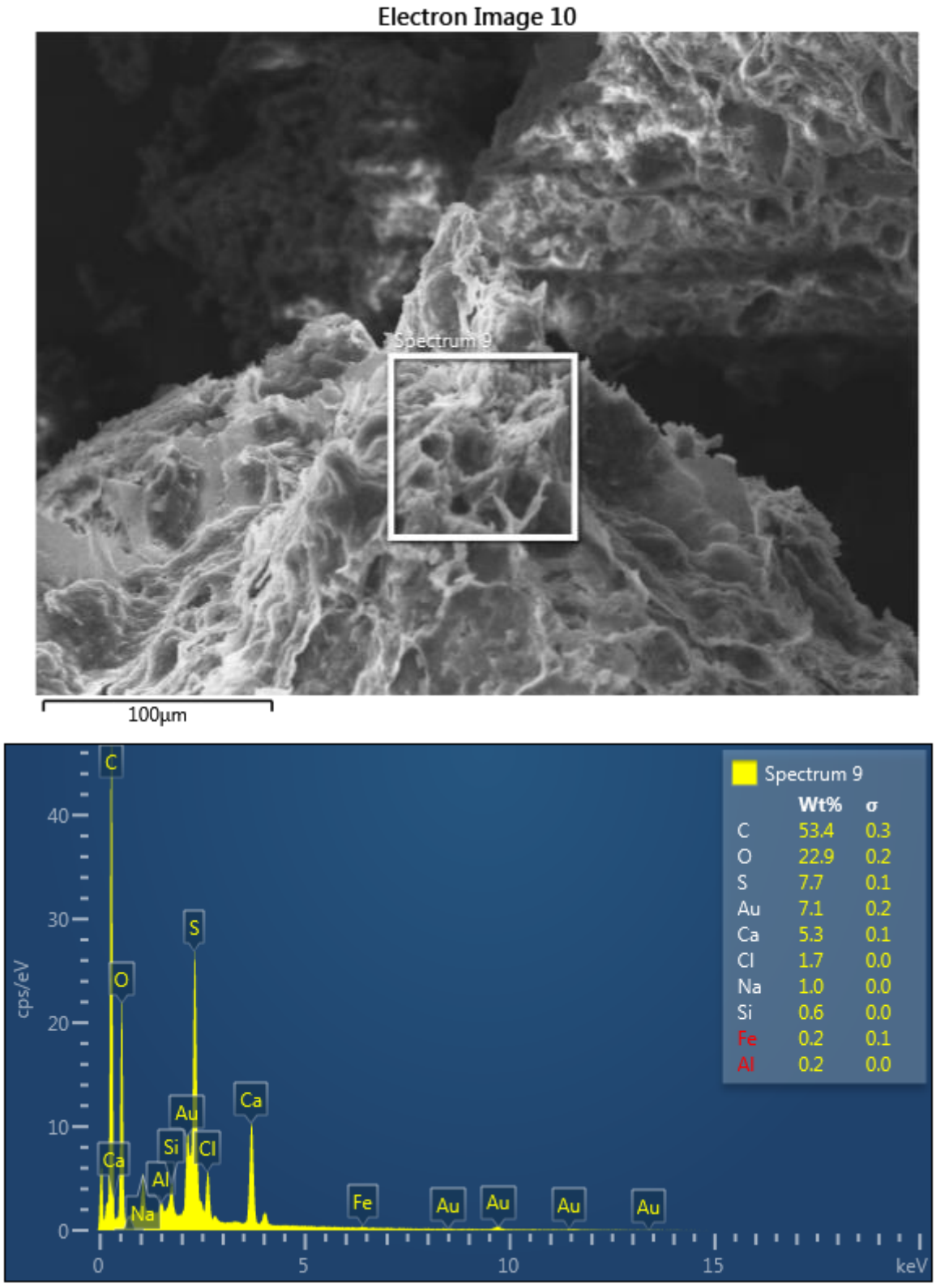

Figure 4-43. XRD results from test C3-1B Site 1

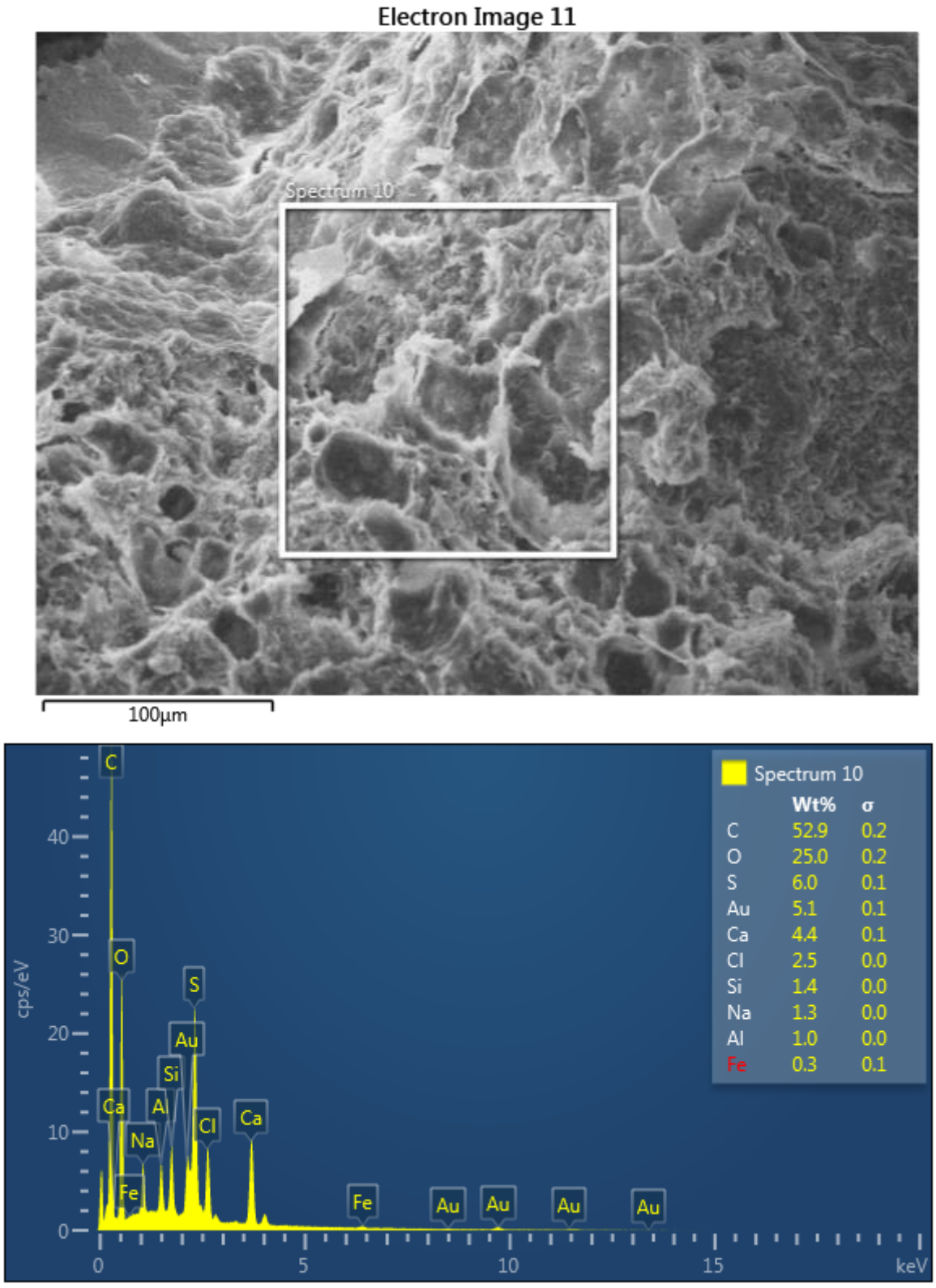

Figure 4-44. XRD results from test C3-1B Site 2

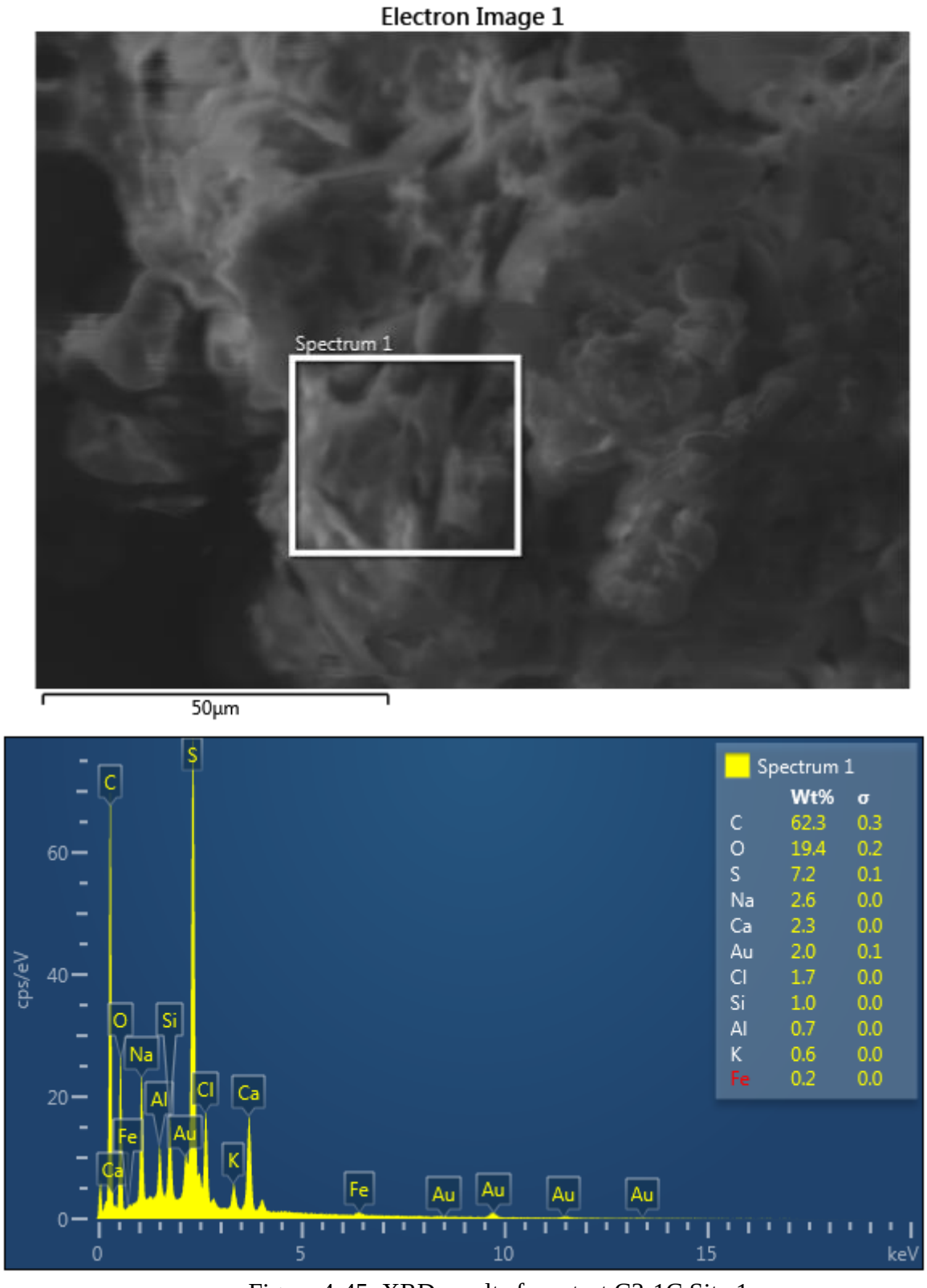

Figure 4-45. XRD results from test C3-1C Site 1

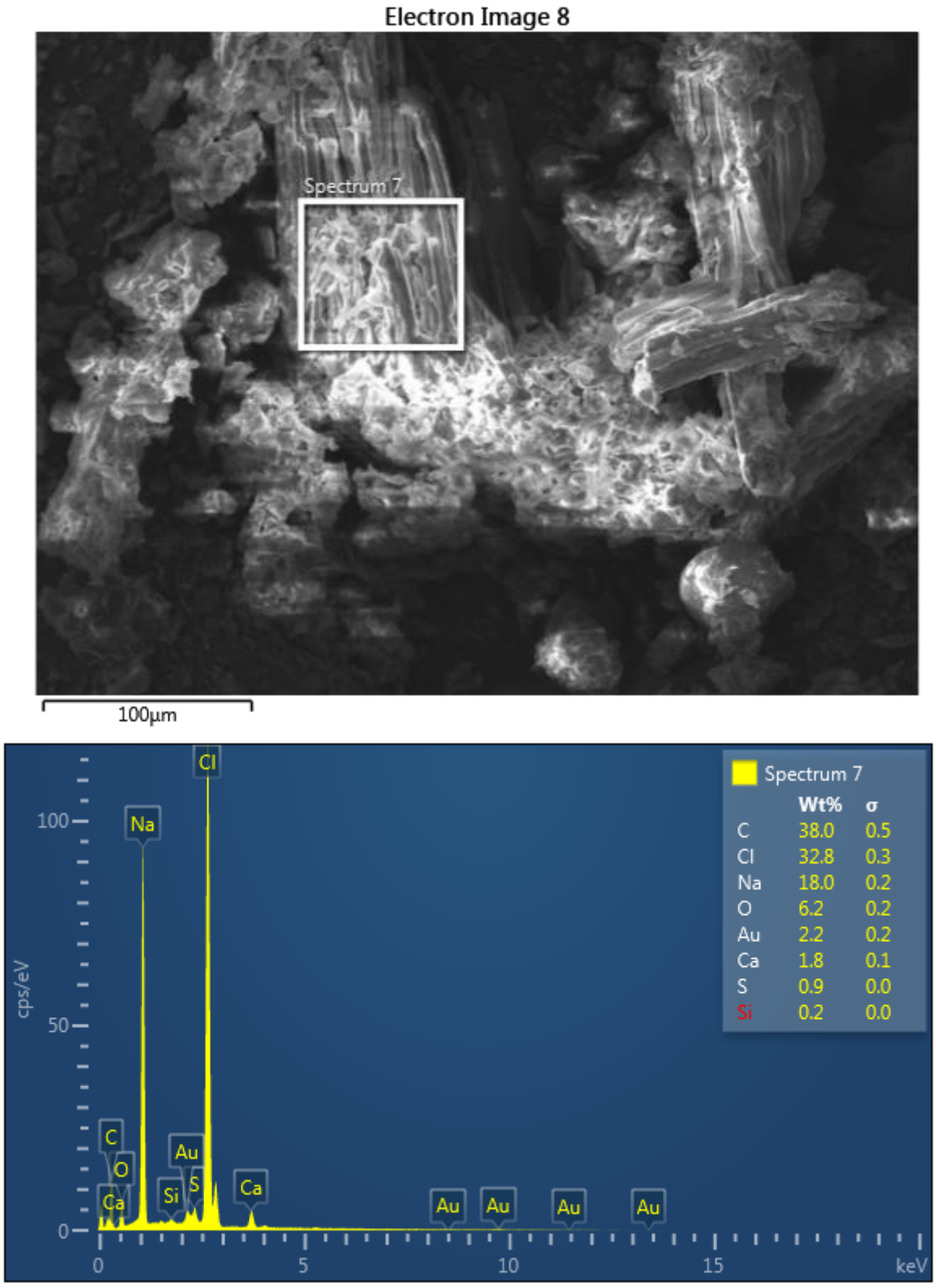

Figure 4-46. XRD results from test C3-1C Site 2

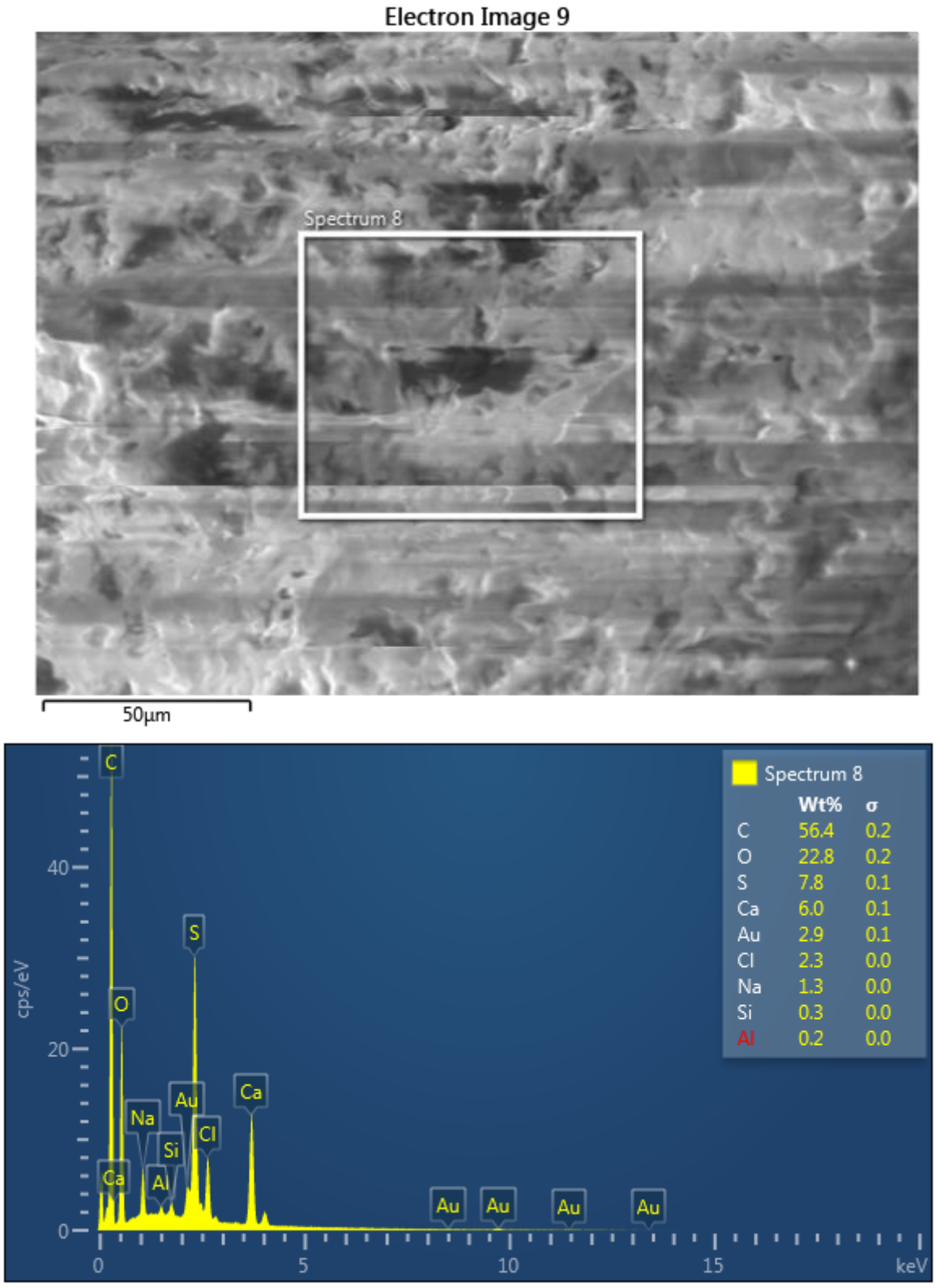

Figure 4-47. XRD results from test C3-1C Site 3

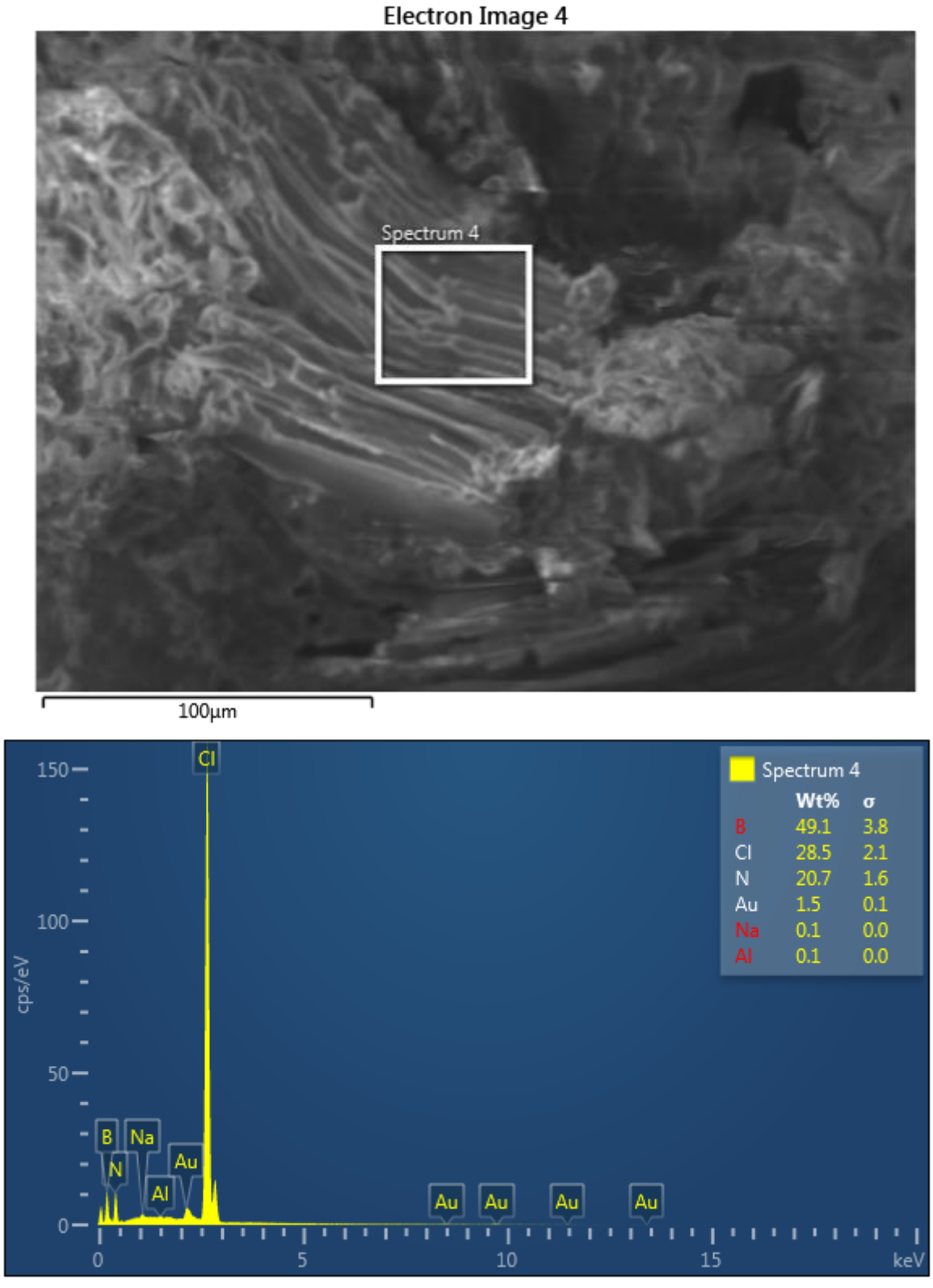

Figure 4-48. XRD results from test C3-2A Site 1

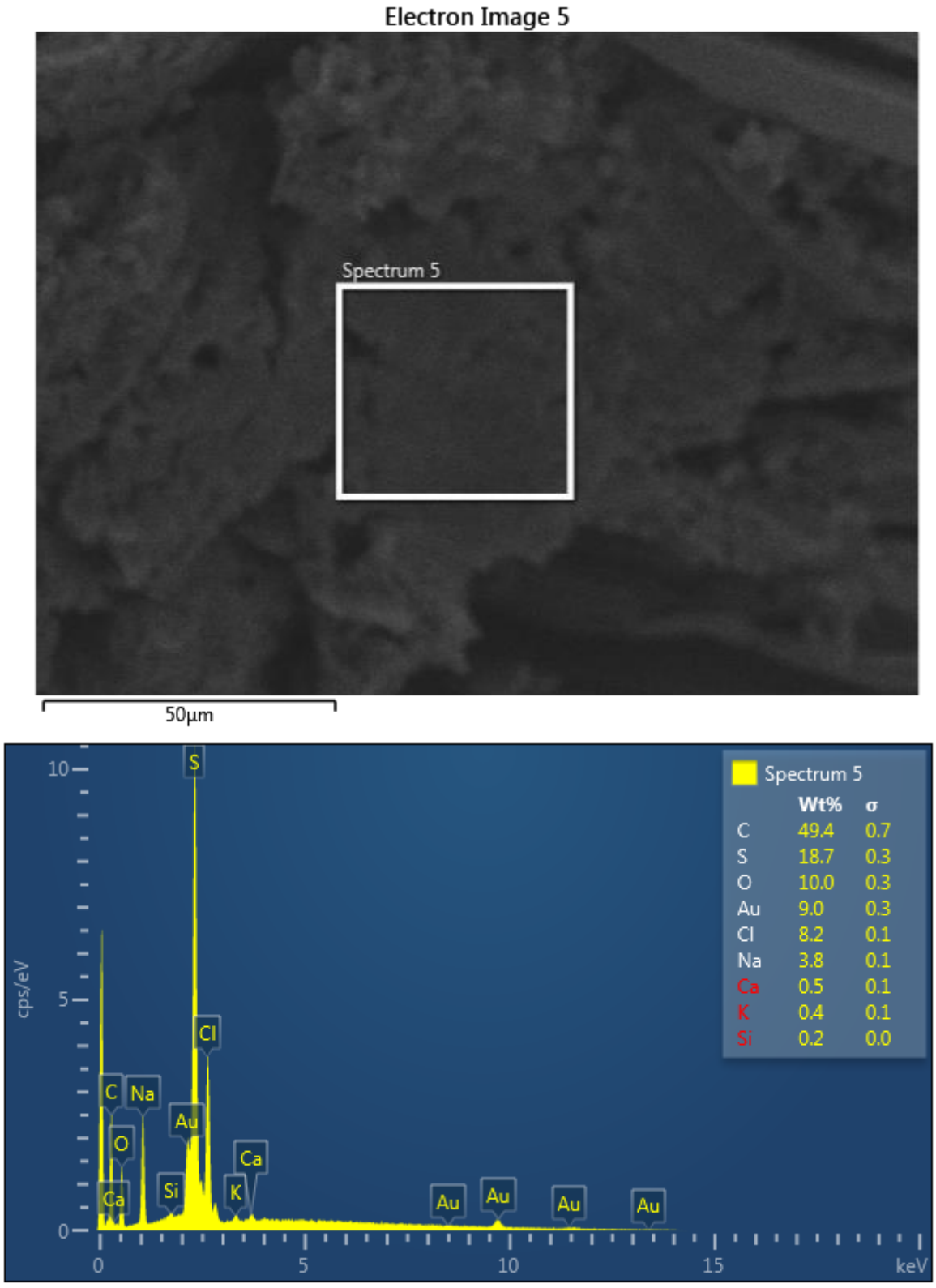

Figure 4-49. XRD results from test C3-2A Site 2

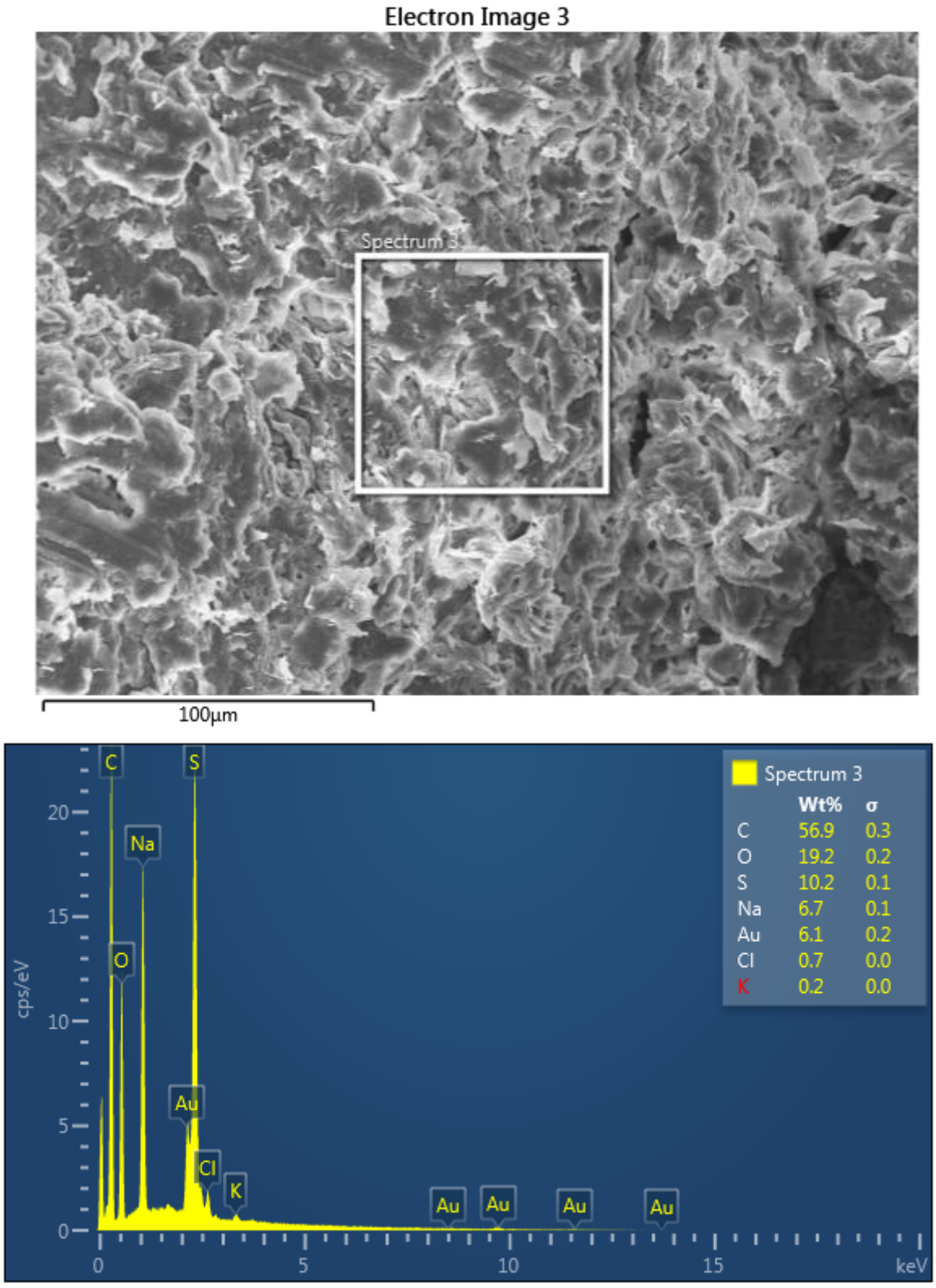

Figure 4-50. XRD results from test C3-2A Site 3

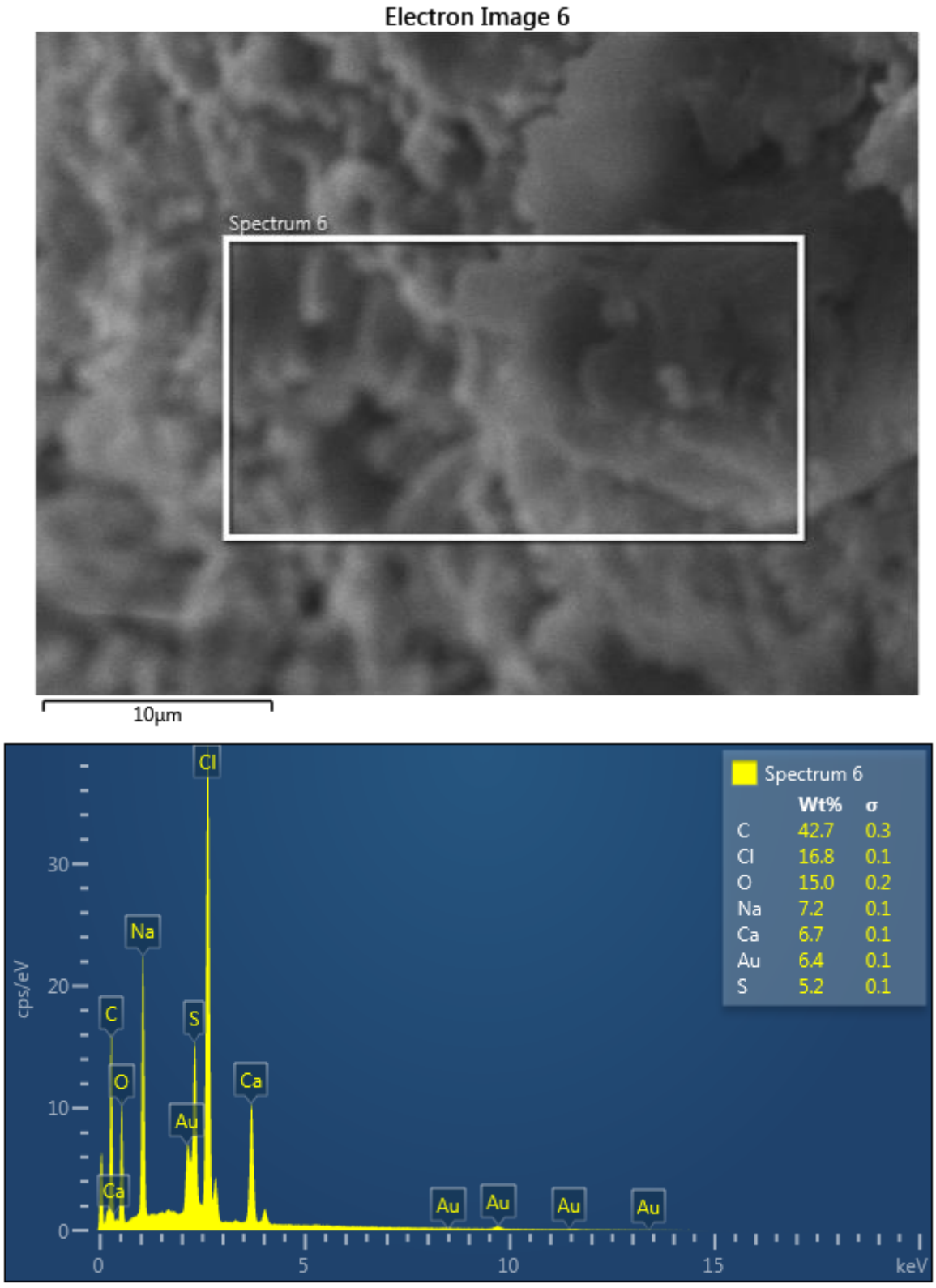

Figure 4-51. XRD results from test C3-2A Site 4

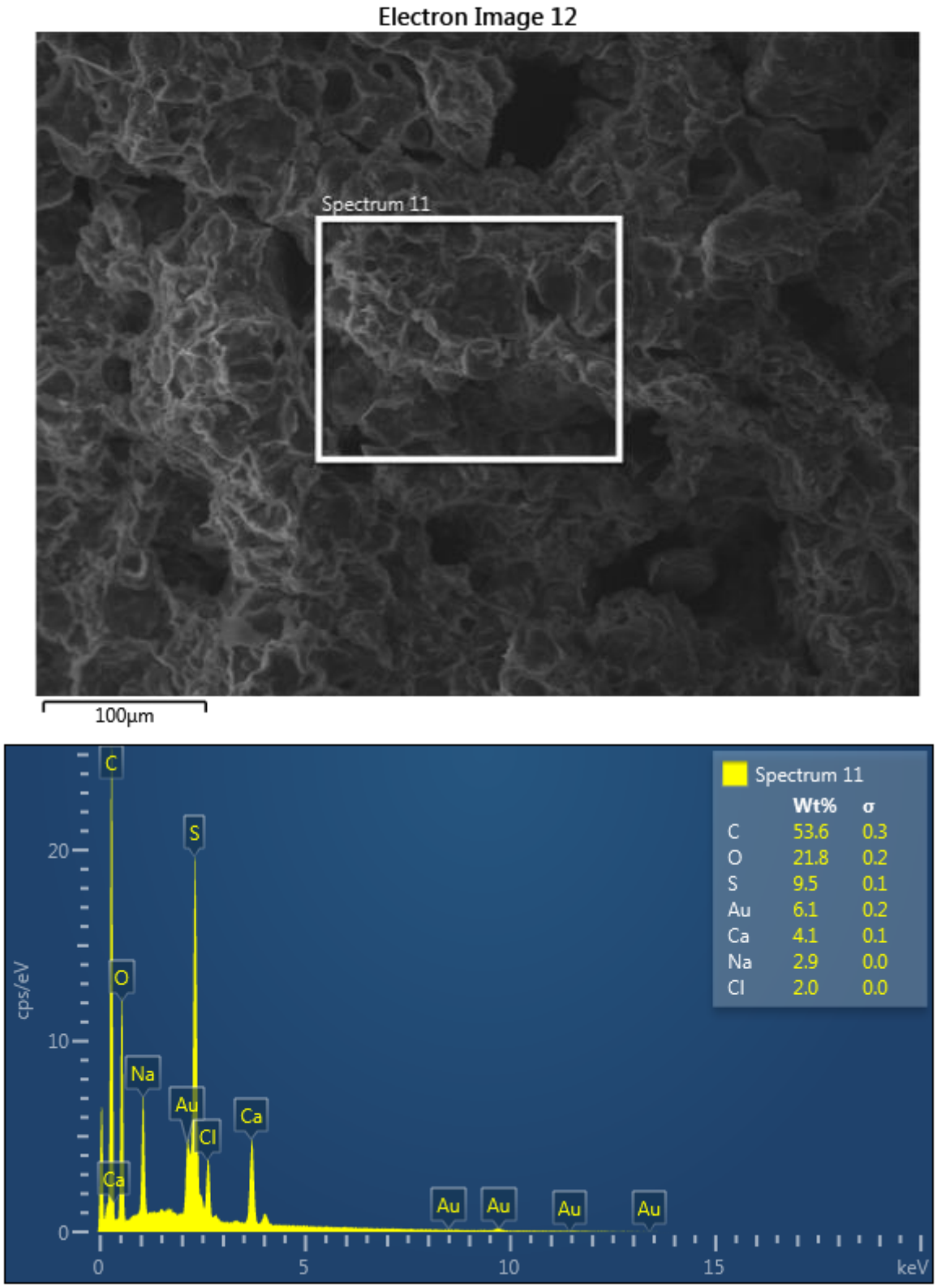

Figure 4-52. XRD results from test C3-2B Site 1

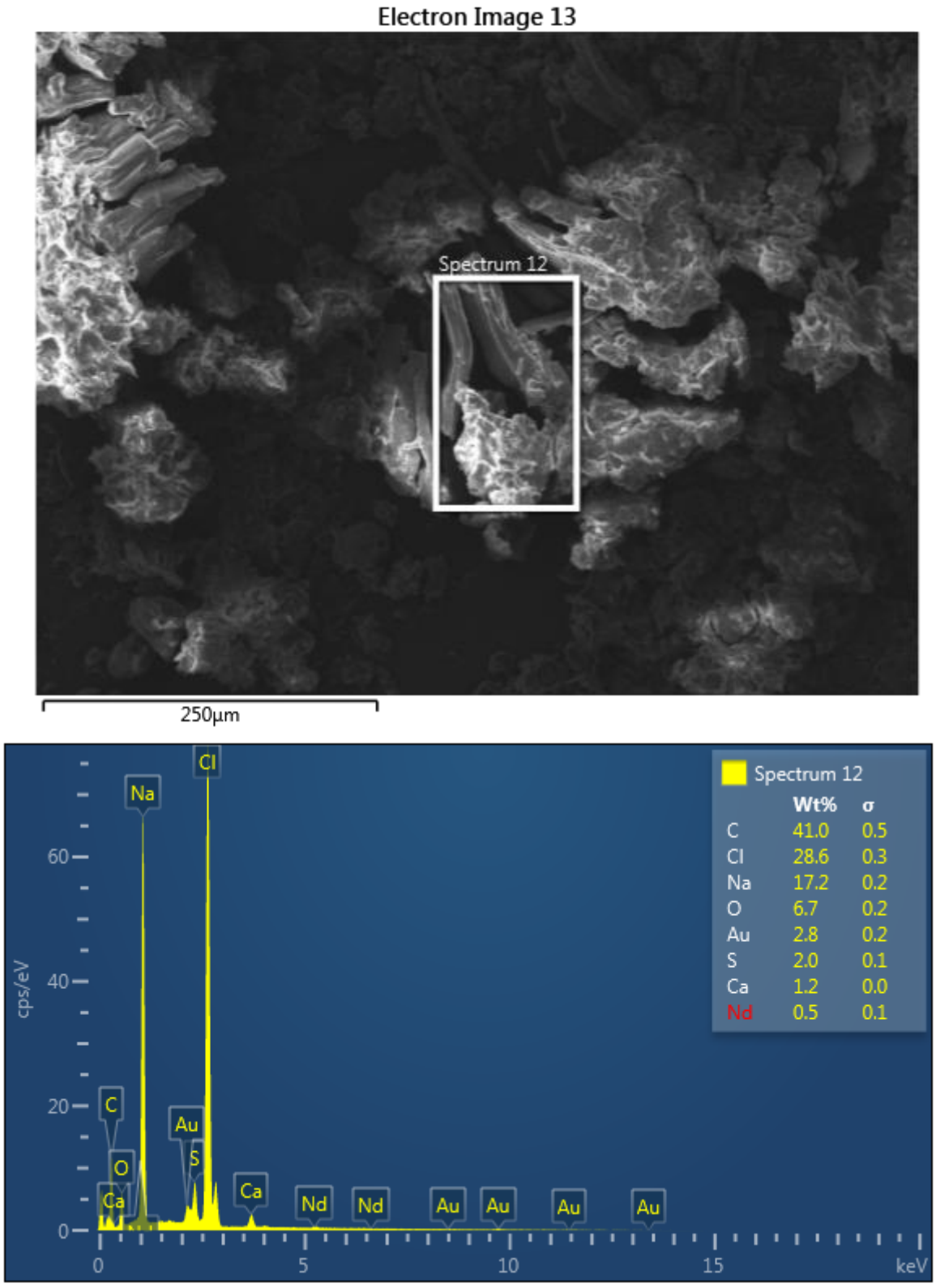

Figure 4-53. XRD results from test C3-2B Site 2

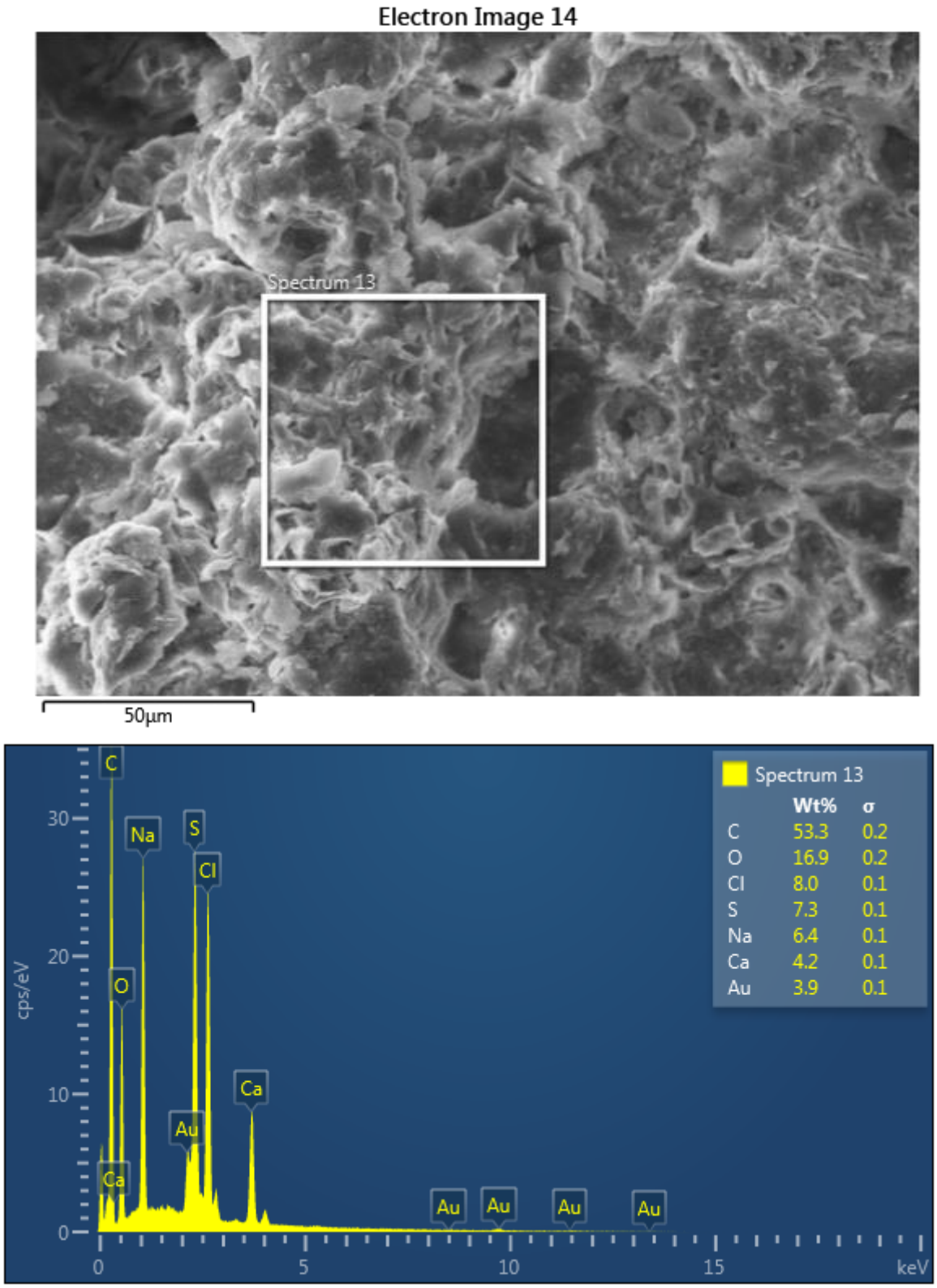

Figure 4-54. XRD results from test C3-2C

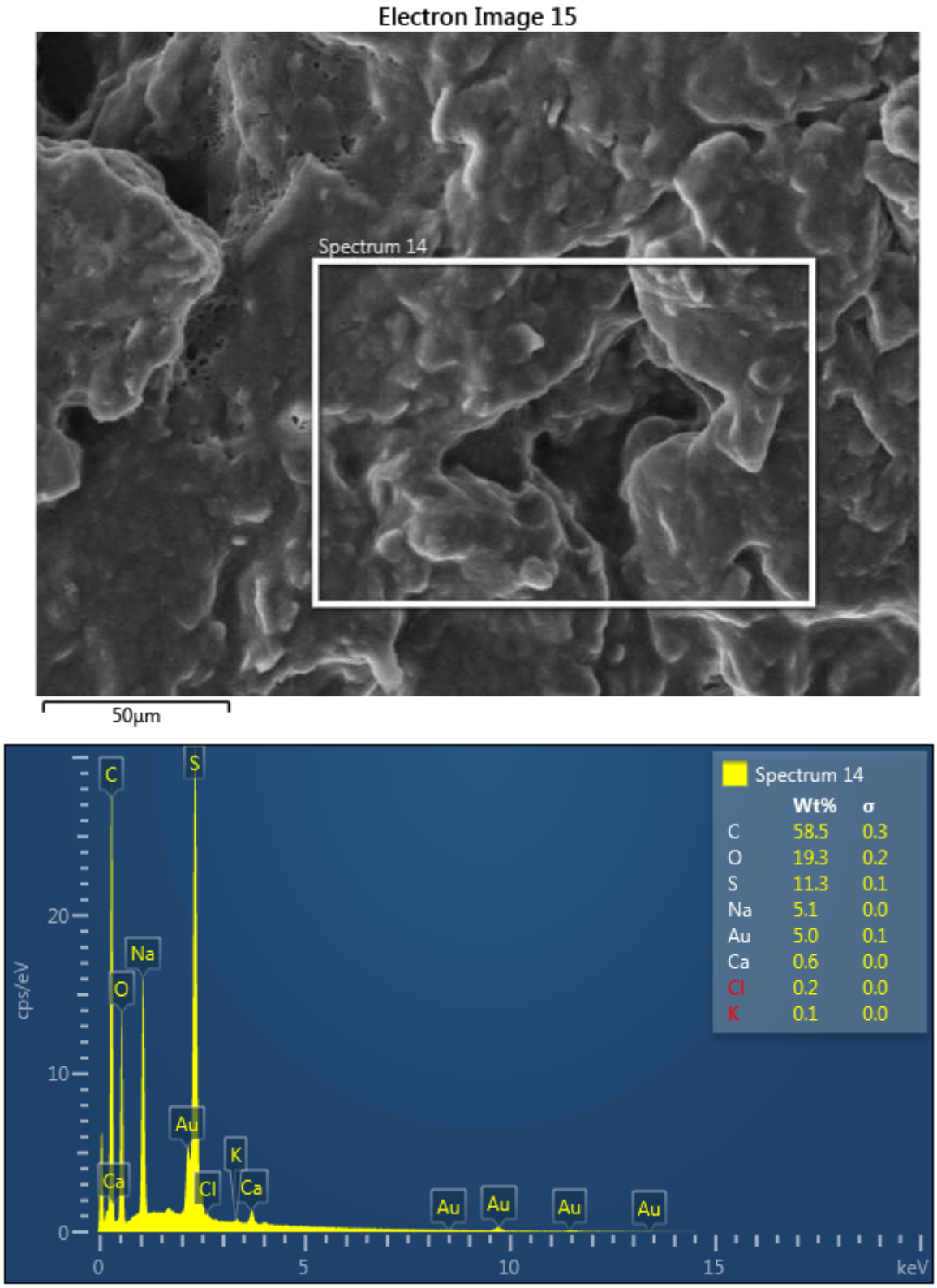

Figure 4-55. XRD results from test C3-3A

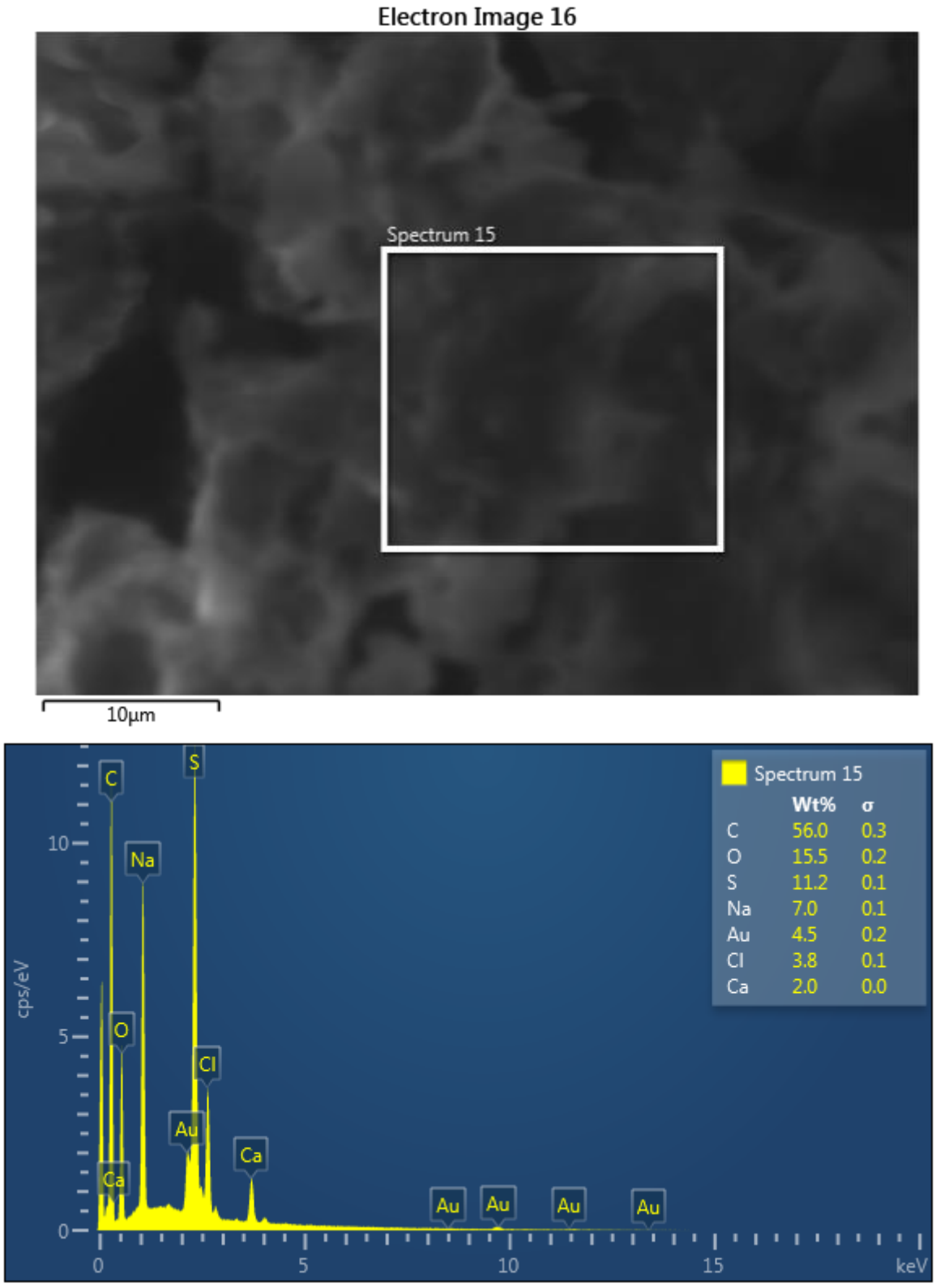

Figure 4-56. XRD results from test C3-3B

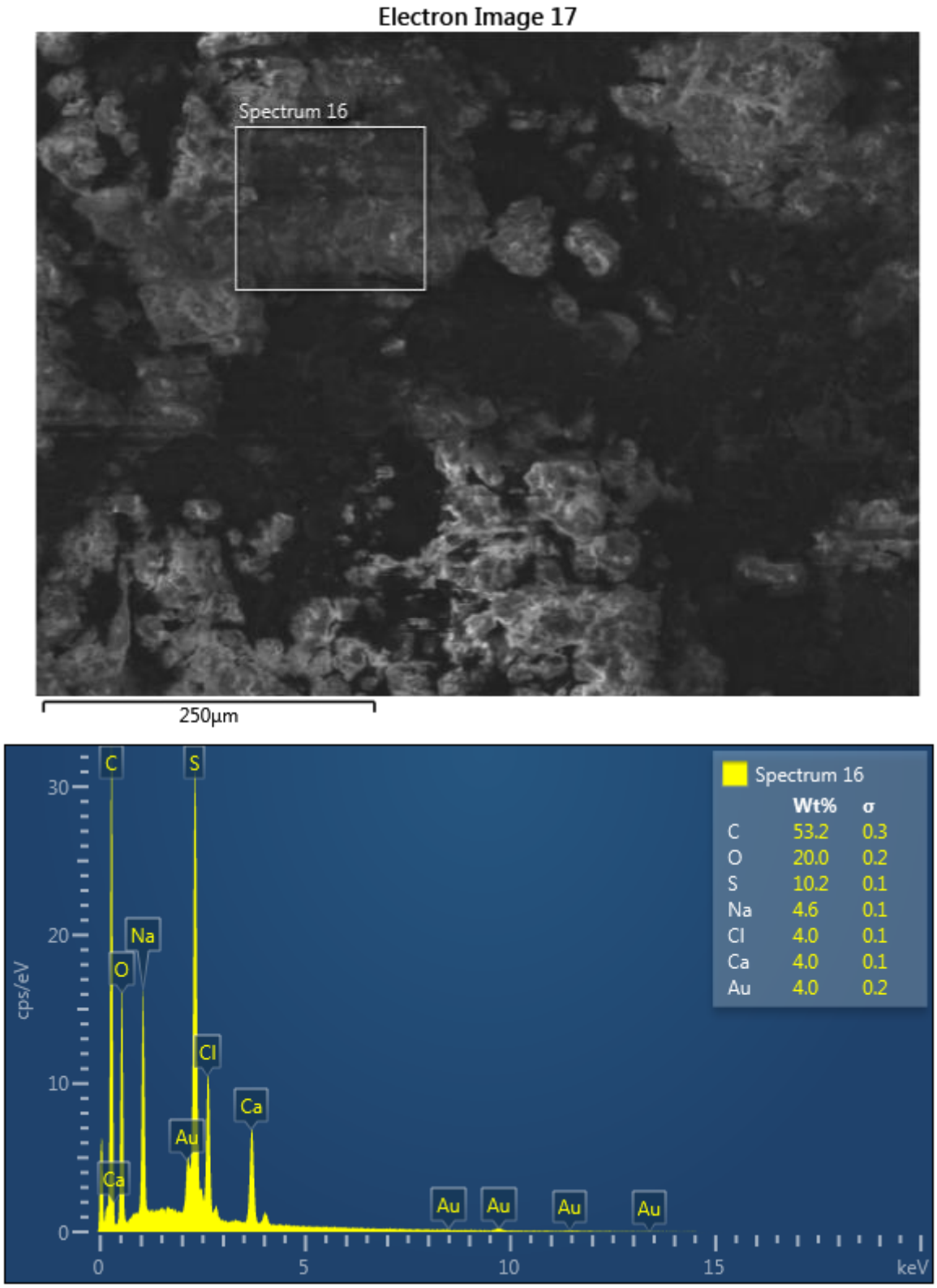

Figure 4-57. XRD results from test C3-3C

4.5.3 Explanation of Results

Summarizing some of the previous findings:

1. The soil mixing-SDS MICP recipe produced specimens that showed apparent strengthening when subjected to UCS testing.

2. Consolidation, triaxial, and dissolution testing showed that the apparent strengthening observed in (1) was dissolvable.

3. Specimens prepared with relatively low SDS percentages and calcium chloride produced soil columns that were not dissolvable.

4. SEM/XRD analysis showed sodium chloride precipitation but very little calcite precipitation in treated columns (both with and without microbes).

Investigators developed a possible explanation for these results. In aqueous solution, the sodium ion from SDS disassociates from its dodecyl sulfate portion of yielding a polar hydrophilic head and a neutrally-charged hydrophobic tail. When the concentration of any surfactant passes its critical micelle concentration (CMC), the hydrophilic heads and the hydrophobic tails tend to align with one another creating micelles (Figure 4-58(a)). As discussed by Zapf (2002), micelle shape may vary depending on interfacial conditions. Common micelle shapes include bilayers, spheres, rod-like structures, disc-like structures, vesicles, lamellae, and a sponge-phase. Regardless of the shape of the micelle, they tend to interact similarly with neutrally-charged particles in aqueous solutions. When in solution, micelle formation results in interior hydrophobic pockets that can absorb neutrally-charged particles coupled with hydrophilic exteriors capable of interacting with water or other polar solvents.

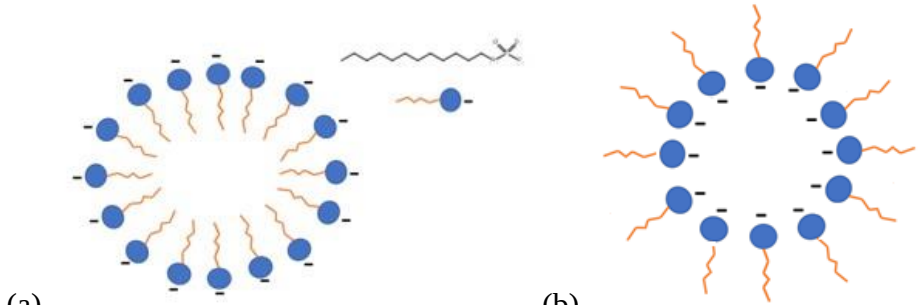

(a) (b)

Figure 4-58 (a) SDS micelle structure in aqueous solution, (b) SDS micelle structure in non-aqueous (hydrophobic) solution (adapted from Davies, 2018)

In this way, organics can absorb into the interior of the micelle and effectively be solubilized into an aqueous media. In hydrophobic solutions (liquid oils), or mixed hydrophobic/hydrophilic solutions, where the mixed solution is far more hydrophobic than hydrophilic, inverted micelles also occur with an interior hydrophilic pocket containing the polar "heads" and a non-polar exterior where the hydrophobic "tails" point outward (Figure 4-78(b)). This occurs to reduce the overall system entropy in hydrophobic media and to align "like" chemical properties.

Overall, Figure 4-78 yields micelles with several negatively-charged tails. In addition, the calcium chloride that was added to the treated soil mixtures is known to dissolve into positive calcium ions (+2) and negatively-charged chlorine ions (-1). It would appear that each calcium ion is bonding with two of the negatively-charged dodecyl sulfate tails to yield a calcium dodecyl sulfate (CDS) complex described in Equation 4-1 and shown at the small scale in Figure 4-59.

$$CaCl_2 + 2NaC_{12}H_{25}O_4S \rightarrow Ca(C_{12}H_{25}O_4S)_2 + 2NaCl \text{ (CDS Complex Formation)} \qquad (4\text{-}1)$$

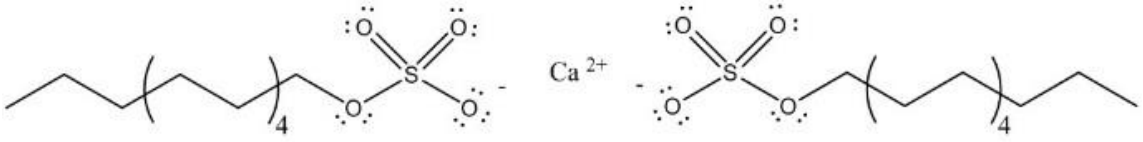

Figure 4-59. Calcium dodecyl sulfate complex

Macroscopically, a multitude of these CDS complexes appear to form inverted micelles above the CMC in a substantially hydrophobic environment. This leads to a secondary matrix of micelles from the combination of positive calcium (+2) ions and the negatively charged (-1) sulfate head/carbon tail portion of the SDS (Figure 4-60).

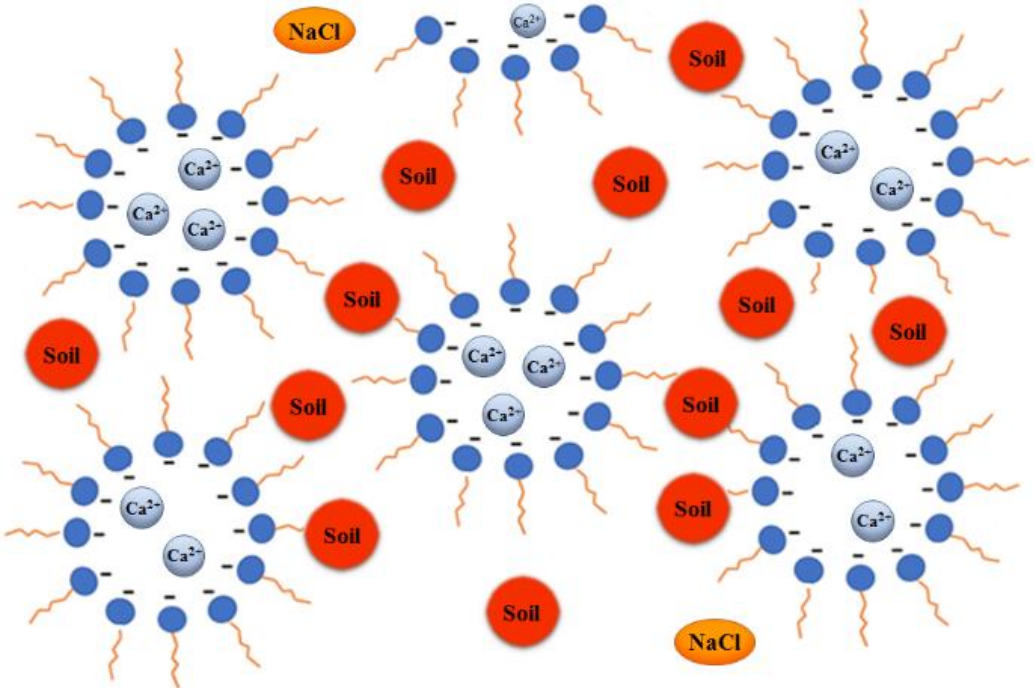

Figure 4-60. Explanation for apparent strengthening from SDS-$CaCl_2$ complex

The formation of the CDS complex prevents the micelle from achieving a hydrophilic exterior as the hydrophilic heads of the micelles are ionically bonded to Ca^{2+} ions. This is likely the reason that treated soil strength increased and that treated specimens were insoluble.

Of course, this explanation does not yet fully address observed results associated with the control dissolution tests nor does this explanation yet fully address observations when combined with uratolytic microbes. It should be noted that when SDS was added to the MICP recipe:

1. A strong smell of ammonium was present throughout testing with microbes.
2. Specimens appeared to "bubble" which indicated that carbon dioxide gas must be produced when specimens were treated with microbes.

These observations would appear to indicate that the microbes were lysing urea, producing ammonia/carbonic acid, and starting the MICP reactions that eventually lead to calcite formation. However, when microbes were included, specimens were weaker than when specimens that were treated with calcium chloride and SDS only. This indicates that some calcium ions are bonding with carbonate while others are bonding to SDS micelles. Overall, this results in a relatively weaker matrix. When urea was added to the recipe, a weaker matrix was also observed. Urea is known to denature organic material; therefore it is likely that its inclusion denatured the soil particles, thereby leading to a weaker CDS complex.

Overall, it appears this CDS complex is very strong and relatively insoluble. This CDS complex is certainly not a form of MICP, but it should be further investigated as a potential method for strengthening organic-rich soil since preliminary results with it were so promising. Preliminarily, soil strengthening via the CDS complex has been dubbed surfactant-induced soil stabilization (SISS). Other types of promising treatments along the same line have been proposed. For instance, Wan Hassan et al. (2017) treated organic soil with magnesium chloride and allowed the specimens to cure for up to 28 days. The authors reported that the formation of magnesium silicate hydrate, a cementitious compound that resulted in rapid increases in the UCS in the first 3 days of curing and up to approximately 14 psi at the end of the 28 days.

4.5.4 Preliminary Further Investigation of the SISS treatment method.

4.5.4.1 First Round of Testing

Investigators prepared several series of specimens using the new SISS treatment technique whereby SDS was mixed with soil and calcium chloride. Curing was allowed to occur both underwater and in air (although, curing method did not appear to affect results). UCS tests were performed on treated specimens. This new data were added to previous results that included the microbes. Preliminary results showed that the new treatment method using SDS and calcium chloride only produced comparable strengths compared to specimens using microbes and urea (Figure 4-61). However, the advantage to this SISS technique is that it appears to be insoluble.

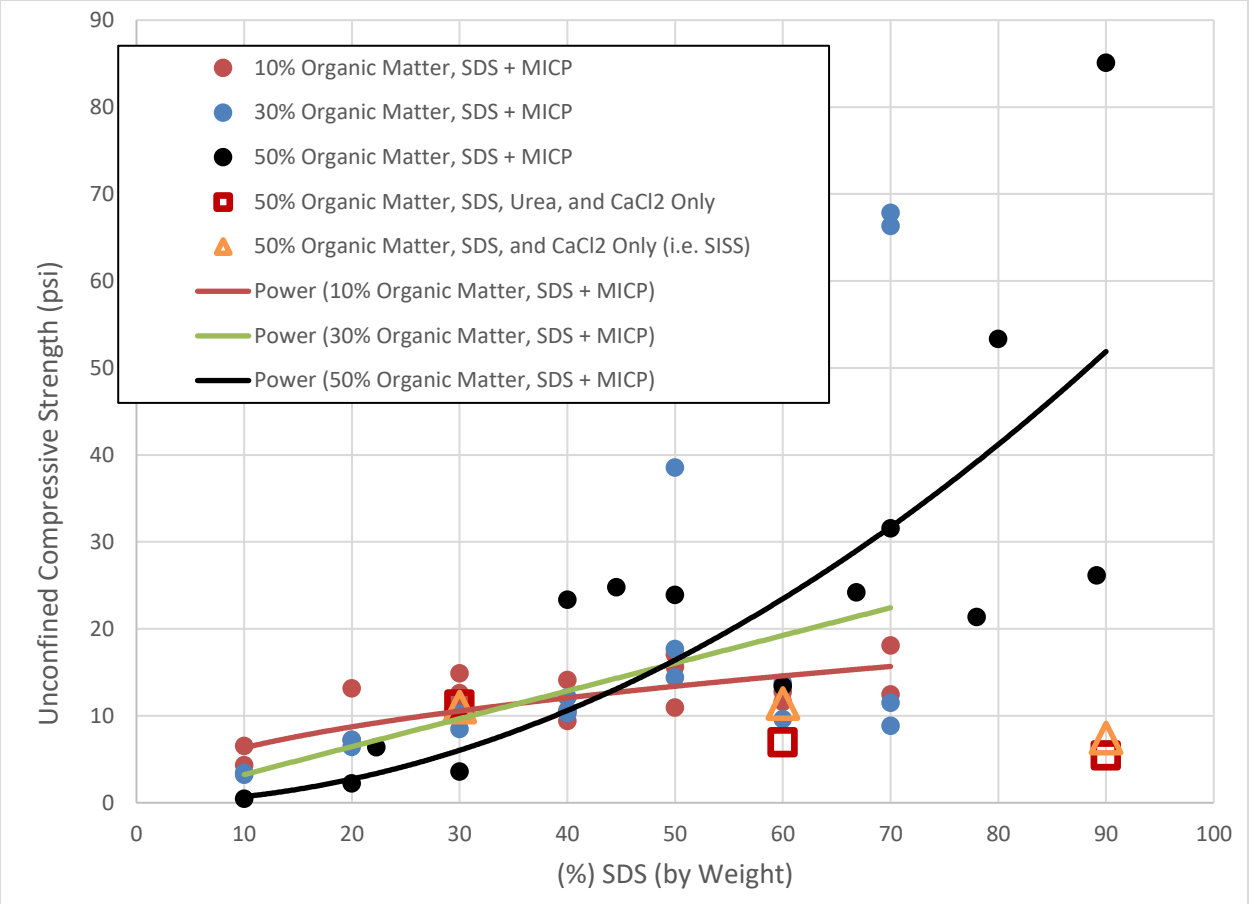

Figure 4-61. UCS vs. % SDS with CDS complex specimen data included

4.5.4.2 Additional Testing

Preliminary testing using other soil specimens was conducted to see if the SISS method would be an effective treatment method for other soil types. In addition, some preliminary optimization tests were conducted using the SISS technique with 50/70 Ottawa sand (soil properties presented in Chapter 2), soil with 30% organic content (soil properties presented in Chapter 3), Tennessee ball clay (TBC), and another clay that was available in the UNF laboratory (Clay 1). Properties of the TBC and Clay 1 are presented below in Table 4-6.

Table 4-6. Properties of clay materials

Clay	**Tennessee Ball Clay (TBC)**	**Clay 1**
Liquid Limit	57.9	30.4
Plastic Limit	26.2	22.9
Plasticity Index	31.7	7.5
USCS Classification	CH	CL
Percent Clay	80%	65%

These soils were mixed with SDS in 2-inch by 4-inch concrete molds. Then, 40-mL of 2.5 M calcium chloride solution was added to the specimens. The specimens were mixed until they were consistent. After mixing, the specimens were allowed to air-dry for a minimum of 48 hours. However, it should be noted that hardening was usually observed within 20 minutes or less. After

drying, the specimens were extracted using a Dremel and UCS tests were performed. Results from these tests are presented below in Figure 4-62.

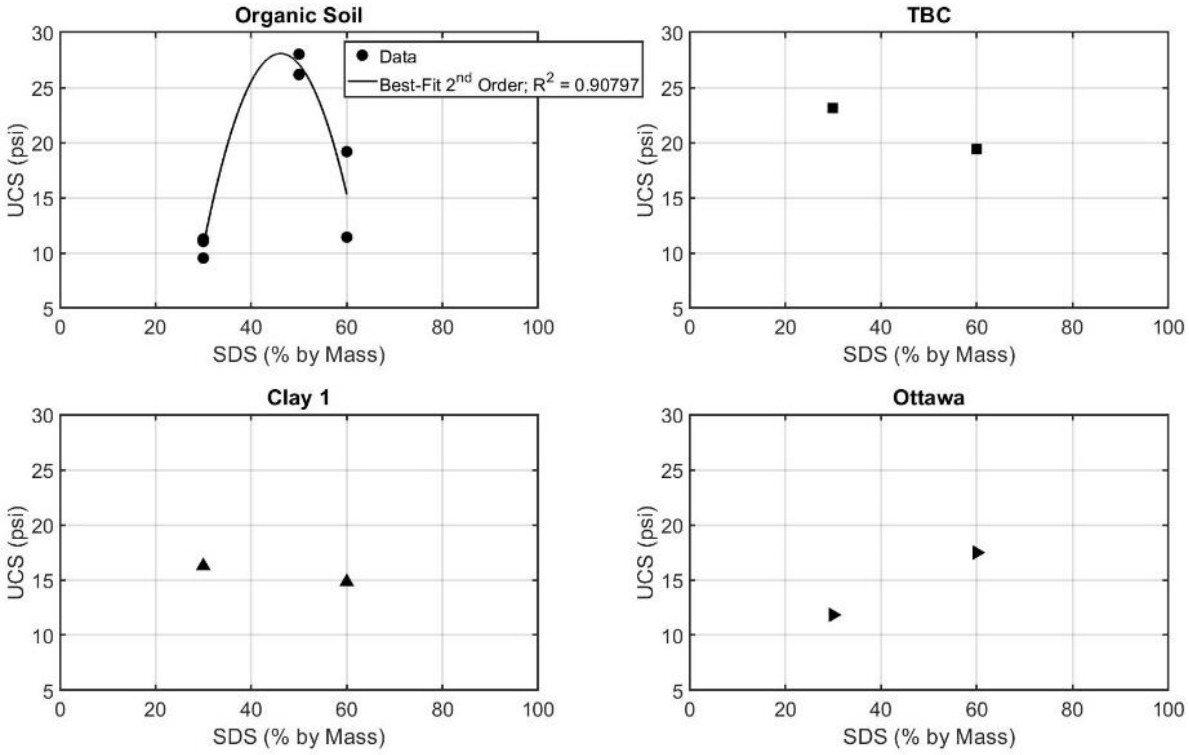

Figure 4-62. Unconfined compressive strength vs. percent SDS for various soil-types

In addition, SISS-treated specimens were broken apart and analyzed qualitatively. Photographs of these specimens are presented below in Figure 4-63.

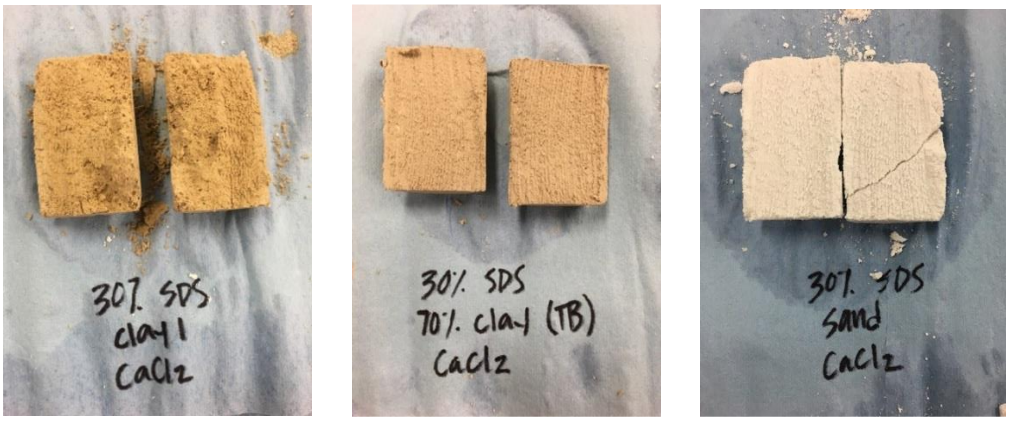

Figure 4-63. Photographs of other soil-types treated via SISS showing clay 1 (left), Tennessee ball clay (middle), and Ottawa sand (right)

Like the soil with high organic content, other soil types also showed relationships between SDS concentration and maximum strength. With the limited data, the Ottawa sand appeared to show a direct relationship between SDS and strength, while the clays tended to show inverse relationships. However, this does not necessarily mean that SISS would be ineffective in clays. Rather, it is possible that a lower SDS percentage (i.e., lower than 30%) may optimize the reaction in these

soils. These relationships and the effect of the clay minerology on the SDS treatment should be further investigated.

Control tests were prepared using the clays. The same procedure used above was repeated with the clays by mixing the clays with water only (no SDS or calcium chloride). After 48 hours, the tubes were cut open. Resulting specimens were not fully dried nor were they hardened as shown below in Figure 4-64. As shown, it was not possible to remove the specimen from its tube so that it could finish drying. On the other hand, the SISS-treated specimens were all sufficiently hardened after 48 hours to allow for "clean" specimen extraction.

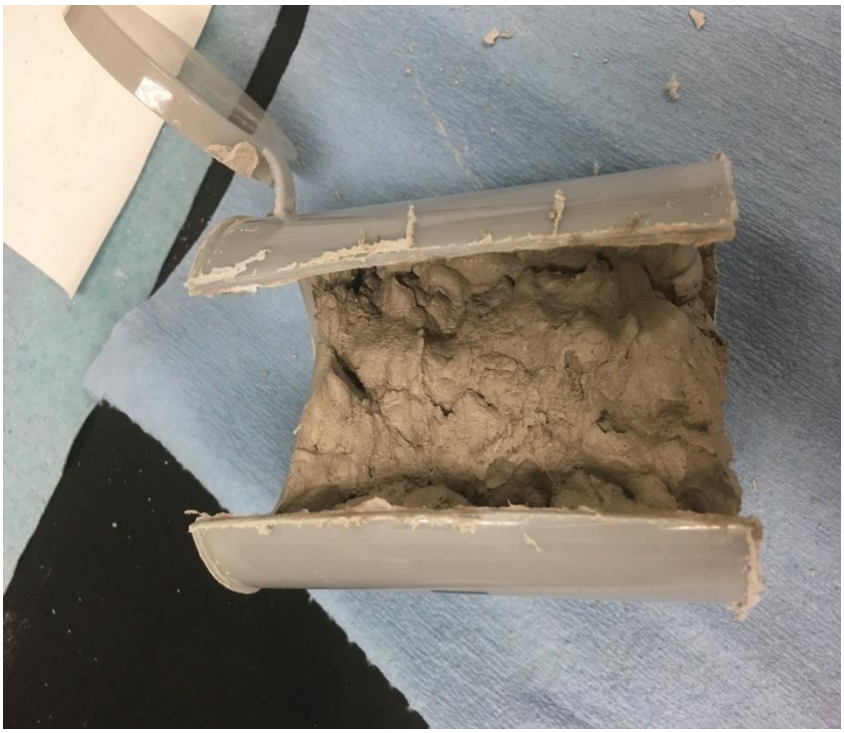

Figure 4-64. Tennessee ball clay after 48 hours mixed with water in concrete tube

A final series of tests was conducted using the 30% organic-rich soil from Polk County. This soil was sieved through a #4 sieve so that soil particles distribution was more-uniform. The SISS treatment components, calcium chloride and SDS, were stoichiometrically balanced and used to treat the sieved soil at various SDS percentages. Results are shown below in Figure 4-65. A clearly-defined optimum SDS/soil ratio was found between 30% and 60% SDS. At this optimum, UCS was on the order of 50 psi. This is much higher than results obtained using MICP and these specimens should be insoluble. This result may also merit further investigation.

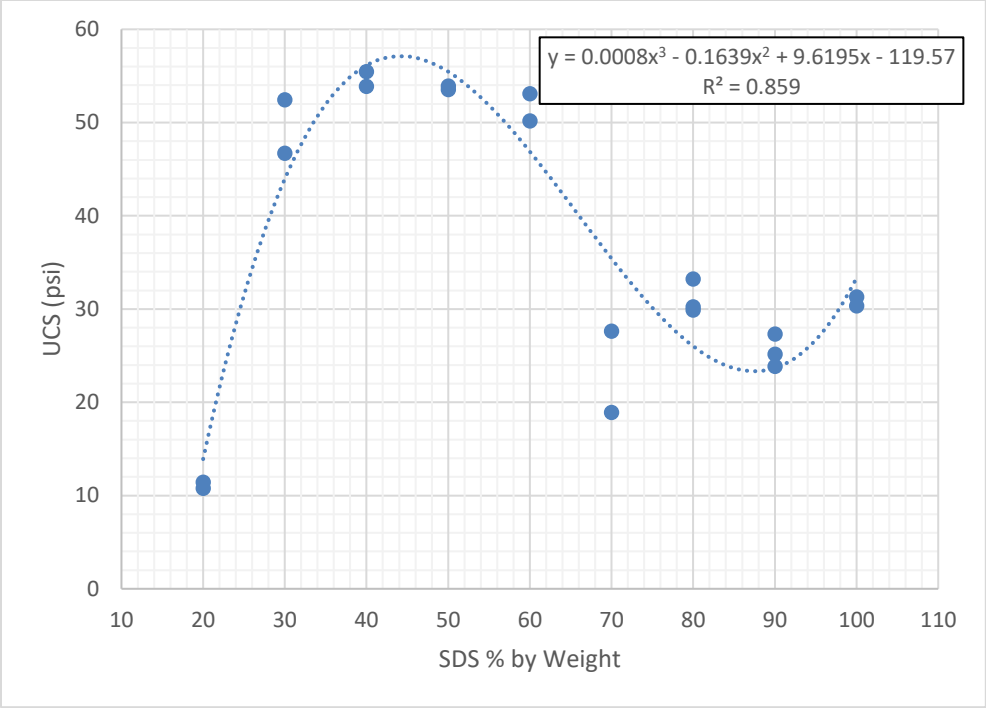

Figure 4-65. SISS treatment results using 30% organic-rich soil from Polk County

CHAPTER 5
A POSSIBLE EXPLANATION FOR MICP'S FAILURE IN ORGANIC SOILS

5.1 Exopolysaccharide Introduction

An investigation was conducted to determine the role of exopolysaccharides (EPS) in MICP calcium carbonate formation. Quartz sands were used throughout this study because MICP in sand tends to be better-understood and relatively easier to characterize and image, with less interferences from organic matter. The DeJong et al. (2006) soil column percolation treatment method was used throughout this study.

EPS are "high-molecular-weight polymers that are composed of sugar residues and are secreted by a microorganism into the surrounding environment" (Staudt, 2004). EPS is a common method of bacteria colonization of surfaces (Staudt, 2004), and there are many advantages of forming EPS biofilms for microbes including assistance in colonizing surfaces with low charge potential, and protection from predators, viruses, antibiotics, and deleterious environmental conditions. Biofilms also promote the maintenance of extracellular enzyme structural integrity and assist in creating the physiological homeostasis of the microbe.

Microorganisms create a wide variety of polysaccharides that mostly consist of monosaccharides and some non-carbohydrate substituents such as acetate, pyruvate, succinate, and phosphate (Suresh, 2009). Exopolysaccharides are generally identified and are classified according to their 'ropy' or 'mucoid' phenotypic appearance. Ropy EPS is characterized by a high resistance to flow and the formation of strands or filaments when extended with an inoculation loop (Dierksen et al., 1997). Mucoid EPS has a shiny, slimy appearance, does not form filaments, and often looks film-like on agar plates. However, these identifiers are highly subjective, as not every slimy and or stringy substance is EPS.

S. pasteurii can produce biofilms. While a few studies have documented the formation of *S. pasteurii* biofilm during the MICP process (e.g., Harris et al., 2016), their potential role in the MICP cementation process has not been studied.

5.2 Goals and Objectives of the EPS Study

The goal of this research was to investigate the role of EPS in MICP. Specifically, it was hypothesized that presence of EPS is critical to calcite formation, i.e cementation, and that this may be more significant than the presence of the bacteria themselves. EPS may serve as a nucleation or template agent (organomineralization) or through some other mechanism. We propose that if EPS is involved in bonding, then EPS should be observed at bonding sites between sand grains. Further, the calcite crystals precipitated during MICP should be formed and immobilized in the EPS and located on soil particle surfaces rather than associated mainly with cells. We might also observe that the bacteria in the MICP soil matrix are present as unbound single cells and are alive rather than encased in calcite, which would be the case if they themselves are nucleating calcite formation. Alternatively, if *S. pasteurii* cells act as nucleation sites, most calcite crystals should be associated with cells and found throughout the MICP materials. We may also find that that the bacteria are not viable after the completion of the MICP process. Put another way, it was hypothesized that the model shown in Figure 5-2 may better explain calcification rather

than the traditional model used to explain MICP as shown below in Figure 5-1. If true, this could have significant implications in terms of MICP's viability for use in organic rich soils.

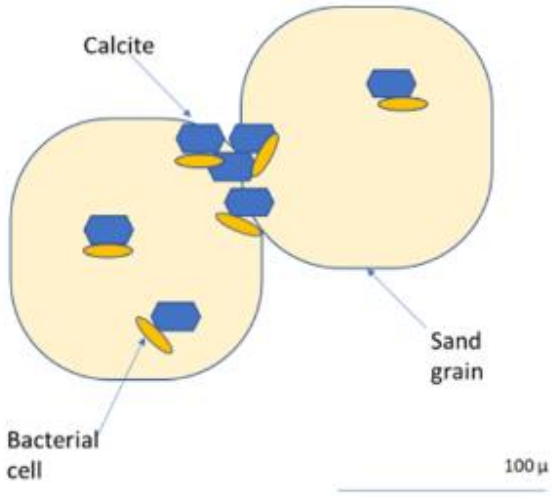

Figure 5-1. Traditional MICP model

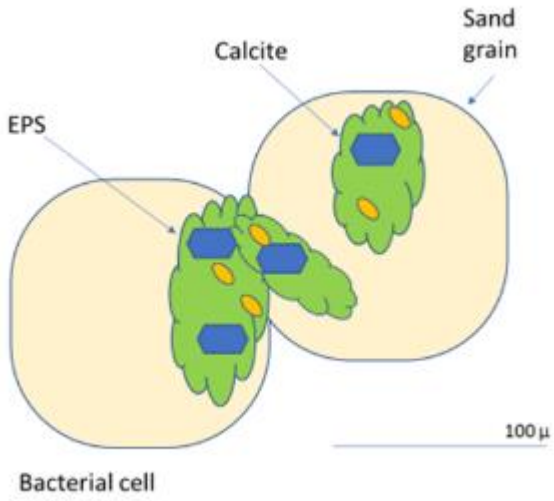

Figure 5-2. Hypothesized modified MICP model

The EPS study tested both hypotheses using the presence of carbonate content based on cementation degree, plate count enumerations, and microscopy/staining techniques that allow one to visualize the relationship between cells, EPS, calcite crystals and sand particles on samples from MICP-cemented sand columns: SEM, autofluorescent imaging, and alcian blue staining. Controls used were: 1) sands that had no microbial additions, 2) samples from sand columns that had been treated with similar additions of microbes and solutions but failed to cement, and 3) samples from upper column uncemented portions of sand columns that cemented in lower column portions.

5.3 Methods during EPS Study

5.3.1 Treatment Method Specifics

As mentioned above, MICP-cemented materials were produced based on the methods of DeJong et al. (2006) and Mortenson et al. (2011), with modification. To summarize, *S. pasteurii* cells were cultured from freezer stocks of the strain (ATCC 6543) obtained from Fischer Scientific by streaking the bacterial suspension on agar plates. These plates were incubated at 28°C for one day in the dark until colonies appeared to be robust. From these plate colonies, a single loop of bacterial mass was used to inoculate liquid growth medium in 500 mL Erlenmeyer flasks aseptically. After shaking these flasks in a dark incubator at room temperature for two days, the bacteria were harvested by centrifugation. Pellets obtained were suspended in DI water, urea and $CaCl_2$ to test for cell viability. Only tests that resulted in calcite precipitation (i.e., cloudy white solution) were used for MICP. Cells were resuspended in an 'inoculation medium' of DI water and low concentrations of NH_4Cl, dextrose, and NaHCO3. This solution was then pumped into the bottom of 7" x 3" diameter acrylic cylinder columns filled with Ottawa sand (pure SiO_2, grain mesh 50-70 microns) using a peristaltic pump and left overnight to "attach" to the soil surfaces (see apparatus photo in Figure 2). The bacteria were then fed a 'treatment mixture' of urea, ammonium chloride, dextrose, bicarbonate, and calcium chloride four times each day for two days. After this, the columns were allowed to cement for a further 2 to 3 days. Chambers were then opened, dried for 24 hours in an oven at 30 °C, and then carefully subsampled longitudinally, at 1.25 cm intervals. Samples were typically extracted from the side of the column so as to allow the remainder of the column to remain intact for physical property testing.

5.3.2 Carbonate Content

Carbonate content was measured by coulometric titration (Engleman et al., 1985) with a UIC/Coulometrics Model 5011 coulometer in which 10 g samples are acidified in closed vials. Addition of 0.2 mL HCl released CO_2, which was quantified on an automated coulometer (UIC) using a coulometric titration technique, with analytical precision ±1% based on analysis of reagent-grade (100%) $CaCO_3$. (Brenner et al., 2005).

5.3.3 Visualizing EPS

Similar to the work with organic-rich soil, SEM was used to visualize treated specimens' surface topographies and compositions. However, SEM is not able to identify organic substances with any certainty. Thus, to identify EPS, alternative methods were required.

Identification of EPS in geological materials is in an early experimental phase, and the majority of research has been done in the fields of dentistry and oncology. However, a recent study, "Molecular and morphological characterization of cyanobacterial diversity in the stromatolites of Highborne Cay, Bahamas," successfully used a staining approach to image EPS formation on the surfaces of carbonate grains (Foster et al, 2009). In this study, both laboratory-created and naturally occurring stromatolites were stained with an alcian blue (AB)/periodic acid (PA) kit, which turns cells that have stored glycogen, glycoproteins or neutral polysaccharides pink, and materials that are rich in anionic groups such as acidic mucopolysaccharides or mucins blue. Using this method, they were able to see the bacterial influence on the structure of stromatolites and also observe differences in EPS and structure between laboratory and natural stromatolites. Though EPS was

more prevalent in laboratory stromatolites, in both natural and laboratory made samples, EPS was shown between sand grains and appeared to show that EPS plays a key role in stromatolite structure. The greater clarity of AB/PA micrographs of stromatolites compared to SEM images, suggest that these staining techniques can provide a clearer picture of the location of individual cells relative to sand particles and precipitated minerals, and can provide information on the role of biofilms in biomineralization.

For this research, SEM and Environmental SEM (ESEM) photomicrographs were collected on a Zeiss EVO MA10 and an Itachi SU-5000 variable pressure FE-SEM, respectively. A Nikon A1RMPsi-STORM 4.0 was used to visualize biologic bonding and indicate whether alcian Blue would be a worthwhile procedure. And lastly, we stained cemented, semi-cemented, and uncemented treated materials with alcian blue and viewed these using both the Nikon E400 and the Leica DM500.

5.4 EPS Study Results and Discussion

5.4.1 Plate Counts

Using the Nikon E400 in this initial experiment, *S. pasteurii* were viable (Figure 5-3). Each individual bright spot in Figure 5-3 represents an individual CFU (colony forming unit), i.e., growing cell colony, of which there were many. This shows that, following the MICP procedure, cells were still viable and not encapsulated in calcite. This observation does not support nucleation theory, and rather suggests that calcite crystals did not form around individual *S. pasteurii* membranes, at least not all of them.

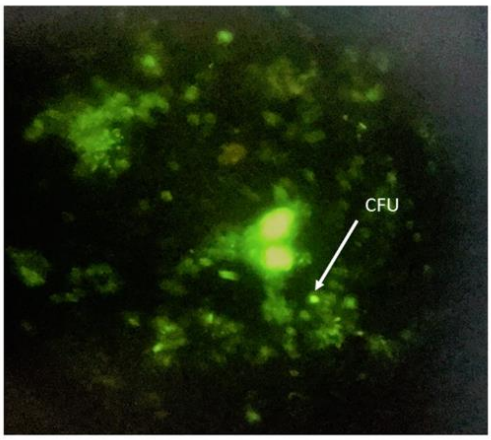

Figure 5-3. Auto-fluorescent photomicrographs of a freshly made enumeration plate of S. pasteurii cells cultured from a moist, treated/cemented MICP sample. CFU = colony-forming unit.

5.4.3 SEM Images

SEM (scanning electron microscopy) is the most common method of visualizing MICP materials, because it is the most widely available visualization tool in materials research. Micrographs from SEM offer clear and precise views of minerals; however, the preparation process requires a sprayed-on metal coating and vacuum desiccation, essentially removing evidence of biological materials. Figure 5-5a shows some sand-calcite and sand-sand bonding material that appears to

differ from the calcite crystals. An amorphous material covered much of these grains that was not present in the treated non-cemented material (Figure 5-4b). While SEM does not clearly show the presence of EPS, it does illustrate a major difference in the sand surface present in cemented and non-cemented materials.

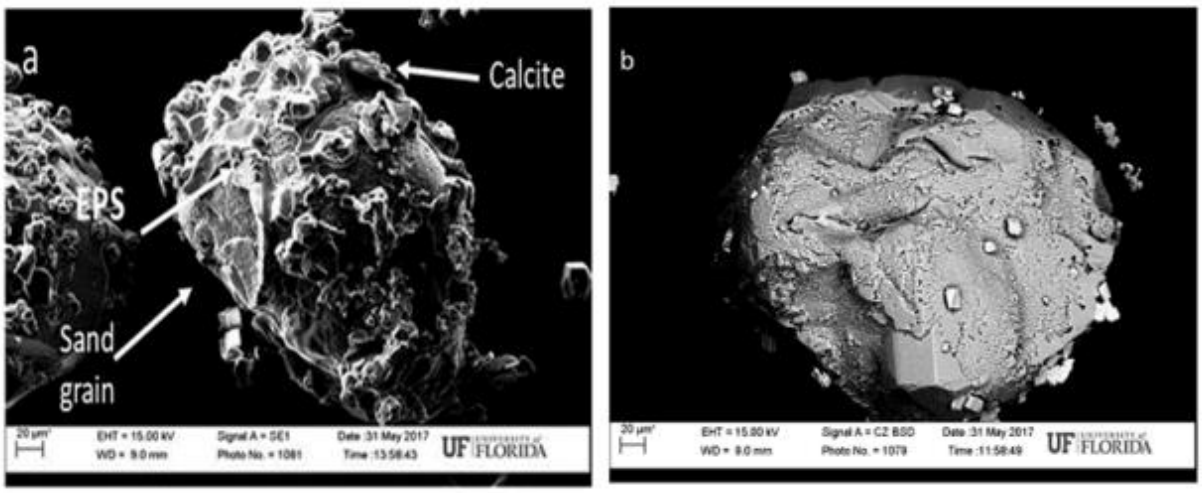

Figure 5-4. SEM images of MICP-cemented sand showing an individual sand grain from (a) cemented and (b) uncemented samples.

5.4.4 ESEM Images

Without the need for desiccation, vacuum or metal coating, the ESEM (environmental scanning electron microscopy) imaging technique allows one to potentially view microscopic biologics. However, the images obtained through this method are often open to interpretation. However, two significant observations that can be made from these images of the MICP products from a lower and upper portion of a cemented column (Figures 5-5a and b, respectively) are: 1) bacteria appeared to be living on the surface of the calcite and do not have calcite crystals growing on their surfaces, and 2) calcite and bacteria appear to be embedded in an amorphous material which may be EPS. These observations contradict the nucleation theory of MICP mechanism.

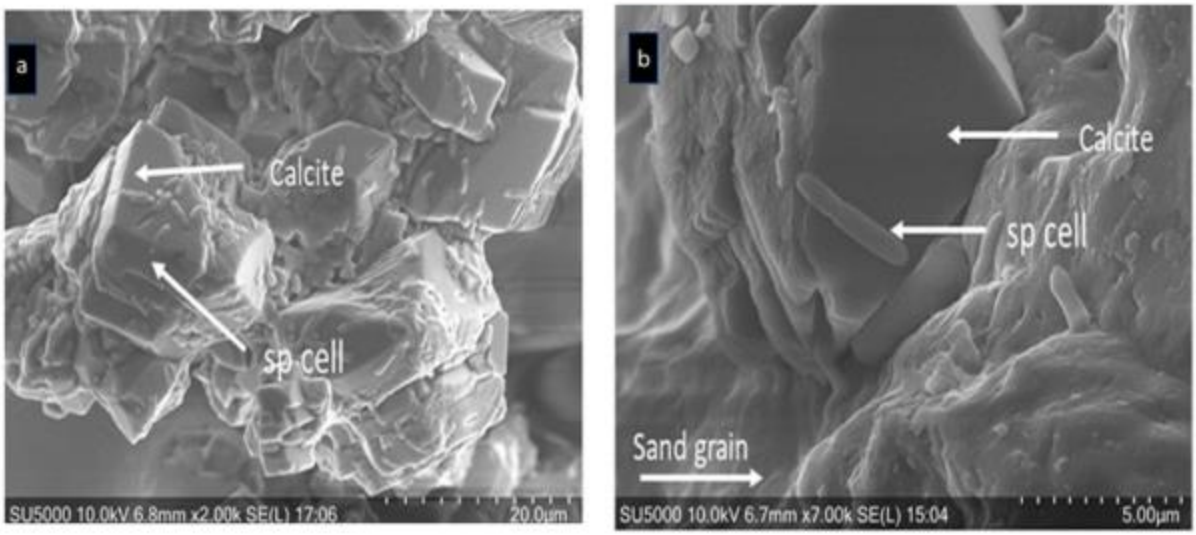

Figure 5-5. ESEM images of individual *S. pasteurii* cells on calcite crystals from moist cemented materials (a) J-NM (0.5 in. height), (b) J-NM (3 in. height).

5.4.5 In Situ Autofluorescence Images

In situ autofluorescence photomicrographs taken with a Nikon A1RMPsi-STORM 4.0 (using settings of FITC: 3500 MS and TRITC: 3000 MS) of unbroken MICP samples showed signs of the presence of EPS in treated/cemented samples (Figures 5-6c and d) that was not present in untreated/uncemented (control) or treated/uncemented samples (Figures 5-6a and b, respectively). Individual calcite crystals can be seen scattered amongst the fluorescing material in Figures 5-6c and 5-6d and can be ruled out as a source of fluorescence. The fluorescent green hue is potentially indicative of a biologic/protein presence and is much brighter in Figure 5-6d (the moist, treated/cemented and fresher sample), perhaps suggesting that this material is more abundant or less degraded, which might occur with EPS. While it cannot be definitely concluded that this florescent material in these images is EPS, it is likely that this coating is some form of protein and could be from individual *S. pasteurii* or EPS.

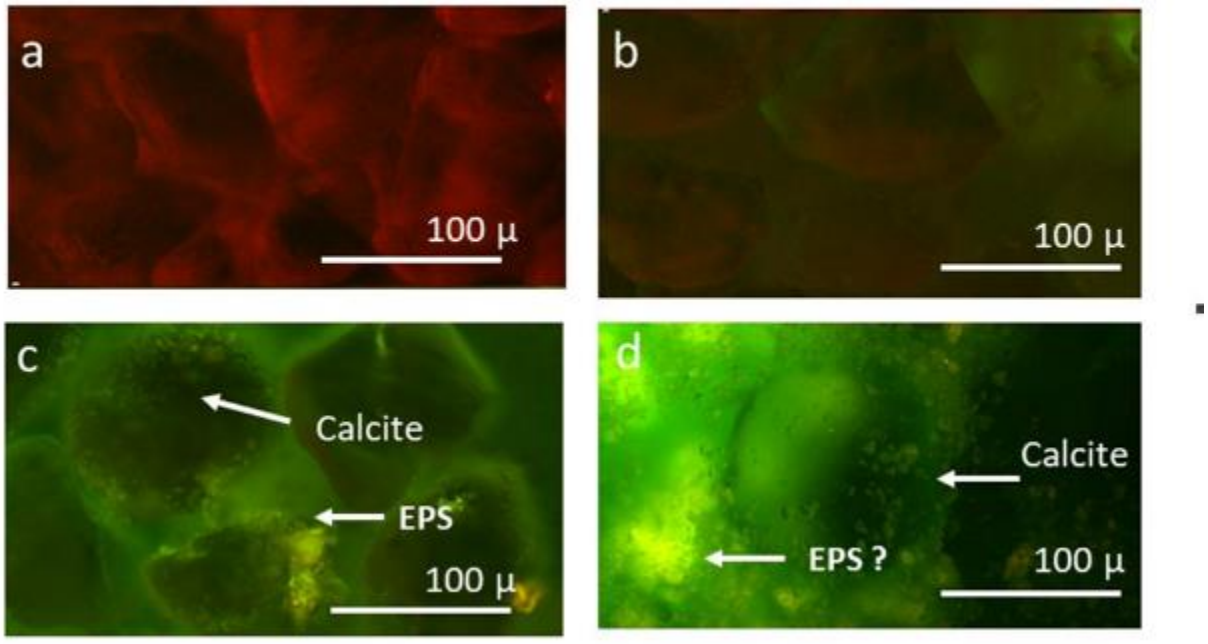

Figure 5-6. In situ auto-florescence photomicrographs of MICP materials captured on Nikon A1RMPsi-STORM 4.0 showing (a) untreated/uncemented (control), (b) treated/ uncemented, (c) treated/cemented/dried, and (d) treated/cemented/ moist sand samples.

5.4.6 Alcian Blue Stained Sample Images

Using the NIKON E400 and a higher magnification, there is a clear difference in the untreated/uncemented and the treated/cemented stained MICP samples (Figures 5-7a and b, respectively). Calcite is more abundant in Figure 5-7b and the stain is darker and more prevalent. There is some evidence of navy "ropy" or "slimy" identifiers of EPS - the former identified by navy, spider web-like tendrils on many sand grains in the image.

Further detail can be seen using a LEICA DM500 which offers higher magnification ability. However, this newer microscope had an LED light source which necessitated the blue wavelength of this light to be filtered out with a yellow film causing each sand grain to act as a prism, producing a rainbow effect. Still, the images clearly suggest less abundance of EPS on the untreated/uncemented vs. treated/cemented samples (Figures 5-8a and b, respectively). Some additional observations suggest the importance of EPS in the biomineralization/biocementation process. The distinct navy coloring of alcian-stained EPS is present at every bonding site but calcite crystals are not always found there. Calcite can be found on non-bonding sites in both images.

A comparison between uncemented and cemented treated sample from the same column (Figures 5-9a and b, respectively) shows that both contain calcite crystals (regular, loose crystals in the former and surface associated variably-shaped crystals in the latter). However, the navy blue stained EPS is only present in the cemented sample (Figure 5-9b). This suggests that EPS is not

needed for calcite to precipitate, but it is needed for calcite to form on sand surfaces and cement sand grains together. This is supported by the carbonate data indicating that uncemented and cemented samples (both MICP treated) had very similar carbonate contents.

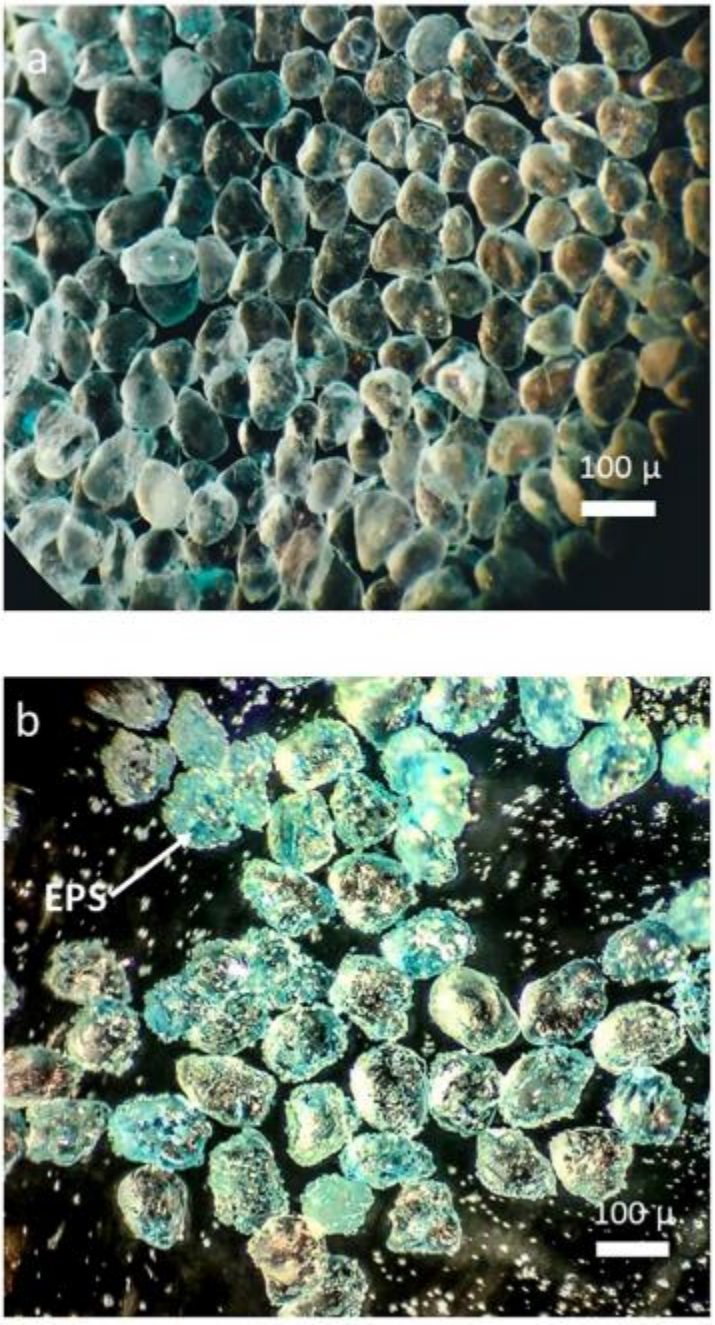

Figure 5-7. Photomicrographs of alcian blue-stained MICP materials captured on a Nikon E400 microscope, with no filter or light adjustment showing (a) untreated/uncemented (control), and (b) treated/cemented sand samples (1.25 cm height).

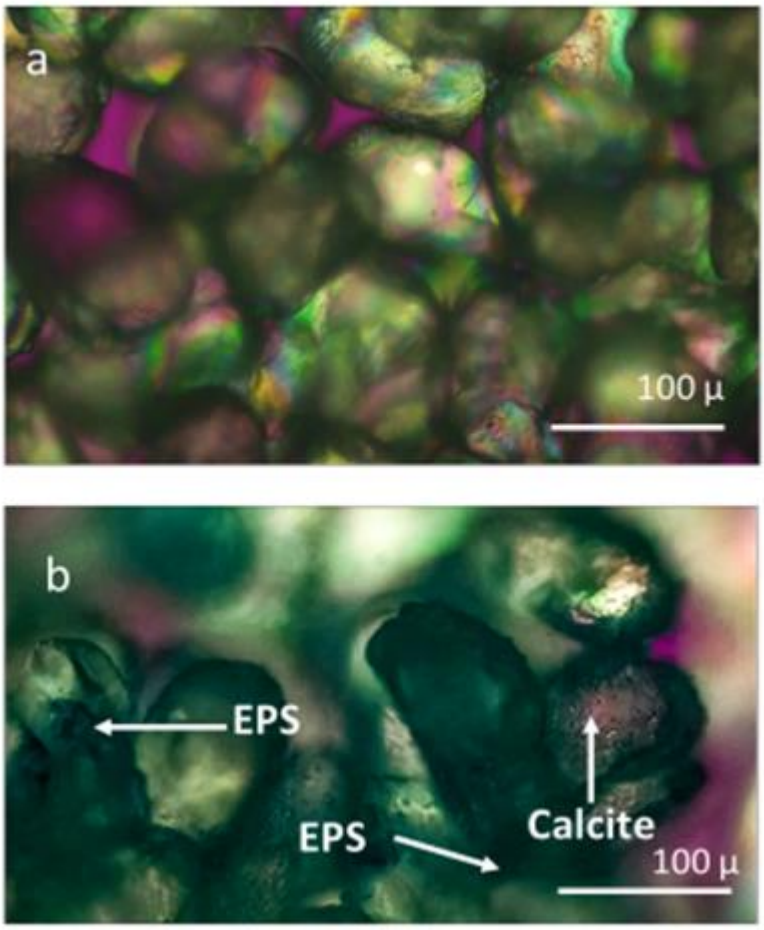

Figure 5-8. Images of alcian blue-stained MICP materials captured on a Leica DM500 with blue light filtered showing (a) untreated/uncemented (control), and (b) a treated/cemented sand samples.

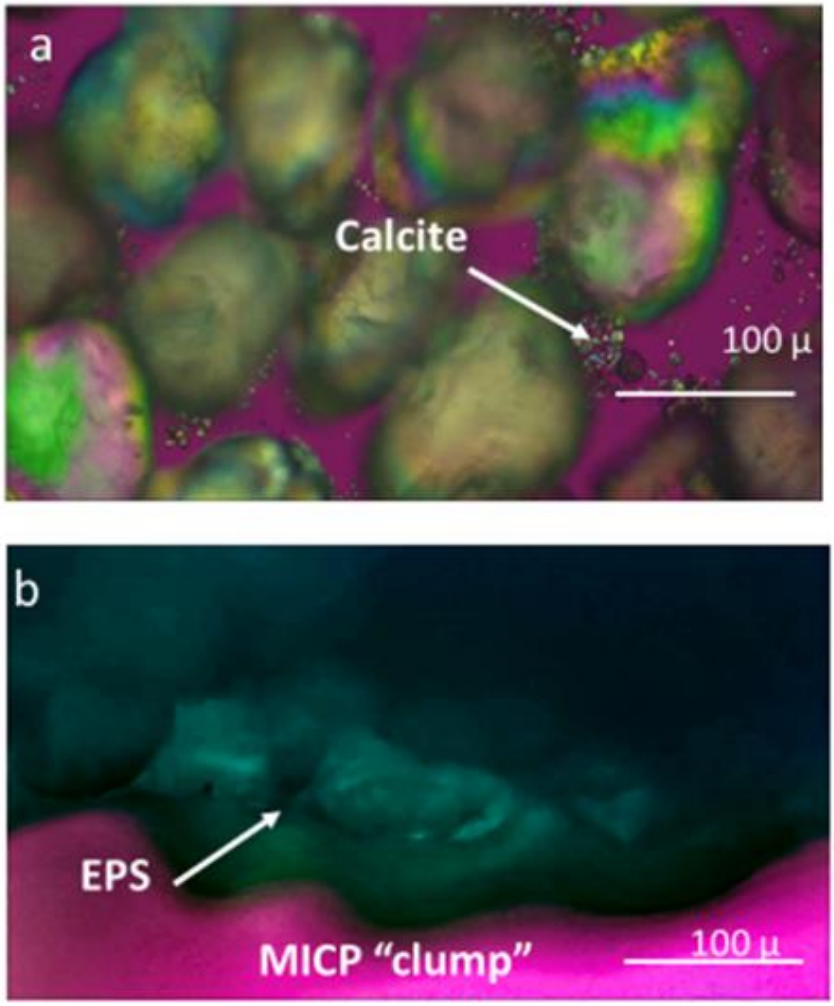

Figure 5-9. Photomicrographs of alcian blue-stained MICP materials captured on a Leica DM500 with blue light filtered out showing (a) treated/uncemented and (b) a treated/cemented sand samples.

5.4.7 Alcian Blue Stained Samples under Fluorescent Lighting

Because alcian blue also has fluorescent properties, imaged samples under a UV light can provide additional information as to the distribution of EPS in MICP samples. These shows that cemented samples (Figure 5-10b) have abundant and widespread EPS (dark blue color in image), whereas uncemented samples have a lack of fluorescent coloring. However, these images were not very clear and show that alcian blue under fluorescent lighting is not the best method of visualizing EPS.

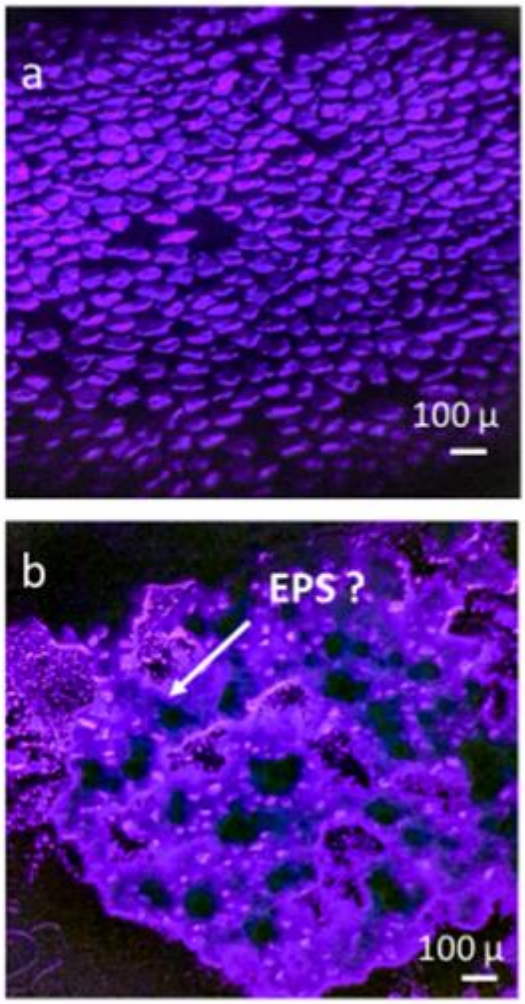

Figure 5-10. Photomicrographs of alcian blue-stained MICP materials captured on a Nikon E400 under UV light showing (a) untreated/uncemented (control) and (b) treated/cemented sand samples.

5.4.8 EPS Study Summary and Conclusions

The observations made during the EPS study do not support the current model of the MICP mechanism, i.e., biologically induced mineralization and cementation via cell nucleation of calcite precipitation. Rather, they suggest the critical involvement of EPS in the MICP process. These observations can be summarized as follows:

1. *S. pasteurii* cells were alive (i.e., viable) after injection into sand and incubation, and not encased in calcite. Cells were well-formed and whole, were found on mineral surfaces and were not observed only as impressions in calcite.

2. EPS was present on most sand surfaces, particularly between cemented sand grains. No evidence of widespread EPS was found in uncemented materials.

3. Calcite was present in uncemented samples, but only as unattached particles (with no or only small amounts of EPS).

Because the presence of calcite and/or cells without EPS did not result in cementation of sand columns, and the large amounts of EPS present on all surfaces in cemented samples, one can conclude that EPS played some role in cementation. There are several possibilities for the nature of this role. First, EPS may catalyze the precipitation of calcite (organomineralization) on the surfaces of sand grains. It may have served as a template for calcite precipitation similar to processes observed in bone or shell formation. Alternatively, EPS may assist precipitation by acting to concentrate Ca or carbonate ions through electrostatic interactions. Second, it may be that EPS and calcite minerals form a 'paste' that itself bonds sand grains. The nature of this 'glue' is currently unknown. It could be that EPS only anchors calcite crystals to sand grains, or is present between all mineral surfaces including calcite. Alternatively, calcification or cementation of sand particles might only be a matter of pore filling and thus, EPS formations only acts to concentrate ions within pore spaces, thus assisting calcite precipitation within pore spaces. The results of this study suggest that MICP may have failed in organic-rich specimens because EPS failed to develop in these soils. The reasons for this are unknown currently but are likely due to biological processes beyond this project's scope. This should be investigated in the future through more advanced EPS visualization techniques. There are other methods that may assist MICP by encouraging EPS formation through microbe stressing methods.

CHAPTER 6
PRELIMINARY BIO-STIMUALTION OF FLORIDA SOILS

6.1 Introduction

As mentioned in Chapter 2, on average, more than 10^9 microbial cells exist per gram of soil in the top meter of soil. At a depth of 30 m, the geomicrobe concentration drops to approximately 10^6 cells per gram of soil (DeJong et al., 2010). As such, there has been speculation in recent years that sufficient *S. pasteurii* or similar ureolytic bacteria may be naturally-present in some soils that could drive MICP-style reactions. Driving MICP reactions without supplementing soil with additional microbes is known as bio-stimulation.

The bio-stimulation option has significant advantages when compared to bio-augmentation. As this study has repeatedly shown, microbes such as *S. pasteurii* may be temperamental in that the bacteria may die, a certain stock may fail to properly grow for any number of reasons, etc. In addition, bio-augmentation requires one to grow a large number of bacteria in large reaction-style vessels. This process may be costly and/or time consuming. As such, part of this project was to preliminarily investigate inducing MICP via bio-stimulation in Florida soils.

6.2 Bio-Stimulation Study Treatment Methodology

When this project's scope was written, it was assumed that it would be possible to drive microbial calcification in organic-rich soils using a one-dose mixing method and that these results would help to guide investigators during the bio-stimulation study. Since MICP treatment via bio-augmentation was unsuccessful in terms of microbially-inducing calcite formation in organic-rich soil, it was unclear how to proceed with the bio-stimulation study in terms of optimized treatment methodologies. The SISS (or CISS) method is a positive step in loose soil improvement, but as mentioned previously, the chemistry governing SISS is unrelated to the chemistry associated with MICP. As a result of all this, investigators believed that the best method for approaching the bio-stimulation study was to repeat the treatment procedure that worked well in Ottawa sand while omitting the supplemented bacteria as this would allow a comparison between similar treatment procedures. A summary of this treatment process is as follows:

- Random soil specimens were obtained from the ground surface at two locations on the University of North Florida campus and from a stockpile of sand that was to be used for the dune restoration project in Flagler Beach, FL provided by Argos. Approximate sample locations for the UNF specimens are shown below in Figure 6-1, while grain-size distributions for these soils are presented in Figure 6-2. Table 6-1 (below) was generated using data from Figure 6-2. As shown, all three soils were classified as SP using the USCS classification system.

Table 6-1. Soil properties for random soil specimens

	Beach Sand	Tree	Light Post
D_{10}	0.09	0.18	0.16
D_{30}	0.15	0.32	0.21
D_{60}	0.27	0.81	0.22
C_u	3.00	4.50	1.38
C_c	0.93	0.70	1.25
USCS Classification	SP	SP	SP

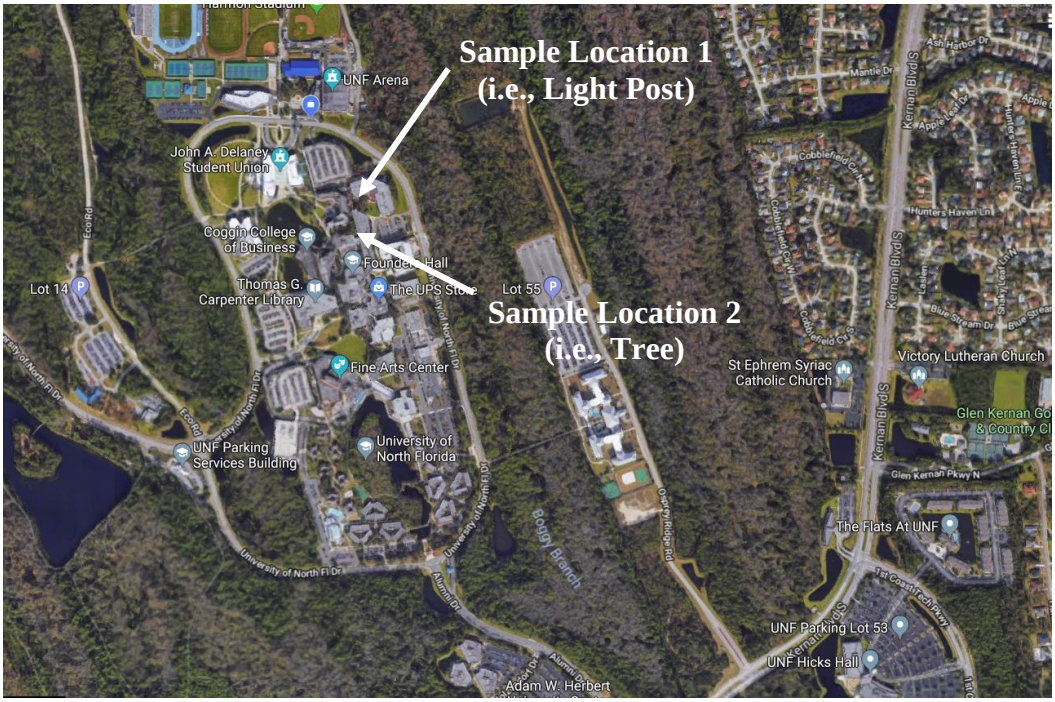

Figure 6-1. Approximate locations of UNF specimens

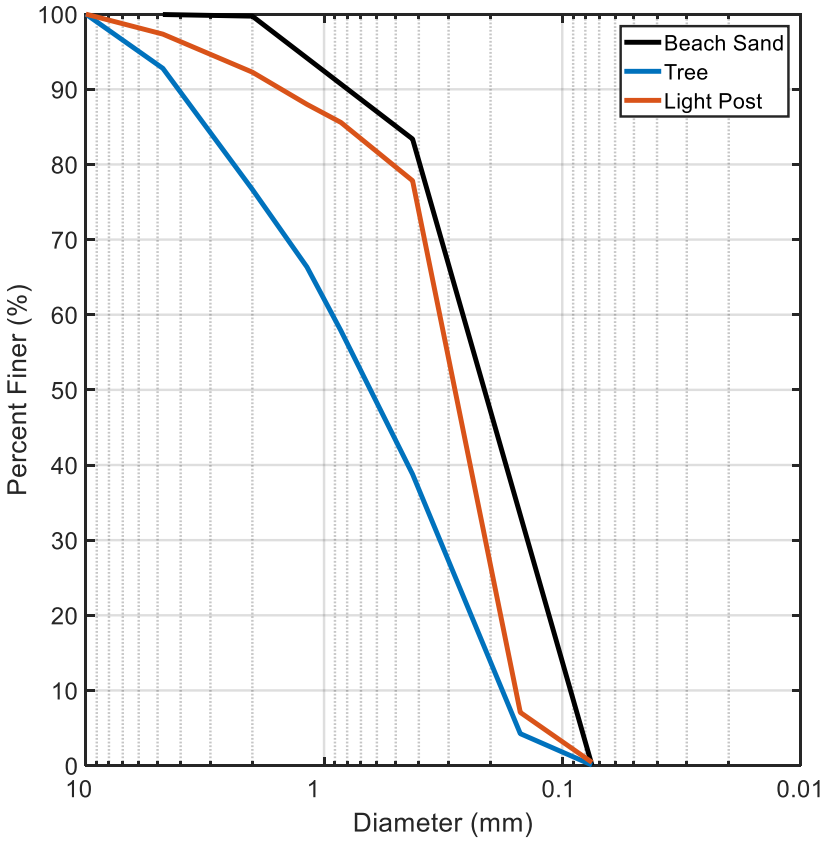

Figure 6-2. Grain-size distributions for random soil specimens

- The specimens were pluviated into 2-inch diameter by 4-inch high plastic molds (i.e., standard concrete molds) until the molds were approximately 75% full.

- 40-mL of a 2.5 M calcium chloride/urea solution was added to the soil in the molds. The mixture was stirred by hand and allowed to air dry for a minimum of 48 hours.

- After 48 hours, the specimens were extracted using a Dremel tool. Unconfined compression testing (UCS) was then performed on each specimen.

6.3 Bio-Stimulation Soil Stabilization Results and Discussion

After drying, most of the specimens associated with the bio-stimulated soil treatment failed to remain intact. However, it was possible to salvage some smaller specimens for UCS testing. Data from these tests are presented below in Figure 6-3.

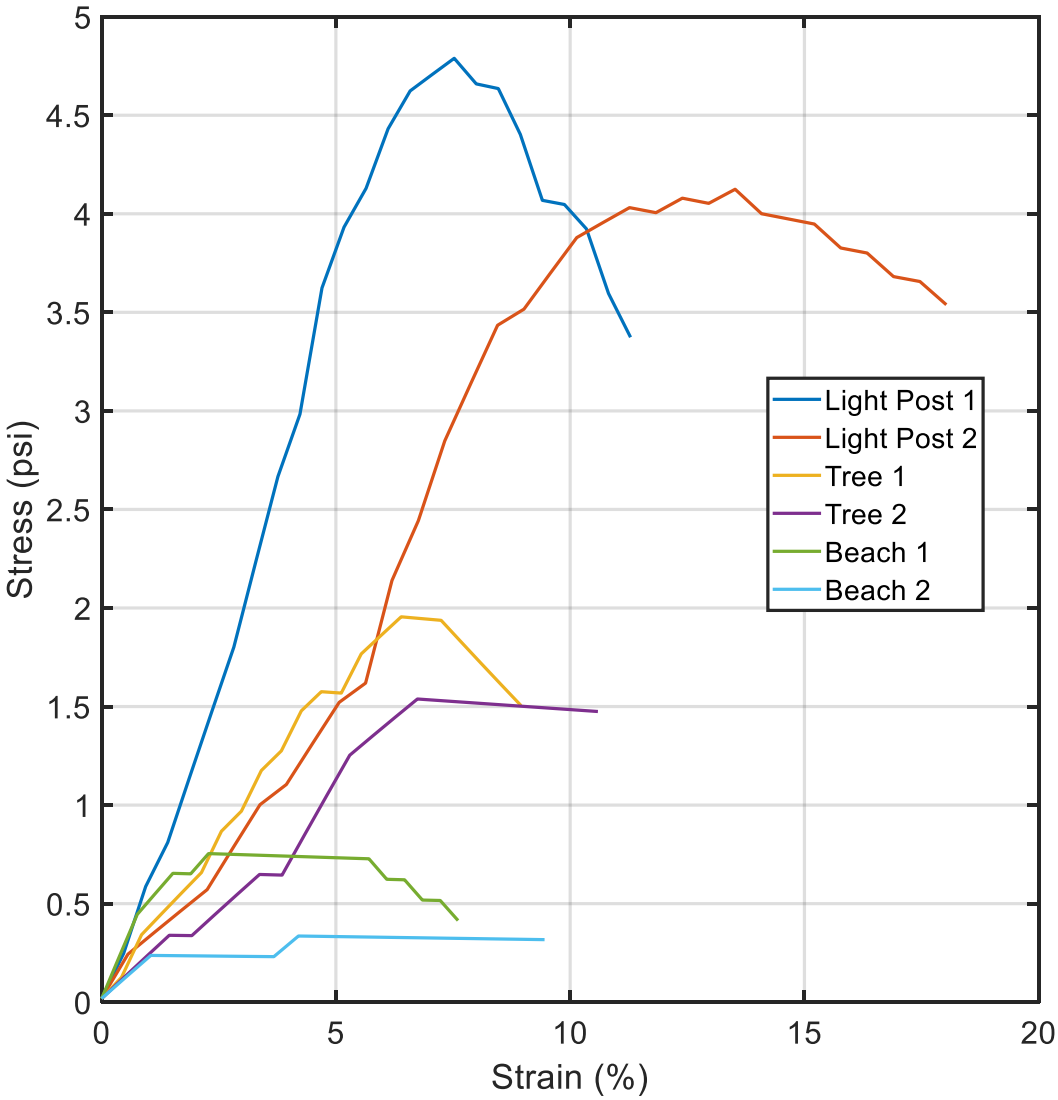

Figure 6-3. UCS Results for specimens treated via bio-stimulation; note, Light Post 1 and Light Post 2; Tree 1 and Tree 2; and Beach 1 and Beach 2 are replicates from the same soils, respectively

As shown in Figure 6-3, specimens treated via bio-stimulation showed very limited unconfined compression strengths. Based upon results presented in Chapter 3 and Chapter 4, this result was expected. It is somewhat interesting that some of the beach sand appeared to be sufficiently strong after treatment to stand upright on its own. However, the observed UCS from all bio-stimulation-treated specimens was much lower than UCS from all SISS-treated specimens. While soil-types were different from test-to-test, SISS-treated specimens tended to see minimum compressive strengths near 10 psi while the highest strength observed for a bio-stimulated via the one-dose mixing method was less than 5 psi. This would appear to indicate that the SISS-treatment method may be a better option for future pursuit than the MICP-related treatment methods.

CHAPTER 7
SUMMARY, CONCLUSIONS, AND RECOMMENDATIONS

7.1 Summary

To summarize the steps followed in this study:

- A thorough literature review about MICP treatment was conducted.

- Several 50/70 Ottawa sand specimens were treated using the MICP treatment techniques outlined extensively by DeJong et al. (2006). Results showed that investigators had successfully induced microbial calcite formation, and treated specimens showed increased strengths and lower compressibilities when compared with untreated specimens. However, treated sand specimens showed significant variability in terms of strength as a function of distance from the injection point. Specimens closer to the injection point were consistently strongest while further form the injection point, specimens were very weak. Maximum effective treatment distance was no more than 4 inches. These issues were thought to be the result of pore clogging.

- To create more-uniform specimens, the treatment technique was changed from the DeJong et al. (2006) percolation method to a pre-mixing-style method. This appeared to produce more-uniform specimens in 50/70 Ottawa sand.

- Several organic-rich soil columns were treated via MICP using both the percolation treatment method and the pre-mixing method. Very little calcification was observed when the percolation method was used. When the mixing method was used, limited calcification was observed when organic content was low (i.e., 10%). When organic content was high (i.e., 50%), very little calcification was observed. When organic content was moderate (i.e., 30%), limited calcification was observed.

- Investigators hypothesized that the reason MICP treatment failed to induce calcite formation in organic specimens may be due to a surface charge issue. SDS was added to the MICP recipe in an attempt to solve this issue. Preliminary results with MICP-SDS specimens were very positive in the sense that visually, strongly-cemented specimens appeared to be produced. However, further investigation showed that these specimens were highly dissolvable. Since calcium carbonate, the byproduct of MICP treatment is relatively insoluble. This meant that another mechanism other than calcium carbonate formation must have been responsible for the preliminary observed strength increases.

- A series of "control" tests were conducted to further characterize the results from the MICP-SDS treatments. These tests involved sequentially omitting an ingredient associated with MICP (i.e., bacteria, urea, and calcium chloride). Results showed that specimens treated with SDS and only calcium chloride performed the best in terms of strength and solubility. This appears to be due to formation of a CDS complex. Results also suggested that the apparent solubility observed during SDS-MICP treatment was due to unbalanced stoichiometry between SDS and calcium chloride, in the sense that the MICP reactions were using calcium ions that would have more effectively strengthened the soil if they had been available for use in the CDS complex.

- The CDS complex was further-investigated since it may be a new and sustainable soil stabilization method that thus far has not been studied by others. Preliminary results show that an optimum ratio between SDS and soil appears to exist that results in maximum soil strength. In addition, it appears that it is possible to form the CDS complex in various soil-types (i.e., organic-rich soil, sand, and clay). Treatment via CDS complex has been dubbed surfactant-induced soil stabilization (SISS). While this method is a promising potential method for loose and/or weak soil stabilization, it is certainly not a form of MICP.

- A study was conducted involving exopolysaccharides' (EPS) role in MICP-induced calcite formation. Results showed that EPS appears to play a role in calcite development. One of the reasons that MICP may have failed to induce calcite in the organic soils could be that EPS failed to form in these soils. These results should be further investigated.

- A preliminary study was conducted to assess the feasibility of using bio-stimulation (as opposed to bio-augmentation) to induce calcite formation in Florida soils. Results showed that soils treated via bio-stimulation were very weak after treatment. However, based upon results from the bio-augmentation studies, these results were expected. It is possible that Florida soils may respond better to bio-stimulation via micro-dosing (others in the literature have shown this to be effective). However, treatment via this technique was outside the scope of this project.

7.2 Recommendations

The most significant outcome from this project was the development of the SISS treatment technique for loose and/or weak soils. Discovery of this new treatment method was unintended, and it was the result of attempts to optimize MICP in organic-rich soils. This method for soil treatment appears to be effective based on very preliminary results and should be further investigated as a potential solution for remediating organic-rich soils in Florida.

LIST OF REFERENCES

Abdel Aal, G. Z., Atekwana, E. A., and Atekwana, E. A. (2010). "Effect of Bioclogging in Porous Media on Complex Conductivity Signatures." *J. Geophys. Res*., 115, pp. G00G07.

Achal, V., Pan, X., and Özyurt, N. (2011a). "Improved Strength and Durability of Fly Ash Amended Concrete by Microbial Calcite Precipitation." *Ecological Engineering*, 37(4), 554-559.

Achal, V., Pan, X., and Zhang, D. (2011b). "Remediation of Copper-Contaminated Soil by Kocuria Flava CR1, Based on Microbially Induced Calcite Precipitation." *Ecological Engineering*, 37(10), 1601-1605.

Al-Thawadi, S (2008). *High Strength In-Situ Biocementation of Soil by Calcite Precipitating Locally Isolated Ureolytic Bacteria*. "Ph.D. Thesis," Murdoch University, Perth, Australia.

Al Qabany, A., Soga, K., and Santamarina, C. (2012). "Factors Affecting Efficiency of Microbially Induced Calcite Precipitation." *J. Geotechnical and Geoenvironmental Engineering*, 138(8), DOI 10.1061/(ASCE)GT.1943-5606.0000666.

Arunachalam, K. D., Sathyanarayanan, K. S., Darshan., and Balaji, R. R. (2010). "Studies on the Characterization of Biosealant Properties of *Bacillus sphaericus*." *International Journal of Engineering Science and Technology*, 2(3), 270-277.

ASTM D1997 (2013). "Standard Test Method for Laboratory Determination of Fiber Content of Peat Samples by Dry Mass." ASTM International, West Conshohocken, PA.

ASTM D2166 (2016). "Standard Test Method for Unconfined Compressive Strength of Cohesive Soils." ASTM International, West Conshohocken, PA.

ASTM D2435 (2011). "Standard Test Methods for One-Dimensional Consolidation Properties of Soils using Incremental Loading." ASTM International, West Conshohocken, PA.

ASTM D2974 (2014). "Standard Test Methods for Moisture, Ash, and Organic Matter of Peat and Other Organic Soils." ASTM International, West Conshohocken, PA.

ASTM D2976 (2015). "Standard Test Method for pH of Peat Materials." ASTM International, West Conshohocken, PA.

ASTM D3080 (2011). "Standard Test Method for Direct Shear Test of Soils under Consolidated Drained Conditions." ASTM International, West Conshohocken, PA.

ASTM D4373 (2014). "Standard Test Method for Rapid Determination of Carbonate Content of Soils." ASTM International, West Conshohocken, PA.

ASTM D4427 (2018). "Standard Classification of Peat Samples by Laboratory Testing." ASTM International, West Conshohocken, PA.

ASTM D4767 (2011). “Standard Test Method for Consolidated Undrained Triaxial Compression Test for Cohesive Soils.” ASTM International, West Conshohocken, PA.

ASTM D4972 (2018). “Standard Test Methods for pH of Soils.” ASTM International, West Conshohocken, PA.

Bachmeier, K. L., Williams, A. E., Bang, S. S., and Warmington, J. R. (2002). "Urease Activity in Microbiologically-Induced Calcite Precipitation." *Journal of Biotechnology*, 93, 171-181.

Barkouki, T. H., Martinez, B. C., Mortensen, B. M., Weathers, T. S., De Jong, J. D., Ginn, T. R., Spycher, N. F., Smith, R. W., and Fujita, Y. (2011). "Forward and Inverse Bio-Geochemical Modeling of Microbially Induced Calcite Precipitation in Half-Meter Column Experiments." *Transport in Porous Media*, 90(1), 23-39.

Bjerrum, L. (1967). “Engineering Geology of Norwegian Normally-Consolidated Marine Clays as Related to Settlements of Buildings.” *Geotechnique*, 17, 81-118.

Brenner, M., Hodell, D. A., Leyden, B. W., Curtis, J. H., Kenney, W. F., Gu, B., and Newman, J. M. (2006). “Mechanisms for Organic Matter and Phosphorus Burial in Sediments of a Shallow, Subtropical, Macrophyte-Dominated Lake.” *Journal of Paleolimnology*, 35, 129-148.

Canakci, H., Sidik, W., and Kilic, H. I. (2015). “Effect of Bacterial Calcium Carbonate Precipitation on Compressibility and Shear Strength of Organic Soil.” *Soils and Foundations*, 55(5), 1211-1221.

Castanier, S., Le Métayer-Levrel, G., and Perthuisot, J. P. (1999). “Ca-Carbonates Precipitation and Limestone Genesis -- the Microbiogeologist Point of View.” *Sedimentary Geology*, 126(1-4), 9-23.

Castanier S., Le Metayer-Levrel, G., and Perthuisot, J. P. (2000). “Bacterial Carbonatogenesis and Applications to Preservation and Restoration of Historic Property.” In: *Of Microbes and Art: The Role of Microbial Communities in the Degradation and Protection of Cultural Heritage*, Ciferri O, Tiano P, and Mastromei G, Eds. Kluwer Academic-Plenum, Amsterdam, 246–262.

Chai, L., Fan Zhang, F., YueHui She, Y., Banat, I., and Hou, D. (2015). "Impact of a Microbial-Enhanced Oil Recovery Field Trial on Microbial Communities in a Low-Temperature Heavy Oil Reservoir." *Nature Environment and Pollution Technology*, 14(3), 455-462.

Chen, Y. M., Clancy, K. A., and Burne, R. A. (1996). “*Streptococcus salivarius U*rease: Genetic and Biochemical Characterization and Expression in a Dental Plaque *Streptococcus*.” *Infection and Immunity*, 64, 585-592.

Cheng, L., and Cord-Ruwisch, R. (2012). "In Situ Soil Cementation with Ureolytic Bacteria by Surface Percolation." *Ecological Engineering*, 42, 64-72.

Cuthbert, M. O., McMillan, L. A., Handley-Sidhu, S., Riley, M. S., Tobler, D. J., and Phoenix, V. R. (2013). "A Field and Modeling Study of Fractured Rock Permeability Reduction using Microbially Induced Calcite Precipitation." *Environmental Science Technology*, 47(23), 13637-13643.

DeJong, J. T., Fritzges, M. B., and Nüsslein, K. (2006). "Microbially Induced Cementation to Control Sand Response to Undrained Shear." *Journal of Geotechnical and Geoenvironmental Engineering*, 132(11), 1381-1392.

DeJong, J. T., Martinez, B. C., Mortensen, B. M., Nelson, D. C., Waller, J. T., Weil, M. H., Ginn, T. R., Weathers, T. S., Barkouki, T. H., Fujita, Y., Redden, G., Hunt, C., Major, D., and Tanyu, B. "Upscaling of Bio-Mediated Soil Improvement ." (2009). *Proc., 17th International Conference on Soil Mechanics and Geotechnical Engineering*, DOI: 10.3233/978-1-60750-031-5-2300.

DeJong, J. T., Mortensen, B. M., Martinez, B. C., and Nelson, D. C. (2010). "Bio-Mediated Soil Improvement." *Ecological Engineering*, 36(2), 197-210.

DeJong, J. T., Soga, K., Kavazanjian, E., Burns, S., Van Paassen, L. A., Al Qabany, A., Aydilek, A., Bang, S. S., Burbank, M., Caslake, L. F., Chen, C. Y., Cheng, X., Chu, J., Ciurli, S., Esnault-Filet, A., Fauriel, S., Hamdan, N., Hata, T., Inagaki, Y., Jefferis, S., Kuo, M., Laloui, L., Larrahondo, J., Manning, D. A. C., Martinez, B., Montoya, B. M., Nelson, D. C., Palomino, A., Renforth, P., Santamarina, J. C., Seagren, E. A., Tanyu, B., Tsesarsky, M., and Weaver, T. (2013). "Biogeochemical Processes and Geotechnical Applications: Progress, Opportunities and Challenges." *Géotechnique*, 63(4), 287-301.

De Moel, P. J., van der Helm, A. W. C., van Rijn, M., van Dijk, V., and van der Meer, W. G. J. (2013). "Assessment of Calculation Methods for Calcium Carbonate Saturation in Drinking Water for DIN 38404-10 Compliance." *Drinking Water Engineering and Science*, 6, 115-124.

De Muynck, W., Debrouwer, D., De Belie, N., and Verstraete, W. (2008). "Bacterial Carbonate Precipitation Improves the Durability of Cementitious Materials." *Cement and Concrete Research*, 38(7), 1005-1014.

De Muynck, W., Verbeken, K., De Belie, N., and Verstraete, W. (2010). "Influence of Urea and Calcium Dosage on the Effectiveness of Bacterially Induced Carbonate Precipitation on Limestone." *Ecological Engineering*, 36(2), 99-111.

Dierksen K. P., Sandine., W .E., and Trempy. J. E. (1997). "Expression of Ropy and Mucoid Phenotypes in Lactococcus Lactis." *J. Dairy Sci.*, 80, DOI: 1528–1536.10.3168/jds.S0022-302(97)76082-X.

Dupraz, S., Parmentier, M., Menez, B., and Guyot, F. (2009). "Experimental and Numerical Modeling of Bacterially Induced pH Increase and Calcite Precipitation in Saline Aquifers." *Chemical Geology*, 265(1–2), 44-53.

Ehrlich, H. (1998). "Geomicrobiology: its Significance for Geology." *Earth-Science Reviews*, 45(1-2), 45-60.

FDOT (2018). Soils and Foundation Handbook. Florida Department of Transportation, State Materials Office, Gainesville, FL.

Feng, K., and Montoya, B. M. (2016). "Influence of Confinement and Cementation Level on the Behavior of Microbial-Induced Calcite Precipitated Sands under Monotonic Drained Loading." *Journal of Geotechnical and Geoenvironmental Engineering*, 142(1), 04015057.

Ferris F. G., Phoenix, V., Fujita, Y., and Smith, R. W. (2003). "Kinetics of Calcite Precipitation Induced by Ureolytic Bacteria at 10^{o}C to 20^{o}C in Artificial Groundwater." *Geochem Cosmochim Acta*, 67, 1701–1722.

Foster, J. S., Green, S. J., Ahrendt, S. R., Golubic, S., Reid, R. P., Hetherington, K. L., and Bebout, L. "Molecular and Morphological Characterization of Cyanobacterial Diversity in the Stromatolites of Highborne Cay, Bahamas." *ISME Journal*, 3.5(2009), 573-87.

Fujita Y., Ferris F. G., Lawson R. D., Colwell F. S., and Smith, R. W. (2000). "Calcium Carbonate Precipitation by Ureolytic Subsurface Bacteria." *Geomicrobiology Journal*, 17, 305–318.

Fujita, Y., Taylor, J. L., Wendt, L. M., Reed, D. W. and Smith, R. W. (2010). "Evaluating the Potential of Native Ureolytic Microbes to Remediate a 90Sr Contaminated Environment." *Environmental Science* Technology, 44(19), 7652–7658.

Fujita, Y., Redden, G. D., Ingram, J. C., Cortez, M. M., Ferris, F. G., and Smith, R. W. "Strontium Incorporation into Calcite Generated by Bacterial Ureolysis." *Geochim Cosmochim Acta*, 68, 3261-3270.

Gat, D., Tsesarsky, M., and Shamir, D. (2011). "Ureolytic Calcium Carbonate Precipitation in the Presence of Non-Ureolytic Competing Bacteria." *Geo-Frontiers*.

Gollapudi, U. K., Knutson, C. L., Bang, S. S., and Islam, M. R. (1995). "A New Method for Controlling Leaching Through Permeable Channels." *Chemosphere*, 30(4), 11.

Gue S. S., Tan Y. C., and Liew S. S. (2002). "Cost Effective Geotechnical Solutions for Roads and Factories Over Soft Ground." *20th Conference of the ASEAN Federation of Engineering Organizations*, Cambodia, September 2-5.

Hammes, F., Seka, A., Knijf, S, and Verstraete W. (2003). "A Novel Approach to Calcium Removal from Calcium-Rich Industrial Wastewater." *Water Resources*, 37, 699–704.

Hammes, F. and Verstraete, W. (2002). "Key Roles of pH and Calcium Metabolism in Microbial Carbonate Precipitation." *Reviews in Environmental Science and Bio/Technology* 1(1), 3-7.

Harkes, M. P., van Paassen, L. A., Booster, J. L., Whiffin, V. S., and van Loosdrecht, M. C. (2010). "Fixation and Distribution of Bacterial Activity in Sand to Induce Carbonate Precipitation for Ground Reinforcement." *Ecological Engineering*, 36(2), 112-117.

Harris, D., Ummadi, J. G., Thurber, A. R., Allau, Y., Verba, C., Colwell, F., Torres, M. E., and Koley, D. "Real-Time Monitoring of Calcification Process by *Sporosarcina pasteuriibiofilm*." *The Analyst*, 141.10(2016), 2887-895.

Holtz, R. D., and Kovacs, W. D. (1981). *An Introduction to Geotechnical Engineering*. Prentice-Hall, Inc, Englewood Cliffs, New Jersey, 733.

Huat, B. B. K., Prasad, A., Asadi, A., and Kazemian, S. (2014). *Geotechnics of Organic Soils and Peat.* CRC Press, Taylor and Francis Group, Boca Raton, FL.

Inagaki, Y., Tsukamoto, M., Mori, H., Sasaki, T., Soga, K., Al Qabany, A., and Hata, T. (2011). "The Influence of Injection Conditions and Soil Types on Soil Improvement by Microbial Functions." *Geo-Frontiers*.

Ivanov, V. and Chu, J. (2008). "Applications of Microorganisms to Geotechnical Engineering for Bioclogging and Biocementation of Soil in Situ. *Reviews in Environmental Science and Bio/Technology*, 7(2), 139-153.

Jarret, P. M. (1995). "Geoguide 6, Site Investigation for Organic Soils and Peat." *JKR Document 20709-0341-95*. Institut Kerja Raya, Malaysia.

Kantzas, A., Stehmeie, L., Marentette, D. F., Ferris, F. G., Jha, K. N., and Maurits, F. M. (1992). "A Novel Method of Sand Consolidation Through Bacteriogenic Mineral Plugging." *Proc., Annual Technical Meeting*, Petroleum Society of Canada.

Khan, J. A. (2011). "Biodegradation of Azo Dye by Moderately Halotolerant Bacillus megaterium and Study of Enzyme Azoreductase Involved in Degradation." *Advanced BioTech*, 10(7), 21-27.

Klein, K. A., and Santamarina, J. C., (2003). "Electrical Conductivity in Soils Underlying Phenomena." *J. Environmental Engineering Geophy*. 8(4), 263–273.

Kile, D. E., Eberl, D. D., Hoch, A. R., and Reddy, M. M. (2000). "An Assessment of Calcite Crystal Growth Mechanisms Based on Crystal Size Distributions." *Geochimica et Cosmochimica Acta*, 64(17), 2937-2950.

Knorre, H. v. and Krumbein, W. E., (2000). "Bacterial Calcification. *Microbial Sediments*. Berlin: Springerverlag, 25-31.

Kucharski, E. S., Cord-Ruwisch, R., Whiffin, V., and Al-Thawadi, S. (2008). "Microbial Biocementation." United States Application US 2008/0245272.

Lee, M. L., Ng, W. S., and Tanaka, Y. (2013). "Stress-Deformation and Compressibility Responses of Bio-Mediated Residual Soils." *Ecological Engineering*, 60, 142-149.

Lee, S. L. and Lo, K. W. (1985). "Ground Improvement by Dynamic Replacements and Mixing." *Third International Geotechnical Seminar*, Soil Improvement Methods, Singapore, Nov.

Li, J., Vasanthan, T., and Bressler, D. C. (2012). “Improved Cold Starch Hydrolysis with Urea Addition and Heat Treatment at Subgelatinization Temperature.” *Carbohydrate Polymers*, 87, 16499-1656.

Li, Z., Kutter, B. L., Wilsone, D. W., Sprott, K., Lee, J.-S., and Santamarina, J.C., (2005). “Needle Probe Application For High-Resolution Assessment of Soil Spatial Variability in the Centrifuge.” *ASCE Geotech*, Special Publ. 130-142, 2087–2101.

Lian, B., Hu, Q., Chen, J., Ji, J., and Teng, H. (2006). “Carbonate Biomineralization Induced by Soil Bacterium *Bacillus megaterium*.” *Geochimica et Cosmochimica Acta*, 70(22), 5522-5535.

Liang, J., Guo, Z., Deng, L., and Liu, Y. (2015). "Mature Fine Tailings Consolidation Through Microbial Induced Calcium Carbonate Precipitation." *Canadian Journal of Civil Engineering*, 42(11), 975-978.

Liang, A., Wang, C., Tong, Z., Ye, W., and Ye, S., (2005). “Bio-Catalytic Nanoparticles with Urease Immobilized in Multilayer Assembled Through Layer-by-Layer Technique.” *Research Institute of Materials Science*, South China University of Technology, Guangzhou, China.

Lin, H., Suleiman, M.T. Brown, D., and Kavazanjian, E. (2015). “Mechanical Behavior of Sands Treated by Microbially Induced Carbonate Precipitation.” *Journal of Geotechnical and Geoenvironmental Engineering*, 142(2), DOI: 10.1061/(ASCE)GT.1943-5606.0001383.

Lo, K. W., Ooi, P. L., and Lee, S. L., (1990). “Unified Approach to Ground Improvement by Heavy Tamping.” *Journal of Geotechnical Engineering*, Vol. 116, No.3, March.

Lu, W., Qian, C. and Wang, R. (2010). “Study on Soil Solidification Based on Microbiological Precipitation of $CaCO_3$.” *Science China Technological Sciences*, 53(9), 2372-2377, FHWA, Washington, D. C.

Lukas, R. (1986). “Dynamic Compaction for Highway Construction, Design and Construction Guidelines, Volume 1.” Federal Highway Administration Report FHWARD-86-133.

Maier, R. M., Pepper, I. L. and Gerba, C. P., (2009). *Environmental Microbiology*. Second Edition, Elsevier Science, China.

Maleki, M., Ebrahimi, S., Asadzadeh, F., and Emami Tabrizi, M. (2016). "Performance of Microbial-Induced Carbonate Precipitation on Wind Erosion Control of Sandy Soil." *International Journal of Environmental Science and Technology*, 13(3), 937-944.

Manahan, S.E. (2010). *Environmental Chemistry*. CRC Press, Taylor and Francis Group, Boca Raton, FL.

Martinez, B. C. and DeJong, J. T. (2009). “Bio-Mediated Soil Improvement: Load Transfer Mechanisms at the Micro- and Macro-scales.” US-China Workshop on Ground Improvement Technologies, ASCE GSP, 10 pp.

Martinez, B. C., Barkouki, T., DeJong, J., Ginn, T. (2011). "Upscaling of Microbial Induced Calcite Precipitation in 0.5-m Columns Experimental and Modeling Results." *Geo-Frontiers* 2011, pp. 4049-4059.

Martinez, B. C. (2012). *Experimental and numerical upscaling of MICP for soil improvement*. "Ph.D. Dissertation," University of California, Davis, CA, USA.

McConnaughey, T. A. and Whelan, J. F. (1997). "Calcification Generates Protons for Nutrient and Bicarbonate Uptake. *Earth-Science Reviews*, 42(1–2), 95-117.

McVay, M. C. and Nugyen, D. (2004). "Evaluation of Embankment Distress at Sander's Creek – SR20." FDOT Final Report No. BC354, RPWO#17, Florida Department of Transportation, Tallahassee, FL.

Meyer, M. E., Zhou, L., and Gonzalez, C. M., (2004). "The use of EPS Geofoam Lightweight Fill in Hollywood, FL." *Fifth International Conference on Cases Histories in Geotechnical Engineering* (April 13-17, 2004), New York, NY.

Mitchell, J. K. and Santamarina, J. C. (2005). "Biological Considerations in Geotechnical Engineering." *Journal of Geotechnical and Geoenvironmental Engineering*, 131(10), 1222-1233.

Mobley, H. L. T., Island, M. D., and Hausinger, R. P. (1995). "Molecular Biology of Microbial Ureases." *Microbiological Reviews*, 59(3), 31.

Mooney, M., Pacheco, C., Prejean, S., Sato, H., Schuster, J., Wapenaar, K., and Wilt, M., (2005). "Advanced Noninvasive Geophysical Monitoring Techniques." *Earth Planet. Sci*. 35, 653–683.

Montoya, B. M., DeJong, J., Boulanger, R., Wilson, D., Gerhard, R., Ganchenko, A., and Chou, J. (2012). "Liquefaction Mitigation using Microbial Induced Calcite Precipitation." *GeoCongress 2012: State of the Art and Practice in Geotechnical Engineering*, Oakland, CA, 1918-1927.

Montoya, B. M., and DeJong, J. T. (2015). "Stress-Strain Behavior of Sands Cemented by Microbially Induced Calcite Precipitation." *Journal of Geotechnical and Geoenvironmental Engineering*, 141(6).

Montoya, B. M., Feng, K., and Shanahan, C. (2013). "Bio-Mediated Soil Improvement Utilized to Strengthen Coastal Deposits." *Proc., 18th International Conference on Soil Mechanics and Geotechnical Engineering*.

Mortensen, B. M., Haber, M. J., DeJong, J. T., Caslake, L. F., and Nelson, D. C. (2011). "Effects of Environmental Factors on Microbial Induced Calcium Carbonate Precipitation." *J. Appl Microbiol*, 111(2), 338-349.

Mortensen, B. M. and DeJong, J. T. (2011). "Strength and Stiffness of MICP Treated Sand Subjected to Various Stress Paths." *Geo-Frontiers 2011: Advances in Geotechnical Engineering*, Dallas, TX, 4012-4020.

Mujah, D., Shahin, M., and Cheng, L. “State-of-the-Art Review of Biocementation by Microbially Induced Calcite Precipitation (MICP) for Soil Stabilization.” *Geomicrobiology*, 34(6) 524-537.

Mullins, G. and Gunaratne (2015). “Soil Mixing Design Methods and Construction Techniques for Use in High Organic Soils.” Florida Department of Transportation, Tallahassee, FL.

Nemati, M. and Voordouw, G. (2003). “Modification of Porous Media Permeability Using Calcium Carbonate Produced Enzymatically in Situ.” *Enzyme and Microbial Technology*, 33(5), 635-642.

Nemati, M., Greene, E. A. and Voordouw, G. (2005). “Permeability Profile Modification using Bacterially Formed Calcium Carbonate Comparison with Enzymic Option.” *Process Biochemistry*, 40(2), 925-933.

Ng, W.-S., Lee, M.-L., and Hii, S.-L. (2012). "An Overview of the Factors Affecting Microbial-Induced Calcite Precipitation and its Potential Application in Soil Improvement." *International Journal of Civil, Environmental, Structural, Construction and Architectural Engineering*, 6(2), 188-194.

Nonakaran, S. H., Pazhouhandeh, M., Keyvani, A., Abdollahipour, F. Z., and Shirzad, A. (2015). "Isolation and Identification of *Pseudomonas azotoformans* for Induced Calcite Precipitation." *World J. Microbiol Biotechnol*, 31(12), 1993-2001.

Okwadha, G. D. and Li, J. (2010). “Optimum Conditions for Microbial Carbonate Precipitation.” *Chemosphere*, 81(9), 1143-1148.

Ramachandran S. K., Ramakrishnan, V., and Bang, S. S. (2001). “Remediation of Concrete using Micro-Organisms.” *ACI Mater J*, 98(1), 3–9.

Rebata-Landa, V., (2007). *Microbial Activity in Sediments: Effects on Soil Behaviour*. “Ph.D. Dissertation,” Georgia Institution of Technology, Atlanta, GA.

Ritvo, G., Dassa, O. and Kochba, M. (2003). “Salinity and pH Effect on the Colloidal Properties of Suspended Particles in Super Intensive Aquaculture Systems.” *Aquaculture*, 218(1-4), 379-386.

Rivadeneyra, M. A., Parraga, J., Delgado, R., Ramos-Cormenzana, A., and Delgado, G. (2004). “Biomineralization of Carbonates by *Halobacillus trueperi* in Solid and Liquid Media with Different Salinities.” *FEMS Microbiology Ecology*, 48(1), 39-46.

Rodriguez-Navarro C, Rodriguez-Gallego M, Chekroun KB, and Gonzalez-Munoz MT. (2003). “Conservation of ornamental stone by *Myxococcus xanthus* Induced Carbonate Biomineralisation.” *Applied and Environmental Microbiology*, 69, 2182–2193.

Rong, H., and Qian, C.-X. (2014). "Binding Functions of Microbe Cement." *Advanced Engineering Materials*, 17(3), 334-340.

Sahrawat, K.L. (1984). “Effects of Temperature and Moisture on Urease Activity in Semi-Arid Tropical Soils.” *Plant and Soil*, 78(3), 401-408.

Salifu, E., MacLachlan, E., Iyer, K. R., Knapp, C. W., and Tarantino, A. (2016). "Application of Microbially Induced Calcite Precipitation in Erosion Mitigation and Stabilisation of Sandy Soil Foreshore Slopes: A Preliminary Investigation." *Engineering Geology*, 201, 96-105.

Sarda, D., Choonia, H. S., Sarode, D. D., and Lele, S. S. (2009). “Biocalcification by *Bacillus pasteurii* urease: A Novel Application.” *Journal of Industrial Microbiology & Biotechnology*, 36(8), 1111-1115.

Siddique, R., Achal, V., Reddy, M. S., and Mukherjee, A. (2008). “Improvement in the Compressive Strength of Cement Mortar by the use of a Microorganism - *Bacillus megaterium*. *Excellence in Concrete Construction through Innovation*, Limbachiya, M. C. and Kew, H. eds. Taylor and Francis, United Kingdom, pp. 27-30.

Simpson, D. C. (2014). *Behavioral Thresholds in mixtures of Sand and Clay*. “M.S. Thesis,” Oregon State University, Corvallis, OR.

Singh, R., Yoon, H., Sanford, R. A., Katz, L., Fouke, B. W., and Werth, C. J. (2015). "Metabolism-Induced CaCO3 Biomineralization During Reactive Transport in a Micromodel: Implications for Porosity Alteration." *Environ Sci Technol*, 49(20), 12094-12104.

Soon, N. W. (2013). *Improvements in Engineering Properties of Tropical Residual Soil by Microbially-Induced Calcite Precipitation*. Master of Engineering Science Thesis, Universiti Tunku Abdul Rahman, Petaling Jaya, Malaysia.

Soper, E. K. and Obson, C. C. (1922). “The Occurrence and Uses of Peat in the United States.” United States Geological Survey, Department of the Interior, Washington, DC.

Staudt, C., Horn, H., Hempel, D. C ., and Neu., T. R. (2004). "Volumetric Measurements of Bacterial Cells and Extracellular Polymeric Substance Glycoconjugates in Biofilms.” *Biotechnology and Bioengineering*, 88.5 (2004), 585–92.

Stocks-Fischer, S., Galinat, J. K., and Bang, S. S. (1999). "Microbiological Precipitation of $CACO_3$." *Soil Biology and Biochemistry*, 31(11), 1563-1571.

Sumner, J.B. (1926). “The Isolation and Crystallization of the Enzyme Urease.” Department of Physiology and Biochemistry, Cornell University Medical College, Ithaca, NY, 435-441.

Suresh and Mody. (2009). "Microbial Exopolysaccharides: Variety and Potential Applications.” *Microbial Production of Biopolymers and Polymer Precursors*. Caister Academic Press, ISBN 978-1-904455-36-3.

Tagliaferri, F., Waller, J., Andò, E., Hall, S. A., Viggiani, G., Bésuelle, P., and DeJong, J. T. (2011). "Observing Strain Localization Processes in Bio-Cemented Sand using X-Ray Imaging." *Granular Matter*, 13(3), 247-250.

Terashi, M., and Tanaka, H. (1981). “Ground Improvement by Deep Mixing Method.” *Soil Mechanics and Foundation Engineering*, *Tenth International Conference*, Stockholm, Sweden, June.

Tiano P. (1995). “Stone Reinforcement by Calcite Crystal Precipitation Induced by Organic Matrix Macromolecules.” *Stud. Conserv.*, 40, 171–176.

Torkzaban, S., Tazehkand, S. S., Walker, S. L., and Bradford, S. A. (2008). “Transport and Fate of Bacteria in Porous Media: Coupled effects of Chemical Conditions and Pore Space Geometry.” *Water Resources Research*, 44(4), W04403.

Wan Hassan, W. H., Rashid, A. S. A., Latifi, N., Horpibulsuk, S., and Borhamdin, S. (2017). “Strength and Morphological Characteristics of Organic Soil Stabilized with Magnesium Chloride.” *Quarterly Journal of Engineering Geology and Hydrogeology*, 50, 454-459.

Warren, L. A., Maurice, P. A. , Parmar, N., and Ferris, F.G. (2001). “Microbially Mediated Calcium Carbonate Precipitation: Implications for Interpreting Calcite Precipitation and for Solid-Phase Capture of Inorganic Contaminants.” *Geomicrobiol J*., 18, 93–115.

Wei, S., Cui, H., Jiang, Z., Liu, H., He, H., and Fang, N. (2015). "Biomineralization Processes of Calcite Induced by Bacteria Isolated from Marine Sediments." *Braz. J. Microbiol*, 46(2), 455-464.

Weil, M. H., De Jong, J. D., Martinez, B., and Mortensen, B. M. (2012). "Seismic and Resistivity Measurements for Real-Time Monitoring of Microbially Induced Calcite Precipitation in Sand." *Geotechnical Testing Journal*, 35(2).

Whiffin, V.S. (2004). *The Reduction of the Permeability of a Lateritic Soil through the Application of Microbially Induced Calcite Precipitation*. “Ph.D. Dissertation,” Murdoch University, Perth, Australia.

Whiffin, V. S., van Paassen, L. A., and Harkes, M. P. (2007). "Microbial Carbonate Precipitation as a Soil Improvement Technique." *Geomicrobiology Journal*, 24(5), 417-423.

Wong, L. S. (2015). "Microbial Cementation of Ureolytic Bacteria from the Genus *Bacillus*: a Review of the Bacterial Application on Cement-Based Materials for Cleaner Production." *Journal of Cleaner Production*, 93, 5-17.

Wright, D. T. (1999). “The role of Sulphate-Reducing Bacteria and Cyanobacteria in Dolomite Formation in Distal Ephemeral Lakes of the Coorong Region, South Australia.” *Sedimentary Geology*, 126(1–4), 147-157.

Vahabi, A., Ramezanianpour, A. A., Sharafi, H., Zahiri, H. S., Vali, H., and Noghabi, K. A. (2015). "Calcium Carbonate Precipitation by Strain *Bacillus licheniformis* AK01, Newly Isolated from Loamy Soil: A Promising Alternative for Sealing Cement-Based Materials." *Journal of Basic Microbiology*, 55(1), 105-111.

Vandevivere, P. and Baveye, P. (1992). "Relationship between Transport of Bacteria and Their Clogging Efficiency in Sand Columns." *Applied Environmental Microbiology*, 58(8), 2523-2530.

van Elsas, J. D. and Penido, E. G. C. (1982). "Characterization of a New *Bascillus megaterium* Bacteriophage, M J-l, from Tropical Soil." *Antonie Van Leeuwenhoek*, 48(4), 365-371.

van Paassen, L. A., Daza, C. M., Staal, M., Sorokin, D. Y., van der Zon, W., and van Loosdrecht, C. M. (2010). "Potential Soil Reinforcement by Biological Denitrification." *Ecological Engineering*, 36(2), 168-175.

van Tittelboom, K., De Belie, N., DeMuynck, W., and Verstraete, W. (2010). "Use of Bacteria to Repair Cracks in Concrete." *Cement and Concrete Research*, 40(1), 157-166.

Vijay, B., Prashant, H. and Darshak, R., (2009). "Bacterial concrete - An Ideal Concrete for Historical Structures." *Concrete Solutions*. CRC Press, Boca Raton, FL.

Yasuhara, H., Neupane, D., Hayashi, K., and Okamura, M. (2012). "Experiments and Predictions of Physical Properties of Sand Cemented by Enzymatically-Induced Carbonate Precipitation." *Soils and Foundations*, 52(3), 539-549.

Zayen, V.D.B., Almeida, M.S.S., Marques, M.E.S., and Fujii, J. (2003). "Behaviour of the Embankment of the Sewage Treatment Plant of Sarapui (in Portuguese)." *Soils and Rocks*, 26, (3), 261-271.

Zhao, Q., Li., L., Li, C., Li, M., Amini, F., and Zhang, H. (2014a). "Factors Affecting Improvement of Engineering Properties of MICP-Treated Soil Catalyzed by Bacteria and Urease." *J. Materials in Civil Engineering*, 26(12), DOI: 10.1061/(ASCE)MT.1943-5533.0001013.

Zhao, Q., Li, L., Li, C., Zhang, H., Amini, F. (2014b). "A Full Contact Flexible Mold for Preparing Samples Based on Microbial-Induced Calcite Precipitation Technology." *Geotechnical Testing Journal* 37(5), 1-5.

APPENDIX A: LITERATURE REVIEW OF BACTERIA TYPES

Microbe Type	Soil (characteristics)	Microbe Growth	Isolation	Urea Medium	Bacterial Solution(s)	Cementation Solution(s)	Source
S. pasteurii	Sand (quartz)	600 mL of microbes grown in Tris-YE medium until cell reached late exponential growth, incubated at 200 rpm One set then autoclaved at 121°C for 20 min	Centrifuged at 5000 g for 10 min, washed twice in in buffer containing sodium phosphate	1^{-1} distilled water, 3 g bacto, 20 g urea, 10 g NH_4Cl, 2.12 g $NaHCO_3$ 25°C Added 1.4, 2.8 and 5.6 g of $CaCl_2$ to different samples	Cells suspended in urea medium and mixed with 100 g of sand	Gravity fed with urea solution for 10 days	(Stocks-Fischer et al., 1999)
S. pasteurii	Sand: Ottawa 50-70 (D_{50} = .12 mm C_u = 1.6 C_c = 0.8 G_s = 2.65 e_{min} = 0.55 e_{max} = 0.87)	Cells initially grown on solid medium then transferred to liquid medium and agitated for 19 hr at 37°C	Centrifuged at 1000rpm, 4°C for 10 min. Afterward the supernatant was removed.	Contains per liter of double distilled water, 3 g Bacto nutrient broth 20 g Urea $NH_2(CO)NH_2$, 10 g NH_4Cl, 2.12 g $NaHCO_3$, Adjust pH of the medium to 6.0 with 5 N HCl prior to sterile filtration	$2x10^6$ cells/mL Bacillus pasteurii, 400 mL Urea medium, 8 mL of $CaCl_2$ stock solution (140 g/L)	400 mL Urea medium, 8 mL of $CaCl_2$ stock solution (140 g/L)	(DeJong et al., 2006)

Microbe Type	Soil (characteristics)	Microbe Growth	Isolation	Urea Medium	Bacterial Solution(s)	Cementation Solution(s)	Source
S. pasteurii	Sand: Itterbeck d10 = 10 µm (10% of the grains have a diameter of this size or lower); d50 = 165 µm; d90 = 275µm) to a dry density of 1.65 g/cm^3 (porosity of 37.8%)	Grown aerobically in medium of 20 g/L yeast extract and 10 g/L NH4Cl at a pH of 9 Grown to early stationary phase (all readily available nutrients consumed) before storing at 4^{0}C for 48 hours	Not described	1.1 M Urea and $CaCl_2$	OD600: 1.583 Injected at 0.35 L/hr for 18 hours followed by 0.05 M $CaCl_2$ at same flow rate for 17 hours	1.1 M Urea and $CaCl_2$ with same flow rate for 25 hours	(Whiffin et al., 2007)
S. pasteurii	Toyoura and No. 3 Silica sand Edosaki and Kushiro peat	Not described	Not described	Varied between 0.25 and 1.5 mol/L	Microbe culture solution	3g nutrient broth, 10 g NH_4Cl, 2.12 g $NaHCO_3$, 0.5 mol $Co(NH_2)_2$, 0.5 mol $CaCl_2$	(Inagaki et al., 2011)
S. pasteurii (mixed with *Bacillus subtilis* (competing bacteria))	N/A	Grown in nutrient broth (NB, Himedia®) with 2% urea (333 mM) until exponential growth phase	Centrifuged and re-suspended in $CaCO_3$	7mM urea, 13 g/L NBu medium	Culture suspended in sterile $CaCO_3$	Urea medium, 16.91 mM Na+, 0.32 mM K+, 2.43 mM Ca2+, 2 mM Mg2+, 1 mM SO42-, 21.53 mM Cl-, 2.56 mM DIC	(Gat et al., 2011)
S. pasteurii	Silica, calcite, iron oxide, feldspar	Grown at 30ºC in ammonium yeast extract (ATCC 1376) Incubated aerobically in shaking water bath at 200 rpm for 40 h (OD_{600} of 0·8-1·0	Centrifuged at 4000 g for 20 min Stored at 4ºC for 14 days	Concentrations described under cementation solution	Microbe culture isolate	Three batches containing (units in mM/L): urea (333, 333, 50), NH_4Cl (187, 374, 56.7), $NaHCO_3$ (25.2, 25.2, 3.8), nutrient broth (3, 3, 0g), and $CaCl_2$ (50)	(Mortensen et al., 2011)

Microbe Type	Soil (characteristics)	Microbe Growth	Isolation	Urea Medium	Bacterial Solution(s)	Cementation Solution(s)	Source
S. pasteurii	Fractured rock	Grown at 30 °C in 1 L glass bottles containing tryptic soy broth and 2% wt urea. 400 mL of liquid containing cells in exponential growth phase, determined by measuring optical density at 600 nm using UV-Vis Spectrophotometer (WPA Lightwave S2000), was transferred to each of four vessels containing 8 L of sterilized growth media. The vessels were then sealed and incubated at 30 °C on an orbital shaker at 100 rpm.	Cells at the late exponential growth stage (24 h incubation) were harvested by centrifugation at 10000 rpm for 10 min	Concentrations described in bacterial and cementation solutions	Culture diluted to OD_{600} = 1 with quarry sump water then added 0.2 mM $CaCl_2$ and 0.4 M urea	Urea and calcium chloride (concentrations not given)	(Cuthbert et al., 2013)
S. pasteurii	Sandy Soil 95% sandy soil, 5% silt, pH: 8	Cultivated in a medium of 10 g/L yeast extract, 5 g/L NH_4Cl, 1.3 mg/L $NiCl_2$, at pH of 8.5. Grown to late exponential growth in shaker incubator at 200 rpm and 25^0 C.	Not described	MICP_1 (0.1 M urea–0.1 M CaCl2), MICP_2 (0.25 M urea–0.25 M CaCl2), MICP_3 (0.5 M urea–0.5 M CaCl2) and MICP_4 (1 M urea–1 M CaCl2)	Microbe culture isolate	100 mL (equal parts bacterial and cementation)	(Maleki et al., 2016)

Microbe Type	Soil (characteristics)	Microbe Growth	Isolation	Urea Medium	Bacterial Solution(s)	Cementation Solution(s)	Source
S. pasteurii	Sand: Ottawa 50-70	20 g/L yeast extract, 10 g/L ammonium sulfate suspended in 0.13 M Tris buffer, pH 9 30^{o} C, aerobic, 200 rpm shaking incubator, OD_{600} = 1.0 (40 hrs)	Centrifuged at 4000 g for 15 min	333 mM urea, 374 mM ammonium chloride,	Microbe culture isolate with urea medium	Urea medium and 50 mM calcium chloride	(Feng and Montoya, 2016)
S. pasteurii	Uniformly Graded Sand Saturated hydraulic conductivity, cm/s: 1.5×10^{-3} Specific gravity Value: 2.65 Coarse sand percentage, %: 0.6 Medium sand percentage, %: 31.9 Fine sand percentage, %: 67.5 D_{60},mm: 0.4 D_{30},mm: 0.3 Effective size (D_{10}),mm: 0.24 Coefficient of curvature (C_c): 0.94 Coefficient of uniformity (C_u): 1.67	Prepared from strain ATCC 11859 stored in agar plates and grown overnight. Harvested at late exponential growth.	Centrifuged a 10000 g for 10 min, diluted to OD_{600} of 1.0	0.7 M of $CaCl_2$ and urea	Microbe culture isolate with urea medium	Urea medium	(Salifu et al., 2016)

Microbe Type	Soil (characteristics)	Microbe Growth	Isolation	Urea Medium	Bacterial Solution(s)	Cementation Solution(s)	Source
E. coli HB101 (studied with plasmids pBU11 and pBR322)	N/A	Maintained in Luria–Bertani (LB) broth containing 50 µM $NiCl_2$ (100 μgmL^{-1} for urease activity and ampicillin) for maintenance of the plasmid. Broth cultures for $CaCO_3$ precipitation experiments were prepared in urea–$CaCl_2$. Grown at 37° C	N/A	Urea and $CaCl_2$ medium containing ampicillin (100 μgmL^{-1}), to which $NiCl_2$ was added to final concentrations of 0, 5, 100, 500, and 1000 µM.	N/A	N/A	(Bachmeier et al., 2002)
Bacillus sphaericus	Silica sand	Cultivated under sterile aerobic batch conditions in a medium consisting of 20 g/L yeast extract, 0.17 M ammonia sulfate and 0.1 mM NiCl2, at pH of 9.25. After 24 h incubation at 28◦C, the culture was collected and stored at 4°C prior to use OD_{600} between 1.5 and 2	Not described	1 M CaCl2 and 1 M urea	Microbe culture	Urea medium	(Cheng and Cord-Ruwisch, 2012)

Microbe Type	Soil (characteristics)	Microbe Growth	Isolation	Urea Medium	Bacterial Solution(s)	Cementation Solution(s)	Source
B. diminuta CP16, S. *soli* CP23 and B. *lentus* CP28		0.5 g of yeast extract, 10 g of dextrose, 5 g of $CaCl_2$, 0.5g of $(NH_4)_2SO_4$, 5 g of $Ca_3(PO_4)_2$, 0.2 g of KCl, 0.1 g of $MgSO_4$, 0.0001 g of $MnSO_4$ and 0.0001 g of $FeSO_4$, 20 g agar, pH 7.0, and grown at 28 °C for 5 days.					(Wei et al., 2015)
Bacillus megaterium	Gravel: 0% Sand: 29% Silt: 55% Clay: 16%	Grown in nutrient broth at temperature of 37°C under aerobic condition. The grown culture (5×10^7 cfu/mL) was harvested at late exponential phase and mixed with air-dried soil specimens.	Not described	0.25 mol urea and calcium chloride	Microbe culture	3 g nutrient broth, 10 g NH4Cl, and 2.12 g NaHCO3 per liter of deionized water mixed with urea medium	(Ng et al., 2012)
Pseudomonas stutzeri	n/a: synthetic homogeneous pore network	Prepared using Bold's basal medium					(Singh et al., 2015)

APPENDIX B: OTTAWA 50/70 SAND CONSOLIDATION DATA

Displacement vs. square root of time for treated sands (J23-0 and J21-0) and untreated sands (U1 and U2).

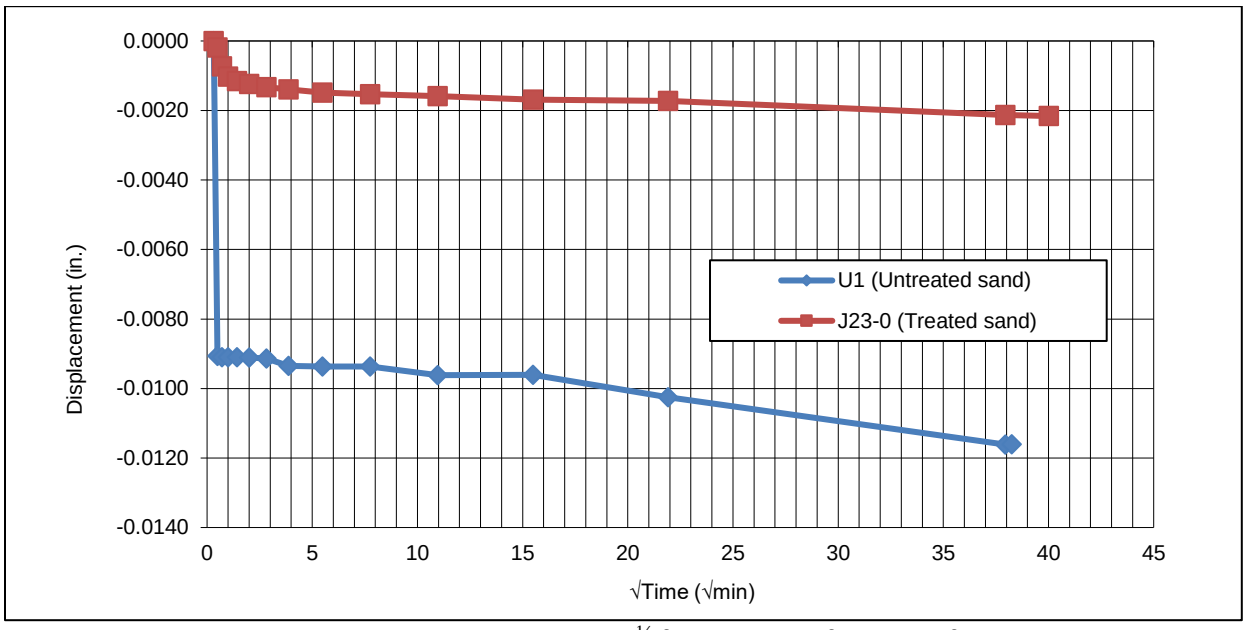

Figure B-1. Displacement vs. time^{½} for 0.0625-tsf loading for J23-0

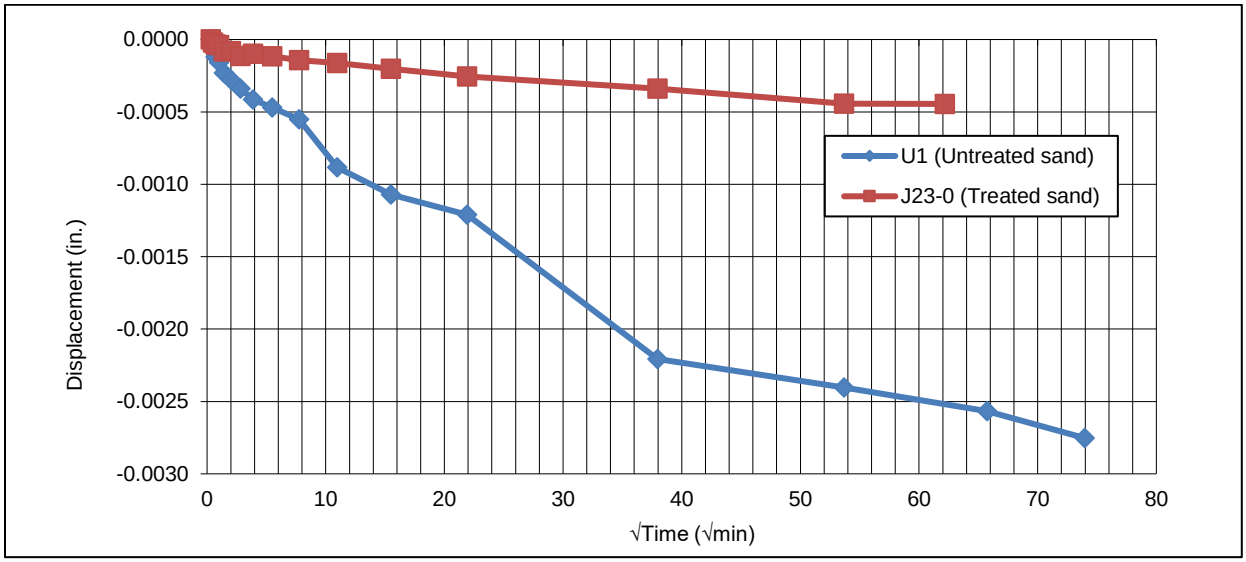

Figure B-2. Displacement vs. time^{½} for 0.125-tsf loading for J23-0

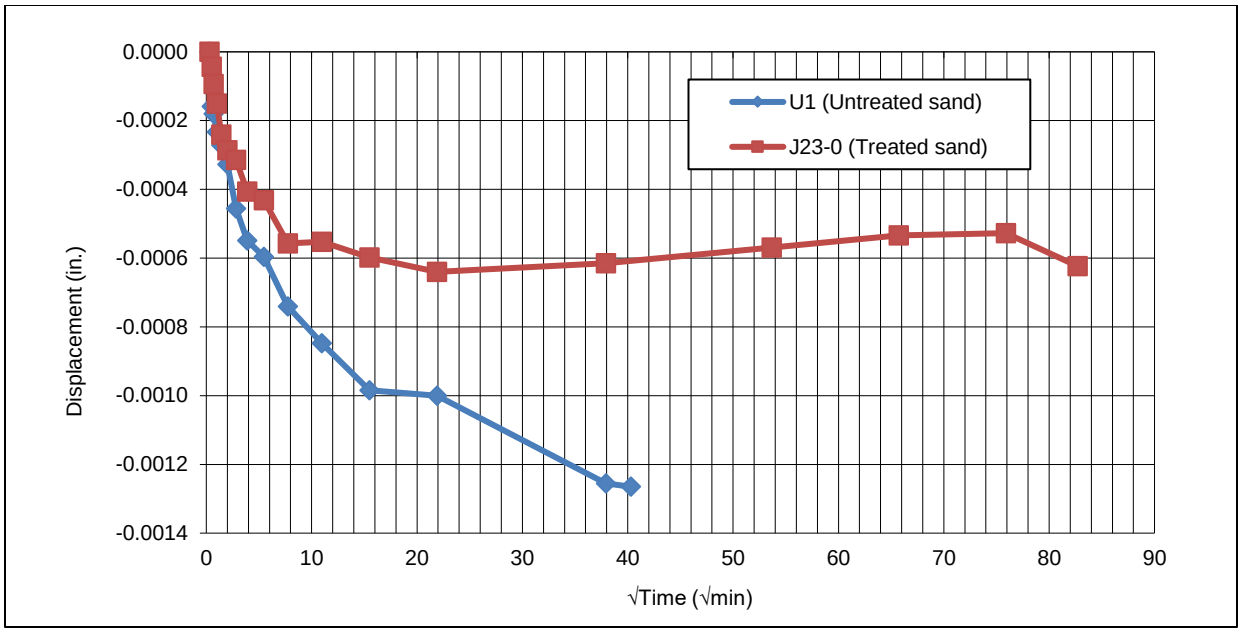

Figure B-3. Displacement vs. time^{½} for 0.25-tsf loading for J23-0

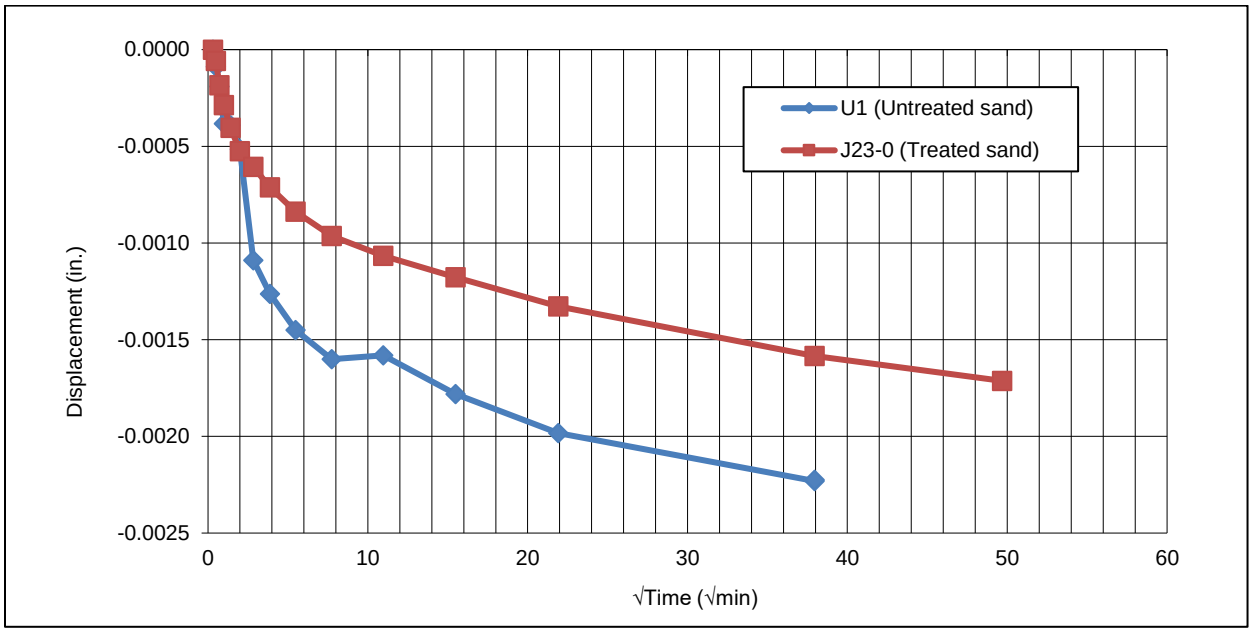

Figure B-4. Displacement vs. time^{½} for 0.5-tsf loading for J23-0

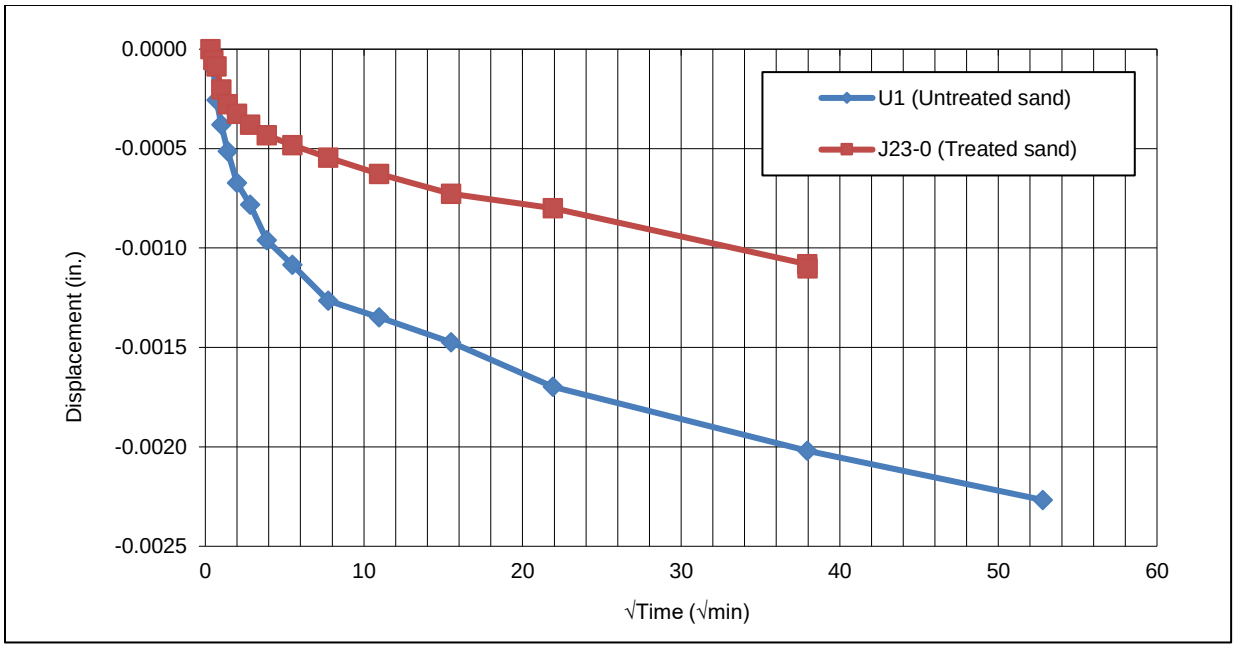

Figure B-5. Displacement vs. time^{½} for 1-tsf loading for J23-0

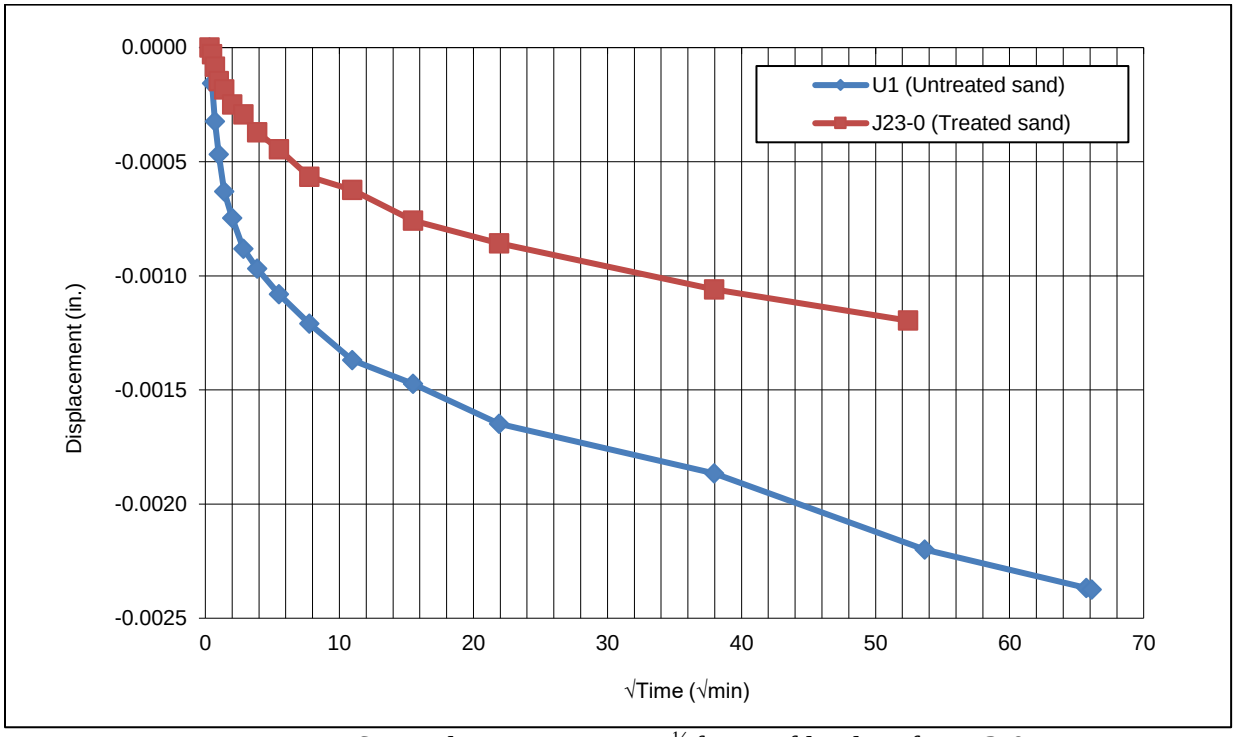

Figure B-6. Displacement vs. time^{½} for 2-tsf loading for J23-0

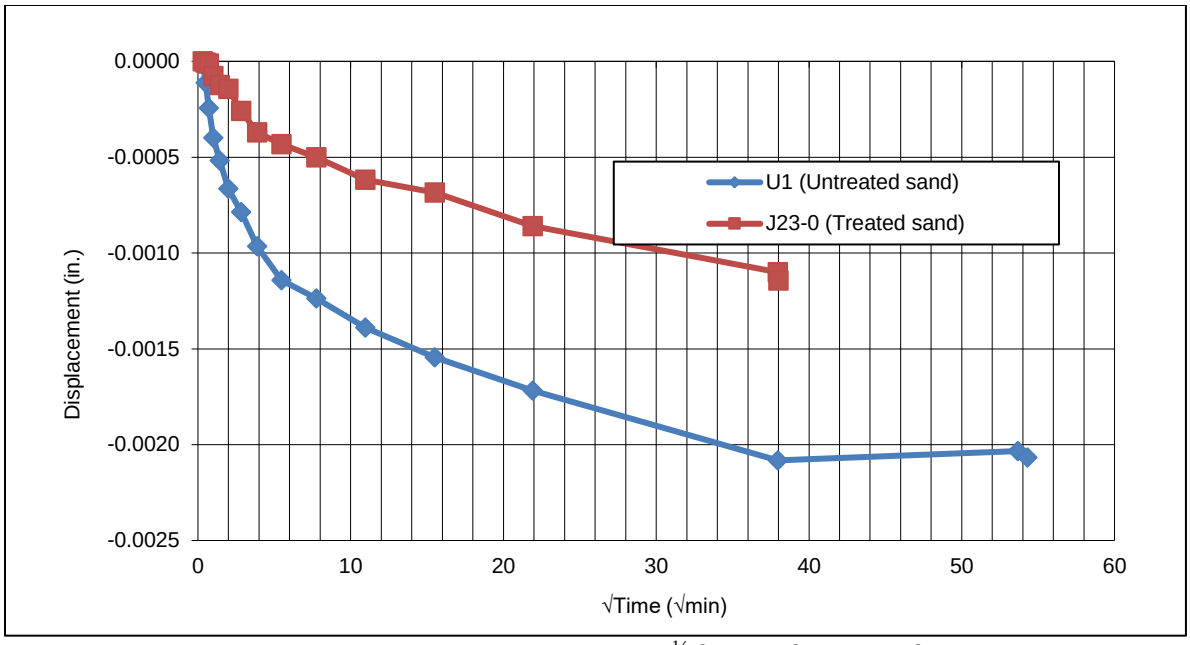

Figure B-7. Displacement vs. time^{½} for 4-tsf loading for J23-0

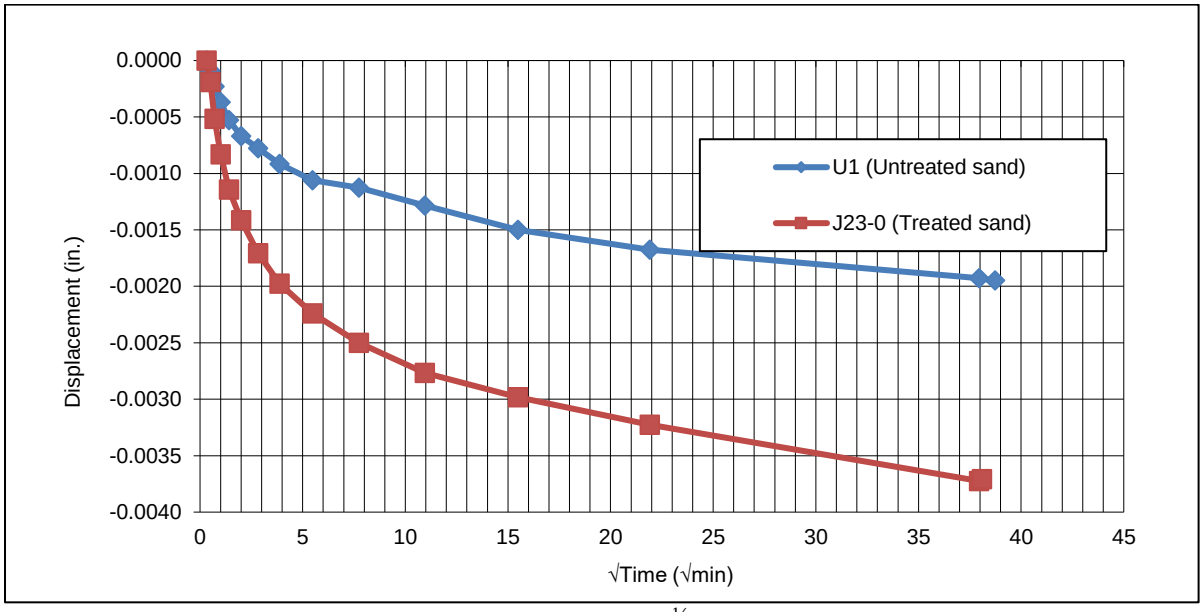

Figure B-8. Displacement vs. time^{½} for 8-tsf loading for J23-0

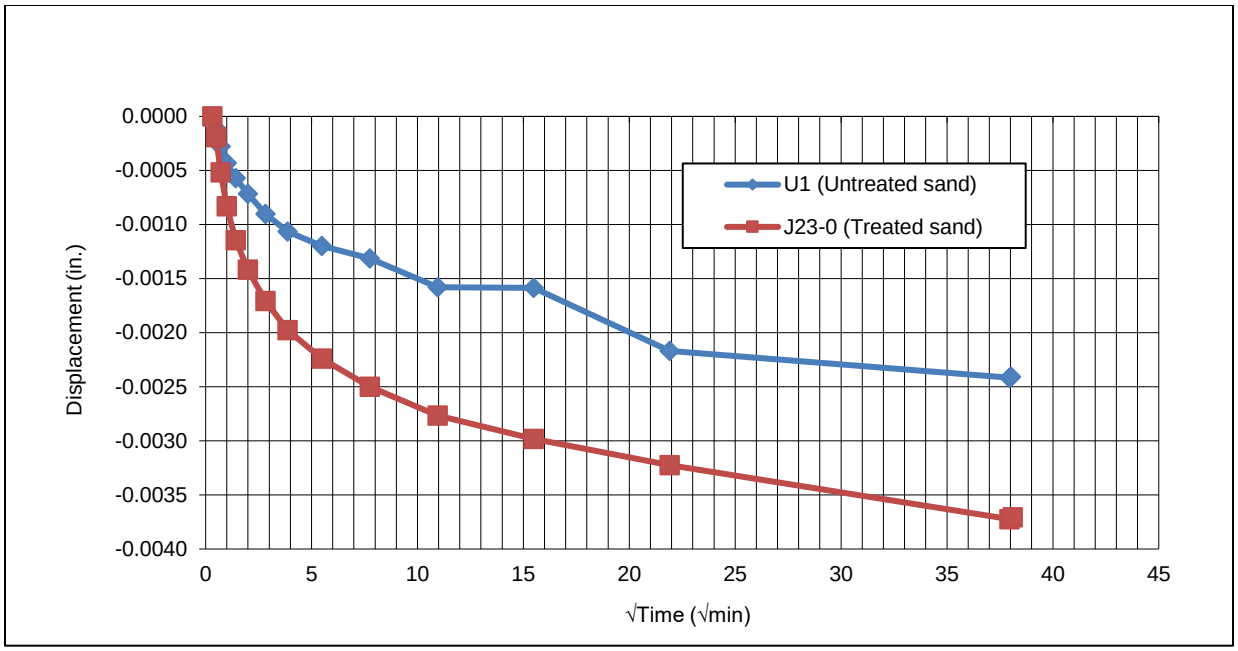

Figure B-9. Displacement vs. time^{½} for 16-tsf loading for J23-0

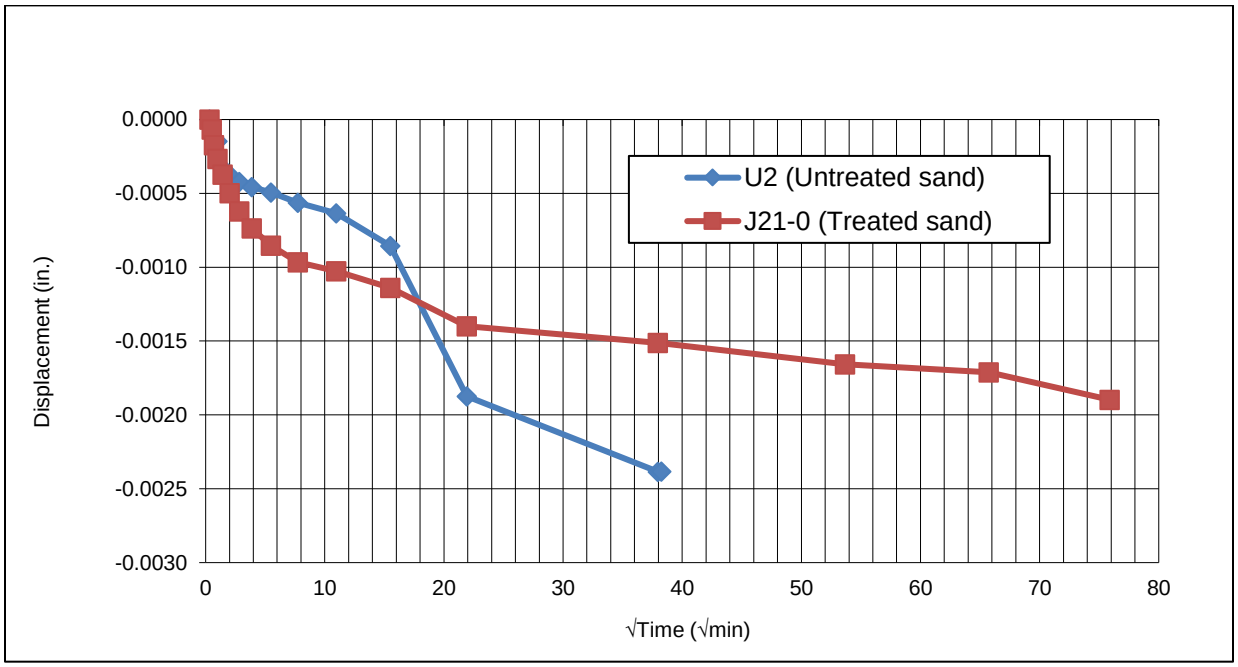

Figure B-10. Displacement vs. time^{½} for 0.0625-tsf loading for J21-0

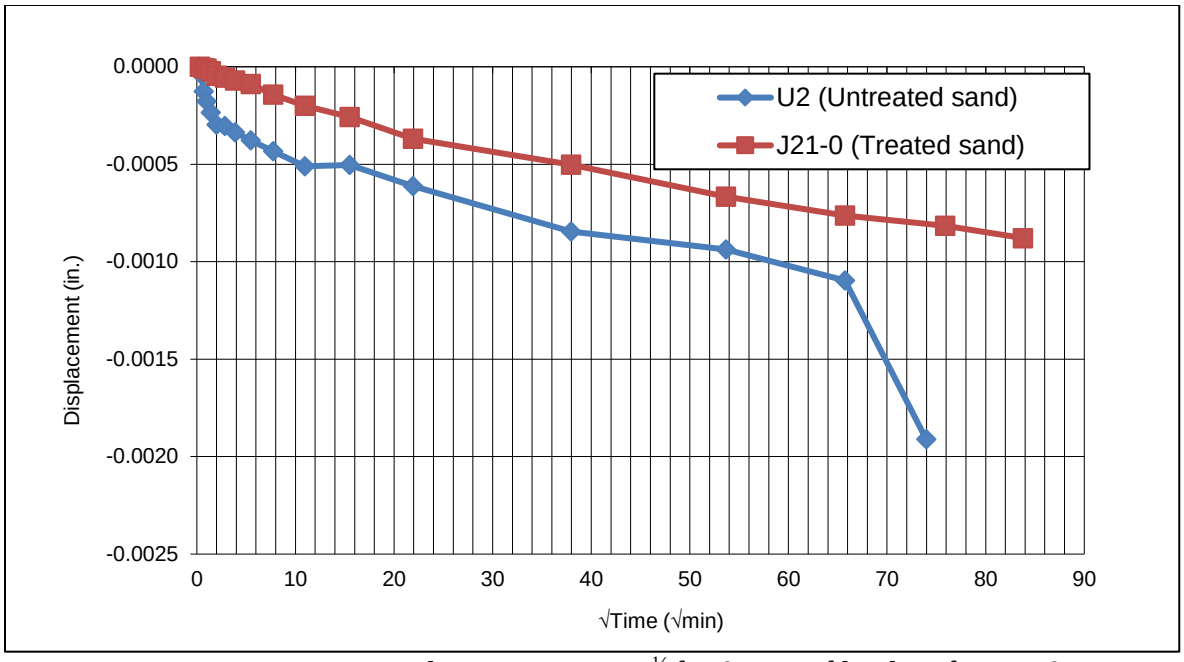

Figure B-11. Displacement vs. time^{½} for 0.125-tsf loading for J21-0

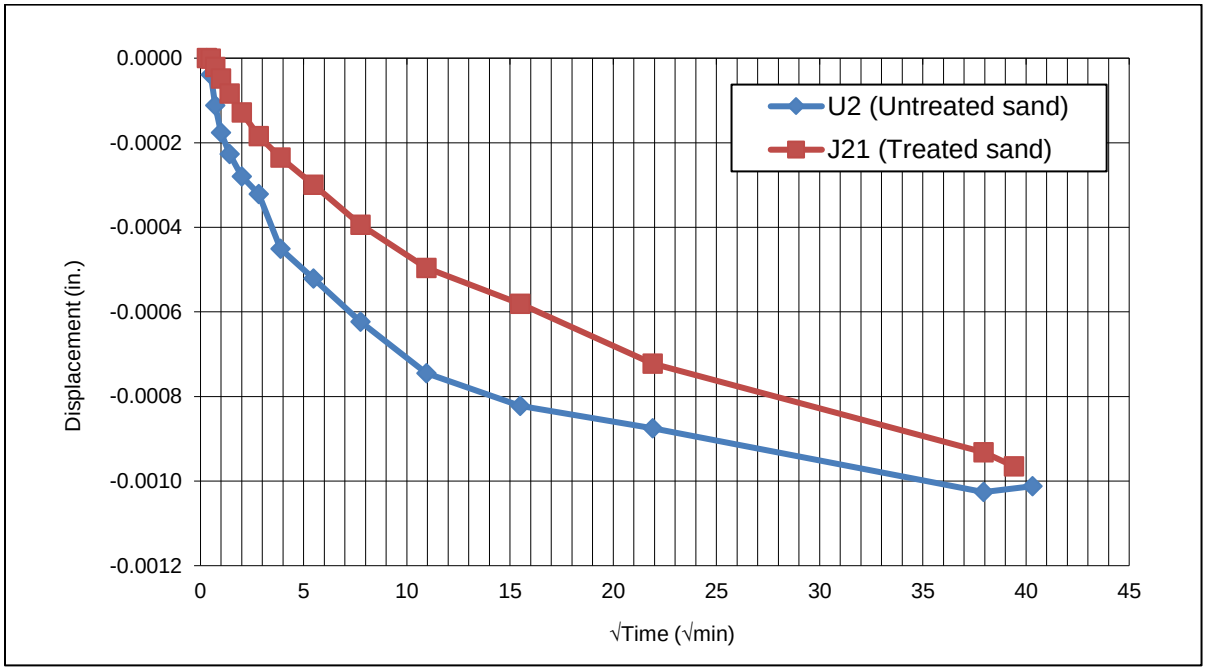

Figure B-12. Displacement vs. time^{½} for 0.25-tsf loading for J21-0

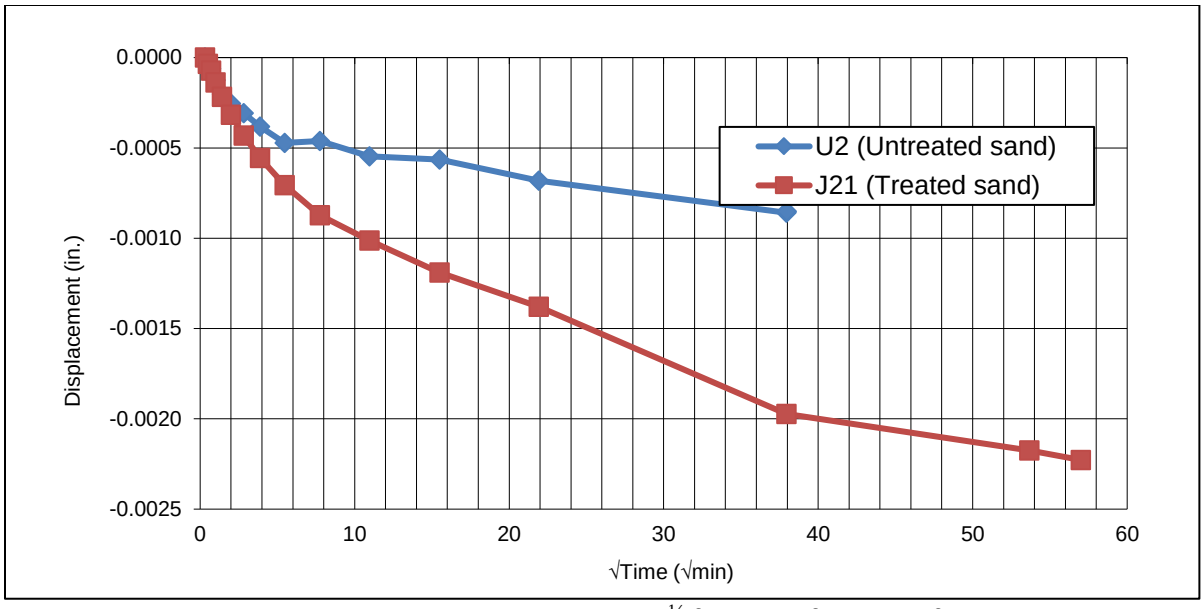

Figure B-13. Displacement vs. time^{½} for 0.5-tsf loading for J21-0

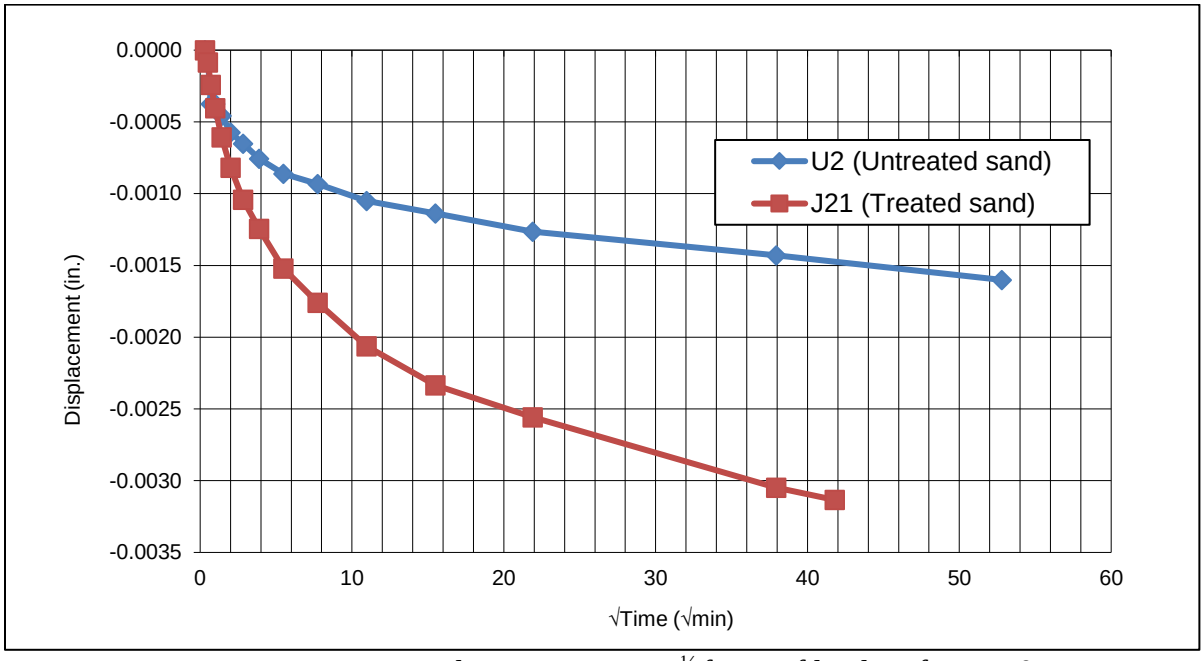

Figure B-14. Displacement vs. time^{½} for 1-tsf loading for J21-0

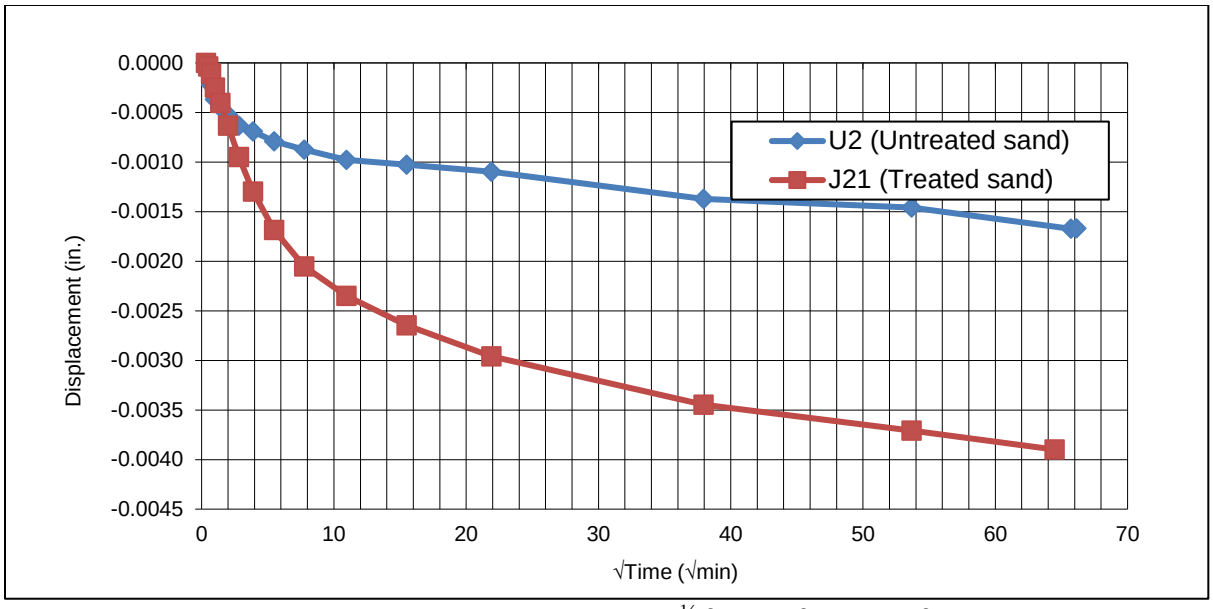

Figure B-15. Displacement vs. time^{½} for 2-tsf loading for J21-0

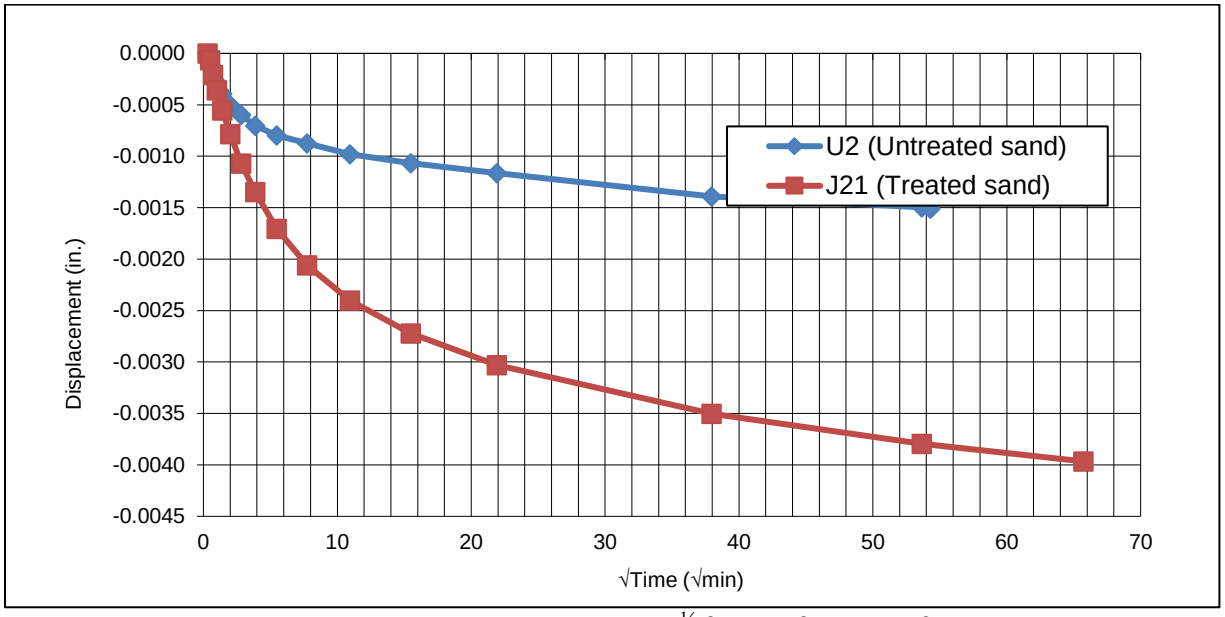

Figure B-16. Displacement vs. time^{½} for 4-tsf loading for J21-0

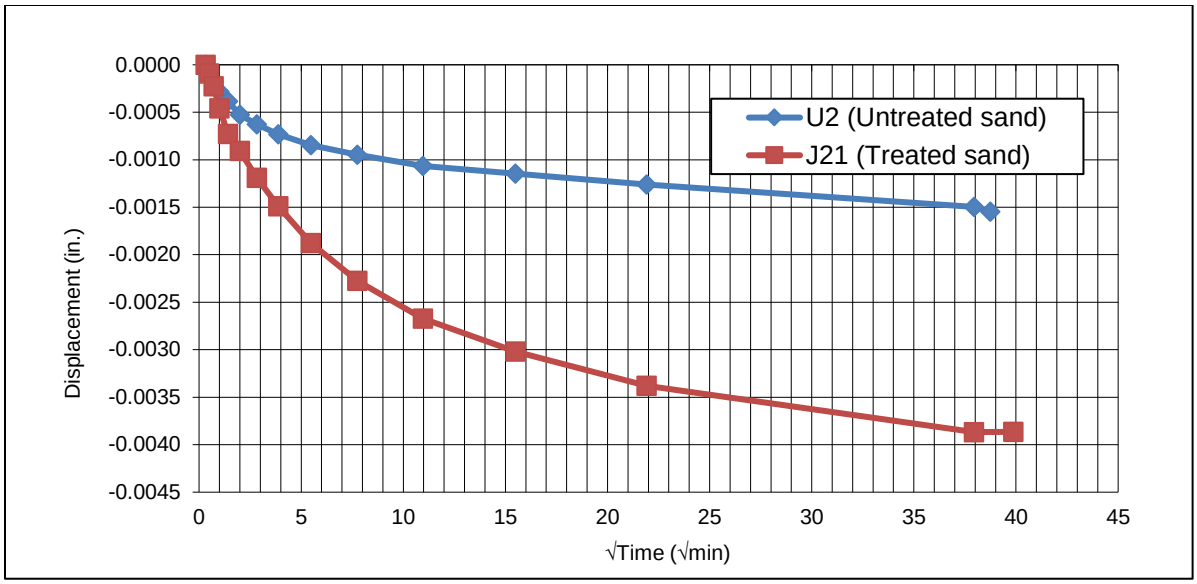

Figure B-17. Displacement vs. time^{½} for 8-tsf loading for J21-0

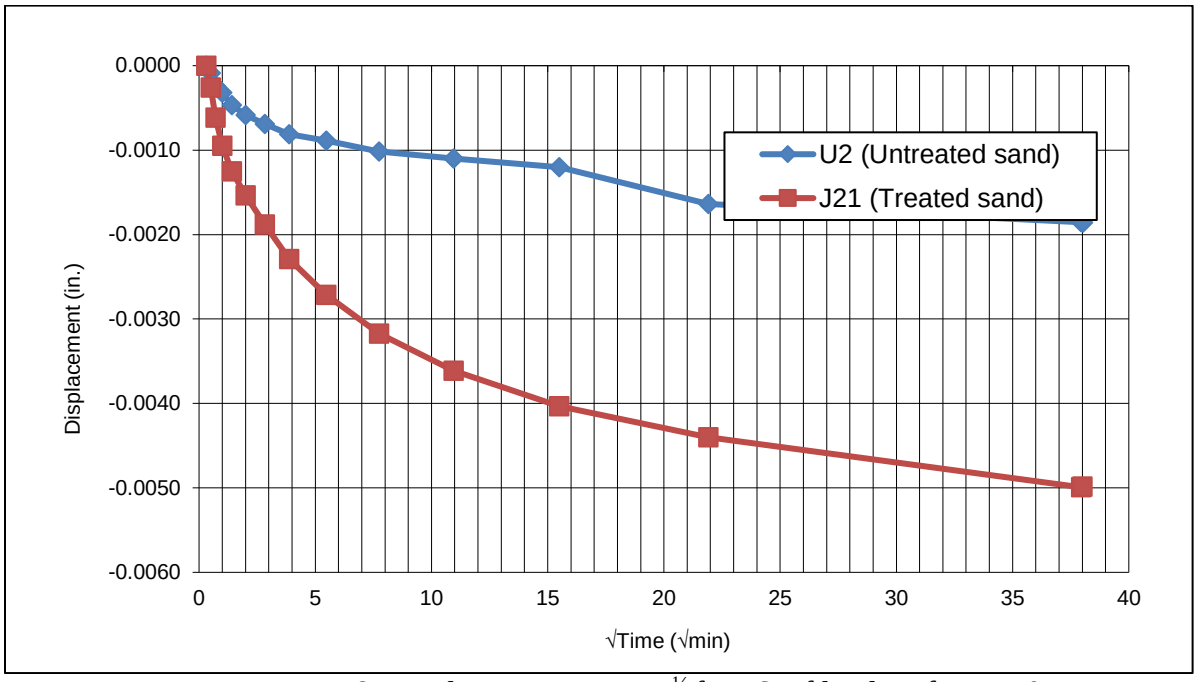

Figure B-18. Displacement vs. time^{½} for 16-tsf loading for J21-0

APPENDIX C: CONSOLIDATION DATA FROM UNTREATED SOIL WITH 50% ORGANIC CONTENT

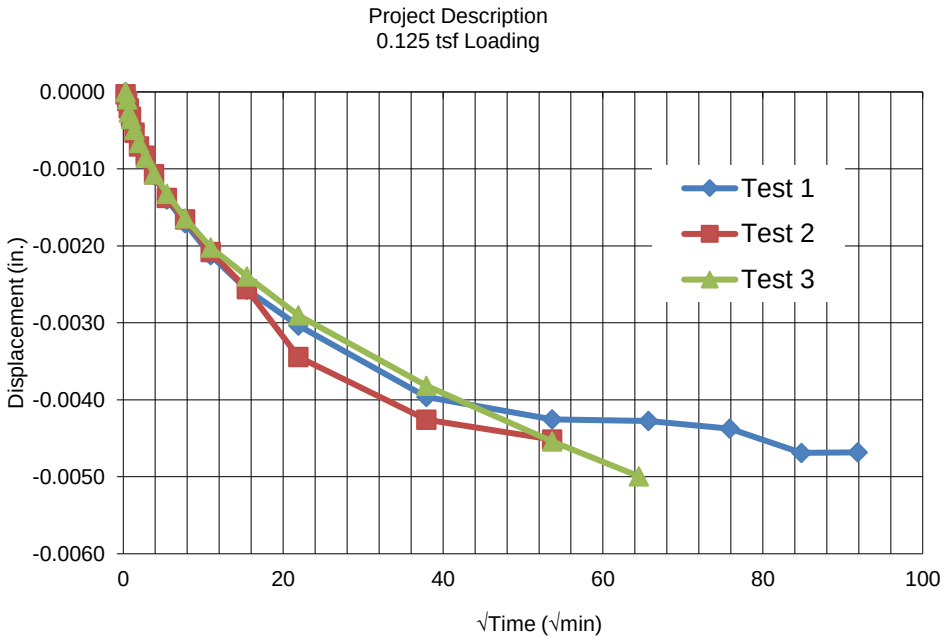

Figure C-1. Deformation vs. time^{½} for untreated soil at 0.125 tsf

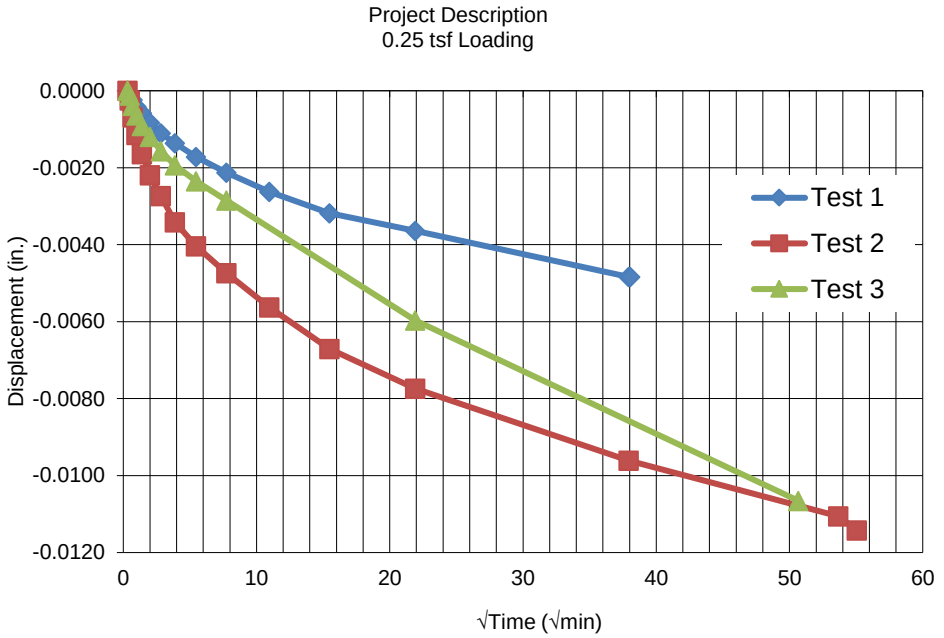

Figure C-2. Deformation vs. time^{½} for untreated soil at 0.25 tsf

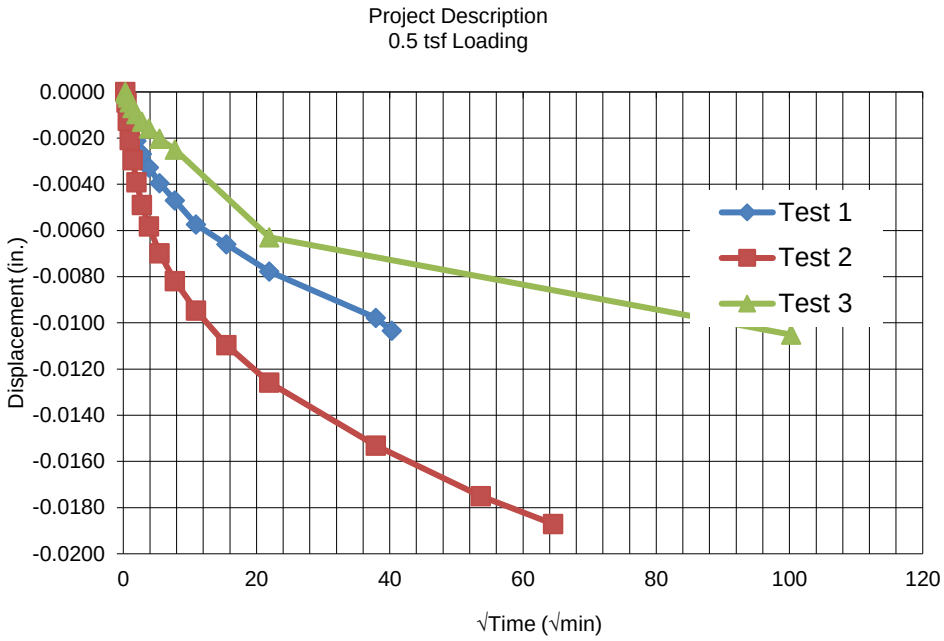

Figure C-3. Deformation vs. time^{½} for untreated soil at 0.5 tsf

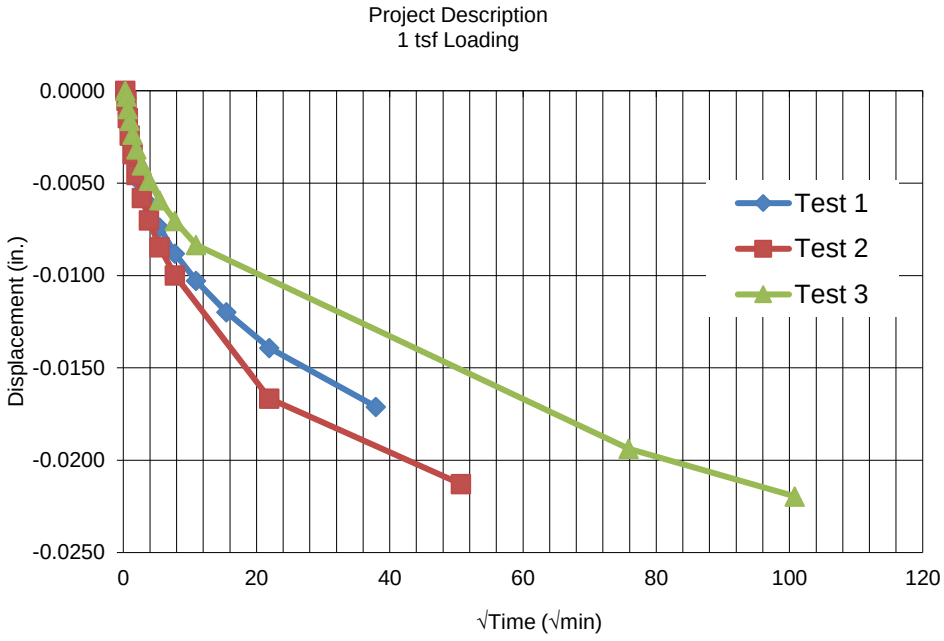

Figure C-4. Deformation vs. time^{½} for untreated soil at 1 tsf

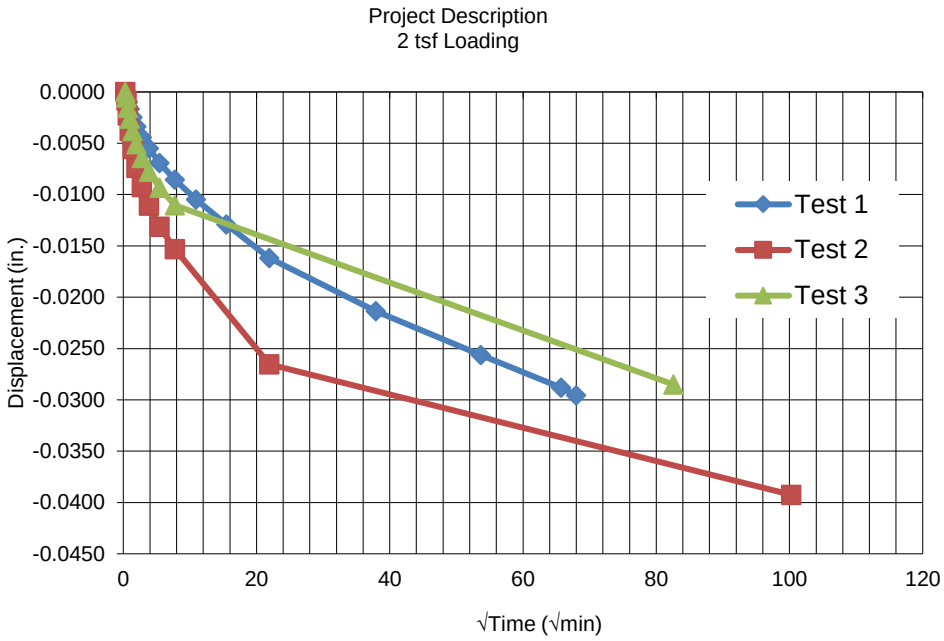

Figure C-5. Deformation vs. time^{½} for untreated soil at 2 tsf

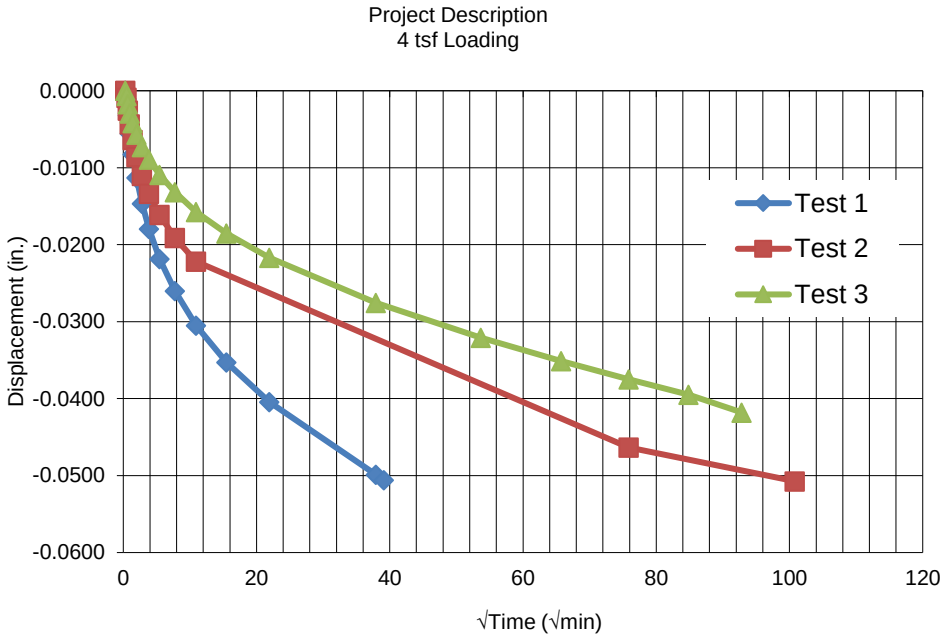

Figure C-6. Deformation vs. time^{½} for untreated soil at 4 tsf

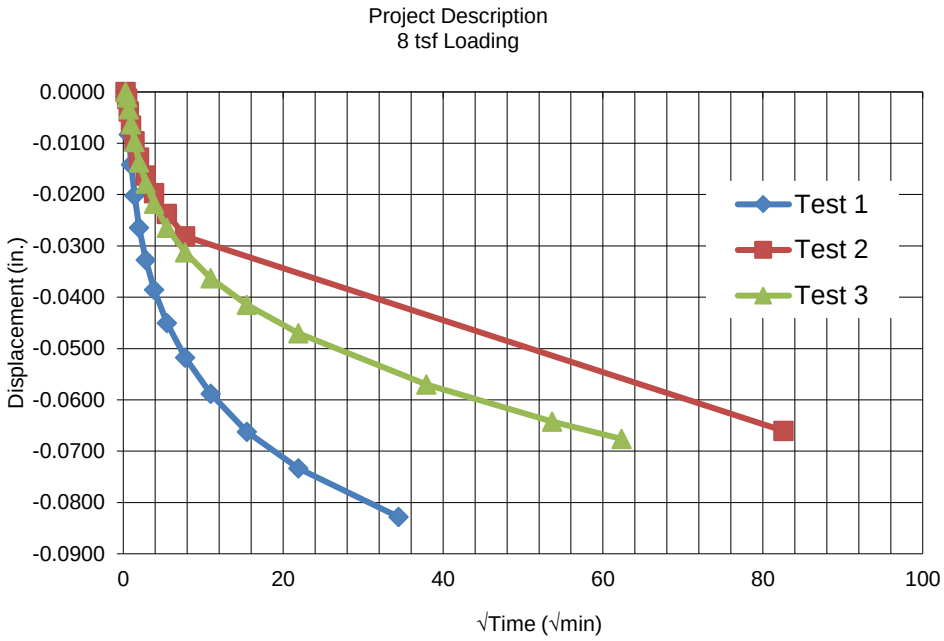

Figure C-7. Deformation vs time^{½} for untreated soil at 8 tsf

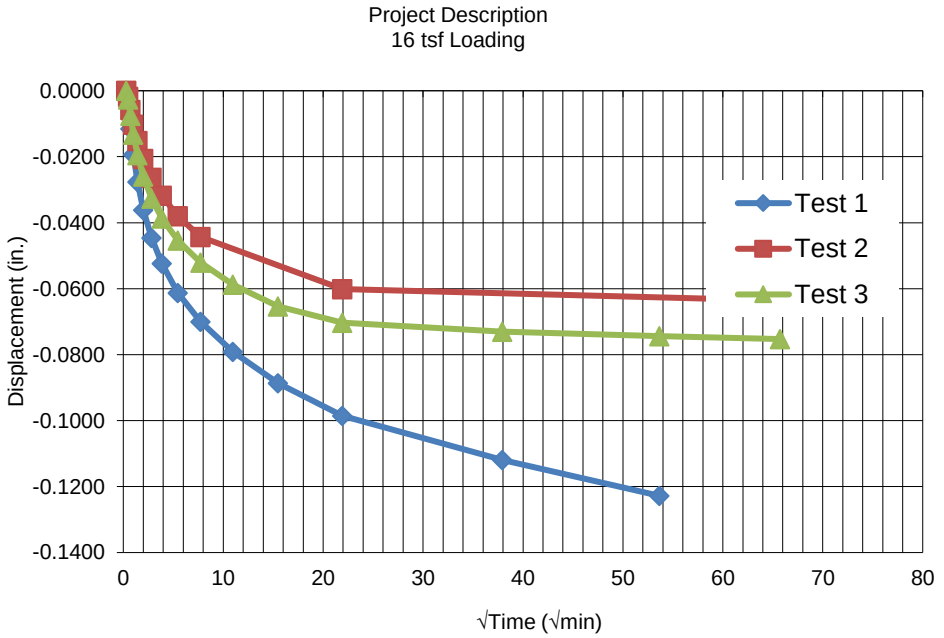

Figure C-8. Deformation vs. time^{½} for untreated soil at 16 tsf

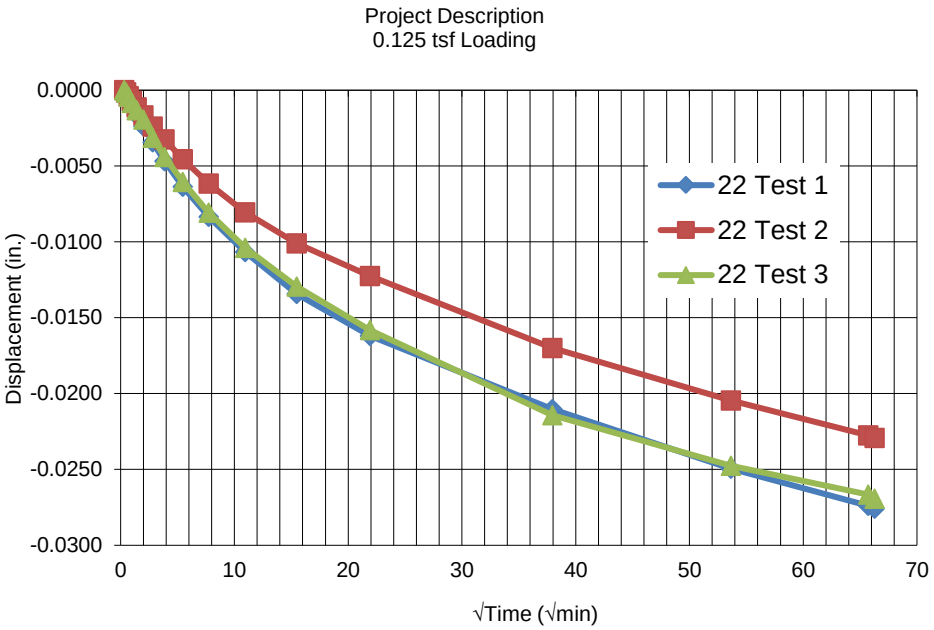

Figure C-9. Deformation vs. time^{½} for sample 22 at 0.125 tsf

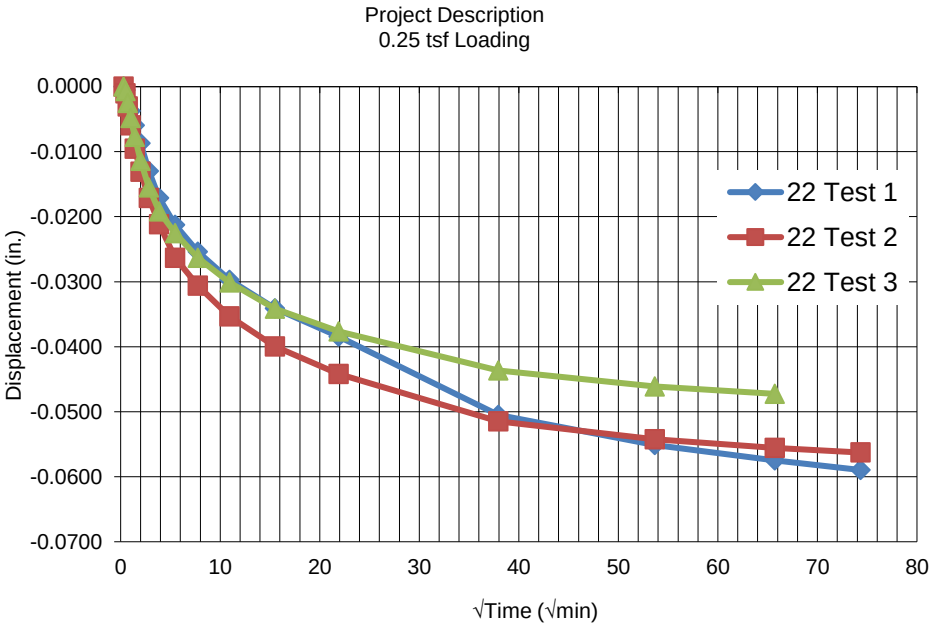

Figure C-10. Deformation vs. time^{½} for sample 22 at 0.25 tsf

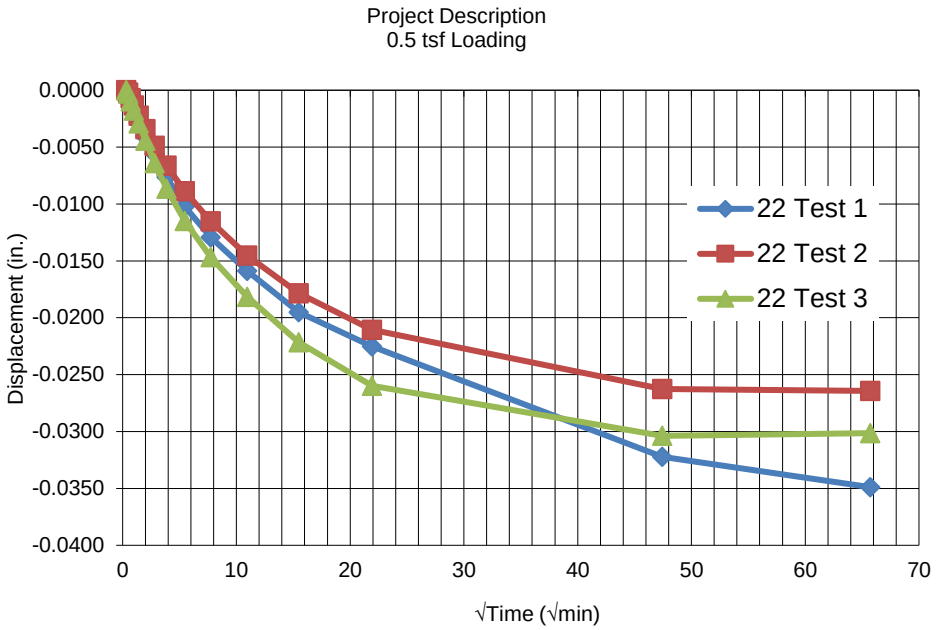

Figure C-11. Deformation vs. time^{½} for sample 22 at 0.5 tsf

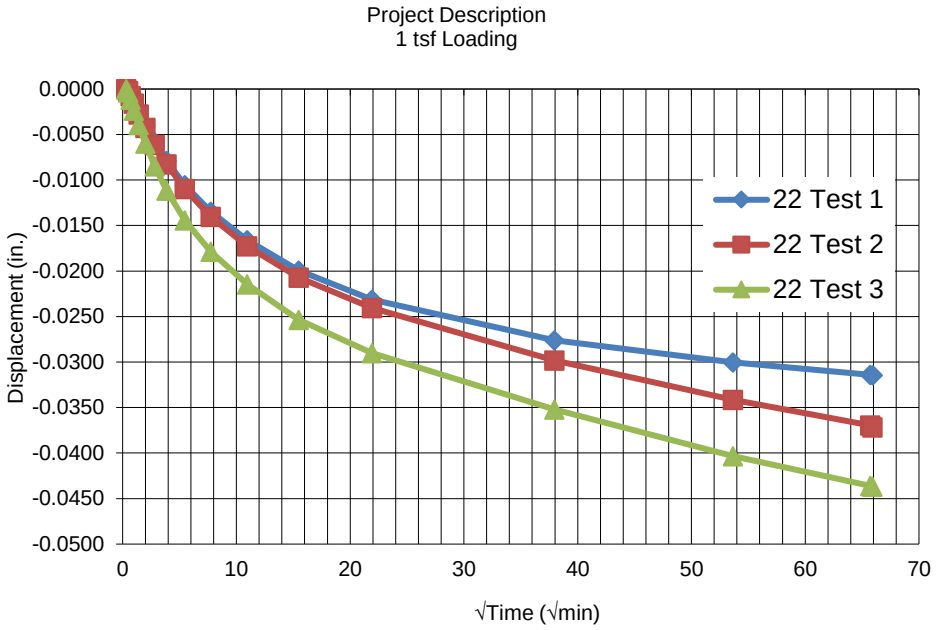

Figure C-12. Deformation vs. time^{½} for sample 22 at 1 tsf

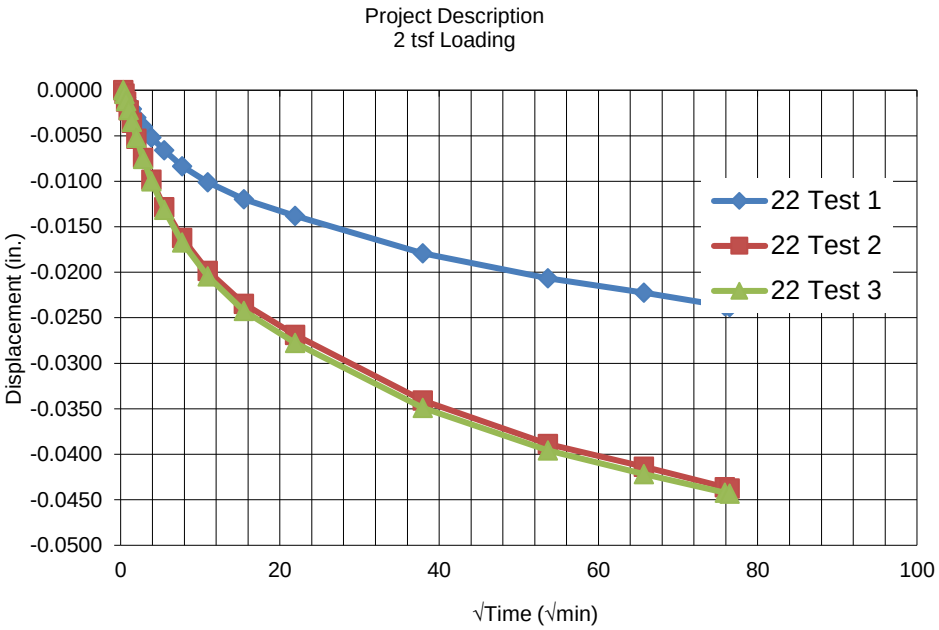

Figure C-13. Deformation vs. time^{½} for sample 22 at 2 tsf

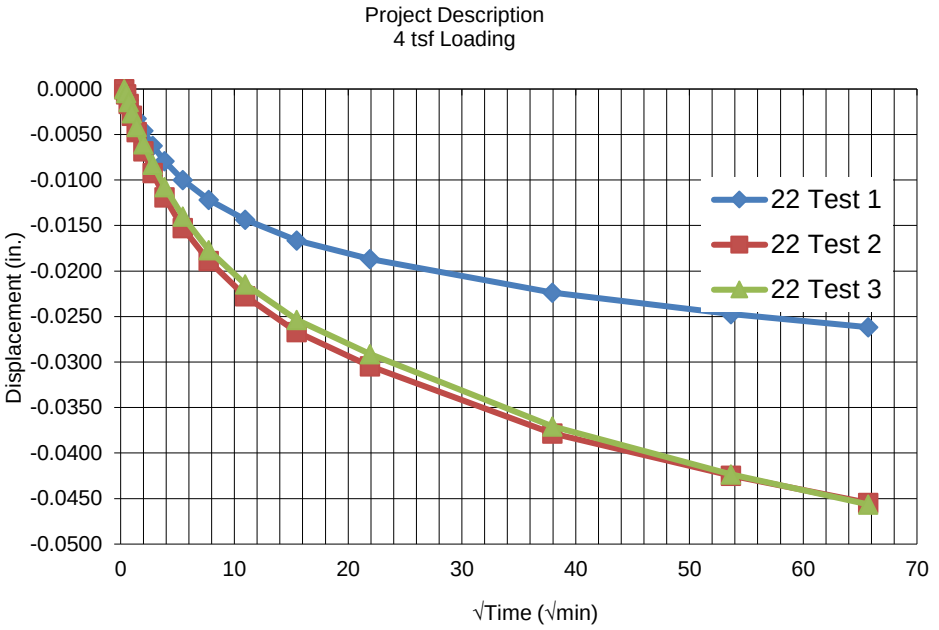

Figure C-14. Deformation vs. time^{½} for sample 22 at 4 tsf

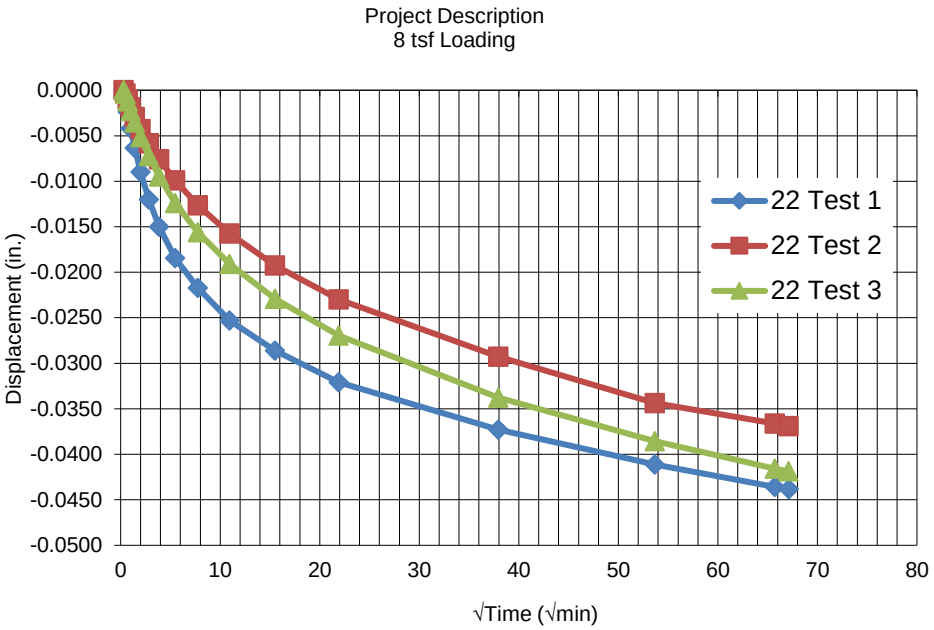

Figure C-15. Deformation vs. time^{½} for sample 22 at 8 tsf

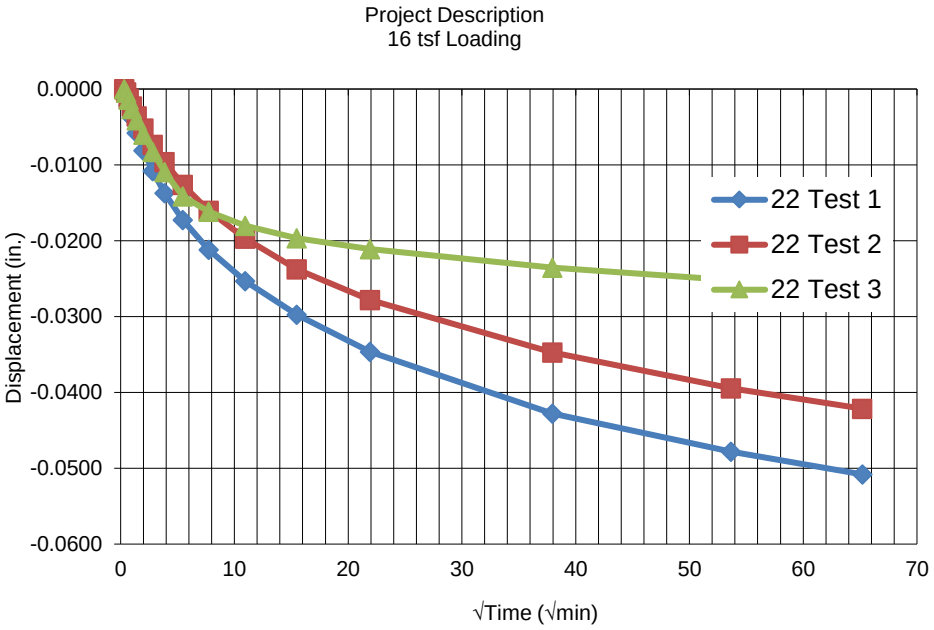

Figure C-16. Deformation vs. time^{½} for sample 22 at 16 tsf

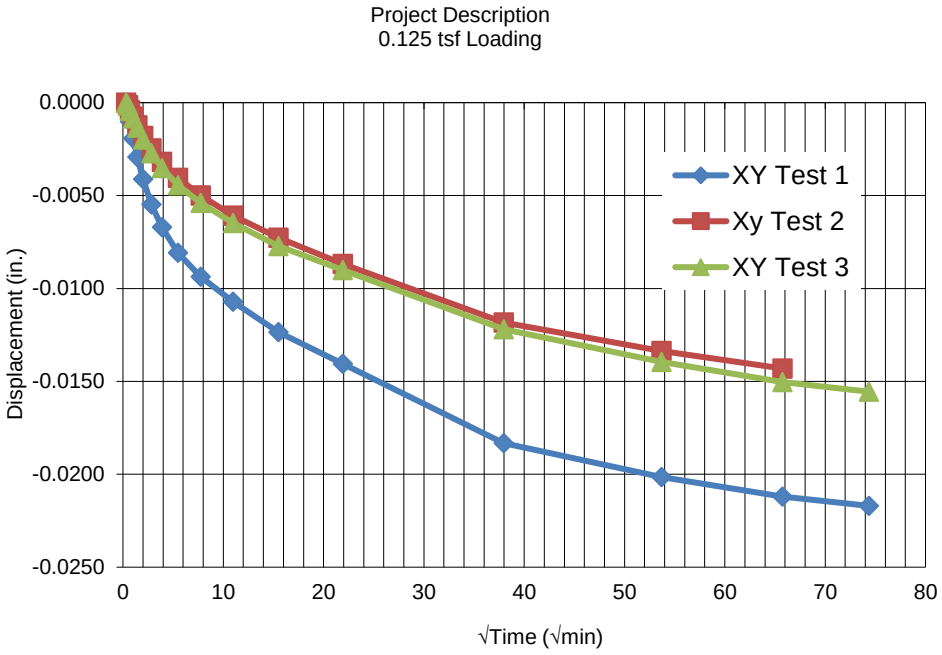

Figure C-17. Deformation vs. time^{½} for sample XY at 0.125 tsf

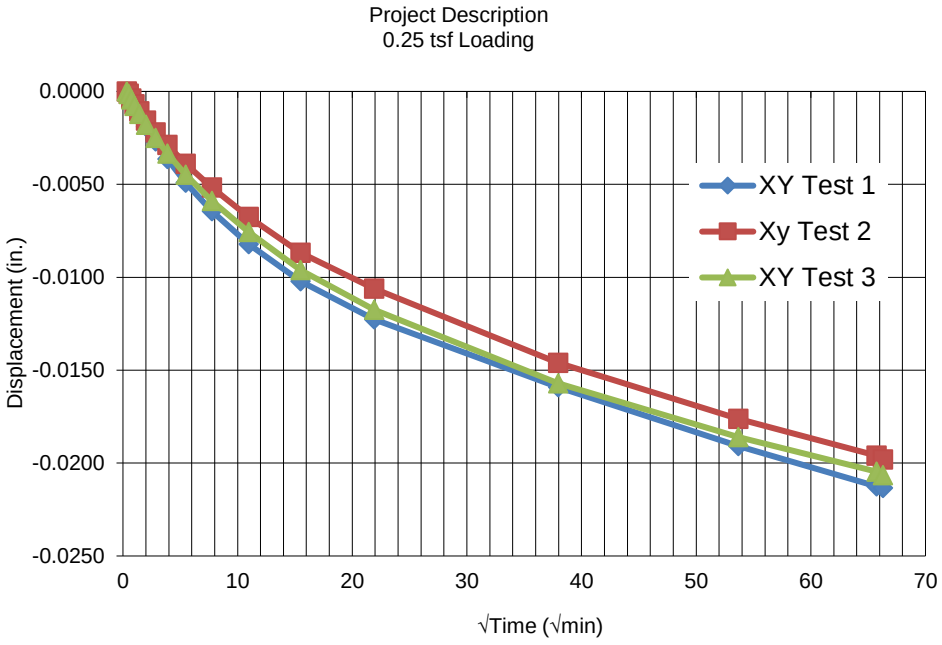

Figure C-18. Deformation vs. time^{½} for sample XY at 0.25 tsf

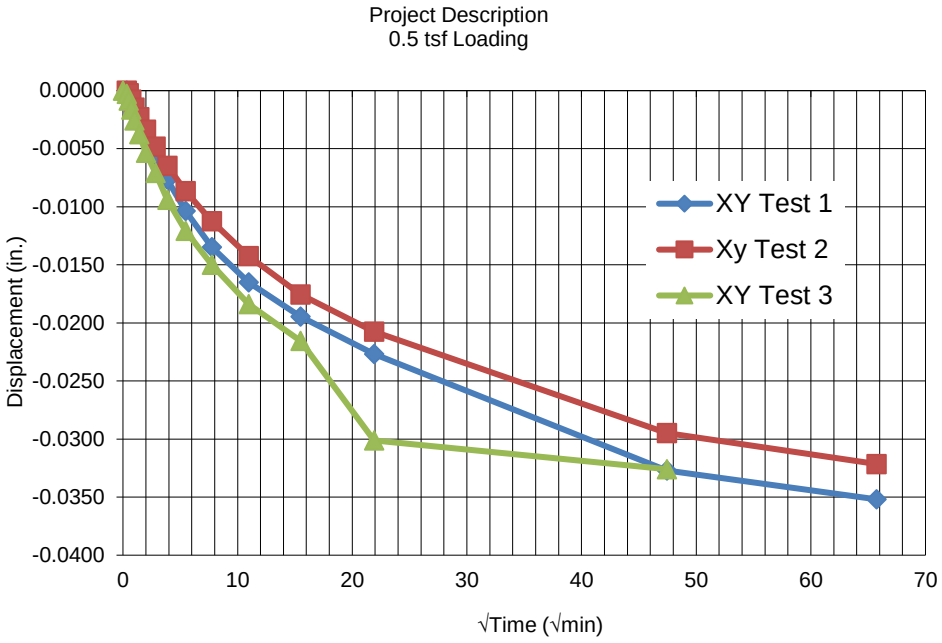

Figure C-19. Deformation vs. time^{½} for sample XY at 0.5 tsf

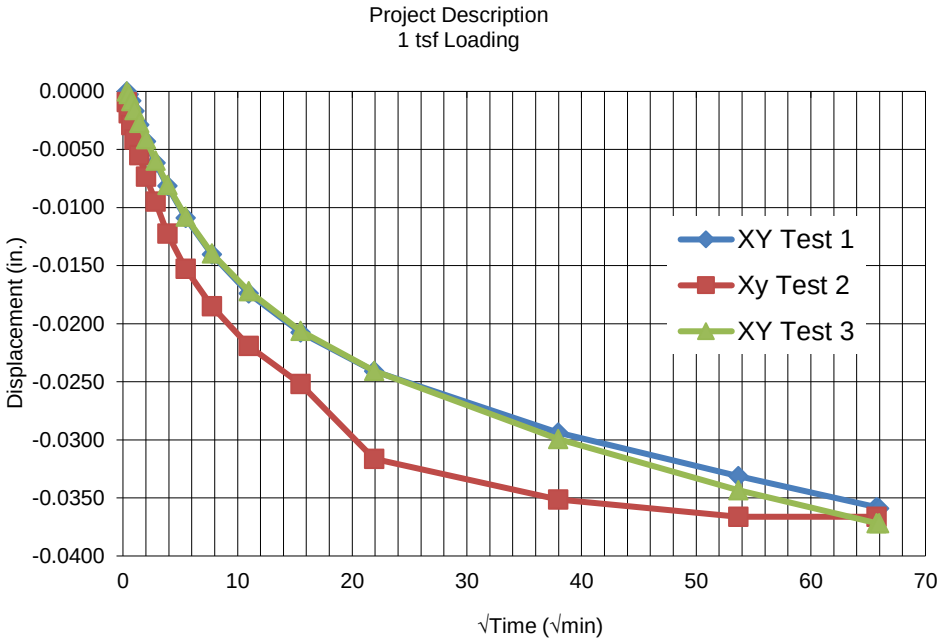

Figure C-20. Deformation vs. time^{½} for sample XY at 1 tsf

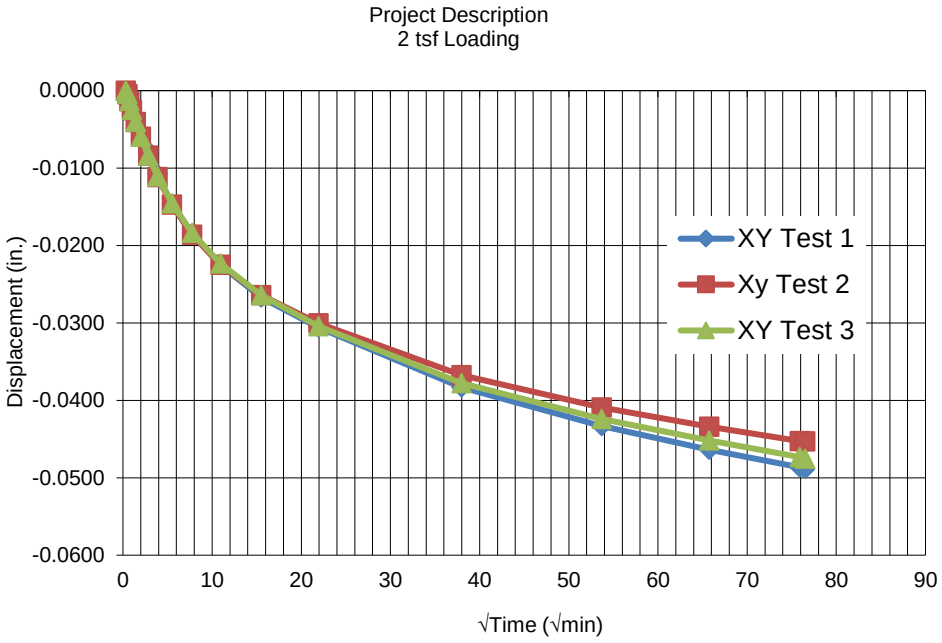

Figure C-21. Deformation vs. time^{½} for sample XY at 2 tsf

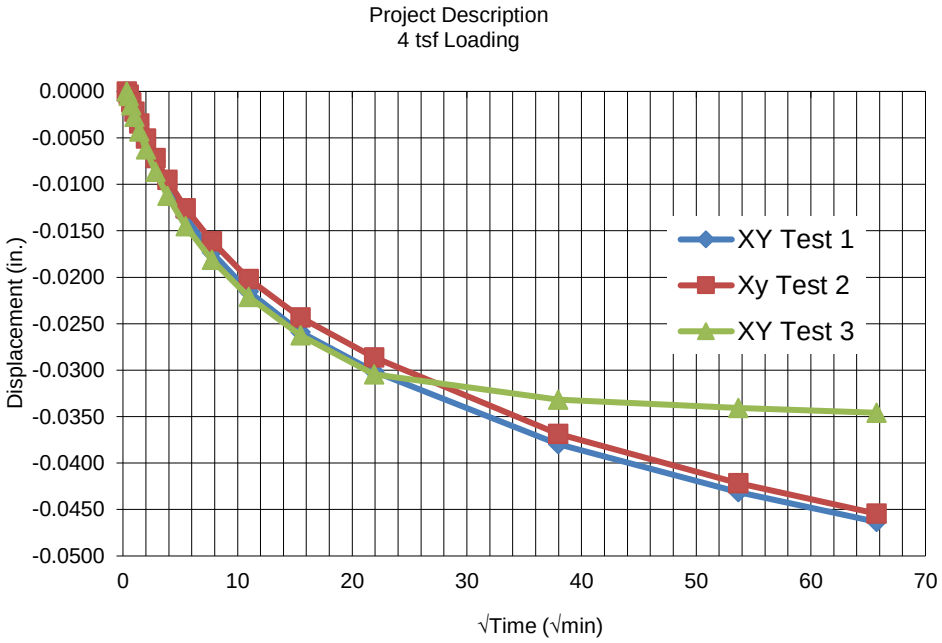

Figure C-22. Deformation vs. time^{½} for sample XY at 4 tsf

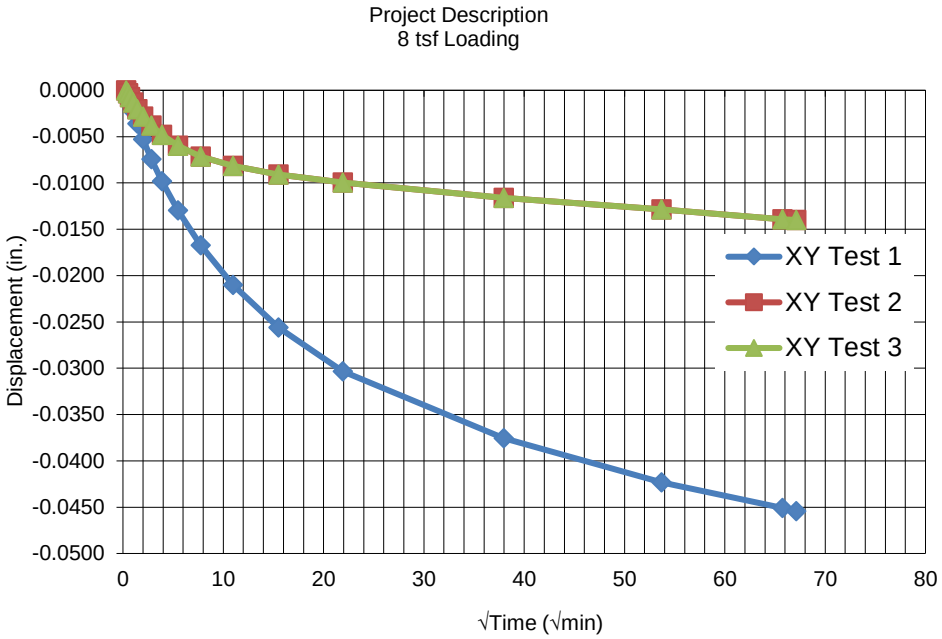

Figure C-23. Deformation vs. time^{½} for sample XY 8 tsf

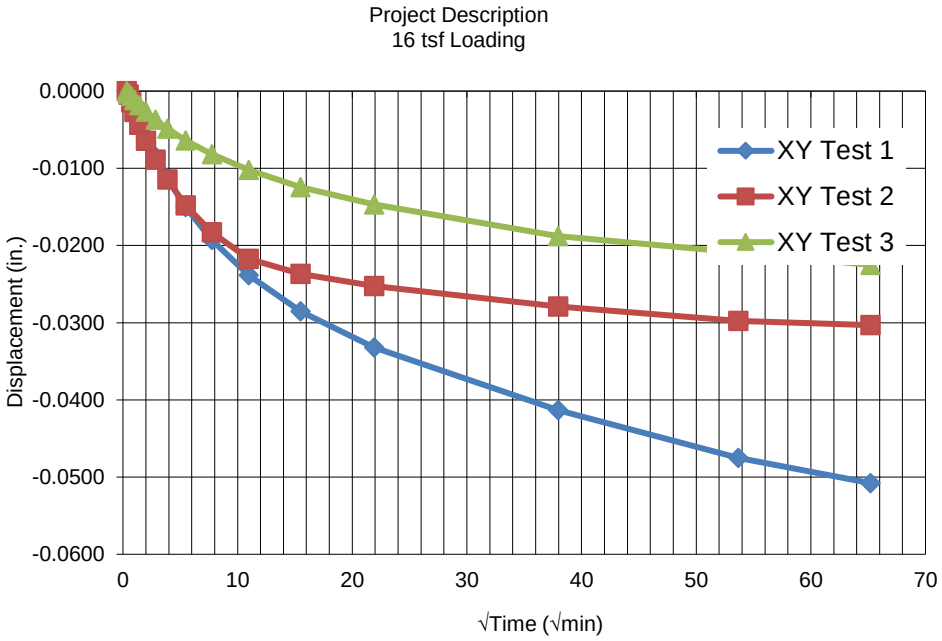

Figure C-24. Deformation vs. time^{½} for sample XY at 16 tsf

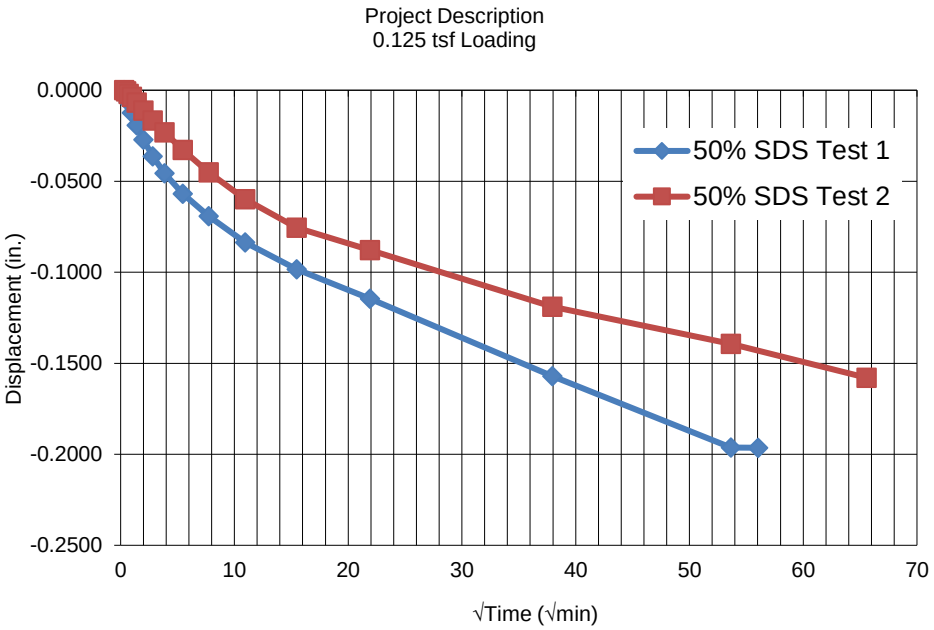

Figure C-25. Deformation vs. time^{½} for sample MD102 at 0.125 tsf

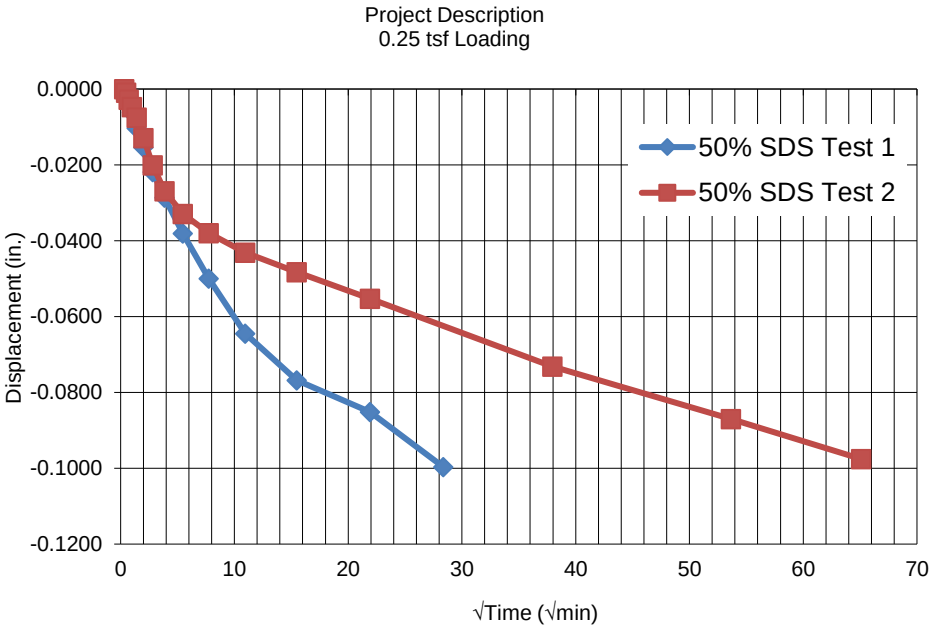

Figure C-26. Deformation vs. time^{½} for sample MD102 at 0.25 tsf

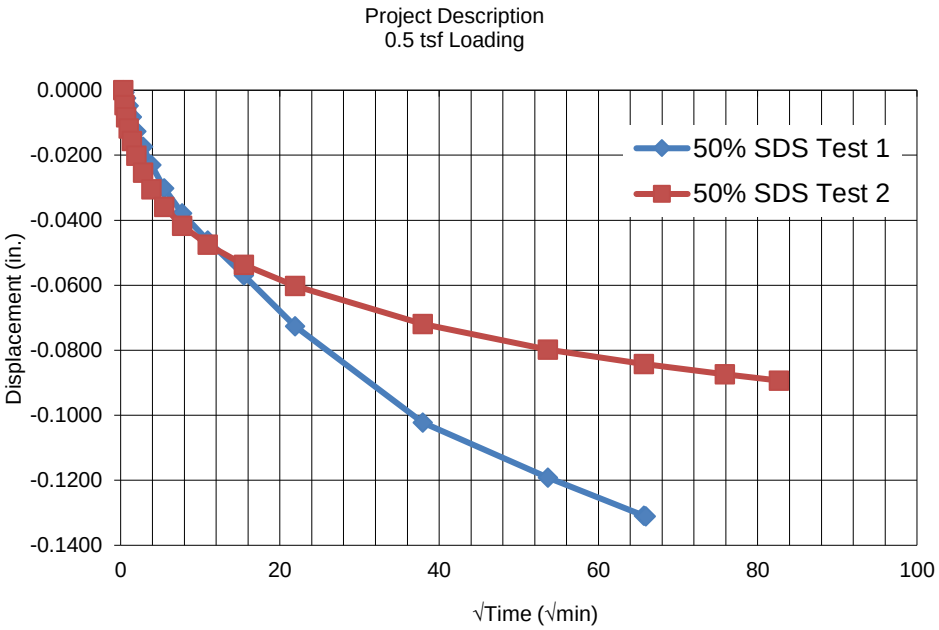

Figure C-27. Deformation vs. time^{½} for sample MD102 at 0.5 tsf

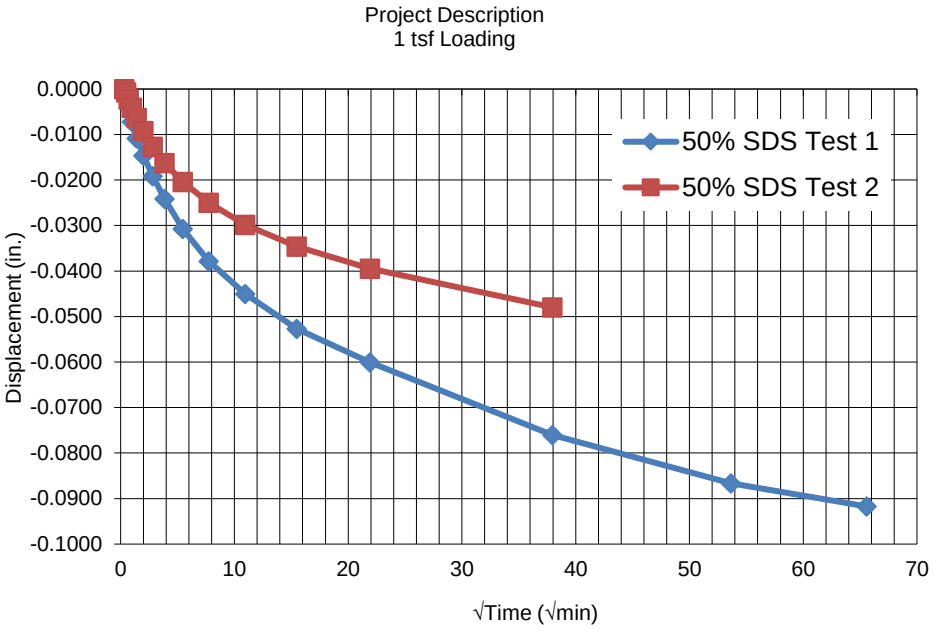

Figure C-28. Deformation vs. time^{½} for sample MD102 at 1 tsf

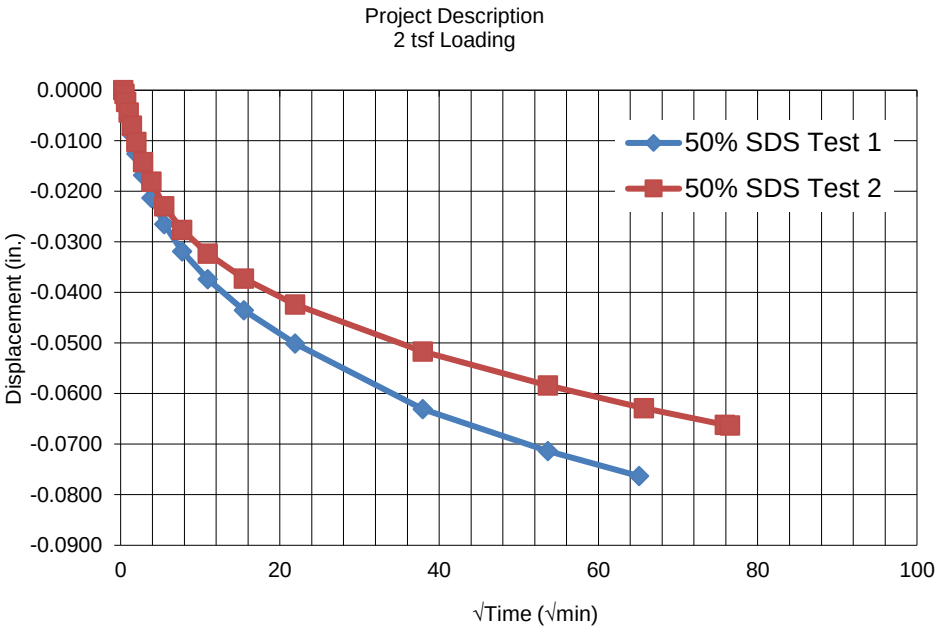

Figure C-29. Deformation vs. time^{½} for sample MD102 at 2 tsf

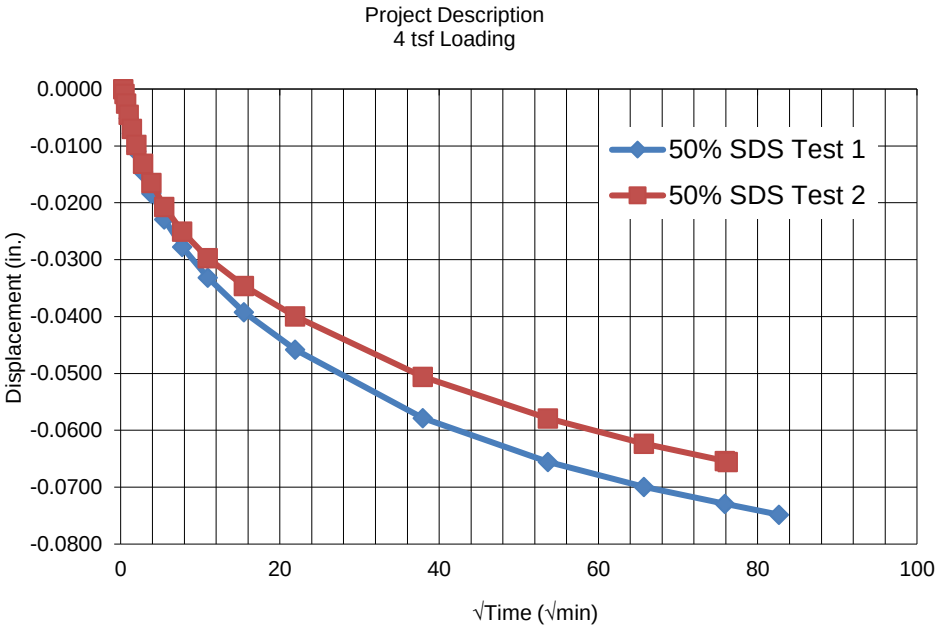

Figure C-30. Deformation vs. time^{½} for sample MD102 at 4 tsf

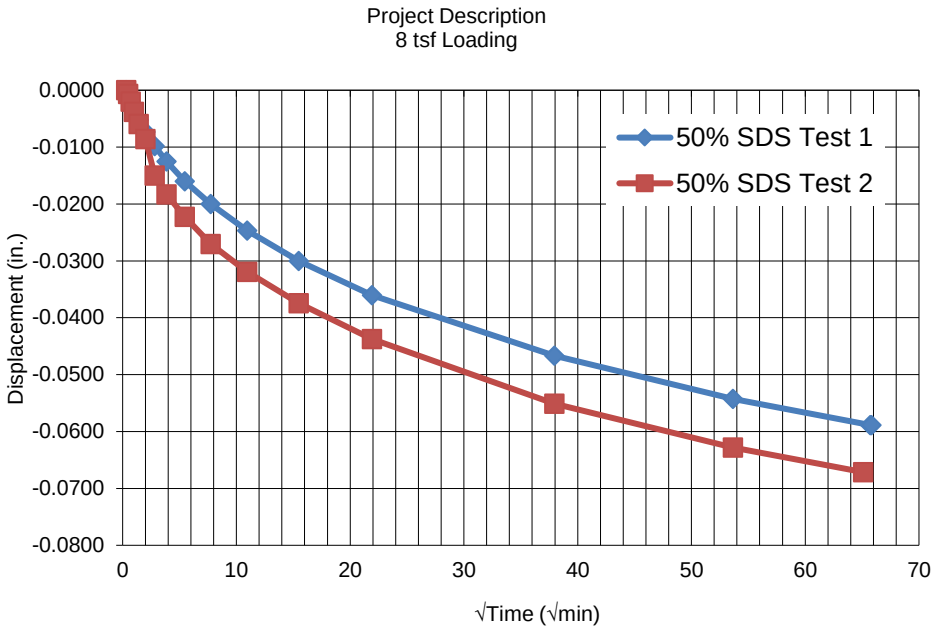

Figure C-31. Deformation vs. time^{½} for sample MD102 at 8 tsf

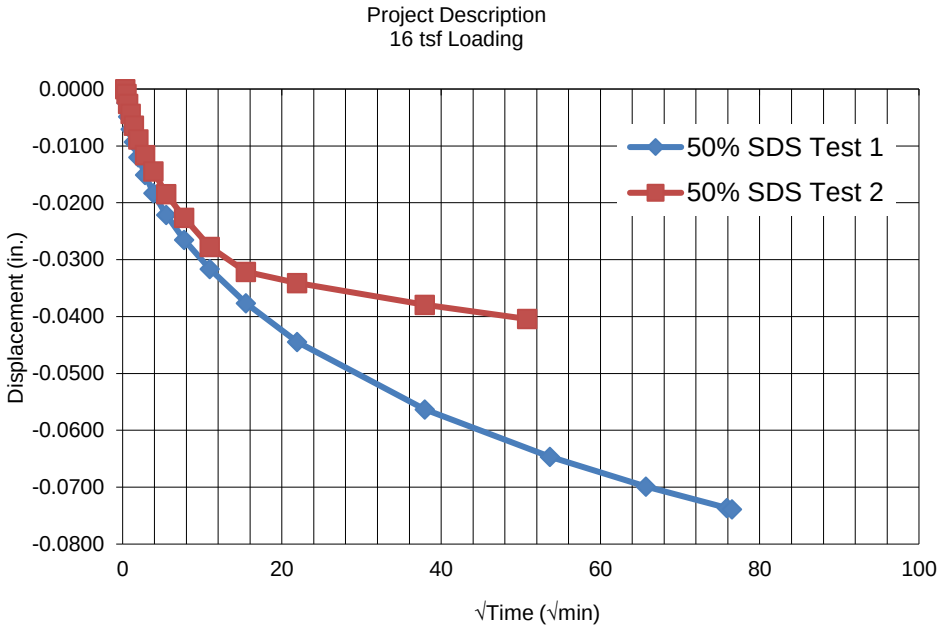

Figure C-32. Deformation vs. time^{½} for sample MD102 at 16 tsf

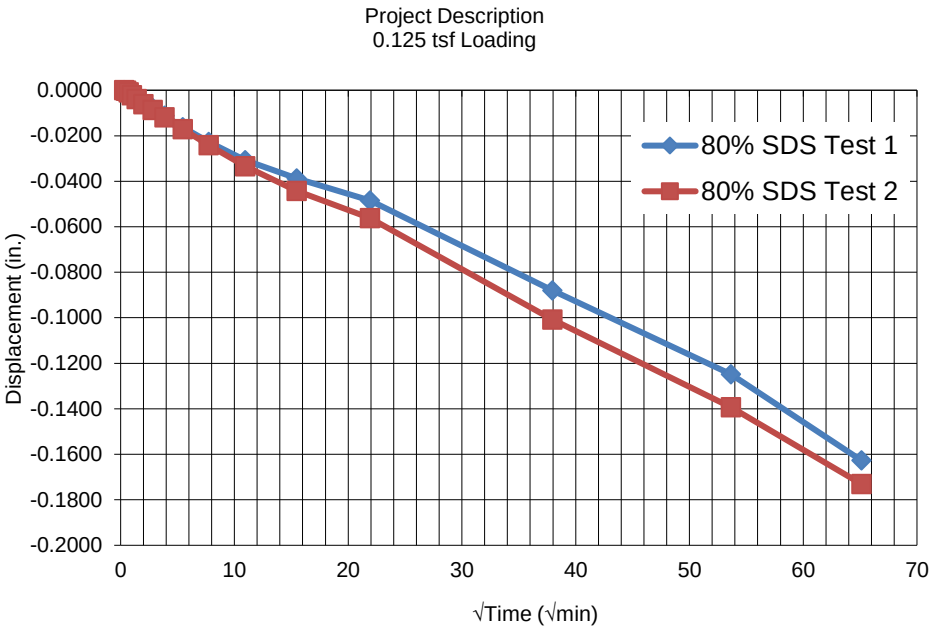

Figure C-33. Deformation vs time^{½} for sample MD202 at 0.125 tsf

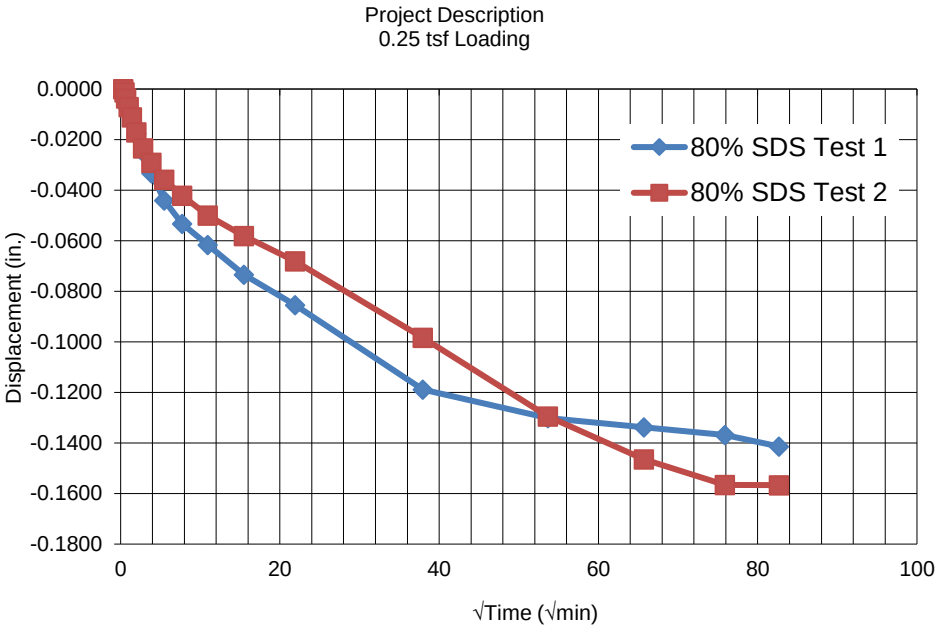

Figure C-34. Deformation vs. time^{½} for sample MD202 at 0.25 tsf

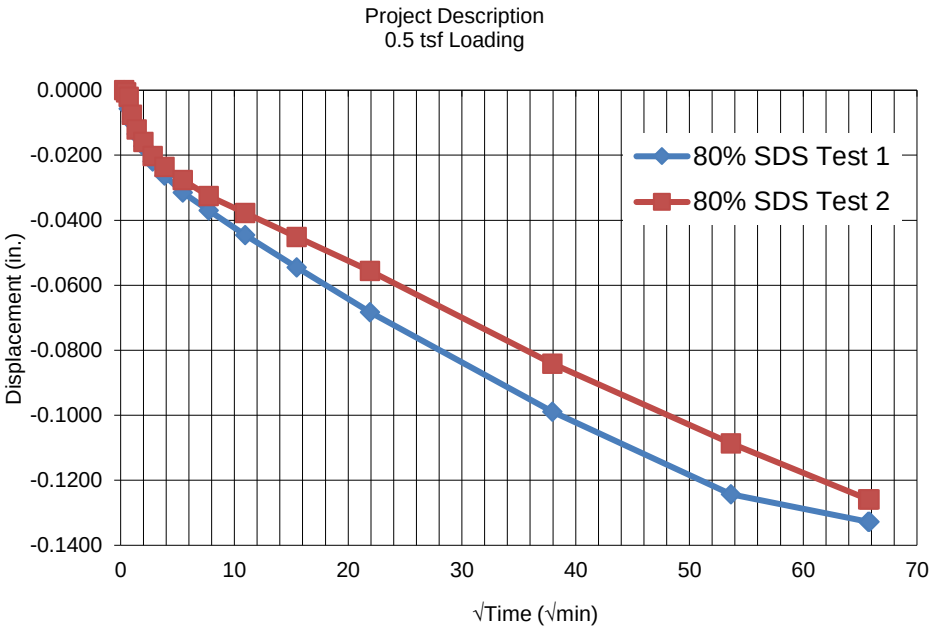

Figure C-35. Deformation vs time^{½} for sample MD202 at 0.5 tsf

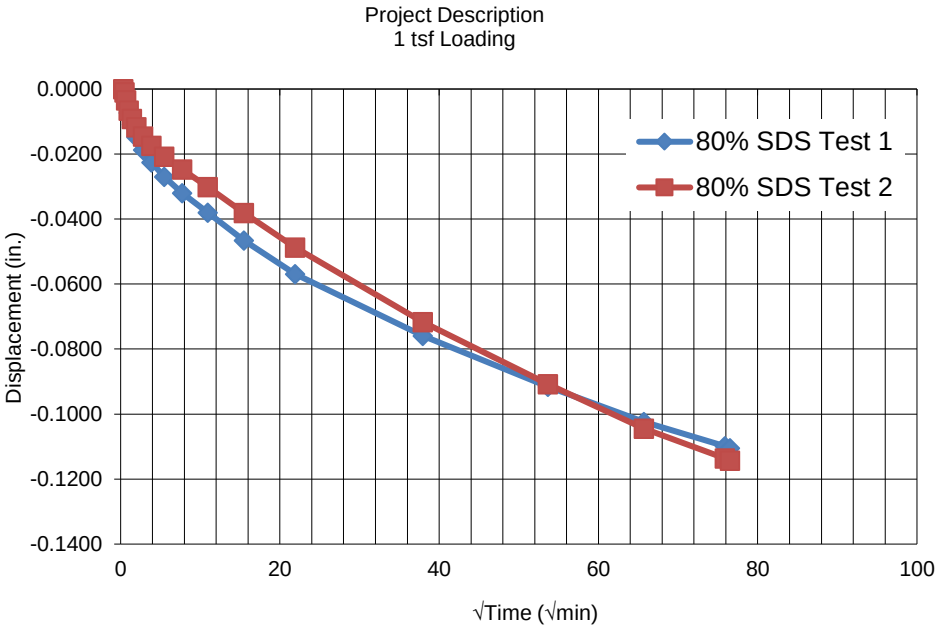

Figure C-36. Deformation vs. time^{½} for sample MD202 at 1 tsf

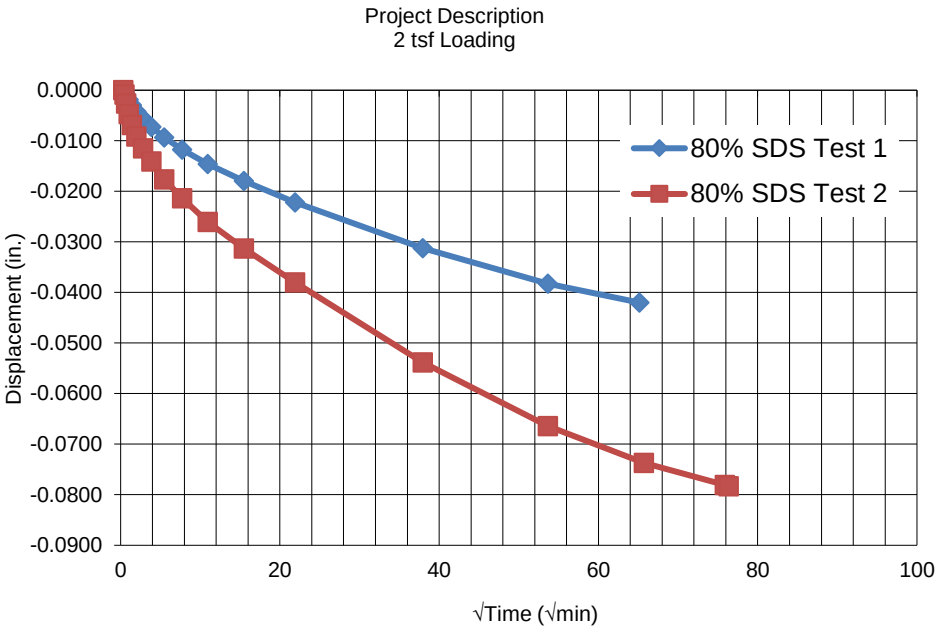

Figure C-37. Deformation vs. time^{½} for sample MD202 at 2 tsf

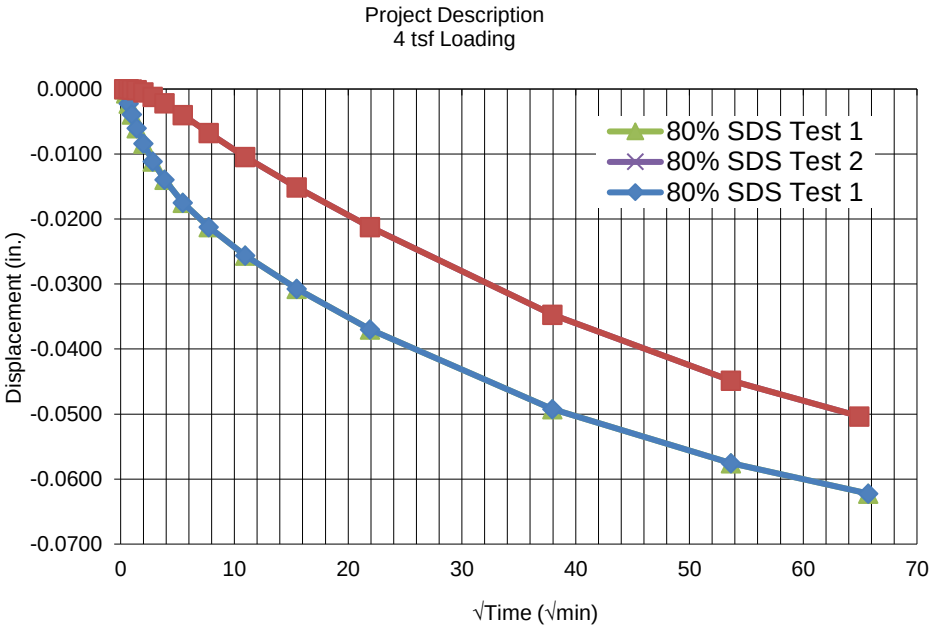

Figure C-38. Deformation vs. time^{½} for sample MD202 at 4 tsf

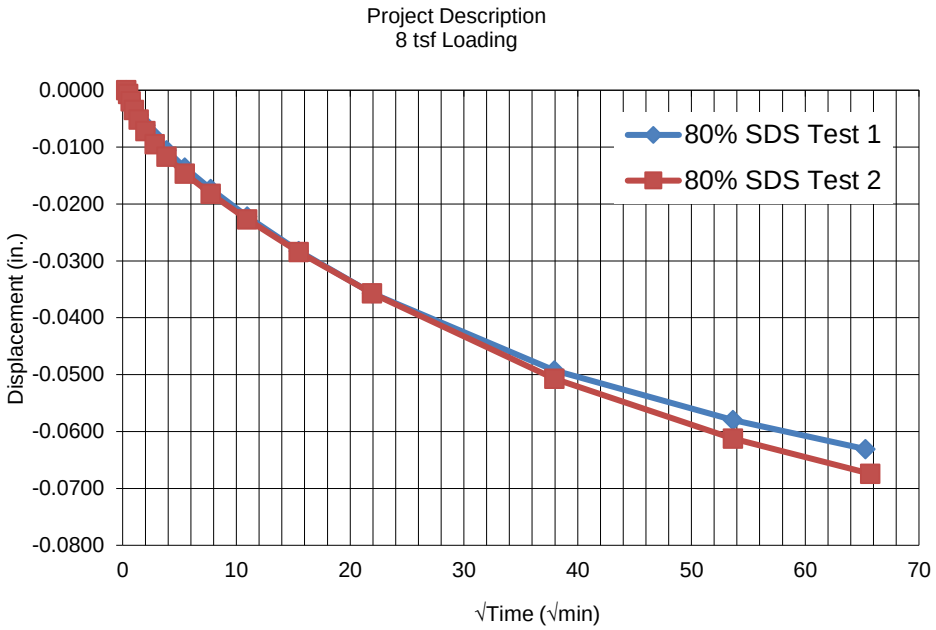

Figure C-39. Deformation vs. time^{½} for sample MD202 at 8 tsf

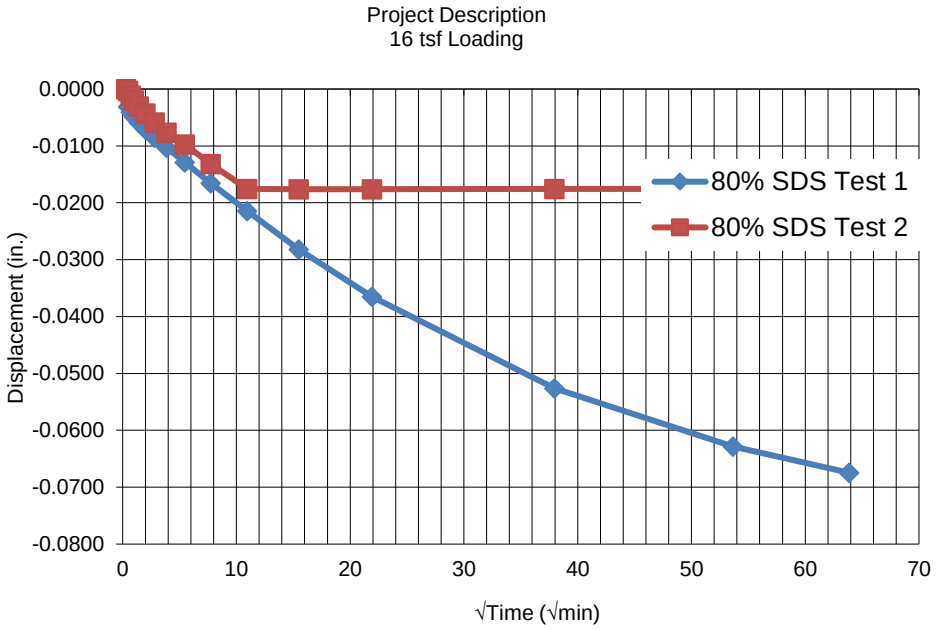

Figure C-40. Deformation vs. time^{½} for sample MD202 at 16 tsf